Precision Utilization of Extracellular Vesicles: From isolation to Application in Treating Bone Defects

Peng Wang

RADBOUD UNIVERSITY PRESS

Radboud Dissertation Series

Precision Utilization of Extracellular Vesicles: From isolation to Application in Treating Bone Defects

Peng Wang

This work was supported by grants from the China Scholarship Council (CSC grant No. 202008440374).

The work presented in this thesis was carried out within the Radboud University Medical Center. Publications of this thesis were financially supported by the Radboud University Medical Center (Radboudumc).

Precision Utilization of Extracellular Vesicles: From isolation to Application in Treating Bone Defects
Peng Wang

Radboud Dissertation Series
ISSN: 2950-2772 (Online); 2950-2780 (Print)

Published by RADBOUD UNIVERSITY PRESS
Postbus 9100, 6500 HA Nijmegen, The Netherlands
www.radbouduniversitypress.nl

Design: Proefschrift AIO | Guus Gijben
Cover: Peng Wang
Printing: DPN Rikken/Pumbo

ISBN: 9789465151915
DOI: 10.54195/9789465151915
Free download at: https://doi.org/10.54195/9789465151915

RADBOUD
UNIVERSITY
PRESS

Precision Utilization of Extracellular Vesicles: From isolation to Application in Treating Bone Defects

Proefschrift ter verkrijging van de graad van doctor
aan de Radboud Universiteit Nijmegen
op gezag van de rector magnificus prof. dr. J.M. Sanders,
volgens besluit van het college voor promoties
in het openbaar te verdedigen op

dinsdag 16 december 2025
om 12.30 uur precies

door

Peng Wang
geboren op 23 juni 1994
te Jiangxi (China)

Promotoren:
Prof. dr. P.M. van der Kraan
Dr. ing. J.J.J.P. van den Beucken

Copromotoren:
Dr. A.A.J. van de Loo
Dr. A.J. Arntz

Manuscriptcommissie:
Prof. dr. J.G.J. Hoenderop
Prof. dr. R.E. Brock
Prof. dr. M.H.M. Wauben (Universiteit Utrecht)

Paranimfen:
Wessel Theeuwes
Xiaosong Xiang

Precision Utilization of Extracellular Vesicles: From isolation to Application in Treating Bone Defects

Dissertation to obtain the degree of doctor
from Radboud University Nijmegen
on the authority of the Rector Magnificus prof. dr. J.M. Sanders,
according to the decision of the Doctorate Board
to be defended in public on

Tuesday, December 16, 2025
at 12.30 pm

by

Peng Wang
born on June 23, 1994
in Jiangxi(China)

Supervisors:
Prof. dr. P.M. van der Kraan
Dr. ing. J.J.J.P. van den Beucken

Co-supervisors:
Dr. A.A.J. van de Loo
Dr. A.J. Arntz

Manuscript Committee:
Prof. dr. J.G.J. Hoenderop
Prof. dr. R.E. Brock
Prof. dr. M.H.M. Wauben (Utrecht University)

Ushers:
Wessel Theeuwes
Xiaosong Xiang

Table of contents

Chapter 1

General Introduction

1. Bone and skeletal system

The skeletal system is a complex organ system that plays a crucial role in supporting the body, facilitating movement, and protecting vital organs. It comprises bones and joints, that work together to enable locomotion and maintain structural integrity [1]. Bones mainly serve as the framework of the body. Bone structure is a complex and dynamic system composed of two primary types: cortical (compact) bone and cancellous (trabecular) bone. Cortical bone, which makes up about 85% of the skeleton, is dense and primarily found in the shafts of long bones, while cancellous bone, comprising the remaining 15%, is more prevalent in the vertebral column and has a larger surface area per unit volume, allowing for greater metabolic activity [2]. Bone tissue also houses red bone marrow, which is responsible for producing blood cells necessary for oxygen transport and immune function [3]. Bone cells are integral to the structure and function of bone, with three main types: osteoblasts, osteoclasts, and osteocytes. Osteoblasts are responsible for bone formation and are derived from mesenchymal stromal cells (MSCs), while osteoclasts, which resorb bones, originate from hematopoietic stromal cells [4]. Osteocytes as the most abundant bone cell type, are derived from osteoblasts and embedded within the bone matrix and play a crucial role in mechanosensation and the regulation of bone remodeling [5].

2. Bone changes in skeletal diseases

Skeletal diseases such as osteoporosis and arthritis significantly impact bone health, leading to changes in bone structure and function [6]. Osteoporosis is characterized by a reduction in bone density, which increases the risk of bone fractures, particularly in postmenopausal women and older adults [7]. In addition, arthritis especially rheumatoid arthritis, exacerbates bone loss through chronic inflammation and the use of glucocorticoids, which can lead to both local and generalized bone loss, contributing to osteoporosis [8]. The interplay between these conditions is further complicated by shared risk factors such as aging, genetics, and systemic inflammation, which can accelerate bone deterioration and increase bone fracture risk [9].

3. Bone defects

Osteoporotic fractures are often accompanied by bone defects due to changes in bone microarchitecture, decreasing deposits of bone mineral and bone matrix components, sparseness of bone trabeculae, decreased bone strength, and increased bone fragility [10]. A bone defect is defined as a significant disruption in the integrity of bone tissue [11, 12]. Globally, fracture-related bone defects such as non-unions and segmental bone defects are significant public health issues. There are approximately 178 million new bone fractures worldwide every year, with a substantial increase in prevalence since 1990 [13]. Bone defects and related conditions can lead to long-term disability, affecting a patient's ability to work and participate in daily activities and reducing the quality of life [14]. Moreover, the treatment of bone defects in the United States incurs an annual cost of approximately $5 billion, with significant expenses related to bone grafts and surgical interventions for non-unions and other complications [15].

The natural healing of bone defects involves a complex interplay of various cell types, each contributing to different phases: inflammation, repair, and remodeling. With blood clot formation, the monocytes have been recruited and differentiated to macrophages and pre-osteoclasts. Pre-osteoclasts fuse to form osteoclasts that resorb damaged or old bone, releasing embedded growth factors that initiate repair [16]. Meanwhile, macrophages clear cellular debris and secrete cytokines that create a regenerative microenvironment [17]. MSCs are known for their immunomodulatory properties and ability to differentiate into pre-osteoblasts [18, 19]. Osteoblasts are responsible for the synthesis, deposition, and mineralization of the bone matrix, playing a crucial role in bone turnover and fracture healing. Additionally, endothelial cells are critical for neovascularization, which is essential for providing nutrients and oxygen and removing waste products during the healing process [20]. The clinical approach to enhance bone healing is to facilitate the integration of these cellular activities using biomaterials and scaffolds that provide structural support and enhance cellular interactions [21]. Overall, the orchestration of these diverse cell types and their interactions is critical for effective bone (defect) healing, highlighting the potential for targeted therapeutic strategies in regenerative medicine.

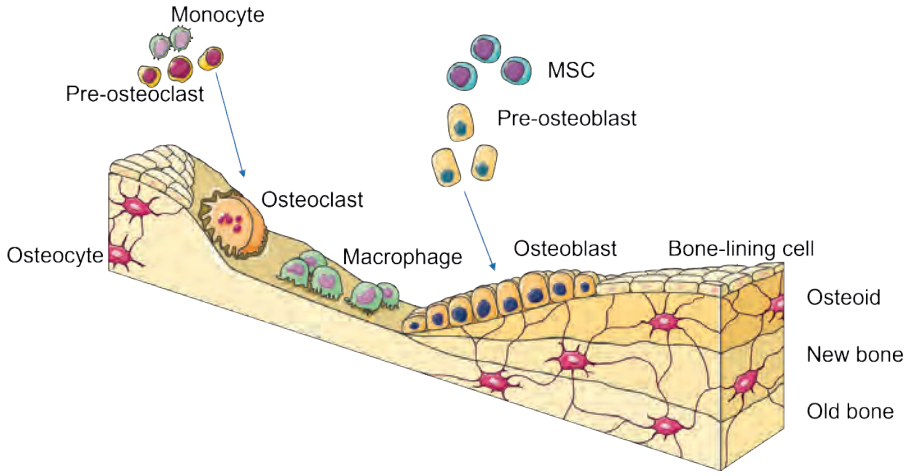

Fig. 1. Schematic representation of the process of bone healing and involved cell types. Monocytes differentiate into pre-osteoclasts, which mature into osteoclasts that break down old bone. Macrophages help clear debris. Next, MSCs differentiate into pre-osteoblasts, which then turn into osteoblasts, with the function of forming new bone. This new bone becomes osteoid, which mineralizes into mature bone, while bone-lining cells cover the surface and osteocytes become embedded in the bone matrix.

4. Standard of Care & Cutting-edge therapies

The current standard for treating bone defects, especially in pathological conditions such as osteoporotic bone, primarily involves surgical interventions that use autologous bone grafts to fill the defects [22], which are considered the gold standard due to their osteoinductive and osteogenic properties. However, this method is not without limitations, including donor site morbidity, limited supply, and variable clinical outcomes [23]. As for allografts and xenografts, they offer key advantages such as wide availability, ease of use, and avoidance of donor-site morbidity [24]. Through they lack osteogenic potential, they provide an effective osteoconductive scaffold and, in some cases (e.g., Demineralized Bone Matrix), limited osteoinductive capacity. Their ready-to-use nature makes them valuable alternatives when autografts are not feasible [25]. Other traditional methods include the Masquelet technique (two-stage surgical method that uses a temporary spacer to induce a biologically active membrane, which later supports bone grafting for bone defect repair), distraction osteogenesis, and vascularized bone grafts, which have shown favorable results in certain cases but still face challenges such as inadequate vascularization and high surgical costs [26].

Emerging cutting-edge therapies in bone tissue engineering (BTE) and regenerative medicine are being developed to address these limitations and improve patient outcomes using the following basis:

i) Biomaterials are essential for creating scaffolds that mimic the natural bone environment, providing structural support and facilitating cell attachment and proliferation. Commonly used biomaterials include calcium phosphate (CaP)-based materials, such as hydroxyapatite (HAP) and biphasic calcium phosphate (BCP) [27]. The physicochemical properties of CaPs, such as their chemical composition, crystal size, and morphology, significantly influence their biological performance, including osteoinductive and osteoconductive capabilities [28]. Moreover, advanced fabrication techniques, including 3D printing and electrospinning, allow for the customization of scaffold properties to enhance their performance and bioactivity. However, the complexity of fabricating scaffolds that incorporate multiple functional components, such as cells, growth factors, and drugs, poses significant technical challenges [29].

ii) Growth Factors such as bone morphogenetic proteins (BMPs), fibroblast growth factor (FGFs), and vascular endothelial growth factor (VEGFs) have been utilized to enhance osteoblast activity and promote bone healing [30]. These growth factors are integral to the reparative processes in bone and cartilage, acting as mediators that regulate cellular growth, proliferation, and differentiation, which are crucial for tissue regeneration [31]. The delivery of these growth factors is a critical aspect of their effectiveness, with various strategies being explored to optimize their therapeutic potential. Techniques such as encapsulation, scaffolding, and the use of hydrogels have been developed to protect growth factors from degradation and to control their release kinetics, ensuring adequate and targeted delivery to the affected areas [32]. However, several potential side effects require careful consideration. For example, high doses of BMP-2, often required due to its short half-life, can lead to adverse events such as inflammation, osteoclast-mediated bone resorption, and inappropriate adipogenesis, as well as ectopic bone formation and even tumorigenesis in some cases [33, 34]. Additionally, the regenerative potential of growth factors can be hindered by proinflammatory signals, such as those mediated by the interleukin-1 receptor, which can desensitize bone-forming cells and accelerate cellular senescence [35].

iii) Cell-based Therapies predominantly using MSCs are being explored for their potential to improve the quality and rate of bone regeneration [36]. For example, the use of iPSCs derived from peripheral blood cells has also been investigated, with studies demonstrating their ability to differentiate into osteoblasts and promote

bone formation when transplanted into animal models [37]. Innovative scaffolding technologies further enhance the efficacy of cell-based therapies by providing a supportive three-dimensional environment that mimics the in vivo conditions necessary for osteogenic differentiation [38]. The integration of bioactive materials, such as the osteoimmunomodulatory biopatch, has been shown to potentiate cell-based therapies by regulating signaling pathways like IL-17 and ferroptosis, thereby improving bone regeneration outcomes in animal models [39]. Despite these advancements, challenges remain, including the need for standardized protocols and further clinical trials to confirm the safety and efficacy of these therapies in humans [40, 41].

iv) Extracellular Vesicles (EVs) are cell-secreted lipid bilayer vesicles that consist of sterols, membrane proteins and enclose an aqueous solution containing proteins, nucleic acids, and metabolites capable of influencing biological functions [42]. The study of EVs began with the discovery of matrix vesicles (MVs). In 1967, Anderson and colleagues first observed these vesicles in cartilage tissue. Released by osteoblasts and chondrocytes, MVs were found to initiate hydroxyapatite crystal formation in the extracellular matrix and play a crucial role in bone and cartilage mineralization. This marked the earliest recognition of vesicle-mediated extracellular functions [43]. Later, in 1983, exosomes—another subtype of EVs—were identified during the maturation of reticulocytes, where they facilitated the disposal of transferrin receptors. These exosomes, originating from multivesicular bodies (MVBs), were subsequently recognized as important mediators of intercellular communication [44]. Currently, EVs are categorized into three main types: exosomes, microvesicles, and apoptotic bodies, each distinguished by their size and biogenesis. Exosomes are small EVs, typically ranging from 30 to 150 nm, and are formed through the fusion of multivesicular bodies with the plasma membrane [45]. Microvesicles, also known as ectosomes, are medium-sized EVs ranging from 50 to 1000 nm and produced by the outward budding of the plasma membrane [46]. Apoptotic bodies are the largest, ranging from 500 to 2000 nm, that result from the disintegration of cells during the late stages of apoptosis. It is generally accepted that these EVs play crucial roles in intercellular communication by transporting proteins, lipids, and nucleic acids as their cargo that influence various physiological and pathological processes [47]. For example, in the context of immunity, EVs are involved in immune cell activation, antigen presentation, and immunomodulation, impacting both innate and adaptive immune responses [48]. In cancer, EVs contribute to tumor growth, metastasis, and immune evasion by transferring oncogenic signals and remodeling the tumor microenvironment [49]. EVs are emerging as a promising cell-free therapeutic strategy in regenerative

medicine [50]. The potential of EVs to deliver bioactive molecules and promote MSCs migration and differentiation makes them a valuable tool in bone regeneration [51].

5. Sources of EVs for bone regeneration

EVs isolated from in vitro cell cultures: EVs can be isolated from cell cultures. The majority of EVs for tissue regeneration come from MSC cultures, and among them the most widely used are bone marrow MSC, periodontal ligament and gingival MSCs. Bone marrow stromal cell-derived EVs have been shown to positively regulate osteogenic genes and promote osteoblastic differentiation without inhibiting cell proliferation. For example, the presence of specific microRNAs, such as miR-196a, within these EVs plays a critical role in enhancing osteoblastic differentiation and gene expression, further supporting their osteogenic capabilities [52]. EVs derived from periodontal ligament MSCs and gingival MSCs have been encapsulated in RGD-modified alginate scaffolds to enhance MSC viability and osteogenic differentiation. This approach has demonstrated significant bone formation in critical size calvarial defects in mice, indicating the potential of these EVs in bone regeneration [53]. In addition, EVs derived from adipose tissue-derived stromal cells (ADSCs) play a role in intercellular communication and have properties like functional MSCs. Using β-tricalcium phosphate (β-TCP) as a carrier, EVs from thermally induced ADSCs promote bone regeneration [54]. For all experimental EV research, however, the main concern of enrichment of MSC-EVs from cell culture media is the contamination with exogenous EVs present in fetal bovine serum (FBS). The presence of FBS-EVs may confound the therapeutic or diagnostic analyses of EVs derived from cultured cells [55].

EVs isolated from body liquid: EVs can be isolated from bodily fluids such as plasma/serum and milk that have shown significant potential in tissue regeneration. For example, EVs derived from platelet-rich plasma (PRP) have been shown to enhance bone regeneration by participating in the regulation of bone repair through the bioactive molecules in their cargo. Specifically, they stimulate angiogenesis through the activation of signaling pathways such as PI3K, ERK, and G protein-coupled receptors in endothelial cells, resulting in improved vascularization. Moreover, PRP-EVs also stimulate the Wnt/β-catenin signaling pathway, which enhances osteogenesis and aids bone tissue regeneration. PRP-EVs contain key growth factors like VEGF, PDGF, bFGF, and TGF-β1, which are critical for tissue repair and regeneration [56]. In addition, EVs derived from human milk (HMEVs) are recognized for their potential roles in infant development and immune modulation [57, 58].

Recent work reported that the BMP2 and MAPK signaling pathways are crucial for the osteogenic effects of HMEVs. These pathways facilitate the differentiation and mineralization of osteoblasts, thereby promoting bone regeneration [59]. However, the use of HMEVs faces limitations due to ethical problems, limited resources, individual heterogeneity that limit scalability and standardization of the EV product which complicates their widespread therapeutic use [60, 61]. Consequently, EVs derived from cow milk have been investigated recently due to the abundance of cow milk and their reported species cross-reactivity for energy supply [62].

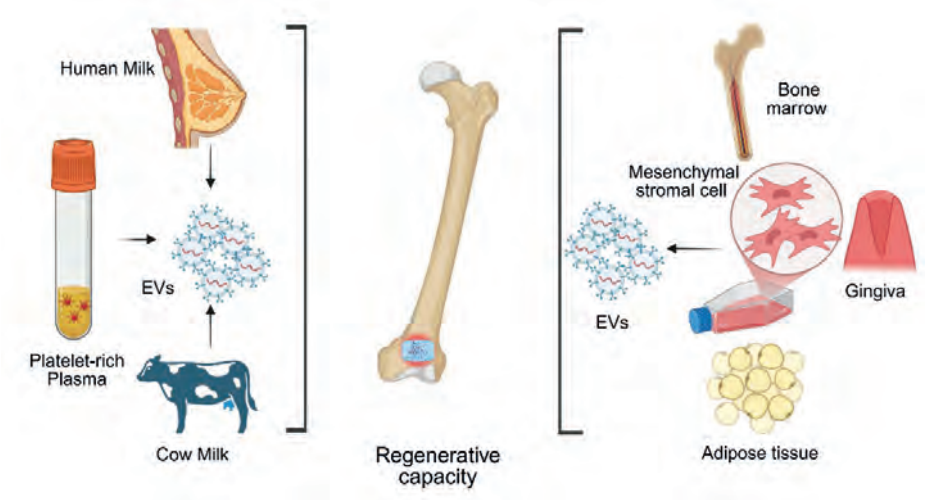

Fig. 2. Sources of EVs with bone-promoting properties. The left section illustrates EVs derived from body fluids such as platelet-rich plasma, human milk, and cow milk, which possess osteogenic potential. The right part mainly presents EVs isolated from the culture supernatants of MSCs from various sources, highlighting their potential applications in bone regeneration. In the central section, EVs loaded into scaffolds, particularly hydrogels—have been implanted into femoral condyle defects, representing the regenerative capacity of EVs in bone repair (created in BioRender.com).

6. Cow milk EVs in bone homeostasis

Cow milk EVs (mEVs) are known for their robust stability, as they can survive the gastrointestinal tract's harsh conditions, making them effective carriers for bioactive molecules and potential drug delivery systems [63]. The scalable isolation of high-quality purified mEVs has been achieved through novel purification methods, which ensure minimal contamination from milk proteins, thus paving the way for their industrial-scale application [64]. Moreover, mEVs have been recognized for their immunomodulatory properties, influencing macrophage differentiation and cytokine production, which could be beneficial in treating conditions like fibrosis and cancer [63].

Previous studies demonstrated that mEVs regulate bone homeostasis through influencing the activity of osteoblasts and osteoclasts [65, 66]. Moreover, mEVs showed systemic osteoprotective properties in an ovariectomized (OVX) murine bone loss model via RANKL/OPG regulation [67]. It has been reported that changes in bioenergetic metabolism significantly impact the balance of bone homeostasis by influencing the energy supply necessary for bone cell functions, such as osteoblast differentiation and bone matrix production [68]. For instance, osteoblasts, the second bone-forming cells, require substantial energy to synthesize and mineralize the bone matrix, and this energy is derived from various metabolic pathways, including glycolysis, fatty acid metabolism and glutamine metabolism. Since mEVs have been implicated in modulating energy status, which can influence metabolic homeostasis [69], investigating the role of mEVs in accelerating osteogenesis in terms of bioenergetic metabolism seems meaningful.

7. EVs-ECM interaction for bone remodeling

Besides uptake by recipient cells, EVs could inherently interact with the extracellular matrix (ECM) meshwork. A large number of surface biomolecules have been identified to anchor on the EV surface for interaction with the ECM [70]. The extracellular matrix (ECM) plays a crucial role in regulating cellular functions and constitutes the primary non-cellular component of tissues [71]. Additionally, the ECM is a naturally occurring substance that contains both biochemical and biophysical components surrounding living cells. In bone, the ECM is mainly composed of type I collagen, a fibrous protein that imparts tensile strength, and (carbonated) hydroxyapatite, a mineral that provides compressive strength. Moreover, non-collagenous proteins like osteocalcin, osteopontin, and bone sialoprotein play vital roles in regulating the remodeling of bone ECM and influencing cell behavior [72].

ECM-binding property of EVs: EVs interact with ECM components such as laminin and collagen through motifs that are recognized by integrins. A recent study found that when MCF10 breast cancer EVs move through the interstitium, those containing integrin α3β1 bind to the laminin-rich ECM. This interaction affects the number of EVs that enter the blood and lymphatic capillaries and further influences the spatial distribution of both bound and free MCF10 EVs within the interstitial space [73]. Moreover, it has been reported that such bonds exist among EVs derived from cells residing in bone tissue and collagen [74]. For example, researchers intravenously administered labeled injured neuron-derived EVs containing fibronectin-1 to rats

with tibial bone or calvarial defects. The EVs entered the bloodstream and migrated to various organs. Using optical imaging, they observed a significant increase in the number of injured neuron-derived EVs within the vicinity of the bone defects. Application of a synthetic FN1-binding inhibitor peptide (GRGDNP) significantly reduced the accumulation of EVs in bone, supporting the idea that FN1 mediates the targeting process through interaction with integrins [75]. Therefore, the ECM-binding properties could be one of many "EV-inherent features", associated with EVs' therapeutic application.

EVs encapsuled in ECM-based biomaterials: Local injections of EVs have been utilized in preclinical studies for therapeutic applications in bone disorders, employing animal models such as mice with femoral fractures [76]. The integration of EVs with scaffolds and other biomaterials has been a focal point of research, aiming to improve the efficacy of bone regenerative therapies based on EVs. Studies have explored the use of EVs encapsulated in ECM-based biomaterials, such as decellularized ECM, specific ECM components, or ECM-mimetic hydrogels, for tissue regeneration applications [77]. ECM-based biomaterials act as biologically compatible delivery platforms that closely resemble the natural tissue environment. The localized delivery of EVs from ECM-based scaffolds offers significant benefits for bone regeneration. Since bone tissue regeneration typically demands extended therapeutic treatments due to slow healing and the need for precise control over biomolecule delivery, ECM-based scaffolds provide a solution by offering adequate release mechanisms that ensure prolonged EV activity at the injury site [78].

8. Objective of this thesis

The main objective of this thesis was to investigate the precision utilization of EVs including characterization, isolation and therapeutic application: Developing methods of eliminating FBS contamination for isolating EVs from *in vitro* cell culture (human ADSCs) and investigating the osteogenic potential of specific subpopulations of EVs isolated from body fluids (cow milk). More specifically, this thesis aimed to answer the following research questions:

1. **Chapter 2**-Which EV-depletion method of FBS is the best to use in MSC cultures to obtain pure MSC-EVs with minimal FBS EV contamination whilst not impairing cell growth and differentiation? To investigate this, we tested three methods: 18h-ultracentrifugation (UC), ultrafiltration (UF), and polyethylene glycol (PEG) precipitation to obtain three EV depleted FBS (EVdFBS) batches

and compared them to FBS and commercial (Com) EVdFBS on human ADSCs growth, differentiation, enrichment of EVs in human ADSCs supernatant and their biological function on collagen metabolism.

2. **Chapter 3**-What is the effect of mEVs on energy metabolism during EV accelerated osteogenic differentiation of human bone marrow MSCs (hBMSCs)? To explore this, we evaluated the impact of mEVs at various concentrations on the osteogenic differentiation of hBMSCs over a 21-day period. Next, we determined the DNA content and adenosine triphosphate (ATP) production of cells, and glucose consumption and lactate production, as well as glutamine consumption in the early phase of hBMSCs osteogenic differentiation (day2 & day6). Moreover, the activities of mitochondria have been investigated by testing mitochondrial-associated genes and the changes of mitochondria volumes and reaction byproducts.
3. **Chapter 4**-What is the significance of ECM-binding properties of EVs in the therapeutic treatment of skeletal diseases? To understand this, we reviewed the available knowledge on EV surface biomolecules and their interactions with ECM components that are crucial for regulating bone remodeling, cartilage maintenance, and immune responses, playing roles in both tissue homeostasis and pathological conditions, such as arthritis and osteoporosis. More importantly, using analyses of animal experimental data, we illustrated the effect of ECM-based biomaterials (e.g. hydrogels, decellularized matrices, and ECM-mimetic scaffolds) as carriers for EVs toward effective EV delivery in regenerative and immunomodulatory therapies in bone and joint tissue. These biomaterials enable sustained release and targeted delivery of EVs, promoting bone and cartilage regeneration.
4. **Chapter 5**-What is the role of the mEV subpopulation with the capacity to bind collagen in preclinical bone regeneration? To investigate this, we utilized collagen-binding to estimate the proportion of mEVs with or without collagen-binding property: collagen-binding mEVs ($^{cb+}$mEVs) and non-collagen binding mEVs ($^{cb-}$mEVs). To assess their osteogenic functionality, we determined EV uptake and calcium deposition by hBMSCs with their stimulation *in vitro*. Moreover, to investigate proteins enriched in $^{cb+}$mEVs that facilitate collagen binding, we performed proteomic profiling of mEVs and $^{cb-}$mEVs. Most importantly, to reveal the functional mEV subpopulation regarding bone regenerative capacity, we implanted the hydrogel constructs encapsulating different mEVs subsets into a femoral condyle defect in osteoporotic rats to evaluate bone defect healing.
5. **Chapter 6**-Can we develop an *ex vivo* vital human bone model to study bone regeneration? To investigate this, we collected femoral heads from

total hip replacement surgery and prepared bone discs for *ex vivo* culture. To demonstrate cellular diversity related to bone biology in this model, we identified BMSCs from bone discs by flow cytometry, and lipopolysaccharide was utilized to observe immune reactions in the bone discs by luminex assay. H&E staining was conducted to investigate the presence of micro vessels and multinucleated cells. Thereafter, we assessed the effect of mEV injection into defects created in the bone discs for stimulating osteogenic responses by performing fluorochrome labeling and RT-qPCR analysis.

References

1. Brotto, M. and M.L. Johnson, Endocrine crosstalk between muscle and bone. Curr Osteoporos Rep, 2014. **12**(2): p. 135-41.
2. Horner, J.H., Bone structure and calcium metabolism. Surgery (Oxford), 2004. **22**(1): p. 24a-24d.
3. Li, G. and W. Niu, Chapter 1 - Challenges toward musculoskeletal injuries and diseases, in Nanoengineering in Musculoskeletal Regeneration, M. Razavi, Editor. 2020, Academic Press. p. 1-41.
4. Brunetti, G., et al., Anatomy and Physiology of Skeletal Tissue: The Bone Cells, in Multidisciplinary Approach to Osteoporosis: From Assessment to Treatment, A. Lenzi and S. Migliaccio, Editors. 2018, Springer International Publishing: Cham. p. 1-23.
5. Klein-Nulend, J., P.J. Nijweide, and E.H. Burger, Osteocyte and bone structure. Curr Osteoporos Rep, 2003. **1**(1): p. 5-10.
6. Huang, K. and H. Cai, The interplay between osteoarthritis and osteoporosis: Mechanisms, implications, and treatment considerations - A narrative review. Exp Gerontol, 2024. **197**: p. 112614.
7. Woolf, A.D. and B. Pfleger, Burden of major musculoskeletal conditions. Bull World Health Organ, 2003. **81**(9): p. 646-56.
8. Kareem, R., et al., The Impact of Rheumatoid Arthritis on Bone Loss: Links to Osteoporosis and Osteopenia. Cureus, 2021. **13**(8): p. e17519.
9. Miyamoto, T., [Analysis of Musculoskeletal Systems and Their Diseases. Pathology and therapy for skeletal disorder]. Clin Calcium, 2015. **25**(8): p. 1182-7.
10. von Rüden, C. and P. Augat, Failure of fracture fixation in osteoporotic bone. Injury, 2016. **47 Suppl 2**: p. S3-s10.
11. Li, Y., et al., Bone defect animal models for testing efficacy of bone substitute biomaterials. J Orthop Translat, 2015. **3**(3): p. 95-104.
12. Hadji, P., et al., The epidemiology of osteoporosis--Bone Evaluation Study (BEST): an analysis of routine health insurance data. Dtsch Arztebl Int, 2013. **110**(4): p. 52-7.
13. Global, regional, and national burden of bone fractures in 204 countries and territories, 1990-2019: a systematic analysis from the Global Burden of Disease Study 2019. Lancet Healthy Longev, 2021. **2**(9): p. e580-e592.
14. Mora, R., et al., Economic Burden and Practical Considerations, in Hexapod External Fixator Systems: Principles and Current Practice in Orthopaedic Surgery, M. Massobrio and R. Mora, Editors. 2021, Springer International Publishing: Cham. p. 285-289.
15. Perez, J.R., et al., Tissue Engineering and Cell-Based Therapies for Fractures and Bone Defects. Front Bioeng Biotechnol, 2018. **6**: p. 105.
16. Sims, N.A. and T.J. Martin, Osteoclasts Provide Coupling Signals to Osteoblast Lineage Cells Through Multiple Mechanisms. Annu Rev Physiol, 2020. **82**: p. 507-529.
17. Hong, H. and X.Y. Tian, The Role of Macrophages in Vascular Repair and Regeneration after Ischemic Injury. Int J Mol Sci, 2020. **21**(17).
18. Majidinia, M., A. Sadeghpour, and B. Yousefi, The roles of signaling pathways in bone repair and regeneration. J Cell Physiol, 2018. **233**(4): p. 2937-2948.
19. Murayama, M., et al., The interactions of macrophages, lymphocytes, and mesenchymal stem cells during bone regeneration. Bone Joint Res, 2024. **13**(9): p. 462-473.

20. Koob, S., et al., Bone formation and neovascularization mediated by mesenchymal stem cells and endothelial cells in critical-sized calvarial defects. Tissue Eng Part A, 2011. **17**(3-4): p. 311-21.
21. Wu, J., et al., Transcriptomic and cellular decoding of scaffolds-induced suture mesenchyme regeneration. Int J Oral Sci, 2024. **16**(1): p. 33.
22. Zhang, H., et al., Expert consensus on the bone repair strategy for osteoporotic fractures in China. Front Endocrinol (Lausanne), 2022. **13**: p. 989648.
23. Jimi, E., et al., The current and future therapies of bone regeneration to repair bone defects. Int J Dent, 2012. **2012**: p. 148261.
24. Ferraz, M.P., Bone Grafts in Dental Medicine: An Overview of Autografts, Allografts and Synthetic Materials. Materials (Basel), 2023. **16**(11).
25. Amini, Z. and R. Lari, A systematic review of decellularized allograft and xenograft-derived scaffolds in bone tissue regeneration. Tissue Cell, 2021. **69**: p. 101494.
26. Vidal, L., et al., Reconstruction of Large Skeletal Defects: Current Clinical Therapeutic Strategies and Future Directions Using 3D Printing. Front Bioeng Biotechnol, 2020. **8**: p. 61.
27. Min, K.H., et al., Biomimetic Scaffolds of Calcium-Based Materials for Bone Regeneration. Biomimetics (Basel), 2024. **9**(9).
28. Hou, X., et al., Calcium Phosphate-Based Biomaterials for Bone Repair. J Funct Biomater, 2022. **13**(4).
29. Alarçin, E., et al., Hydrogel Biomaterial in Bone Tissue Engineering, in Biomaterial-based Hydrogels: Therapeutics Carrier and Tissue Regeneration, S. Jana, Editor. 2024, Springer Nature Singapore: Singapore. p. 387-427.
30. Makhdom, A.M. and R.C. Hamdy, The role of growth factors on acceleration of bone regeneration during distraction osteogenesis. Tissue Eng Part B Rev, 2013. **19**(5): p. 442-53.
31. Qasim, M., D.S. Chae, and N.Y. Lee, Bioengineering strategies for bone and cartilage tissue regeneration using growth factors and stem cells. J Biomed Mater Res A, 2020. **108**(3): p. 394-411.
32. Takematsu, E., et al., Optimizing Delivery of Therapeutic Growth Factors for Bone and Cartilage Regeneration. Gels, 2023. **9**(5).
33. Tateiwa, D. and T. Kaito, Advances in bone regeneration with growth factors for spinal fusion: A literature review. N Am Spine Soc J, 2023. **13**: p. 100193.
34. James, A.W., et al., A Review of the Clinical Side Effects of Bone Morphogenetic Protein-2. Tissue Eng Part B Rev, 2016. **22**(4): p. 284-97.
35. Julier, Z., et al., Enhancing the regenerative effectiveness of growth factors by local inhibition of interleukin-1 receptor signaling. Sci Adv, 2020. **6**(24): p. eaba7602.
36. Rodham, P., et al., Cellular therapies for bone repair: current insights. J Orthop Traumatol, 2024. **25**(1): p. 28.
37. Kato, H., et al., Bone regeneration of induced pluripotent stem cells derived from peripheral blood cells in collagen sponge scaffolds. J Appl Oral Sci, 2022. **30**: p. e20210491.
38. Kirankumar, S., et al., Modern approaches on stem cells and scaffolding technology for osteogenic differentiation and regeneration. Exp Biol Med (Maywood), 2022. **247**(5): p. 433-445.
39. Liu, S., et al., An Osteoimmunomodulatory Biopatch Potentiates Stem Cell Therapies for Bone Regeneration by Simultaneously Regulating IL-17/Ferroptosis Signaling Pathways. Adv Sci (Weinh), 2024. **11**(35): p. e2401882.
40. Pérez-Leal, M., et al., Efficacy of stem cells in bone rehabilitation in patients with alveolar bone atrophy: a systematic review. Med Oral Patol Oral Cir Bucal, 2023. **28**(3): p. e247-e254.

41. Varshney, S., A. Dwivedi, and V. Pandey, Efficacy of autologous stem cells for bone regeneration during endosseous dental implants insertion - A systematic review of human studies. J Oral Biol Craniofac Res, 2020. **10**(4): p. 347-355.
42. Kumar, M.A., et al., Extracellular vesicles as tools and targets in therapy for diseases. Signal Transduct Target Ther, 2024. **9**(1): p. 27.
43. Anderson, H.C., Electron microscopic studies of induced cartilage development and calcification. J Cell Biol, 1967. **35**(1): p. 81-101.
44. Pan, B.T. and R.M. Johnstone, Fate of the transferrin receptor during maturation of sheep reticulocytes in vitro: selective externalization of the receptor. Cell, 1983. **33**(3): p. 967-78.
45. Jadamba, B., Y. Jin, and H. Lee, Harmonising cellular conversations: decoding the vital roles of extracellular vesicles in respiratory system intercellular communications. Eur Respir Rev, 2024. **33**(174).
46. H, U.S., D. Brotherton, and J. Inal, Communication is key: extracellular vesicles as mediators of infection and defence during host-microbe interactions in animals and plants. FEMS Microbiol Rev, 2022. **46**(1).
47. Aloi, N., et al., Extracellular Vesicles and Immunity: At the Crossroads of Cell Communication. Int J Mol Sci, 2024. **25**(2).
48. Möbs, C. and A.L. Jung, Extracellular vesicles: Messengers of allergic immune responses and novel therapeutic strategy. Eur J Immunol, 2024. **54**(5): p. e2350392.
49. Ma, Y., et al., Extracellular vesicles in cancers: mechanisms, biomarkers, and therapeutic strategies. MedComm (2020), 2024. **5**(12): p. e70009.
50. Kaur, S., et al., Future Perspectives of Bone Tissue Engineering with Special Emphasis on Extracellular Vesicles, in Tissue Engineering in Oral and Maxillofacial Surgery, R. Seppänen-Kaijansinkko, Editor. 2019, Springer International Publishing: Cham. p. 159-169.
51. Lamichhane, T.N., et al., Emerging roles for extracellular vesicles in tissue engineering and regenerative medicine. Tissue Eng Part B Rev, 2015. **21**(1): p. 45-54.
52. Qin, Y., et al., Bone marrow stromal/stem cell-derived extracellular vesicles regulate osteoblast activity and differentiation in vitro and promote bone regeneration in vivo. Sci Rep, 2016. **6**: p. 21961.
53. Moshaverinia, A., et al., Bone regeneration potential of stem cells derived from periodontal ligament or gingival tissue sources encapsulated in RGD-modified alginate scaffold. Tissue Eng Part A, 2014. **20**(3-4): p. 611-21.
54. Akdeniz-Dogan, Z., et al., The Role of Extracellular Vesicles Secreted From Thermal Stress-Induced Adipose-Derived Stem Cells on Bone Regeneration. J Craniofac Surg, 2021. **32**(6): p. 2245-2250.
55. Eitan, E., et al., Extracellular vesicle-depleted fetal bovine and human sera have reduced capacity to support cell growth. J Extracell Vesicles, 2015. **4**: p. 26373.
56. Wu, J., et al., Platelet-rich plasma-derived extracellular vesicles: A superior alternative in regenerative medicine? Cell Prolif, 2021. **54**(12): p. e13123.
57. Ascanius, S.R., et al., Milk-Derived Extracellular Vesicles Suppress Inflammatory Cytokine Expression and Nuclear Factor-κB Activation in Lipopolysaccharide-Stimulated Macrophages. 2021. **2**(2): p. 165-178.
58. Chutipongtanate, S., et al., Prenatal SARS-CoV-2 Infection Alters Human Milk-Derived Extracellular Vesicles. Cells, 2025. **14**(4).
59. Jiao, Y., et al., Advances in the Study of Extracellular Vesicles for Bone Regeneration. Int J Mol Sci, 2024. **25**(6).

60. Miracle, D.J., et al., Contemporary ethical issues in human milk-banking in the United States. Pediatrics, 2011. **128**(6): p. 1186-91.
61. Chutipongtanate, S., A.L. Morrow, and D.S. Newburg, Human Milk Extracellular Vesicles: A Biological System with Clinical Implications. Cells, 2022. **11**(15).
62. Sanwlani, R., et al., Milk-Derived Extracellular Vesicles in Inter-Organism, Cross-Species Communication and Drug Delivery. Proteomes, 2020. **8**(2).
63. Barathan, M., et al., Milk-Derived Extracellular Vesicles: A Novel Perspective on Comparative Therapeutics and Targeted Nanocarrier Application. Vaccines (Basel), 2024. **12**(11).
64. Marsh, S.R., et al., Novel Protocols for Scalable Production of High Quality Purified Small Extracellular Vesicles from Bovine Milk. Nanotheranostics, 2021. **5**(4): p. 488-498.
65. Oliveira, M.C., et al., Milk extracellular vesicles accelerate osteoblastogenesis but impair bone matrix formation. J Nutr Biochem, 2016. **30**: p. 74-84.
66. Oliveira, M.C., et al., Milk-Derived Nanoparticle Fraction Promotes the Formation of Small Osteoclasts But Reduces Bone Resorption. J Cell Physiol, 2017. **232**(1): p. 225-33.
67. Oliveira, M.C., et al., Bovine Milk Extracellular Vesicles Are Osteoprotective by Increasing Osteocyte Numbers and Targeting RANKL/OPG System in Experimental Models of Bone Loss. Front Bioeng Biotechnol, 2020. **8**: p. 891.
68. Shen, L., G. Hu, and C.M. Karner, Bioenergetic Metabolism In Osteoblast Differentiation. Curr Osteoporos Rep, 2022. **20**(1): p. 53-64.
69. Wang, L., et al., Bovine milk exosomes attenuate the alteration of purine metabolism and energy status in IEC-6 cells induced by hydrogen peroxide. Food Chem, 2021. **350**: p. 129142.
70. Belov, L., et al., Extensive surface protein profiles of extracellular vesicles from cancer cells may provide diagnostic signatures from blood samples. J Extracell Vesicles, 2016. **5**: p. 25355.
71. Theocharis, A.D., et al., Extracellular matrix structure. Adv Drug Deliv Rev, 2016. **97**: p. 4-27.
72. Bailey, S., et al., Structural role of osteocalcin and its modification in bone fracture. Appl Phys Rev, 2023. **10**(1): p. 011410.
73. Sariano, P.A., et al., Convection and extracellular matrix binding control interstitial transport of extracellular vesicles. J Extracell Vesicles, 2023. **12**(4): p. e12323.
74. Bailey, S., et al., The role of extracellular matrix phosphorylation on energy dissipation in bone. Elife, 2020. **9**.
75. Xia, W., et al., Damaged brain accelerates bone healing by releasing small extracellular vesicles that target osteoprogenitors. Nat Commun, 2021. **12**(1): p. 6043.
76. Furuta, T., et al., Mesenchymal Stem Cell-Derived Exosomes Promote Fracture Healing in a Mouse Model. Stem Cells Transl Med, 2016. **5**(12): p. 1620-1630.
77. De Jong, O.G., et al., Extracellular vesicles: potential roles in regenerative medicine. Front Immunol, 2014. **5**: p. 608.
78. Wang, P., et al., ECM-binding properties of extracellular vesicles: advanced delivery strategies for therapeutic applications in bone and joint diseases. Cell Commun Signal, 2025. **23**(1): p. 161.

Chapter 2

Polyethylene Glycol Precipitation is an Efficient Method to Obtain Extracellular Vesicle-Depleted Fetal Bovine Serum

Peng Wang, Onno J. Arntz, Johanna F.A. Husch, Van der Kraan PM,
Jeroen J.J.P. van den Beucken, Fons A.J. van de Loo.

PLoS One. 2023 Dec 5;18(12):e0295076.

ABSTRACT

Mesenchymal stromal/stem cell derived-extracellular vesicles (MSC-EVs) have gained interest as drug delivery nanoparticles, having immunoregulatory and potentiating tissue repair property. To maintain growth of MSCs the culture media should contain fetal bovine serum (FBS) free of EVs, as the presence of FBS-EVs confounds the true capabilities of MSC-EVs. Currently, 18h ultracentrifugation (UC) and ultrafiltration (UF) as well as using commercial EV depleted FBS strategy are common FBS-EV depletion methods in MSC-EV research, but all vary in terms of depletion efficiency. Therefore, we tested three methods: UC, UF, and polyethylene glycol (PEG) precipitation to obtain three EV depleted FBS (EVdFBS) batches and compared them to FBS and commercial (Com) EVdFBS on human adipose stem cell (hADSC) growth, differentiation, enrichment of EVs in hADSC supernatant and their biological function on collagen metabolism. FBS EV depletion was comparable between PEG (95.6%) and UF (96.6%) but less by UC (82%), as compared to FBS. FBS protein loss was markedly different among PEG (47%), UF (87%), and UC (51%), implying the ratio of EV depletion over protein loss was PEG (2.03), UF (1.11), and UC (1.61). Typically, a significant decrease of TGFβ/Smad signaling, involving in MSC growth and physiology, was observed by UF. After 96 hours of exposure to 5% FBS or 5% EVdFBS cell growth media, the osteogenesis ability of hADSCs was not impaired but slightly lower mRNA expression level of Col2a observed in EVdFBS media during chondrogenesis. In consistent with poor confluency of hADSCs observed by optical microscope, cell proliferation in response to 5% UF EVdFBS media was affected significantly. Importantly, more and purer ADSCs EVs were obtained from ADSCs cultured in 5% PEG EVdFBS media, and they retained bioactive as they upregulated the expression of Col1a1, TIMP1 of human knee synovial fibroblast. Taken together, this study showed that PEG precipitation is the efficient method to obtain EV depleted FBS for MSC EVs enrichment with minimal FBS EV contamination.

INTRODUCTION

Increasing attention has been paid on MSC-based therapy due to its anti-inflammatory, oxidative stress, apoptotic, and angiogenic effects [1, 2]. Specifically, the immunoregulatory and regenerative properties of MSC-sourced secretome have been persistently reported [3, 4]. Compared to parent cells which might cause immune responses and tumor formation [5, 6], extracellular vesicles (EVs) derived from MSC, one of secretome factors, are more effective and stable. Through transferring various contents such as nucleic acids, proteins, and lipids into recipient cells, MSC-EVs regulate phenotype, function, survival of resident cells and homing of immune cells, and participate in tissue maintenance and repair such as cartilage restoration and wound healing [7-9]. However, the main concern of enrichment of MSC-EVs from cell culture media is the contamination with exogenous EVs derived from fetal bovine serum (FBS). The presence of FBS-EVs may confound the therapeutic or diagnosis analyses of EVs derived from cultured cells [10, 11].

Based on an international survey conducted by International Society for Extracellular Vesicles (ISEV) in 83% of *invitro* and preclinical EV studies, cell culture media was used to enrich various cell-EVs [12]. Furthermore, FBS is used as a common and important additive in MSCs culture, because it contributes to stable cell adhesion and alleviates cellular stresses associated with in vitro environment through providing various serum factors and other constitutes [13, 14]. Therefore, to date an increasing number of studies use EV depleted FBS (EVdFBS) to support growth of MSC and obtain pure MSCs-EVs [7, 15, 16].

The common FBS-EVs depletion method used to obtain EVdFBS is performing ultracentrifugation (UC) at 120,000g for 18h in diluted FBS and considered to be the gold standard [17]. Shelke and colleagues conducted a study on EV depletion protocol using different centrifugation times for FBS: one short (1.5 h) and one long (18 h) and collected two UC EV-depleted FBS. They isolated EVs from the media containing UC EV depleted FBS and observed 1.5 h of ultracentrifugation reduced FBS-derived EV RNA content by approximately 50%, while 18 h of centrifugation reduced it by 95%. However, distinguishing FBS-derived EVs from those released by cells remained challenging due to their similar characteristics, such as round morphology and RNA profile. The researchers demonstrated 18 h of ultracentrifugation was the optimal time, even though it did not completely eliminate EV contaminants from FBS [18]. This observation was later confirmed in a comparison of EV depleted FBS through 18 hours UC EV depleted FBS with commercially available EV depleted FBS [19]. Interestingly, both EV depleted

FBS still contained a significant number of nano-sized particles, as evidenced by nanoparticle tracking analysis (NTA). Electron microscopy images of media supplemented with UC EV depleted FBS revealed nanoparticles without the typical cup-shaped morphology of EVs, suggesting they could be lipoprotein particles. The efficiency of EV depletion was approximately 70% for UC EV depleted FBS and 75% for commercially available EV-depleted FBS. Pham *et al* later challenged the UC protocol and investigated the particles remaining in FBS after EV depletion through UC, showing that certain nanoparticles were not depleted after 18 h of ultracentrifugation [20]. For UF FBS EV depletion, *Kornilov et al* utilized ultra-15 centrifugal filters in 2018. They subjected FBS to 55 minutes of centrifugation at 3000 × g to obtain UF EV depleted FBS, which was compared with EV depleted FBS obtained through UC and commercially EV-depleted FBS. Transmission electron microscopy revealed that UF EV depleted FBS had no detectable EVs, distinguishing it from commercially EV-depleted FBS and UC EV depleted FBS. To assess whether the UF protocol impacted FBS ability to support cell growth or modify cell phenotype, they supplemented the media with different EV depleted FBS and unprocessed FBS. They analyzed the proliferation of three cancer cell lines (HSC3, PC-3, and HOS143b) and found that media supplemented with all types of tested FBS exhibited similar capabilities to support cell growth [21]. Another emerging option involves commercially available EV-depleted FBS. However, the specific protocols for depleting FBS from EVs lack detailed descriptions. Given that certain studies have revealed contaminants in commercial EV-free FBS, caution should be exercised when using such material for in vitro EV studies. In our view, the depletion of FBS-EVs from FBS is a one-step procedure, different with routine isolation of EVs from original materials. For EV isolation, the sucrose gradient UC can remove lipoprotein particles that are similar in size of EVs but different in density, and the size exclusion chromatography (SEC isolation) separates EVs from soluble proteins, and the original materials could be discarded. However, considering retrieve of the EVdFBS, it is limited to apply these methods in FBS-EVs depletion [22]. Not only are current techniques time-consuming and relatively expensive, but also the selectivity of FBS-EV depletion remains unclear. During the FBS-EVs depletion process, the serum factors (proteins, lipids, and lipoproteins) tend to become aggregated and removed from FBS, leaving a less potent and incomplete cell culture media supplement. Therefore, studying the best method for high selective FBS-EVs depletion is necessary. In this study, we tested three techniques: UC, UF, and polyethylene glycol (PEG) precipitation to obtain three different EVdFBS batches and compared them to FBS and commercial (Com) EVdFBS on human adipose stem cell (hADSC) growth, differentiation, enrichment of EVs in hADSC supernatant and their biological function on collagen metabolism.

MATERIALS AND METHODS

Preparation of different EV depleted FBS (Fig 1A)

Ultracentrifugation method. Culture media or PBS was used to dilute FBS before performing UC using an AH629 rotor (k-factor 284.7, Beckmann-Coulter) at 120,000g for 18h. UC EVdFBS was obtained from the supernatant (approximately 90%), and the precipitate on the bottom was denoted as UC isolated FBS EVs.

Ultrafiltration method. Similarly, after 55 min centrifugation at 3000g, FBS in the Amicon ultra-15 centrifugal filters (ref: UFC910024, 100kDa Merk Millipore Ltd.) had been separated in two parts: the permeate on the external tube ascribed as UF EVdFBS and UF isolated FBS EVs in the retentate room.

PEG precipitation method. To obtain PEG EVdFBS, FBS were supplemented with 50% w/v stock solution of PEG 6000 (Sigma-Aldrich, Taufkirchen, Germany) to the various final concentrations of PEG. The PEG EVdFBS could be collected from the supernatant of mixture after incubation overnight at 4°C and 30 min centrifugation at 1500g. Also, the pellet was regarded as PEG isolated FBS EVs on the bottom.

Nanoparticle tracking analysis (NTA)

Particle size distribution was estimated by the Brownian motion of the particles in a NanoSight 300 using Nanoparticle Tracking Analysis 2.3 software (Nanosight Ltd, Amesbury, UK). Particles were diluted in PBS, till a suitable concentration for analysis was reached, and the concentration value between 20 to 80 particles/frame was deemed as effective measurement. Major particle concentration was evaluated for the particles between 30–300nm in diameter. 30s video was recorded using camera level 10 and detection threshold 5.

Protein content

Total protein content of FBS and four different EVdFBS batches as well as three isolated FBS EVs was evaluated by the bicinchoninic acid micro-BCA protein assay kit (Pierce, Rockford, IL, USA). Using the 96-well plates, protein analysis was carried out according to the manufacturer's instructions, and the 2mg/ml BSA was the standard protein sample.

XTT assay

To examine the quantification of human adipose tissues (hADSCs) proliferation cultured in FBS and four different EVdFBS batches, the Cell Proliferation Kit II (XTT) was used (Dojindo, US). The XTT reagent, which is a tetrazolium-based compound,

is sensitive to cellular redox potential and cellular respiration converts this substrate into an orange-colored formazan product. The assay was done according to the manufacturer's instructions in 48 hours, 5 days to hADSCs, and measured at wavelength 450 nm using a microplate reader. The blank well on the same row and the wavelength >650 nm were taken as the references.

Western blot

To detect the EV-specific markers Alix, CD81 and HSP-70 as well as the lipoprotein marker ApoE in the three isolated FBS EVs sample, equal amounts of protein were loaded onto 12% SDS-PAGE, together with protein ladder, and subsequently transferred onto a 0.45 μm nitrocellulose membrane for 120 min at 350mA. The membrane was blocked with 5% skim milk for 1 h at room temperature. After washing 3 times with Tris-buffered saline containing 0.1% Tween 20 (TBST), the membranes were incubated, respectively, with 1:500 anti-Alix (Santa Cruz Biotechnology, Inc., Dallas, TX, USA; Cat # sc-53540, 1:2000 anti-CD81 (Santa Cruz Biotechnology, Inc., Dallas, TX, USA; Cat # sc-166029), 1:2000 anti-HSP70 antibody (Santa Cruz Biotechnology, Inc., Dallas, TX, USA; Cat # sc-32239) and 1:1000 anti-ApoE (Sanbio, Rosemont, USA; Cat # 18254-1-AP) at 4°C overnight. After washing in TBST for 3 times (5 min for each time), the membrane was incubated with horseradish peroxidase-linked secondary antibodies (anti-mouse or rabbit) for 2 h at room temperature. After washing five times with TBST, proteins were detected with ECL western blotting detection reagent (GE Healthcare, UK; Cat # lot 16961643) according to the manufacturer's instructions.

CAGA12-Luciferase reporter assay [23]

To examine serum growth factor TGFb in FBS and four different EVdFBS batches, mouse embryonic fibroblasts (3T3 fibroblasts) were seeded at 30.000 cells per 96-well plate and transduced with SMAD-sensitive CAGA-Luc reporter adenovirus the next day for 2.5 hours in serum-free DMEM condition. Then after a 20-hour recovery period using DMEM containing FBS, Cells were serum deprived for 8 hours and then were stimulated with DMEM alone (control) or with recombinant human TGF- β1 or FBS and four different EVdFBS batches, respectively. Using 50 μl reporter assay lysis buffer, cells were lysed 16 hours after stimulation (Promega). Thereafter, an equal amount of BrightGlow was added and luciferase was measured immediately with a microplate reader (Clariostar). Constitutively GFP expression by the CAGA-luc reporter was used to determine transduction efficiency and to control/compensate for TGFβ-unrelated biological and technological variations.

Osteogenic and chondrogenic differentiation

Human subcutaneous adipose tissue from two healthy male donors, with an age range of 33–47 years, was obtained from the Department of Plastic Surgery (Radboudumc) after ethical approval (Commissie Mensgebonden Onderzoek; dossier number #3252) and informed consent. The tissue was excised into pieces and then minced in a 0.1% collagenase type II (Mannheim, Germany) solution with 1% bovine serum albumin (BSA, Sigma, St. Louis, USA) for 1 h at 37 °C under shaking conditions, as described previously [24]. Initially, cells were treated with FBS or four different EVdFBS (5%) media for 96 hours. After that, cells were washed carefully with PBS, and osteogenic differentiation was induced using with regular osteogenic induction media (FBS media supplemented with 20mM β-glycerophosphate, 100nM dexamethasone, and 50μM ascorbic acid phosphate) for 21 days. Cells were washed with PBS twice and fixed with 70% ethanol for 10 min and stained with 0.5% alizarin red S (pH 4.1) for 20 min and then washed three times with deionized water.

As for chondrogenic differentiation, a micromass culture system was employed [25]. Cells were seeded at a concentration of 10^7 cells/ml in the 24-well plate. The first 2 hours, the plates were incubated at 37 °C with 5% CO_2 without extra culture media. Then cells were washed with PBS and treated with FBS or four different EVdFBS (5%) media. After 96 hours, chondrogenic induction medium (CIM, high glucose media supplemented with 10 ng/ml transforming growth factor-1, 1μM dexamethasone, 0.2 mM ascorbate-2-phosphate, 1mM sodium pyruvate and 1:100 diluted ITS + Premix) were replaced every other day to induce chondrogenic differentiation. After 14 days of induction, cells were lysed for total RNA extraction.

EV treatment

To investigate the role of ADSC-EVs on collagen metabolism, human knee synovial fibroblasts were treated with $2*10^8$ particles/ml EVs enriched from ADSCs FBS media, ADSCs-PEGEVdFBS media, ADSCs-serum free media or FBS-EVs. The cells were seeded at 10^5 cells in 24-wells plates and incubated for 12h in serum-free RPMI medium with EVs enriched from hADSCs-PEG EVdFBS media. EVs enriched from hADSCs-FBS growth media and hADSCs-serum free media as well as vehicle (PBS) were deemed as the references. The cells were collected for subsequent total RNA extraction.

RNA extraction and real-time PCR

RNA extraction from cells was performed using TRI reagent according to the manufacturer's procedure. The cells were mixed with 0.5 mL TRI reagent and 100μl chloroform, vortexed for 15 seconds, then incubated at room temperature for

2 minutes. The supernatant was transferred to a new tube and 250µl isopropanol was added after centrifugation at 12,000g for 15 minutes at 4°C. The mixture was centrifuged at 12,000g for 30 minutes at 4°C to remove the supernatant after an overnight incubation, and the RNA pellet was washed twice with 75% ethanol. After centrifugation at 12,000g for 5 minutes at 4°C, the ethanol was aspirated and the RNA pellet was air dried for 10 minutes and resolved in 8 µl of RNase-free water.

Synthesis of cDNA was accomplished by reverse transcription PCR an oligo(dT) primer and Moloney murine leukemia virus Reverse Transcriptase. Quantitative real-time PCR was performed using SYBR Green real-time PCR master mix on a Step-One according to the manufacturer's instructions. Primer sets for individual genes were used (**supplementary table**).

Statistical analysis

The graphs (Figures 1B-1D, 2A-C, 2E-2F, 3B-D, 3F-H, and Figure 4) show the biological and/or technical replicates (n=3 or 4). Statistical analyses were performed using GraphPad Prism 9 (GraphPad Software Inc., CA) statistical software. For XTT assay, CAGA12-Luciferase reporter assay, Brown-Forsythe and Welch one way ANOVA with Dunnett T3 multiple comparisons tests was used for statistical analysis, and $p<0.05$ or less was deemed significant.

RESULTS

Comparison among EV depletion methods

Diluting FBS prior to performing UC is required to improve EV-depletion efficiency. The EV protein content (fg/particle), a purity index of the isolated FBS EV samples [26], was the lowest in UC isolated FBS EVs, isolated from 25% diluted FBS. This coincided with a marked reduction in particle numbers of UC EVdFBS batch. Moreover, comparable proliferations of hADSC were observed in FBS and UC EVdFBS, obtained through performing UC of 25% diluted FBS.

By performing UF of FBS, though more particles were removed from FBS compared to that by UC (**Fig 1C**), the purity of UF isolated FBS EVs was much worse as higher protein content was detected in UF isolated FBS EVs (**Fig 1B**). Meanwhile, the proliferation of hADSC was significantly decreased when using UF EVdFBS as culture media supplement.

Using different final concentration of PEG 6K for EVs isolation with a desirable effect on EVs precipitation, has been reported recently [27, 28]. To choose the optimal one for high selectivity of FBS-EVs depletion, a final incubation concentration in the range of 16%-10% PEG in FBS was investigated. We found an inverse relationship between the concentration of PEG and the particle number of batches and purity of isolated EVs. More importantly, though the amount of particle depletion was almost comparable between PEG precipitation and UF (**Fig 1C**), (concentration 10%) PEG EVdFBS could support hADSC growth (**Fig 1D**). Based on the results above, UC method using 25% diluted FBS and 10% PEG addition to FBS were selected for further analysis.

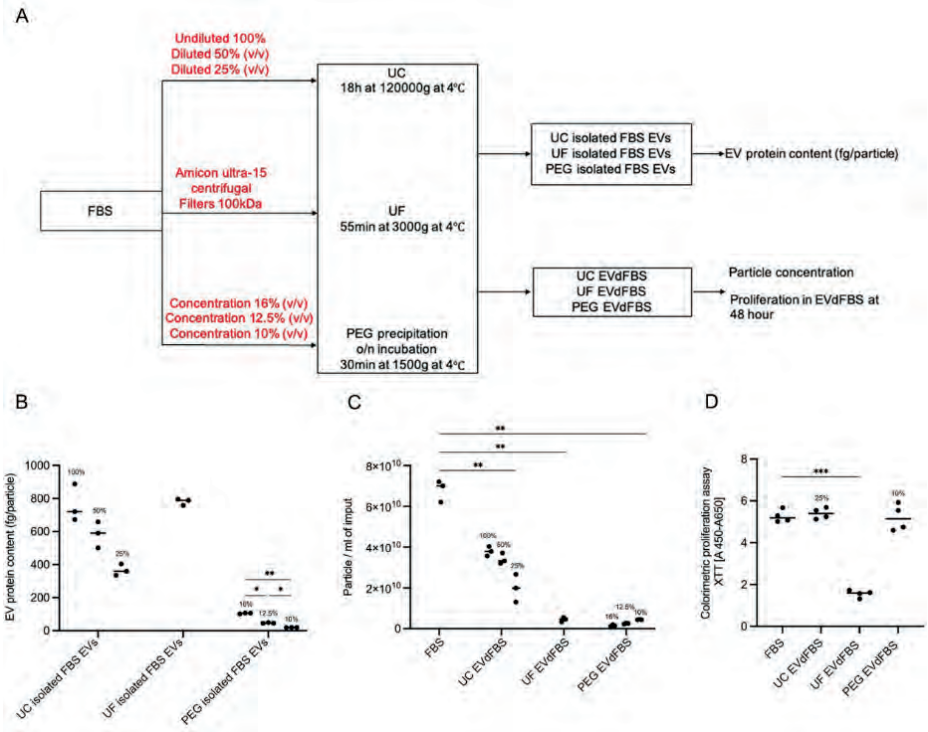

Fig. 1. Comparison among EV depletion methods. (A) The working procedure to obtain UC/UF/PEG EVdFBS. (B) The EV protein contents of UC/UF/PEG isolated FBS EVs were calculated based on protein level determined by microBCA and particle concentration measured by NTA (in triplo). (C) Particle concentration of corresponding UC/UF/PEG EVdFBS measured by NTA (in triplo). (D) hADSCs proliferation at 48-hour in 5% FBS or UC/UF/PEG EVdFBS determined by XTT assay (in quadruple). For panel C, the p was determined by student two tailed t test, values are mean. And for panels B and D were calculated by one way ANOVA tests. *** $p<0.01$.

PEG had the highest selectivity of FBS-EVs depletion

Compared to FBS, the amount of particle depletion was almost comparable between PEG (95.6%) and UF (96.6%) but less by UC (82%) (**Fig 2A**), but FBS protein loss was markedly different among PEG (47%), UF (87%), and UC (51%) (**Fig 2B**), therefore the ratio of EV depletion over protein loss was PEG (2.03), UC (1.61), and UF (1.11). A thorough EV depletion was observed by UF and PEG precipitation, simultaneously, much protein aggregation in the FBS was co-isolated with FBS-EVs by UF, leading the lowest total protein concentration in UF EVdFBS. Typically, compared by FBS group, a significantly decreased TGFβ/Smad signalling induced by UF EVdFBS was determined using CAGA12- luciferase reporter construct (**Fig 2C**). Interestingly, compared by UC, more particles were depleted but slightly less protein loss by PEG precipitation, implying the non-particle proteins including protein aggregates as well as lipoproteins are the main component in the FBS. Of note, the commercial EV depleted FBS (Com EVdFBS) exhibited comparable amount of particle concentration, protein content and TGFb bioactivity with UC EVdFBS and PEG EVdFBS. In addition, we characterized the isolated FBS EVs in more detail to determine the best depletion method. PEG isolated FBS EVs showed less serum colour, compared with other two (**Fig 2D**). A less size variation of nanoparticles (30-300nm) was seen in PEG isolated FBS EVs (**Fig 2E**), with lower EV protein content (**Fig 2F**). Moreover, only in the PEG isolated FBS EVs, Alix, CD81 and HSP-70 were clearly detectable. UC isolated FBS EVs had higher expression on ApoE, one marker of high-density lipoproteins (1.063-1.21 g/ml) that overlap in density with EVs (1.10-1.19 g/ml), compared with PEG did (**Fig 2G**), showing it is inevitable that lipid loss happened during UC and PEG precipitation. Notably, though the much protein aggregation loss happened by performing UF due to its low selectivity, the faint band of ApoE was observed in UF isolated FBS EVs, meaning some high-density lipoproteins (molecule weight below 100 kDa) could be retained in UF EVdFBS. Above all, the results implied PEG precipitation had the highest selectivity of FBS-EVs depletion among all techniques.

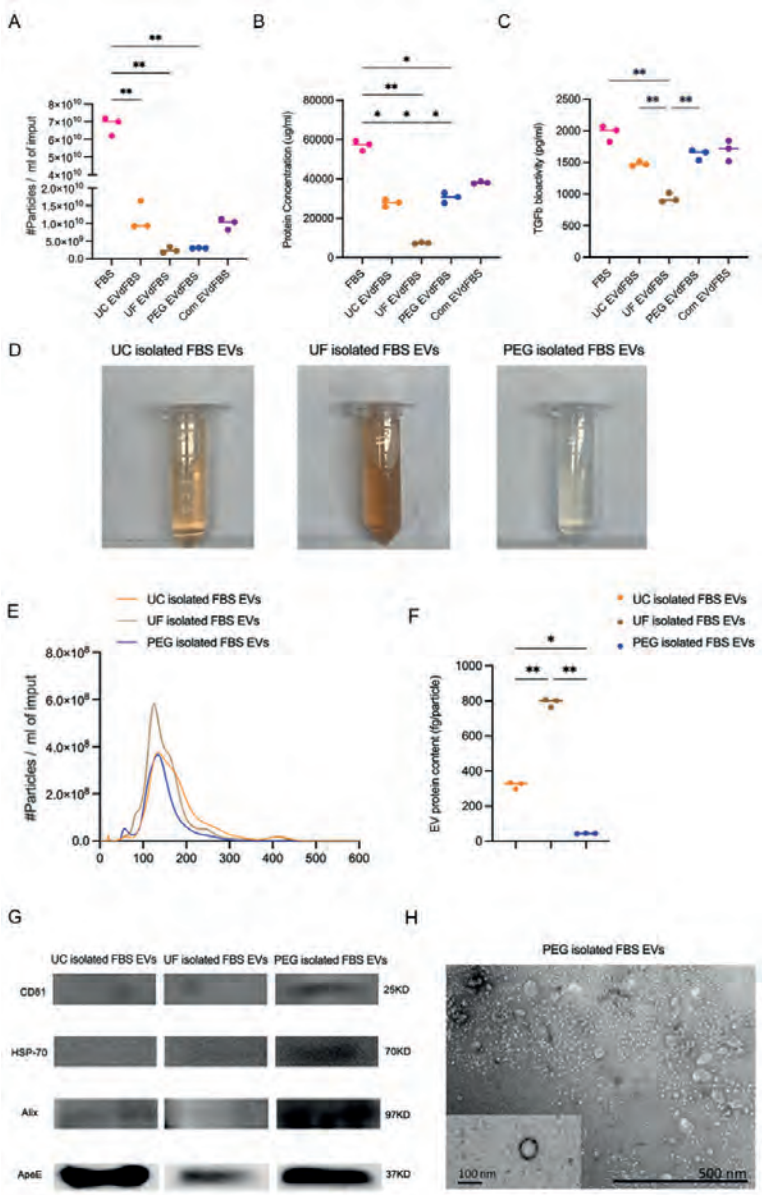

Fig. 2. Comparison among five FBS batches and three isolated FBS EVs samples. (A) Particle concentration was determined by the NTA (in triplo). (B) Protein concentration was measured using micro-BCA kit (in triplo). (C) TGF-β activity was determined using CAGA-LUC reporter assay (in triplo). (D) Colors of isolated FBS EVs by UC, UF, and PEG (n=3, in independent experiments). (E) Particle size distribution of UC, UF, and PEG isolated FBS EVs was determined using NTA (in triplo). (F) EV protein content was based on the ratio of the particle concentration over protein content, determined respectively by NTA and microBCA. (G) Detection of EV-markers Alix, CD81 and HSP70 as well as the lipoprotein maker ApoE by western blotting in UC, UF, or PEG isolated FBS EVs. Statistical differences were determined by one way ANOVA tests. Values are mean, *$p<0.05$, **$p<0.005$.

PEG EVdFBS media supported hADSC growth, differentiation and enrichment of purer hADSC-EVs

The microscopic morphology of hADSC cultured in FBS and the four EVdFBS (5%) media was observed after 72h incubation. The poor confluency of cells was observed in UF EVdFBS media (**Fig 3A**). Consistently, the colorimetric absorbance for proliferation as well as the mRNA level CCND1 and SIRT1 that genes important for cell growth were decreased UF EVdFBS media (**Fig 3B-D**). To evaluate whether the ADSCs retained their differentiation capacity, the alizarin Red S staining assay was done, and results exhibited the comparable calcium deposit in all cell layers after 96 hours expose in FBS and four EVdFBS media and subsequent regular osteogenic differentiation lasting for 21 days (**Fig 3E**). Interestingly, slightly lower mRNA expression levels of Col2a were observed in all EVdFBS media during chondrogenic differentiation (**Fig 3F**). As for enrichment of EVs, purer ADSC EVs could be obtained from hADSC-UF EVdFBS and hADSC-PEG EVdFBS media according to the higher ratio of EVs present in hADSC-EVdFBS media (EVs mixture) over the corresponding cell-free EVdFBS media (FBS-EVs) (**Fig 3G**). Furthermore, the area of size distribution exhibited more ADSC EVs were in the PEG EVdFBS media, compared to those in hADSC-UF EVdFBS media (**Fig 3H**).

EVs enriched from ADSCs-PEG EVdFBS media positively regulate collagen metabolism

To determine whether EVs enriched from ADSC-PEG EVdFBS media retained their tissue regenerative potential, 12-hour serum-free expose with EVs stimulation was conducted. Quantitative real-time RT-PCR showed that the mRNA levels of Col1a1 and TIMP1 of human knee synovial fibroblasts increased significantly with EVs stimulation, compared to those with vehicles (**Figure 4**).

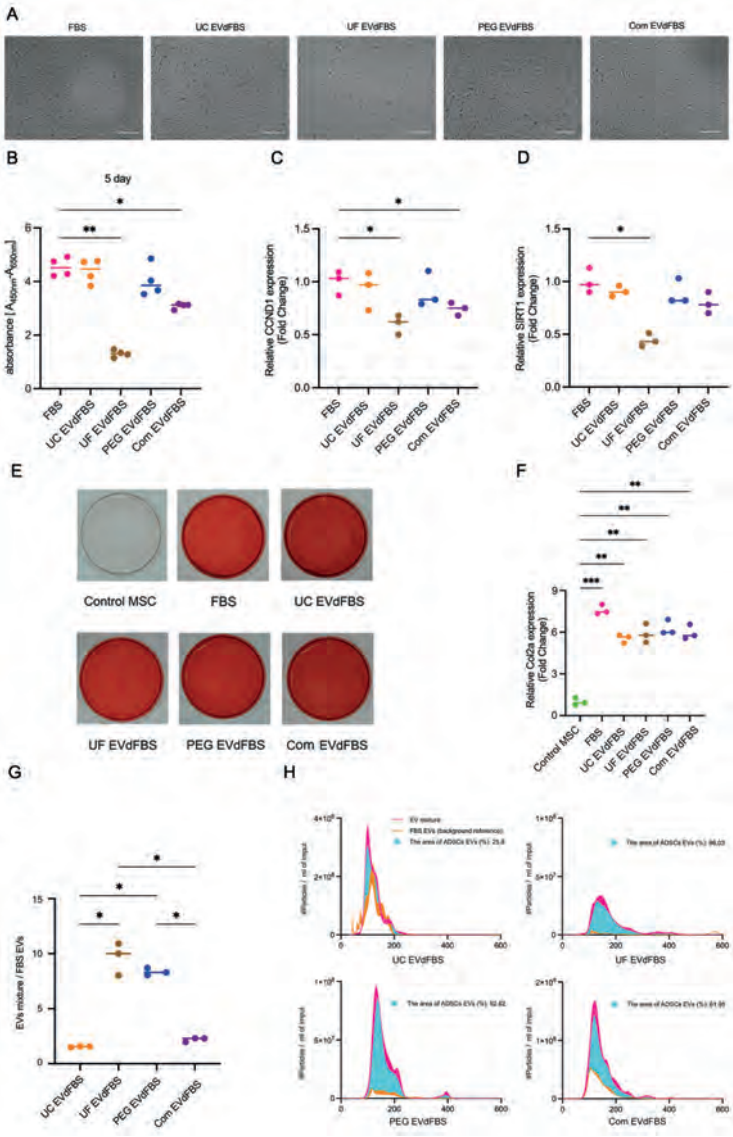

Fig. 3. Growth, differentiation and EV-release of human ADSCs cultured in five different FBS batches. (A) Microscopic morphology of human ADSCs cultured in 5% FBS or four different EVdFBS batches. (B) Proliferation of ADSCs cultured in 5% FBS and four EVdFBS batches for 5 days determined using XTT assay (in quadruple). (C-D) CCND1, SIRT1 mRNA level of human ADSCs exposed to 5% FBS or four different EVdFBS batches were determined (fold change) using RT-qPCR (in triplo). (E) Osteogenic differentiation observed by alizarin Red S staining after ADSCs cultured in 5% UT FBS or four different EVdFBS batches for 96 hours (in triplo). (F) Determined chondrogenic differentiation marker (Col2a) in MSC cultured in different FBS batches by RT-qPCR (in triplo). (G) The ratio of particle concentration of ADSC EVs to FBS-EVs (in triplo). (H) Particle size distribution was determined using NTA (in triplo). For panel B-D and F-G, statistical differences were determined by one way ANOVA tests. Values are mean, *$p<0.05$, **$p<0.005$, ***$p<0.001$.

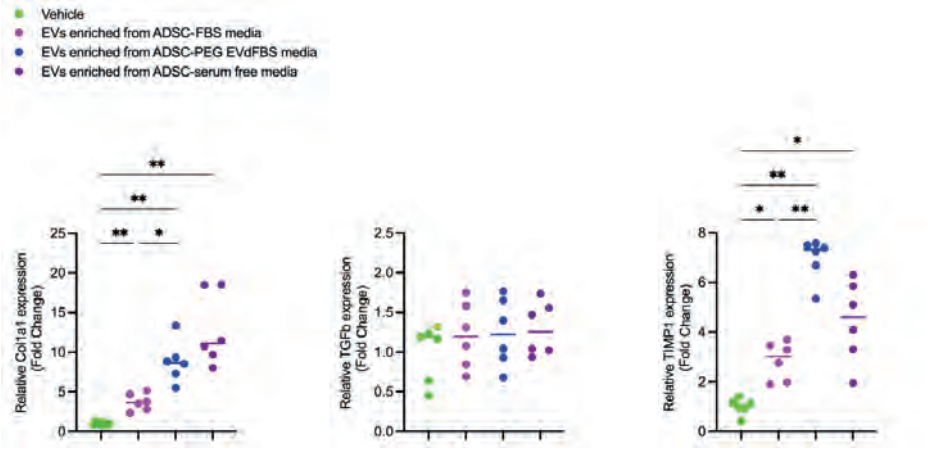

Fig. 4. Gene expression associated with collagen metabolism. Col1a1, TGFb, TIMP1 mRNA levels of human knee synovial fibroblast exposed to different sources of EVs were determined (fold change) using RT-qPCR (n=6). Statistical differences were determined by one way ANOVA tests. Values are mean, *$p<0.05$, **$p<0.005$.

DISCUSSION

Recent publications have investigated some FBS-EV depletion methods regarding cellular physiology state and function [10, 19]. Nevertheless, barely any specific attention has been paid on depletion efficiency of these methods through evaluation of isolated FBS-EVs sample and EVs enriched from cell EVdFBS media. In this study, we demonstrated PEG precipitation is the optimal method to deplete EVs in FBS. Due to its high selectivity of EVs depletion, PEG EVdFBS could be used as culture media supplement for MSC culture to obtain purer MSC-EVs.

FBS-EVs have been continuously reported to be bioactive as they can be internalized by the recipient cells and influence cellular physiology, such as cell migration [18, 29], inevitably disturbing the analysis of cargo content and the biological properties of EVs released by the cultured cells. Of note, co-isolated non-EV particles could be removed from EVs mixture through further wash by sucrose gradient ultracentrifugation and SEC isolation [30], but separating two kinds of EVs (FBS-EVs and cell-EVs) directly is impossible with the available isolation techniques [31]. Therefore, making FBS devoid of bovine EVs with minimal loss of serum protein is essential when using it as a culture medium supplement to maintain cell growth and performance and enrich pure cell-EVs.

The most commonly used method to obtain EV dFBS is UC, but our study showed that this is not only a time-consuming method but also insufficient to remove FBS-EV. By UF and PEG, comparable amount of particle depletion was achieved, but the higher EV protein content in UF isolated FBS-EVs sample and reduced ADSCs proliferation in UF EVdFBS media implied UF had low selectivity of FBS-EV depletion. Considering FBS contains proteins, growth factors, as well as lipids, vitamins, carbohydrates, all of which are essential for cell attachment and maintenance, we speculated much protein loss in UF EVdFBS was one of the potential cause UF EVdFBS influenced morphology and barely support growth of hADSC [32]. Moreover, it is essential and desirable to make an assessment on the isolated FBS-EVs sample through a series of EV characterization parameters [33]. The serum color caused by bilirubin, which is transported as an albumin complex in blood under normal condition [34], were deeper in the isolated FBS EVs obtained by UC and UF implied the presence of more non-EV particles like albumin aggregates. The EV specific markers Alix, CD81, HSP-70 were only clearly detectable in PEG isolated FBS-EVs, which meant purer FBS-EVs were isolated by PEG precipitation. Interestingly, though the much essence loss happened by UF due to its low selectivity, the faint band of ApoE was observed in UF isolated FBS EVs, meaning some high-density lipoproteins (molecule weight below 100 kDa) without aggregation could be retained in UF EVdFBS. Of note, it was tricky to explain that compared to the positive results observed by Kornilov and colleagues, UF protocol might not a suitable method on FBS EV depletion in our study. we meticulously replicated the UF procedure outlined in Kornilov and colleagues' work, employing the identical UF product (UFC910024, 100K Merk Millipore Ltd). As anticipated, our findings aligned with the earlier study, demonstrating a similar degree of EV depletion (approximately 96% in Kornilov's findings). However, despite observing diminished cellular dimensions of human adipose stem cells cultivated in UF EV depleted FBS media group over 96 hours, as evidenced by microscopic analysis, the metabolic activity per cell exhibited no statistically significant divergence from the FBS control group in their study. In our view, the divergent experimental outcomes were attributed to the variation in FBS concentration (5% versus 10%).

Although hADSC still possessed differentiation ability after 96 hours exposure in four EVdFBS media, a slightly lower expression of Col2a was detected in four EVdFBS media compared to that in FBS media, which implied equal differentiation condition for 14 days could not completely diminish the difference of chondrogenic differentiation capacity between hADSC in FBS media and in four EVdFBS media. It seemed the initial 96-hour EVdFBS exposure affected chondrogenic differentiation ability of hADSCs. Indeed, it was reported that serum-supplementation could

increase the frequency of chondrogenic cells and ECM accumulation to enhance chondrogenesis of aging MSCs [35]. Therefore, using serum-free culture media for MSCs culture and EVs enrichment might cause cells to go into adaptation and survival mode, and change the cargo of their EVs and therapeutic property, making further research inaccurate [36, 37]. In addition, a large scale of MSC-EVs production for clinical application requires sustainable and normal MSC culture condition [38]. Using EV-depleted culture media is a standard and specific option, which has no impact on persistent use of MSC.

The considerable proportion that FBS-EVs were in EVs mixture implied the highly impure ADSC-EVs were enriched from ADSC-UC EVdFBS and ADSC-Com EVdFBS media. Furthermore, EVs mixture in ADSC-UF EVdFBS media had broader particle size range, which might influence property of EVs and analysis at a functional level of EVs-mediated intercellular signaling [39, 40]. Moreover, we speculated that the genes associated with EV production and trafficking (e.g.VPS4A) [41] were affected when hADSCs were cultured in TGFβ deficient condition [42], causing less distinct peak of EVs mixture.

It was reported that EVs derived from ADSCs potentiating tissue repair [9, 43, 44]. Of note, the UC EVdFBS media and serum-free media were used for supporting ADSCs growth and EVs enrichment in these publications. Therefore, we treated knee synovial fibroblast with EVs derived from ADSC-FBS media, ADSC-PEG EVdFBS media, ADSC-serum free media. FBS-EVs were used as a reference. Based on the published study [45, 46], the mRNA levels of Col1a1, TIMP1 in vaginal fibroblasts/ scleral fibroblasts were determined to evaluate the collagen metabolism. In our study, the results showed EVs enriched from ADSC-PEG EVdFBS media participate in the processes of extracellular matrix remodeling, mainly collagen metabolism. Interestingly, higher mRNA levels of Col1a1 and TIMP1 were expressed in EVs enriched from ADSC-PEG EVdFBS media and ADSC serum free media groups, compared to that from ADSC-FBS media group. It seemed a competitive relationship exists between FBS-EVs and cell-EVs, influencing the therapeutic use of cell-EVs. Of note, *Azadeh et al* demonstrated the effective particles could be removed from FBS through PEG 4K precipitation, with 3.2 % PEG in final solution [47]. However, we selected the common concentration range of PEG employed in previous literature, and in our study the particles in PEG EVdFBS have increased following the decrease of final solution, which is likely to be ascribed to different commercial FBS. In terms of the status of cells cultured in PEG EVdFBS, the authors observed that the primary adipose tissue derived cells cultured in 10% PEG 4K mediated EVdFBS expressed CD44 (99.7%), CD105 (99.8%) and CD29 (97.2%), as markers for stem cells. While we

focused on the differentiation capacity of cells, which was not affected. Moreover, in our study the cell-derived EVs obtained from PEG EVdFBS supernatant were obtained and still retained bioactive, meaning the PEG EVdFBS supports cell-EVs enrichment.

For clinical use, utilizing MSC EVs necessitates an expansion of EV production on a larger scale, adherence to rigorous good manufacturing practice (GMP) protocols [38], and other various regulatory requisites. Among the critical safety considerations, the adoption of animal-free or bovine EV-free media stands out. In this context, our PEG precipitation depletion protocol emerges as a noteworthy advancement. This protocol enables the generation of FBS EV-free serum, effectively supporting both the production and inherent properties of cell derived EVs. More importantly, this approach holds promising applicability to a wide range of serums, including human serum. As a result, it presents a compelling avenue for future GMP-compliant EV production tailored to clinical applications in the realms of regenerative medicine and therapy

Limitation

In our investigation, our primary focus centered on FBS-derived extracellular vesicles (EVs) and protein contents stemming from FBS contaminants. However, our scrutiny did not extend to examining the RNA component within the FBS milieu. As reported by Shelke and colleagues [18], due attention must be directed towards the extracellularly circulating microRNA (exRNA) introduced in FBS. The persisting RNA complexes introduce confounding variables into an array of experimental outcomes, particularly those involving the evaluation of RNA species associated with EVs. Regrettably, a comprehensive comprehension remains elusive regarding the specific RNA categories that engage with EVs versus other extracellular carriers of exRNA. Likewise, there remains ambiguity concerning that the subset of RNA carriers lingers in solution post-FBS EV-depletion. Interestingly, an observation emerges from Turchinovich and colleagues indicating this particular class of exRNA exhibits resilience against efficient removal from UC EV-depleted FBS, but they seem prone to co-isolation with in vitro-generated EVs during polymer-based EV isolation procedures [48].

In addition, the subtype of MSCs (cells isolated from different tissues) studied was insufficient in this study. Traditionally, MSCs have been isolated from bone marrow or adipose tissue, which have been mainly induced into mesoderm-type cells such as osteoblasts, adipocytes and chondrocytes. During the recent years, MSC-like populations have been obtained from a wide range of skin and foreskin [49],

synovial fluid [50], Wharton's jelly [51] for specific tissue regeneration. The common cell surface markers of BMSCs or ADSCs or Wharton's jelly MSCs are CD73, CD90, CD105, while CD44 is present on MSCs from skin and synovial fluid. Furthermore, the EVs derived from MSC-like populations are capable of restoring an extensive range of damaged or diseased tissues and organs [52]. To make the conclusion more convincing and enrich the applicable field of PEG precipitation FBS EV depletion protocol, various types of MSCs should be incorporated.

In conclusion, our research has successfully demonstrated the straightforward preparation of PEG EVdFBS within any conventional research laboratory setting. The PEG precipitation method we've developed not only boasts cost-effectiveness but also offers a standardization process. Notably, it facilitates the sustained proliferation of MSCs for a minimum of 5 days. The integration of our PEG precipitation protocol within the broader MSC EV research community holds great potential. By adopting this method, researchers can acquire pure MSC EVs, enhancing the robustness and reliability of their investigations. In effect, the quality of their research endeavors stands to benefit significantly. In light of these advancements, PEG EVdFBS emerges as a compelling and viable alternative to conventionally used UC EVdFBS as well as UF EVdFBS and serum-free conditions in future MSC EV-related studies.

REFERENCES

1. Arshi, A., et al., Stem Cell Treatment for Knee Articular Cartilage Defects and Osteoarthritis. Curr Rev Musculoskelet Med, 2020. **13**(1): p. 20-27.
2. Choi, D.H., et al., Tonsil-derived mesenchymal stem cells incorporated in reactive oxygen species-releasing hydrogel promote bone formation by increasing the translocation of cell surface GRP78. Biomaterials, 2021. **278**: p. 121156.
3. Harrell, C.R., et al., Molecular Mechanisms Responsible for Anti-inflammatory and Immunosuppressive Effects of Mesenchymal Stem Cell-Derived Factors. Adv Exp Med Biol, 2019. **1084**: p. 187-206.
4. Yao, X., et al., In-cytoplasm mitochondrial transplantation for mesenchymal stem cells engineering and tissue regeneration. Bioeng Transl Med, 2022. **7**(1): p. e10250.
5. Wu, H., et al., Extracellular vesicles containing miR-146a attenuate experimental colitis by targeting TRAF6 and IRAK1. Int Immunopharmacol, 2019. **68**: p. 204-212.
6. Liu, H., et al., Immunomodulatory Effects of Mesenchymal Stem Cells and Mesenchymal Stem Cell-Derived Extracellular Vesicles in Rheumatoid Arthritis. Front Immunol, 2020. **11**: p. 1912.
7. Cosenza, S., et al., Mesenchymal stem cells-derived exosomes are more immunosuppressive than microparticles in inflammatory arthritis. Theranostics, 2018. **8**(5): p. 1399-1410.
8. Wong, K.L., et al., Intra-Articular Injections of Mesenchymal Stem Cell Exosomes and Hyaluronic Acid Improve Structural and Mechanical Properties of Repaired Cartilage in a Rabbit Model. Arthroscopy, 2020. **36**(8): p. 2215-2228.e2.
9. Choi, J.S., et al., Functional recovery in photo-damaged human dermal fibroblasts by human adipose-derived stem cell extracellular vesicles. J Extracell Vesicles, 2019. **8**(1): p. 1565885.
10. Eitan, E., et al., Extracellular vesicle-depleted fetal bovine and human sera have reduced capacity to support cell growth. J Extracell Vesicles, 2015. **4**: p. 26373.
11. Wei, Z., et al., Fetal Bovine Serum RNA Interferes with the Cell Culture derived Extracellular RNA. Sci Rep, 2016. **6**: p. 31175.
12. Gardiner, C., et al., Techniques used for the isolation and characterization of extracellular vesicles: results of a worldwide survey. J Extracell Vesicles, 2016. **5**: p. 32945.
13. Kim, K., et al., Stable cell adhesion affects mesenchymal stem cell sheet fabrication: Effects of fetal bovine serum and human platelet lysate. J Tissue Eng Regen Med, 2020. **14**(5): p. 741-753.
14. Brunner, D., et al., Serum-free cell culture: the serum-free media interactive online database. Altex, 2010. **27**(1): p. 53-62.
15. Cosenza, S., et al., Mesenchymal stem cells derived exosomes and microparticles protect cartilage and bone from degradation in osteoarthritis. Sci Rep, 2017. **7**(1): p. 16214.
16. Li, B., et al., Labial gland-derived mesenchymal stem cells and their exosomes ameliorate murine Sjögren's syndrome by modulating the balance of Treg and Th17 cells. Stem Cell Res Ther, 2021. **12**(1): p. 478.
17. Théry, C., et al., Isolation and characterization of exosomes from cell culture supernatants and biological fluids. Curr Protoc Cell Biol, 2006. **Chapter 3**: p. Unit 3.22.
18. Shelke, G.V., et al., Importance of exosome depletion protocols to eliminate functional and RNA-containing extracellular vesicles from fetal bovine serum. J Extracell Vesicles, 2014. **3**.
19. Lehrich, B.M., et al., Fetal Bovine Serum-Derived Extracellular Vesicles Persist within Vesicle-Depleted Culture Media. Int J Mol Sci, 2018. **19**(11).

20. Pham, C.V., et al., Bovine extracellular vesicles contaminate human extracellular vesicles produced in cell culture conditioned medium when 'exosome-depleted serum' is utilised. Arch Biochem Biophys, 2021. **708**: p. 108963.
21. Kornilov, R., et al., Efficient ultrafiltration-based protocol to deplete extracellular vesicles from fetal bovine serum. J Extracell Vesicles, 2018. **7**(1): p. 1422674.
22. Yuana, Y., et al., Co-isolation of extracellular vesicles and high-density lipoproteins using density gradient ultracentrifugation. J Extracell Vesicles, 2014. **3**.
23. Pieters, B.C., et al., Commercial cow milk contains physically stable extracellular vesicles expressing immunoregulatory TGF-β. PLoS One, 2015. **10**(3): p. e0121123.
24. Ma, J., et al., Adipose tissue-derived mesenchymal stem cells as monocultures or cocultures with human umbilical vein endothelial cells: performance in vitro and in rat cranial defects. J Biomed Mater Res A, 2014. **102**(4): p. 1026-36.
25. Schelbergen, R.F., et al., Alarmins S100A8/S100A9 aggravate osteophyte formation in experimental osteoarthritis and predict osteophyte progression in early human symptomatic osteoarthritis. Ann Rheum Dis, 2016. **75**(1): p. 218-25.
26. Webber, J. and A. Clayton, How pure are your vesicles? J Extracell Vesicles, 2013. **2**.
27. Ludwig, A.K., et al., Precipitation with polyethylene glycol followed by washing and pelleting by ultracentrifugation enriches extracellular vesicles from tissue culture supernatants in small and large scales. J Extracell Vesicles, 2018. **7**(1): p. 1528109.
28. Lee, H., et al., Low concentration of polyethylene glycol facilitates separation of extracellular vesicles from bronchoalveolar lavage fluid. Am J Physiol Lung Cell Mol Physiol, 2021. **320**(4): p. L522-L529.
29. Liao, Z., et al., Serum extracellular vesicle depletion processes affect release and infectivity of HIV-1 in culture. Sci Rep, 2017. **7**(1): p. 2558.
30. Merten, O.-W., et al., Manufacturing of viral vectors: part II. Downstream processing and safety aspects. Pharmaceutical Bioprocessing, 2014. **2**: p. 237-251.
31. Urzì, O., R.O. Bagge, and R. Crescitelli, The dark side of foetal bovine serum in extracellular vesicle studies. J Extracell Vesicles, 2022. **11**(10): p. e12271.
32. Gstraunthaler, G., Alternatives to the use of fetal bovine serum: serum-free cell culture. Altex, 2003. **20**(4): p. 275-81.
33. Lötvall, J., et al., Minimal experimental requirements for definition of extracellular vesicles and their functions: a position statement from the International Society for Extracellular Vesicles. J Extracell Vesicles, 2014. **3**: p. 26913.
34. Kang, W., et al., Early prediction of adverse outcomes in infants with acute bilirubin encephalopathy. Ann Clin Transl Neurol, 2020. **7**(7): p. 1141-1147.
35. Kisiday, J.D., et al., Culture Conditions that Support Expansion and Chondrogenesis of Middle-Aged Rat Mesenchymal Stem Cells. Cartilage, 2020. **11**(3): p. 364-373.
36. Gudbergsson, J.M., et al., Systematic review of factors influencing extracellular vesicle yield from cell cultures. Cytotechnology, 2016. **68**(4): p. 579-92.
37. Potier, E., et al., Prolonged hypoxia concomitant with serum deprivation induces massive human mesenchymal stem cell death. Tissue Eng, 2007. **13**(6): p. 1325-31.
38. Riazifar, M., et al., Stem Cell Extracellular Vesicles: Extended Messages of Regeneration. Annu Rev Pharmacol Toxicol, 2017. **57**: p. 125-154.
39. Wu, S.C., et al., Subpopulations of exosomes purified via different exosomal markers carry different microRNA contents. Int J Med Sci, 2021. **18**(4): p. 1058-1066.

40. Giebel, B., On the function and heterogeneity of extracellular vesicles. Ann Transl Med, 2017. **5**(6): p. 150.
41. Aswad, H., A. Jalabert, and S. Rome, Depleting extracellular vesicles from fetal bovine serum alters proliferation and differentiation of skeletal muscle cells in vitro. BMC Biotechnol, 2016. **16**: p. 32.
42. Lin, H., et al., miR-4454 Promotes Hepatic Carcinoma Progression by Targeting Vps4A and Rab27A. Oxid Med Cell Longev, 2021. **2021**: p. 9230435.
43. Ren, S., et al., Microvesicles from human adipose stem cells promote wound healing by optimizing cellular functions via AKT and ERK signaling pathways. Stem Cell Res Ther, 2019. **10**(1): p. 47.
44. Zhang, W., et al., Cell-free therapy based on adipose tissue stem cell-derived exosomes promotes wound healing via the PI3K/Akt signaling pathway. Exp Cell Res, 2018. **370**(2): p. 333-342.
45. Xie, Y., X. Ouyang, and G. Wang, Mechanical strain affects collagen metabolism-related gene expression in scleral fibroblasts. Biomed Pharmacother, 2020. **126**: p. 110095.
46. Liu, X., et al., Exosomes secreted by adipose-derived mesenchymal stem cells regulate type I collagen metabolism in fibroblasts from women with stress urinary incontinence. Stem Cell Res Ther, 2018. **9**(1): p. 159.
47. Haghighitalab, A., et al., Cost-effective Strategies for Depletion of Endogenous Extracellular Vesicles from Fetal Bovine Serum. Journal of Cell and Molecular Research, 2020. **11**(2): p. 42-54.
48. Turchinovich, A., et al., Characterization of extracellular circulating microRNA. Nucleic Acids Res, 2011. **39**(16): p. 7223-33.
49. Riekstina, U., et al., Characterization of human skin-derived mesenchymal stem cell proliferation rate in different growth conditions. Cytotechnology, 2008. **58**(3): p. 153-62.
50. Morito, T., et al., Synovial fluid-derived mesenchymal stem cells increase after intra-articular ligament injury in humans. Rheumatology (Oxford), 2008. **47**(8): p. 1137-43.
51. Hou, T., et al., Umbilical cord Wharton's Jelly: a new potential cell source of mesenchymal stromal cells for bone tissue engineering. Tissue Eng Part A, 2009. **15**(9): p. 2325-34.
52. Tsiapalis, D. and L. O'Driscoll, Mesenchymal Stem Cell Derived Extracellular Vesicles for Tissue Engineering and Regenerative Medicine Applications. Cells, 2020. **9**(4).

SUPPLEMENTAL INFORMATION

Table 1. Sequence of primers for real-time PCR analysis.

Gene	Forward	Reverse
GAPDH	ATCTTCTTTTGCGTCGCCAG	TTCCCCATGGTGTCTGAGC
COL2A1	CACGTACACTGCCCTGAAGGA	CGATAACAGTCTTGCCCCACTT
CCND1	ATCAAGTGTGACCCGGACTG	CTTGGGGTCCATGTTCTGCT
SIRT1	AGAGCCTCACATGCAAGCTCTAG	GCCAATCATAAGATGTTGCTGAAC
COL1A1	AGATCGAGAACATCCGGAG	AGATCGAGAACATCCGGAG
TGFb1	GAGGTCACCCGCGTGCTA	TGCTTGAACTTGTCATAGATTTCGTT
TIMP1	CAATTCCGACCTCGTCATCAG	TATACATCTTGGTCATCTTGATCTCATAAC

Chapter 3

Milk Extracellular Vesicles Enhance Osteogenic Differentiation of Bone Marrow Stromal Cells Through Mitochondrial Oxidative Phosphorylation

Peng Wang, Onno J. Arntz, Xinlai Chen, Theodoros Ioannis Papadimitriou, Peter M. van der Kraan, Jeroen J.J.P. van den Beucken, Arjan van Caam, Fons A.J. van de Loo.

In preparation

ABSTRACT

Extracellular vesicles derived from cow milk (mEVs) have been implicated in regulating bone remodeling. Recently, bioenergetic metabolism has emerged as an important regulatory node in bone formation by modulating osteogenic differentiation of mesenchymal stromal cells (MSCs). In the present study, we demonstrated that mEVs promoted osteogenic differentiation and ATP production *in vitro* through strengthening aerobic metabolism. More importantly, flow cytometry and qRT-PCR data demonstrated that mEVs contributed to human bone marrow MSCs (hBMSCs) osteogenic differentiation through activating mitochondrial oxidative phosphorylation (OXPHOS), as evidenced by moderately increasing mitochondrial membrane potential and superoxide production, as well as regulating mitochondrial dynamics and transcription-related genes. Taken together, mEVs facilitate osteogenic differentiation of hBMSCs through activating classical mitochondrial aerobic metabolism, providing a new insight to improve EVs-based bone regenerative treatment.

Keywords: milk, extracellular vesicles, bone marrow mesenchymal stromal cell, bone homeostasis, mitochondrial function

INTRODUCTION

Bone is a dynamic tissue that undergoes continuous renewal. Bone formation and bone resorption are integral components of the bone remodeling process, and essential for maintaining skeletal integrity and homeostasis throughout life [1]. Bone remodeling is a tightly regulated process referred to as coupling, in which osteoclasts resorb bone and osteoblasts form new bone [2]. Osteoblasts are derived from mesenchymal stromal cells (MSCs), which play a pivotal role in bone tissue regeneration and repair due to their multipotent capabilities [3, 4]. To date, most studies on MSCs have concentrated on the activity of the nuclear genome during differentiation, while the characteristics of mitochondrial function have received comparatively less attention.

Mitochondria are double-membrane-bound organelles found in nearly all eukaryotic cells, often referred to as the "powerhouses of the cell" due to their critical role in energy production through oxidative phosphorylation (OXPHOS) [5]. These organelles are responsible for generating the majority of cellular ATP, which is essential for fueling various biochemical reactions within the cell [6]. It has been reported that during osteogenic differentiation, MSCs undergo a transition from glycolysis to aerobic mitochondrial OXPHOS, marked by mitochondrial biogenesis, and increased membrane potential, as well as higher intracellular ATP levels [7]. This metabolic shift is crucial as it supports the energy-intensive process of osteogenic differentiation.

In recent years extracellular vesicles (EVs) have been widely investigated for their ability to modulate bone formation. EVs are lipid bilayer vesicles that consist of parent-cell specific sterols, membrane proteins and encloses an aqueous solution containing proteins, nucleic acids, and metabolites capable of influencing biological functions [8]. EVs derived from cow milk (mEVs) have been recognized for their immunomodulatory properties, influencing macrophage differentiation and cytokine production [9]. Our previous studies showed that mEVs contribute to bone homeostasis by modulating the activity of osteoblasts and osteoclasts *in vitro* [10, 11]. Additionally, in an ovariectomized (OVX) bone loss mouse model, mEVs exhibited systemic osteoprotective effects through regulation of the RANKL/OPG signaling pathway [12]. However, the mechanism(s) how mEVs achieve these effects is/are yet unclear. The possibility that mEVs modulate cell energy status has been suggested before [13], but the effects of mEVs on bioenergetic metabolism during osteogenic differentiation are yet unclear.

In the present study, we aim to investigate the role of mEVs stimulation in energy metabolism during the early phase of osteogenic differentiation of human bone marrow MSCs (hBMSCs). We demonstrated that a low concentration of mEVs promoted osteogenic differentiation and ATP production *in vitro* through strengthening aerobic metabolism. More importantly, through flow cytometry and qRT-PCR, we demonstrated that mEVs contributed to mitochondrial activation in hBMSCs during osteogenic differentiation, as evidenced by increasing mitochondrial membrane potential and superoxide production, as well as regulating mitochondrial dynamics and transcription-related genes.

MATERIALS AND METHODS

Cell culture

Passage 2-5 hBMSCs were maintained in a log phase in a humidified atmosphere with 5% CO_2 at 37°C with cell culture media composed of α-MEM (A14090, Gibco) supplemented with 10% fetal bovine serum (Gibco) and 1% penicillin–streptomycin (Gibco). hBMSCs were isolated from bone fragments obtained as surgical excess material following total hip arthroplasty at the Department of Orthopedics (Radboudumc, Nijmegen, the Netherlands) from anonymized patients. In line with the criteria as set by the International Society for Cellular Therapy (ISCT), hBMSCs were immunophenotypically characterized to express MSC markers (>95% immunopositive for CD90 and CD105, and >85% immunonegative for CD45).

Osteogenic differentiation *in vitro*

To initiate osteogenic differentiation, hBMSC were cultured in basic osteogenic induction media (OM) of α-MEM containing 10% v/v EV-depleted FBS prepared by 18 hours UC [14] and 1% penicillin-streptomycin, as well as 10mM β-glycerophosphate disodium salt hydrate, 10^{-8}M dexamethasone and 50 μg/ml ascorbic acid. On day 7 of osteogenic differentiation the production of type I collagen by cells was measured by western blotting (WB). Cells were washed with PBS and RIPA lysis buffer (Millipore) with a proteinase inhibitor cocktail (Roche diagnostics, cOmplete™) was added. Equal protein amounts were loaded onto 10% SDS-PAGE and subsequently transferred on ice to 0.45 μm nitrocellulose membrane for 120 min at 275 mA using Towbin buffer. The membrane was blocked with 5% skim milk overnight at 4°C. After that, blots were incubated overnight with anti-col1a1 (1:1000, Merck ABT257).

The alkaline phosphatase enzymatic activity (ALP) and the calcium content were tested as previously described [15]. Briefly, 0.5 M alkaline buffer solution (Sigma) and samples (1:5) were incubated with substrate solution (5mM pNPP disodium salt hexahydrate) (Sigma) for 1 hour at 37°C. The conversion in this assay results in 4-Nitrophenol, and the absorbance was read at 405 nm with Clariostar spectrometer (BMG Labtech). To measure calcium content the cell culture wells were incubated overnight in 0.5 M acetic acid at room temperature. The working solution consisted of 5% 14.8 M ethanolamine (Merck)/boric acid buffer (BOOM) [pH 11], 5% Ortho-Cresolphthalein Complexone (Merck), and 2% hydroxyquinoline (Sigma). Samples mixed with working solution and incubated at RT for 10 minutes. The absorbance of the plates was measured with Clariostar spectrometer (BMG Labtech) at 570 nm.

mEVs labeling and cellular uptake

mEVs were labeled with DiD stain (Invitrogen) according to the manufacturer's instructions. Briefly, EVs were mixed with DiD stain (10 µM) and incubated at room temperature for 15 min in the dark. Labeled EVs were then washed two times with PBS at 100,000 g for 90 min at 4°C. The final EVs pellet was suspended in PBS. For cell uptake, 3E+04 hBMSCs were seeded in each well of tissue culture plastic and incubated with DiD-labeled EVs at 37 °C. After 6 h, cells were washed with PBS and fixed with 4% paraformaldehyde. The cell actin filaments were stained with phalloidin, and nuclei were stained with DAPI. The imaging was performed using a confocal laser-scanning microscopy (Nikon, Japan).

DNA quantification

On days 2, 6, or 14 of osteogenic differentiation under different concentrations of mEVs, cells were subjected to a single freeze-thaw cycle in lysis buffer, followed by DNA quantification using the PicoGreen assay (Quant-iT PicoGreen dsDNA Kit; Invitrogen), and measured using a Clariostar (BMG Labtech).

ATP analysis

The cellular ATP level was assessed using the Cell Titer-Glo® 2.0 Cell Viability kit (G9241, Promega) according to the manufacturer's instructions. In brief, the culture medium per condition was removed on days 2 and 6 of osteogenic differentiation, and each well was supplemented with 100 µL of pre-warmed lysis buffer. Luminescence intensity was measured using Clariostar spectrometer (BMG Labtech).

Glucose and Lactate measurements

The glucose consumption and lactate production were determined using the Glucose-Glo™ kit (J6022, Promega) and Lactate-Glo™ kit (J5022, Promega) according to the manufacturer's instructions. The culture medium per condition was collected on days 2, 6 of osteogenic differentiation. The luminometry was measured with Clariostar spectrometer. Results were quantified using a standard curve.

Glutamine measurements

The glutamine consumption was determined using the Glutamine-Glo™ kit (J8021, Promega) according to the manufacturer's instructions. The culture medium per condition was collected on days 2, 6 of osteogenic differentiation. The luminometry was measured with Clariostar spectrometer. Results were quantified using a standard curve.

Flow cytometric analysis

2.4E+05 cells per condition were used for flow cytometric staining. Cells were incubated with Mitotracker Deep Red FM Dye (M46753, Invitrogen™) and/or MitoSox Mitochondrial Superoxide Indicators (M36006, Invitrogen™). Cells were then washed twice with PBS in 96 wells v-bottom and incubated with viability dye efluor780 (1 : 1000 PBS, eBioscience) for 30 min at 4°C in the dark. Followingly, cells were washed twice with FACS buffer (PBS + 1% BSA) and acquired in a Beckman Coulter Cytoflex LX 21-color flow cytometer. Flow cytometry data were analyzed using Kaluza software version 2.1.3 (Beckman Coulter). To quantify the intensity of mitoRed and mitoGreen dye emission the values of the geometric mean of mean fluorescence intensity (MFI) were utilized.

RNA extraction and real-time PCR

RNA extraction from cells was performed using TRI reagent according to the manufacturer's procedure. The cells were mixed with 0.5 mL TRI reagent and 100 µl chloroform, mixed for 15 seconds, then incubated at room temperature for 2 minutes. After centrifugation at 12,000 × *g* for 15 minutes at 4°C, the supernatant was transferred to a new tube and 250 µl isopropanol was added and incubated overnight at -20 °C.This mixture was then centrifuged at 12,000 × *g* for 30 minutes at 4°C and supernatant was removed. The RNA pellet was then washed twice with 75% ethanol. After centrifugation at 12,000 × *g* for 5 minutes at 4°C, the ethanol was aspirated, and the RNA pellet was air dried for 10 minutes and dissolved in RNase-free water.

Synthesis of cDNA was accomplished by reverse transcription PCR an oligo (dT) primer and Moloney murine leukemia virus Reverse Transcriptase. Quantitative real-time PCR was performed using SYBR Green real-time PCR master mix on a Step-One according to the manufacturer's instructions. Primer sets for individual genes were used (**supplementary table 1**).

Statistical analysis

Data are expressed as the mean±SD. All data were analyzed for normality of distribution using Shapiro-Wilk test and were found to be normally distributed. Two group comparisons were analyzed by Student's T tests. Comparisons among three or four groups were evaluated by one-way ANOVA followed by Dunnett test. The statistical analysis was performed using GraphPad Prism (GraphPad Software, La Jolla, CA, USA). A p-value below 0.05 ($p<0.05$) was considered to be statistically significant.

RESULTS

mEVs stimulate osteogenic differentiation of hBMSCs in an inverse dose-dependent manner

The uptake of mEVs by hBMSCs was evaluated using vesicles labeled with fluorescent dye. hBMSCs demonstrated noticeable internalization of mEVs after 6 hours of incubation (Fig. **1A**). To determine the effect of mEVs on osteogenic differentiation of hBMSCs, we performed an mEVs dose–response experiment. We exposed hBMSCs to basic OM in the absence or presence of mEVs at different concentrations (5E+08, 5E+07, 5E+06 particles/ml). Supplementation with mEVs (5E+06 particles/ml) led to a 2.2-fold increase in type I collagen expression at day 7 compared to OM without mEVs as analyzed by WB, and 5E+07 and 5E+08 particles/mL mEVs resulted in 1.9-fold and 1.5-fold increase, respectively (Fig. **1B**). At day 14, ALP activity significantly increased 40% and 30% when the medium of hBMSCs was supplemented with mEV at concentrations of 5E+06 and 5E+07 particles/mL (Fig. **1C**). At day 21 of culture, only enhanced calcium deposition (20% increase) was observed with a low dose of mEV (5E+06 particles/mL; Fig. **1D**). Collectively, these results imply that mEVs stimulate osteogenesis of hBMSCs in an inverse dose-dependent manner.

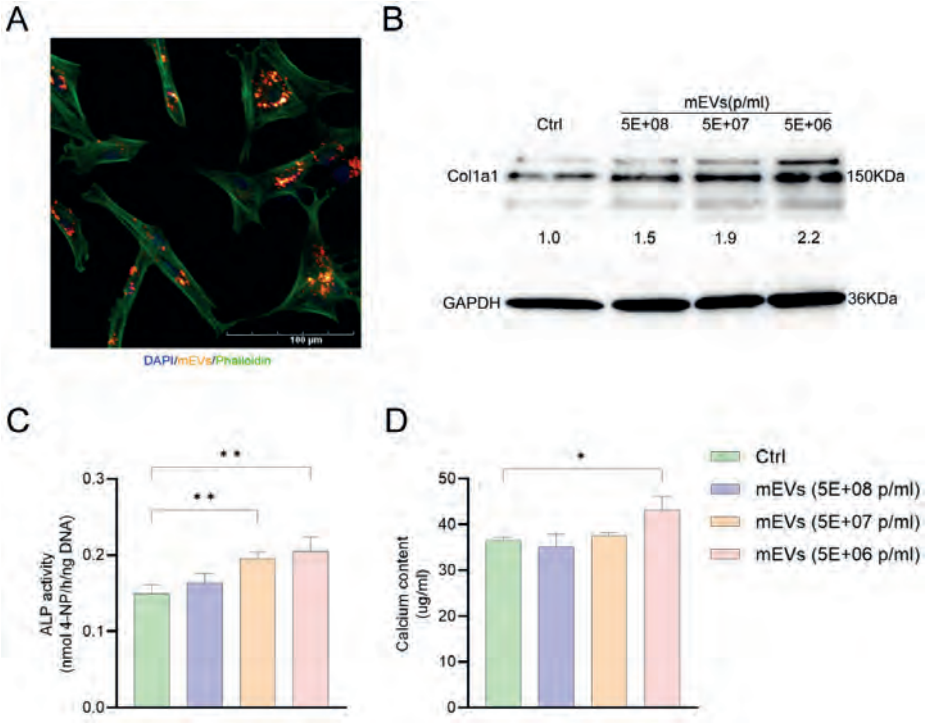

Fig. 1. mEVs stimulate osteogenic differentiation of hBMSCs in an inverse dose-dependent manner. (A) Confocal fluorescence analysis showed that mEVs labelled with DiD (yellow) were taken up by hBMSC labelled with DAPI (blue) and Phalloidin (green) after 6h. (B) Western blotting for Col1a1 protein expressions of hBMSC that received different concentrations of mEVs (5E+08, 5E+07 and 5E+06 particles/ml) at day 7 and C) Alkaline phosphatase enzymatic activity at day 14 (n=3), as well as D) Calcium content of hBMSCs at day 21 (n=3). Data were expressed as means ± standard deviation (SD). **p < 0.05, **p < 0.01*.

mEVs at lower dose increased ATP production in the early phase of osteogenic differentiation of hBMSCs

To assess the impact of mEVs stimulation on ATP production, we determined the cellular ATP amount at days 2 and 6 of hBMSCs osteogenesis. The PicoGreen assay data showed that dsDNA content of all groups decreased with prolonged osteogenic differentiation induction, suggesting cells gradually exited the cell cycle and focus on osteogenic commitment [16]. In more detail, compared to the PBS control (213.4±9.3 ng/ml), at day 2 the dsDNA content under concentrations of mEVs (5E+08, 5E+07, 5E+06 particles/ml) was 203.2±8.9 ng/ml, 190.9±5.8 ng/ml and 192.3±15.2 ng/ml, respectively; At day 6 of osteogenesis of hBMSCs, the dsDNA content showed a further decline: measuring 180.0 ± 15.7 ng/ml in the PBS control, 175.3 ± 7.3 ng/ml at the highest mEVs dose, 149.1 ± 6.1 ng/ml at the medium

dose, and 148.5 ± 13.2 ng/ml at the lowest dose (Fig. **2A)**. In contrast, CellTiter-Glo Luminescent data implied that cellular ATP production of all groups increased with prolonged osteogenic differentiation induction, meeting up with the high energy demand for osteogenic maturation [17]. Specifically, at day 2 compared to the PBS control, a significant 20% increase in ATP production has been determined following mEV stimulation at the 5E+06 particles/ml; At day 6 both 5E+07 and 5E+06 particles/ml mEVs stimulated 10% increases in ATP production (Fig. **2B**). More importantly, at day 2, mEV stimulation at the 5E+07 and 5E+06 particles/ml resulted in a significant 20% and 30% increase in ATP levels (normalized to DNA content), respectively. By day 6, these stimulations showed a 30% increase in ATP levels (normalized to DNA content) compared to the PBS control (Fig. **2C**). Collectively, these data demonstrated that mEVs at lower dose boost ATP production in the early phase of osteogenesis of hBMSCs.

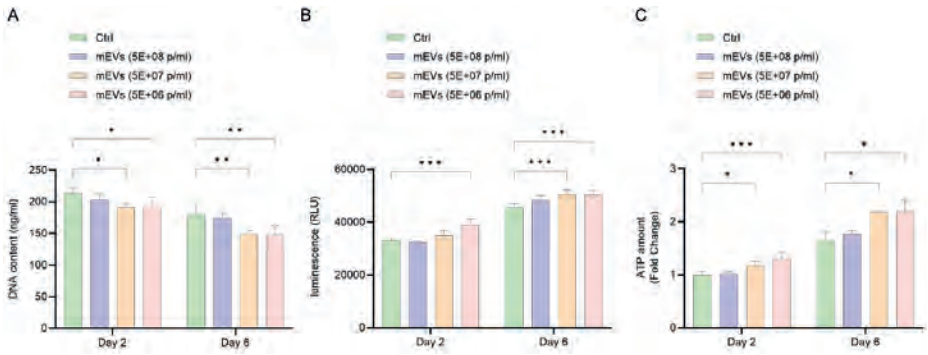

Fig. 2. mEVs at lower dose increased ATP production in the early phase of osteogenic differentiation of hBMSCs. (A) Pico Green assay performed on hBMSCs cultured in OM (Ctrl) or OM within different concentrations of mEVs (5E+08, 5E+07 and 5E+06 particles/ml) at day 2 & day 6 (n=4). (B) The total ATP production by the CellTiter-Glo® Assay (n=4) and C) the ATP amount per DNA of hBMSC (fold change) that received different concentrations of mEVs at day 2 & day 6 (n=4). Data were expressed as means ± standard deviation (SD). *$p < 0.05$, **$p < 0.01$.

mEVs at lower dose strengthen aerobic energy metabolism in the early phase of osteogenic differentiation of hBMSCs

To investigate energy metabolism during the early phase of hBMSCs osteogenic differentiation with mEVs stimulation, we determined glucose consumption, lactate production and glutamine consumption at days 2 and 6. At day 2 a significant decrease of glucose in the culture supernatant by 4%, 4%, and 12% upon stimulation with 5E+08, 5E+07, 5E+06 particles/ml mEVs, respectively, indicating the cells use up more glucose at lower dosage of mEV. At day 6, only mEVs at 5E+06 particles/ml induced an obvious reduction (7%) in glucose residue compared to the PBS

control (Fig. **3A**). Thereafter, lactate production as a hallmark of glycolysis [18] was determined. At day 2 only the low concentration of mEVs stimulation resulted in the lowest lactate production, at 85% of the PBS control, and no obvious difference was observed in lactate production among the groups at day 6 (Fig. **3B**). Next, to investigate the consumption of amino acid as another fuel source for energy [19], we determined glutamine concentrations in cell culture supernatants. Specifically, on day 2, stimulation with mEVs at concentrations of 5E+07 and 5E+06 particles/ml led to increases in glutamine residue levels by 14.7% and 19.3%, respectively, compared to the control. This indicated the cells took up less glutamine as energy source. By day 6, however, glutamine levels showed no notable differences among groups. Taken together, these data demonstrate that mEVs strengthened aerobic energy metabolism with glucose as main source of energy production in the early phase of osteogenic differentiation of hBMSCs. Since 5E+06 particles/ml mEVs showed the most obvious effect at day 2 of osteogenesis, we focused on this concentration in subsequent experiments.

mEVs increase mitochondrial membrane potential and superoxide production

Mitochondria are central to aerobic energy metabolism [20]. To evaluate mitochondrial activity under the mEVs stimulation, mitochondrial membrane potential and superoxide production [21, 22] were investigated. Representative images of flow cytometry plots identified two distinct cell clusters (Fig. 4). In more detail, one cell cluster in upper/right region could not be presented along with the main cell cluster due to higher MFI in cell viability and MitoRed, implying that osteoprogenitor cells were induced in OM culture condition [23]. In addition, for the main cell cluster in the mEV-treated cells, the density center of this BMSC population shifts rightward obviously along the MitoRed axis, indicating an increase in mitochondrial membrane potential (Fig. **4A**). Quantitatively, mEVs significantly increased the mitochondrial membrane potential of hBMSCs compared to PBS control. However, the contribution of mEVs to mitochondrial membrane potential of osteoprogenitor cells was negligible (Fig. **4B**). Consistently, the osteoprogenitor cells cluster with higher MFI in cell viability and MitoGreen was in upper/right region. More importantly, mEVs stimulation resulted in moving rightward of the center of the BMSCs cluster, suggesting that increased mitochondrial superoxide production due to enhanced mitochondrial activity (Fig. **4C**). Quantitatively, mEVs induced the increase in mitoGreen MFI of hBMSCs compared to the PBS control, while it barely contributed to mitoGreen MFI of osteoprogenitor cells (Fig. **4D**). To evaluate whether the ROS level is excessive to impact the osteogenic transcription, the mRNA expression level of RUNX2 and SOD2 at day 2 was determined. qRT-PCR

results revealed that mEVs stimulation resulted in 90% and 100% increases in RUNX2 and SOD2 mRNA expression levels, respectively, compared to the PBS control (Fig S1). Taken together, these results imply that mEVs activated mitochondria in hBMSCs during osteogenic differentiation.

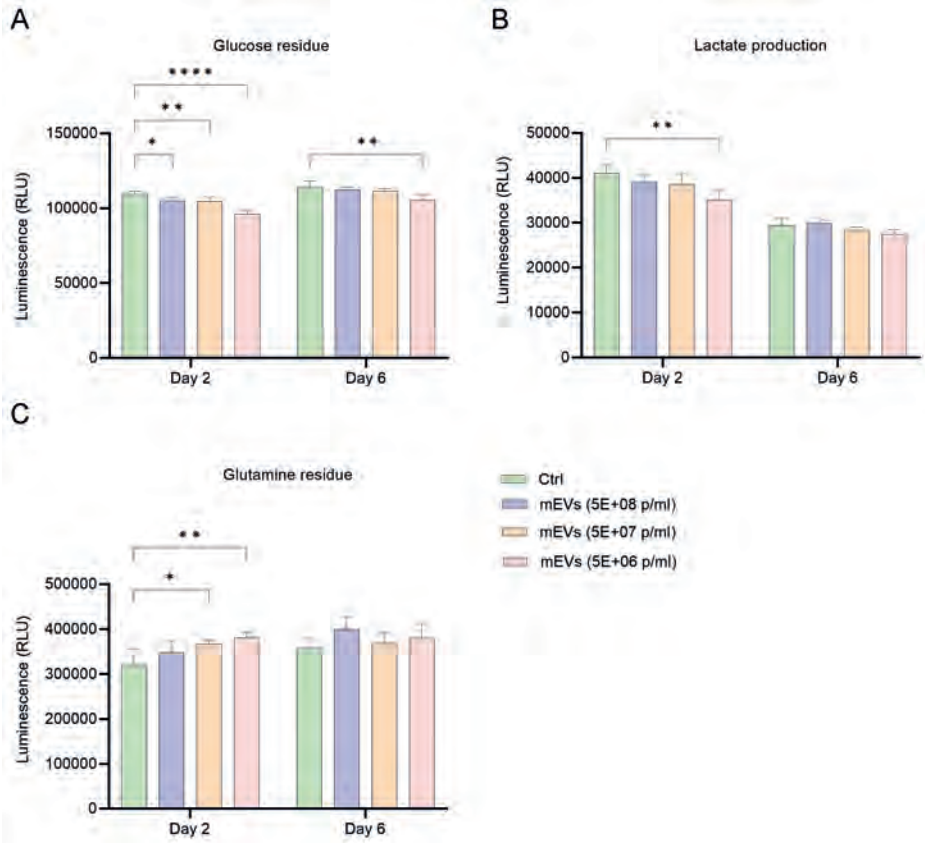

Fig. 3. mEVs at lower dose strengthen aerobic energy metabolism in the early phase of osteogenic differentiation of hBMSCs. (A) Glucose residue in supernatant of hBMSCs with or without different concentrations of mEVs (5E+08, 5E+07 and 5E+06 particles/ml) stimulation at day 2 & day 6 (n=4). (B) The lactate production by hBMSC that received different concentrations of mEVs at day 2 & day 6 (n=4). (C) Glutamine residue in supernatant of hBMSCs with or without different concentrations of mEVs (5E+08, 5E+07 and 5E+06 particles/ml) stimulation at day 2 & day 6 (n=4). Data were expressed as means ± standard deviation (SD). *$p < 0.05$, **$p < 0.01$, ****$p < 0.0001$.

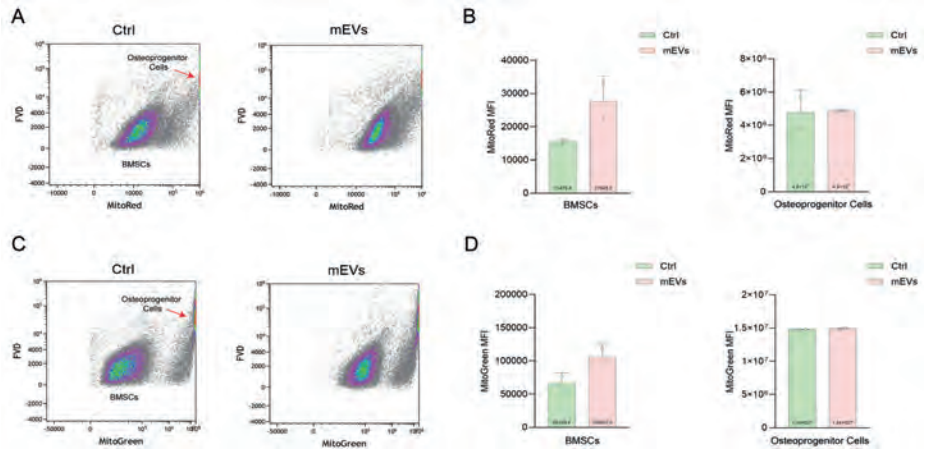

Fig. 4. mEVs increased mitochondrial membrane potential and superoxide production. (A) Representative flow cytometry plots of MitoRed labeled cells with or without at day 2, and (B) Quantification of MitoRed (mitotracker) mean fluorescence intensity (MFI) of labeled BMSCs and osteoprogenitor cells (n=2). (C) Representative flow cytometry plots of MitoGreen labeled cells with or without mEVs at day 2, and (D) Quantification of MitoGreen (mitosox) MFI of labeled BMSCs and osteoprogenitor cells. Data were expressed as means ± standard deviation (SD).

mEVs regulated mitochondrial dynamics and transcription-related genes

To further investigate mitochondrial dynamics and function under the stimulation with mEVs at day 2 osteogenic differentiation, the expressions of mitochondrial regulatory genes have been determined. MFN1 and MFN2 as mitochondrial fusion genes have been investigated. Of note, mEVs stimulation led to a 40% increase in MFN2 mRNA expression, while having little effect on MFN1 compared to the PBS control (Fig. **5A**). Moreover, the expression of mitochondrial fission genes such as DRP1, Fis1 have been determined. qRT-PCR data showed a significant decrease in DRP1 expression by 27% within the mEVs stimulation. Fis1 expression level did not change obviously under the mEVs supplementation (Fig. **5B**). More importantly, we included TEFM and TFB2M as mitochondrial transcription genes. Specifically, mEVs stimulation resulted in a noticeable 140% upregulation of TEFM mRNA and a 30% increase in TFB2M mRNA levels compared to the control PBS group (Fig. **5C**). Collectively, these data indicate that mEVs promoted mitochondrial remodeling toward a fused, functionally active state in hBMSCs during osteogenic differentiation.

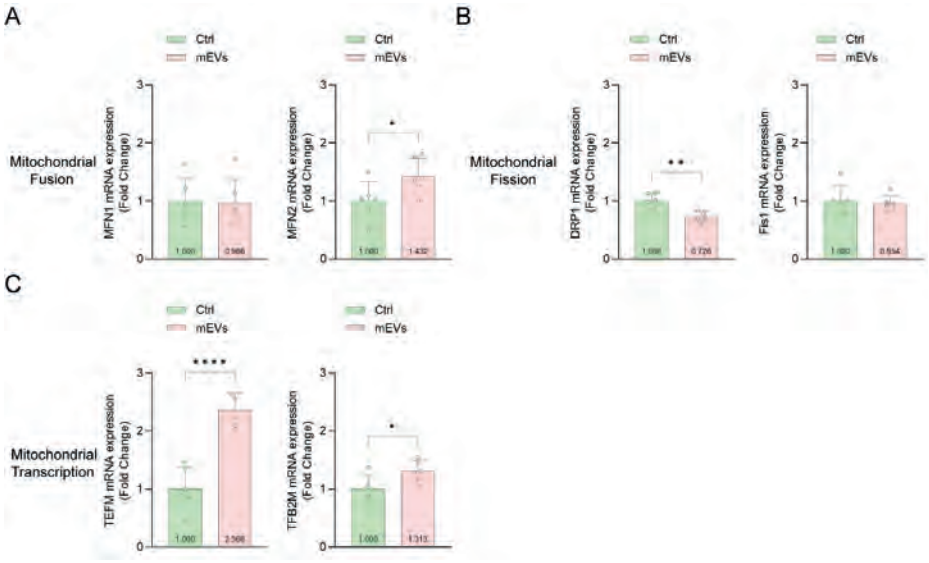

Fig. 5. mEVs regulated mitochondrial dynamics and transcription-related genes. (A) quantitative real-time reverse transcriptase–polymerase chain reaction (qRT-PCR) analysis of mitochondrial fusion (MFN1, MFN2) mRNA expression of hBMSCs with or without mEVs at day 2 (n=6), and (B) mitochondrial fisslon (DRP1, Fis1) mRNA expression (n=6), as well as (C) mitochondrial transcription (TEFM, TFB2M) mRNA expression (n=6). Data were expressed as means ± standard deviation (SD). *$p < 0.05$, **$p < 0.01$, ****$p < 0.0001$.

DISCUSSION

The energy metabolism of MSCs plays a crucial role in their osteogenic differentiation, a process essential for bone formation and repair [24]. Osteogenesis transforms MSCs into metabolically active, matrix-producing osteoblasts, demanding a robust and sustained supply of energy to support this functional transformation [25]. In this study, low-dose stimulation with mEVs enhanced the osteogenic differentiation of hBMSCs, accompanied by increased ATP production and elevated mitochondrial activity. These data explained that mEVs-induced osteogenesis is accompanied by enhanced mitochondrial metabolism.

In the present study, the data showed that cow milk EVs stimulate osteogenic differentiation of hBMSCs in an inverse dose-dependent manner. Higher doses of EVs stimulation failed to drive osteogenic differentiation, aligning with recent reports that raise concerns about potential adverse effects of excessive cow milk consumption on bone health [24, 25]. One recent paper demonstrated that the dose of EVs critically shapes the cellular response [26]. Researchers showed that

high doses of EVs stimulation are more likely to trigger a generalized response of cells that are characterized by downregulation of exocytosis and membrane trafficking genes and increased lysosomal size and activity. While lower doses of EVs drive targeted, specific signaling for therapeutic applications. Herein, we revealed that at low dose mEVs could be internalized immediately by hBMSCs within 6 h and promote osteogenesis of hBMSCs. During the 21-day OM culture, we followed the standard protocol by replenishing the OM supplemented with varying concentrations of mEVs every three days [27, 28]. Given that cells exited the cell cycle and stopped proliferating during OM culture, we speculated that the overwhelming cellular processing machinery had been aggravated due to the higher doses of mEVs accumulation, leading to a reduced effect on promoting osteogenesis, especially during the later phase of osteogenic induction.

The energy has been utilized to support the synthesis of extracellular matrix proteins, activation of osteogenic enzymes like alkaline phosphatase, and the mineralization process. In undifferentiated MSCs, most of the energy is directed toward supporting cell proliferation [29]. Once exposed to osteogenic differentiation conditions, cell proliferation rapidly slows as the cells begin committing to the osteogenic lineage. In our study, DNA content significantly decreased over time in the osteogenic medium meanwhile higher ATP levels were observed in viable cells treated with mEVs, suggesting a strong effect of mEVs in improving energy production for osteogenic maturation. Glucose is the primary and most common energy source in cell cultures [30]. Glycolysis is a fundamental metabolic pathway in which glucose is broken down into pyruvate, producing energy in the form of ATP and NADH [31]. Thereafter, pyruvate enters mitochondria or is converted to lactate by lactate dehydrogenase for continued glycolysis. In our study, lactate production markedly decreased from day 2 to day 6, indicating that the cells underwent a typical osteogenic process involving a metabolic shift from glycolysis toward OXPHOS [32]. More importantly, with mEVs stimulation this transition was accelerated. In addition, despite the fact that glutamine is another energy source in cell cultures and a key anaplerotic substrate for the TCA cycle and fueling OXPHOS [33], it has been reported that glutamine consumption is common in rapidly dividing cells or under glucose-limited conditions [34]. We showed lower glutamine consumption upon mEVs supplementation, implying osteogenic differentiation stimulation with mEVs obey with the glucose-dependent energy metabolism.

It is well established that differentiating osteoblasts are marked by a high abundance of mitochondria with elevated transmembrane potential [35], which is a critical indicator of mitochondrial activity and function [36]. By this, in combination

with the larger size of cell clusters (data not shown) the osteoprogenitor cells have been identified in the present study. Another identified cell cluster consists of undifferentiated BMSCs. Staining with the potential-dependent dye MitoRed revealed that mEV stimulation enhanced mitochondrial activity in these cells, indicating increased energy demand in preparation for further differentiation. In addition, mitochondria are the primary sources of superoxide in mammalian cells, with their production closely linked to mitochondrial activity [37]. Mitochondrial superoxide, a type of reactive oxygen species (ROS), is a byproduct of mitochondrial respiration and plays a dual role in bone physiology. While low levels of ROS are necessary for normal cellular signaling and osteoblast differentiation, excessive ROS, including superoxide, can lead to oxidative stress, which is detrimental to bone health [38, 39]. Herein, higher superoxide production of hBMSCs was observed upon mEVs stimulation, suggesting that higher levels of ROS compared to the PBS control at day 2. Mitochondrial ROS can act as signaling molecules in the cell. Previously, it has been shown that this oxidative stress can lead to the degradation of RUNX2, a critical transcription factor for osteoblast differentiation, thereby inhibiting bone formation [40]. Therefore, we measured the expression of this gene, but this was not affected. Moreover, enhancing superoxide dismutase 2 (SOD2) known as a key antioxidant enzyme can alleviate oxidative stress and promote osteogenesis of BMSCs [41]. Therefore, the qRT-PCR data showed that expressions of RUNX2 and SOD2 were elevated with mEVs stimulation at day 2, implying that the elevated ROS level induced by mEVs was under control and had no detrimental impact on osteogenic differentiation.

Mitochondria are highly dynamic organelles that maintain their morphology via continuous fission and fusion, also known as mitochondrial dynamics [42]. Typically, mitochondria undergo fusion during the early stages of osteogenic differentiation, transitioning to fission at the later stages [43]. MFN1 and MFN2 are essential for mitochondrial fusion, a process that maintains mitochondrial network integrity and function, crucial for mitochondrial DNA (mtDNA) maintenance [44]. Here, the data demonstrated that mEVs induced an increase in MFN2 expression while simultaneously reducing DRP1, a key protein involved in mitochondrial fission. Earlier work reported that stiff ECM conditions promote mitochondrial fusion by increasing MFN1 and MFN2 expression while inhibiting fission by reduced DRP1 expression. This mechanical cue from the microenvironment thus supports osteogenic differentiation through modulation of mitochondrial dynamics [45]. In addition, mitochondrial transcription is essential for mitochondrial activity. This process ensures the production of mitochondrial-encoded proteins required for OXPHOS, which is crucial for ATP generations [46]. TEFM, or the mitochondrial

transcription elongation factor, enhances the processivity of mitochondrial RNA polymerase, which is essential for efficient transcription elongation [47]. TFB2M is a transcription initiation factor that, along with TFAM and mtRNAP, is vital for recognizing mitochondrial promoters and initiating transcription. TFB2M cooperatively interacts with mtRNAP to recognize bases near transcription start sites, which is crucial for species-specific promoter recognition and mitonuclear coevolution [48]. In our study, the data showed that mEVs strongly improved TEFM and TFB2M expression at day 2 of osteogenic differentiation, indicating that more active mitochondrial transcription.

Despite the fact that we clearly demonstrated that mEVs accelerate osteogenic commitment of hBMSCs through active mitochondria, some limitations exist in the present study. Firstly, OXPHOS uses NADH and $FADH_2$ to power the electron transport chain and produce ATP [49]. These molecules can come from the metabolism of glucose, amino acids or fatty acids [50]. We concluded that mEVs-induced osteogenic differentiation is involved in typical glycolysis towards OXPHOS through determining the glucose and glutamine consumption, while the investigation on utilization of fatty acid derived from fetal bovine serum *invitro* culture conditions remains unclear. Secondly, to investigate the true effect of mEVs on bone remodeling, *invivo* experiments need to be conducted. The bone fracture/defect rat models could be established. Besides observing the bone regeneration within local delivery of some biomaterials laden with mEVs, the bone tissue-specific uptake of ^18F-FDG for glucose metabolism could be determined by positron emission tomography imaging [51, 52]. Thirdly, the mEV cargo responsible for the observed osteogenic and mitochondrial effect has not yet been elucidated. The inverse-dose related effect suggests that potentially mEVs harbor both stimulatory (seen at low dose) and inhibitory (seen with higher dosages) osteogenic properties. As the mEVs are a heterogenous population the counteracting properties can reside on different mEV subpopulations making it worthwhile to investigate if an osteogenic promoting mEV population can be identified and selected.

CONCLUSION

We demonstrated that mEVs exhibit osteogenic functionality in an inverse dose-dependent manner. Notably, focusing on biogenetic metabolism, we found that mEV supplementation enhanced ATP production through strengthening aerobic metabolism with glucose as main substrate during the early stage of osteogenic induction. Furthermore, using flow cytometry and qRT-PCR, we showed that

mEVs moderately increased mitochondrial membrane potential and superoxide generation, meanwhile promoted mitochondrial remodeling toward a fused, functionally active state in hBMSCs during osteogenic differentiation.

REFERENCES

1. Bolamperti, S., I. Villa, and A. Rubinacci, Bone remodeling: an operational process ensuring survival and bone mechanical competence. Bone Res, 2022. **10**(1): p. 48.
2. Durdan, M.M., R.D. Azaria, and M.M. Weivoda, Novel insights into the coupling of osteoclasts and resorption to bone formation. Semin Cell Dev Biol, 2022. **123**: p. 4-13.
3. Ding, D.C., W.C. Shyu, and S.Z. Lin, Mesenchymal stem cells. Cell Transplant, 2011. **20**(1): p. 5-14.
4. Chow, S.K., et al., The Advantages and Shortcomings of Stem Cell Therapy for Enhanced Bone Healing. Tissue Eng Part C Methods, 2024. **30**(10): p. 415-430.
5. Tao, M., et al., Animal mitochondria: evolution, function, and disease. Curr Mol Med, 2014. **14**(1): p. 115-24.
6. Piomboni, P., et al., The role of mitochondria in energy production for human sperm motility. Int J Androl, 2012. **35**(2): p. 109-24.
7. Li, Q., et al., The role of mitochondria in osteogenic, adipogenic and chondrogenic differentiation of mesenchymal stem cells. Protein Cell, 2017. **8**(6): p. 439-445.
8. Kumar, M.A., et al., Extracellular vesicles as tools and targets in therapy for diseases. Signal Transduct Target Ther, 2024. **9**(1): p. 27.
9. Barathan, M., et al., Milk-Derived Extracellular Vesicles: A Novel Perspective on Comparative Therapeutics and Targeted Nanocarrier Application. Vaccines (Basel), 2024. **12**(11).
10. Oliveira, M.C., et al., Milk extracellular vesicles accelerate osteoblastogenesis but impair bone matrix formation. J Nutr Biochem, 2016. **30**: p. 74-84.
11. Oliveira, M.C., et al., Milk-Derived Nanoparticle Fraction Promotes the Formation of Small Osteoclasts But Reduces Bone Resorption. J Cell Physiol, 2017. **232**(1): p. 225-33.
12. Oliveira, M.C., et al., Bovine Milk Extracellular Vesicles Are Osteoprotective by Increasing Osteocyte Numbers and Targeting RANKL/OPG System in Experimental Models of Bone Loss. Front Bioeng Biotechnol, 2020. **8**: p. 891.
13. Wang, L., et al., Bovine milk exosomes attenuate the alteration of purine metabolism and energy status in IEC-6 cells induced by hydrogen peroxide. Food Chem, 2021. **350**: p. 129142.
14. Shelke, G.V., et al., Importance of exosome depletion protocols to eliminate functional and RNA-containing extracellular vesicles from fetal bovine serum. J Extracell Vesicles, 2014. **3**.
15. Husch, J.F.A., et al., Comparison of Osteogenic Capacity and Osteoinduction of Adipose Tissue-Derived Cell Populations. Tissue Eng Part C Methods, 2023. **29**(5): p. 216-227.
16. Adithya, S.P., K. Balagangadharan, and N. Selvamurugan, Epigenetic modifications of histones during osteoblast differentiation. Biochim Biophys Acta Gene Regul Mech, 2022. **1865**(1): p. 194780.
17. Sigmarsdottir, T.B., et al., Metabolic and Transcriptional Changes across Osteogenic Differentiation of Mesenchymal Stromal Cells. Bioengineering (Basel), 2021. **8**(12).
18. Rogatzki, M.J., et al., Lactate is always the end product of glycolysis. Front Neurosci, 2015. **9**: p. 22.
19. Ling, Z.N., et al., Amino acid metabolism in health and disease. Signal Transduct Target Ther, 2023. **8**(1): p. 345.
20. Erecińska, M. and D.F. Wilson, Regulation of cellular energy metabolism. J Membr Biol, 1982. **70**(1): p. 1-14.
21. Kondapalli, C., et al., PINK1 is activated by mitochondrial membrane potential depolarization and stimulates Parkin E3 ligase activity by phosphorylating Serine 65. Open Biol, 2012. **2**(5): p. 120080.

22. Nishikawa, T., et al., Normalizing mitochondrial superoxide production blocks three pathways of hyperglycaemic damage. Nature, 2000. **404**(6779): p. 787-90.
23. Lin, C., et al., Impaired mitochondrial oxidative metabolism in skeletal progenitor cells leads to musculoskeletal disintegration. Nat Commun, 2022. **13**(1): p. 6869.
24. Mishra, S., et al., Dairy intake and risk of hip fracture in prospective cohort studies: non-linear algorithmic dose-response analysis in 486 950 adults. J Nutr Sci, 2023. **12**: p. e96.
25. Bierhals, I.O., et al., Milk consumption, dietary calcium intake and nutrient patterns from adolescence to early adulthood and its effect on bone mass: the 1993 Pelotas (Brazil) birth cohort. Cad Saude Publica, 2019. **35**(8): p. e00192418.
26. Hagey, D.W., et al., The cellular response to extracellular vesicles is dependent on their cell source and dose. Sci Adv, 2023. **9**(35): p. eadh1168.
27. Faqeer, A., et al., Cleaved SPP1-rich extracellular vesicles from osteoclasts promote bone regeneration via TGFβ1/SMAD3 signaling. Biomaterials, 2023. **303**: p. 122367.
28. Dong, M., et al., Milk-derived small extracellular vesicles: nanomaterials to promote bone formation. J Nanobiotechnology, 2022. **20**(1): p. 370.
29. Pattappa, G., et al., The metabolism of human mesenchymal stem cells during proliferation and differentiation. J Cell Physiol, 2011. **226**(10): p. 2562-70.
30. Torimoto, K., et al., Glucose consumption of vascular cell types in culture: toward optimization of experimental conditions. Am J Physiol Cell Physiol, 2022. **322**(1): p. C73-c85.
31. Fernie, A.R., F. Carrari, and L.J. Sweetlove, Respiratory metabolism: glycolysis, the TCA cycle and mitochondrial electron transport. Curr Opin Plant Biol, 2004. **7**(3): p. 254-61.
32. Chen, C.T., et al., Coordinated changes of mitochondrial biogenesis and antioxidant enzymes during osteogenic differentiation of human mesenchymal stem cells. Stem Cells, 2008. **26**(4): p. 960-8.
33. Bornstein, R., et al., Glutamine metabolism in diseases associated with mitochondrial dysfunction. Mol Cell Neurosci, 2023. **126**: p. 103887.
34. Cruzat, V., et al., Glutamine: Metabolism and Immune Function, Supplementation and Clinical Translation. Nutrients, 2018. **10**(11).
35. Komarova, S.V., F.I. Ataullakhanov, and R.K. Globus, Bioenergetics and mitochondrial transmembrane potential during differentiation of cultured osteoblasts. Am J Physiol Cell Physiol, 2000. **279**(4): p. C1220-9.
36. Ouyang, Y., et al., Phosphate starvation signaling increases mitochondrial membrane potential through respiration-independent mechanisms. Elife, 2024. **13**.
37. Mailloux, R.J., An Update on Mitochondrial Reactive Oxygen Species Production. Antioxidants (Basel), 2020. **9**(6).
38. Schoppa, A.M., et al., Osteoblast lineage Sod2 deficiency leads to an osteoporosis-like phenotype in mice. Dis Model Mech, 2022. **15**(5).
39. Marques-Carvalho, A., H.N. Kim, and M. Almeida, The role of reactive oxygen species in bone cell physiology and pathophysiology. Bone Rep, 2023. **19**: p. 101664.
40. Hu, G., et al., Glutathione limits RUNX2 oxidation and degradation to regulate bone formation. JCI Insight, 2023. **8**(16).

41. Jin, Z.H., S.F. Wang, and W. Liao, Zoledronic acid accelerates osteogenesis of bone marrow mesenchymal stem cells by attenuating oxidative stress via the SIRT3/SOD2 pathway and thus alleviates osteoporosis. Eur Rev Med Pharmacol Sci, 2020. **24**(4): p. 2095-2101.
42. Ren, L., et al., Mitochondrial Dynamics: Fission and Fusion in Fate Determination of Mesenchymal Stem Cells. Front Cell Dev Biol, 2020. **8**: p. 580070.
43. Liu, J., et al., TMEM135 maintains the equilibrium of osteogenesis and adipogenesis by regulating mitochondrial dynamics. Metabolism, 2024. **152**: p. 155767.
44. Sidarala, V., et al., Mitofusin 1 and 2 regulation of mitochondrial DNA content is a critical determinant of glucose homeostasis. Nat Commun, 2022. **13**(1): p. 2340.
45. Na, J., et al., Extracellular matrix stiffness as an energy metabolism regulator drives osteogenic differentiation in mesenchymal stem cells. Bioact Mater, 2024. **35**: p. 549-563.
46. Mohammadalipour, A., S.P. Dumbali, and P.L. Wenzel, Mitochondrial Transfer and Regulators of Mesenchymal Stromal Cell Function and Therapeutic Efficacy. Front Cell Dev Biol, 2020. **8**: p. 603292.
47. Van Haute, L., et al., TEFM variants impair mitochondrial transcription causing childhood-onset neurological disease. Nat Commun, 2023. **14**(1): p. 1009.
48. Zamudio-Ochoa, A., et al., Mechanisms of mitochondrial promoter recognition in humans and other mammalian species. Nucleic Acids Res, 2022. **50**(5): p. 2765-2781.
49. Nolfi-Donegan, D., A. Braganza, and S. Shiva, Mitochondrial electron transport chain: Oxidative phosphorylation, oxidant production, and methods of measurement. Redox Biol, 2020. **37**: p. 101674.
50. Houten, S.M., et al., The Biochemistry and Physiology of Mitochondrial Fatty Acid β-Oxidation and Its Genetic Disorders. Annu Rev Physiol, 2016. **78**: p. 23-44.
51. Suchacki, K.J., et al., A Systems-Level Analysis of Total-Body PET Data Reveals Complex Skeletal Metabolism Networks in vivo. Front Med (Lausanne), 2021. **8**: p. 740615.
52. Sheppard, A.J., et al., Emerging Role of (18)F-NaF PET/Computed Tomographic Imaging in Osteoporosis: A Potential Upgrade to the Osteoporosis Toolbox. PET Clin, 2023. **18**(1): p. 1-20.

SUPPLEMENTAL INFORMATION

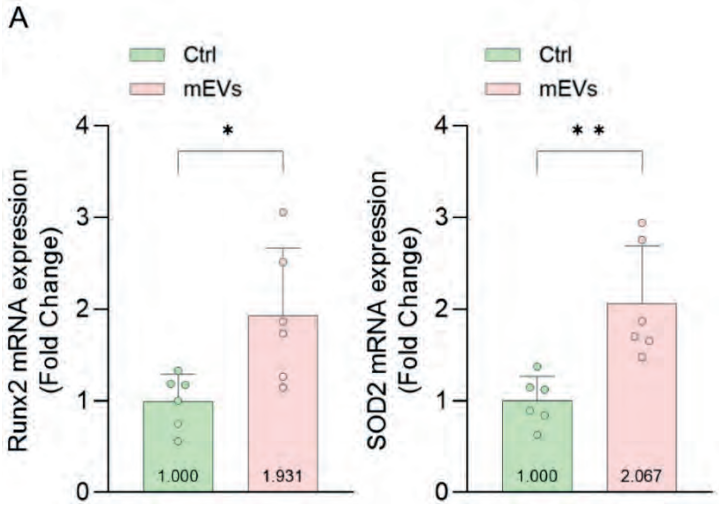

Fig. S1. mEVs improved Runx2 and SOD2 mRNA expression levels at day 2 of osteogenesis. (A) qRT-PCR analysis of Runx2 and SOD2 mRNA expressions with or without mEVs at day 2 (n=6). Data were expressed as means ± standard deviation (SD). *$p < 0.05$, **$p < 0.01$.

Table S1. List of primers used for qPCR.

Gene	Forward primer sequence (5′-3′)	Reverse primer sequence (3′-5′)
MFN1	CCTGGCATCCAGGAGTTAGA	TGGTTCCAGCAATGCGATTT
MFN2	TGCAGGTGTAAGGGACGATT	GAGGCTCTGCAAATGGGATG
DRP1	CAAAGCAGTTTGCCTGTGGA	TCTTGGAGGACTATGGCAGC
Fis1	CCAAATCCTGAAGGAGACGC	GCTGAAGGCCACAGAGGATA
TEFM	TGAGAAAGCTCCTCAAACCAGAC	CAGTCCAGCACTGTCAACTTACG
TFB2M	GGGAAAACCAAGTAGACCTCCAC	TTTCGAGCGCAACCACTTTGGC
Runx2	GCAAGGTTCAACGATCTGAGA	TTCCCGAGGTCCATCTACTG
SOD2	CAGTGCCTGCCCTAGTCATA	TTGCTTCCTTGTTTTGCTCCAA
RPS27a	TGGCTGTCCTGAAATATTATAAGGT	CCCCAGCACCACATTCATCA

Chapter 4

ECM-Binding Properties of Extracellular Vesicles: Advanced Delivery Strategies for Therapeutic Applications in Bone and Joint Diseases

Peng Wang, Johanna F.A. Husch, Onno J. Arntz, Peter M. van der Kraan, Fons A.J. van de Loo, Jeroen J.J.P. van den Beucken

Cell Commun Signal. 2025 Apr 2;23(1):161.

ABSTRACT

Extracellular vesicles (EVs) and the extracellular matrix (ECM) are essential in maintaining bone and joint health by facilitating intercellular communication, regulating tissue processes and providing structural support. EVs with a large surface area carry diverse biomolecules to steer the function of cells in their surroundings. To understand how EVs localize to specific sites, we here review the available knowledge on EV surface biomolecules and their interactions with ECM components that are crucial for regulating bone remodeling, cartilage maintenance, and immune responses, playing roles in both tissue homeostasis and pathological conditions, such as arthritis and osteoporosis. More importantly, using analyses of animal experimental data, we illustrate the effect of ECM-based biomaterials (e.g. hydrogels, decellularized matrices, and ECM-mimetic scaffolds) as carriers for EVs toward effective EV delivery in regenerative and immunomodulatory therapies in bone and joint tissue. These biomaterials enable sustained release and targeted delivery of EVs, promoting bone and cartilage regeneration. The insights of this review can be utilized to advance the development of cutting-edge therapies for skeletal tissue regeneration and disease management.

Keywords: bone, extracellular vesicles, extracellular matrix, delivery system, joint

INTRODUCTION

Bones and joints protect the integrity of skeletal structures with unique yet interconnected functions. Clinicians face substantial clinical challenges in addressing various bone and joint diseases, such as osteoporosis and arthritis [1, 2]. Globally, osteoporosis affects about 6.3% and 21.2% of men and women over 50, respectively. It is a socioeconomic burden due to healthcare expenses and the rising incapacity to work with patient aging. Moreover, bone fractures/defects are more common in osteoporotic patients [3]. Enhancing bone repair is required for faster fracture healing, and improved implant engraftment is currently pursued by injecting bone replacement materials and functionalizing these materials with growth factors. In addition, osteoarthritis (OA) characterized by chronic pain and loss of mobility is the most common form of arthritis in adults. OA is rising because of population growth and ageing, and the lack of an effective cure. The demand on health systems for care of patients with OA, including joint replacements is increasing [4, 5]. The cause of OA remains to be determined, whilst all patients present loss of cartilage as the main characteristic for this disease. Repairing the affected cartilage is difficult, as this tissue is not vascularized and has naturally a much slower turnover. For OA, the use of hydrogels to enhance cartilage repair is under investigation [6].

Osteoclasts, osteoblast, chondrocytes, as well as synovial cells and immune cells are the main cell types involved in bone and joint homeostasis and dysregulation. Besides, the extracellular matrix (ECM) is essential to cellular functions and represents the major acellular component of bones and joints. ECM is a naturally occurring substance that includes biochemical and biophysical components in the direct vicinity of the living cells [7]. Bone ECM is primarily composed of type I collagen, the fibrous protein that provides tensile strength, and a mineral referred to as (carbonated) hydroxyapatite that provides compressive strength. Furthermore, non-collagenous proteins such as osteocalcin, osteopontin and bone sialoprotein, play critical roles in regulating bone ECM remodeling and cell behavior [8]. In addition, ECM in cartilage and synovial tissues involves cell migration on the microscale and load bearing on the macroscale of the joint [9]. In contrast to bone ECM, cartilage ECM is primarily composed of type II collagen and proteoglycans. Proteoglycans are large molecules with a protein core and multiple glycosaminoglycan (GAG) chains, which are negatively charged and provide the cartilage with its characteristic compressive resistance. The synovium envelops the joint cavity, consisting of two unique layers: a lining layer and a fibrous-areolar sub-lining layer. The lining features an intermittent ECM composed of type III collagen

along with laminin, which plays a crucial role in controlling joint lubrication and nutrient exchange through the synovial fluid [10]. Consequently, pathological changes of bones and joints will occur in response to atypical alterations in the structure and composition of tissue specific ECM.

Over the past years, explorations on the diagnostic and therapeutic potency of extracellular vesicles (EVs) have emerged for bone and joint research [11, 12]. EVs are lipid bilayer vesicles with broad size ranges from 30-2000 nm. Based on size, EVs are categorized as (endosomal derived) exosomes and microvesicles derived from plasma membrane/cell surface (30-1000nm), and larger sized (>1000nm) apoptotic bodies, as well as large oncosomes [13]. EVs contain cargos comprising proteins, lipids, metabolites, and nucleic acids, and hence have been recognized as an essential means for intercellular communication [14]. For example, the signaling pathways for Wnt/β-catenin and NF-kB are involved in EV-mediated bone metabolism [15, 16]. Various proteins in the EV cargo, including transforming growth factor beta (TGF-β), osteoprotegerin, and EGFR ligand amphiregulin (AREG), contribute to the biological effects of EVs [17-19]. Additionally, EVs derived from infiltrating immune cells and fibroblast-like synoviocytes (FLSs) mediate communication in the deregulation of joints during local inflammation. The TNF-positive EVs derived from FLSs in rheumatoid arthritis (RA) have been confirmed to induce apoptosis resistance in T cells [20]. Furthermore, T cell EVs increased synthesis of matrix metalloproteinase (MMPs) and prostaglandin E_2 (PGE_2) by FLSs, causing ECM degradation in cartilage [21]. Through increasing the expression of MMPs-inhibitor TIMP-3 and lowering the level of ADAMTS-5 (A Disintegrin and Metalloproteinase with Thrombospondin motifs 5) of articular chondrocytes, our group previously reported that bovine milk EVs carrying TGF-β positively regulate chondrocyte homeostasis and protect against cartilage destruction [22].

EV luminal loading

It has been widely reported that EVs carry cargos, such as proteins, RNA, and small molecules as therapeutic delivery systems. Two primary approaches have been commonly used: passive loading that cargo is naturally incorporated into the EVs, and active loading, which involves techniques like electroporation to increase loading efficiency [23]. For instance, recombinant proteins such as Yap1 have been loaded into platelet-derived EVs through electroporation to promote tendon stem cell rejuvenation for tendon regeneration [24]. Likewise, CCL2-siRNA has been loaded into neural stem cells to treat traumatic injury in the spinal cord, highlighting the potential for regenerative medicine [25]. In addition, genetically engineered cells have also been used to produce EVs containing specific therapeutic proteins

or RNA. For example, long non-coding RNA MEG3 was used in EV-based therapy for osteosarcoma cells. The EVs were isolated from MSCs that have been transfected with MEG3 and these EVs were then used to inhibit osteosarcoma cell growth. In these contexts, EVs serve as highly effective delivery vehicles, protecting the inside cargo from degradation and ensuring targeted delivery to the tissues.

EV surface interactions

A large number of surface biomolecules have been identified to anchor on the EV surface for molecular interactions [26], attracting much attention from various fields of biomedicine due to some critical functional significances. For instance, autocrine EVs derived from HT1080 human fibrosarcoma cells have been reported to promote efficient and directional parent cell motility by transporting fibronectin and connecting with multiple integrins to form nascent adhesions [27]. In autoimmune diseases, EVs associate with autoantibodies to form pro-inflammatory immune complexes which contribute to disease pathology. Specially, the efficacy of antigen presentation has shown to be increased largely when B cell-derived EVs carry the functional peptide major histocompatibility complex (MHC) [28]. Our previous work demonstrated that the presence of IgM rheumatoid factor on circulating EVs in a subset of rheumatoid arthritis patients reflects changes in pre-B-cell immunity and disease activity more rapidly than changes in circulating levels of "free" IgM rheumatoid factor, which is associated with higher disease activity [29].

EV-ECM interactions

The interactions of EV surface molecules with ECM components likely regulate both cellular activities and the physical properties of tissues. Cells receive cues from the ECM, which in turn influences internal signaling that governs the formation of EVs [30]. After being released, a range of biomolecular and physical factors decide if EVs are integrated into the ECM at their site of release to participate in ECM activities either to be taken up by other cells or to be distributed to more distant tissues [31]. Once enveloped in the macromolecular ECM environment, it has been reported that EVs are categorized as an integral ECM component [32] **(Fig.1)**. On the one hand, EVs interact with ECM such as fibronectin and collagen via hydrogen bonds facilitated by heparin-binding domains rich in basic amino acids. These amino acids comprising positively charged groups form hydrogen bonds with negatively charged phosphates on EV membranes. It has been reported that such bonds exist among EVs derived from cells residing in bone tissue and collagen [33]. On the other hand, some other binding domains such as the arginine (R), glycine (G), and aspartic acid (D) (RGD) or Globular N-terminal link are key factors enabling

the diversity in receptors on the membrane of EVs to attach to the ECM components including α4β1 integrin [34] and CD44 [35].

In view of the importance of the interactions between EVs and the ECM, we here review the available knowledge on EV surface biomolecules toward understanding the interaction between EVs and ECM; we will not focus on biophysical EV–ECM network interactions as this has been done in detail in recent excellent review [36]. Furthermore, using analyses of animal experimental data, we illustrate the effect of ECM-based biomaterials encapsulating EVs for efficient EV delivery in regenerative and immunomodulatory therapies in bone and joint tissue pathologies.

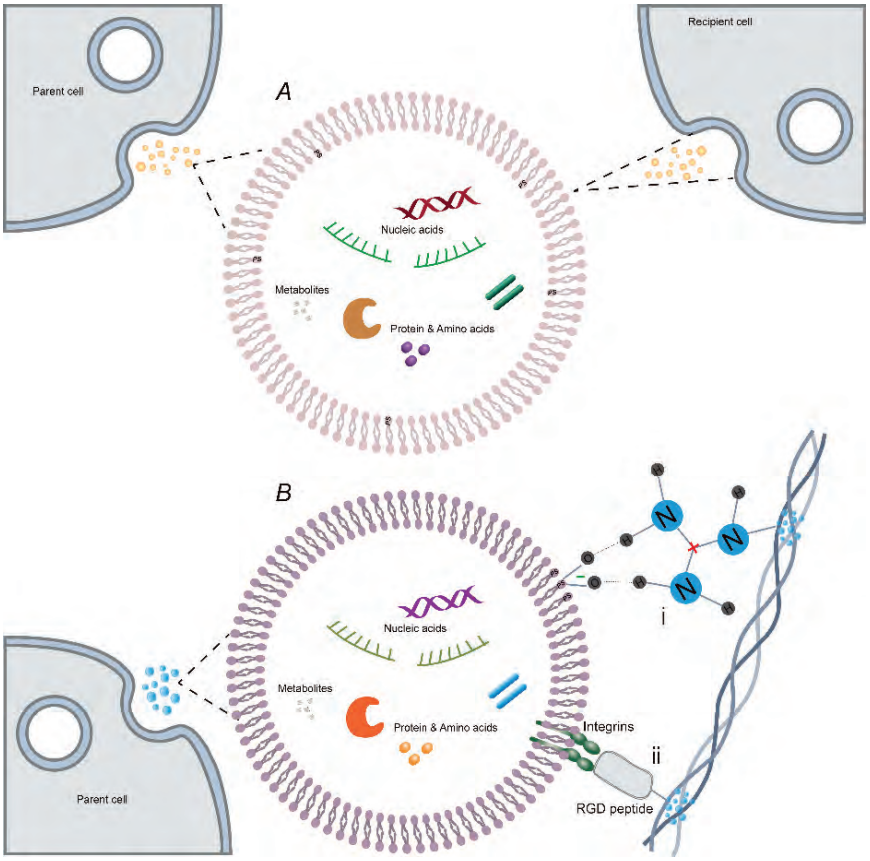

Fig. 1. Biomolecular interactions between EV surface and the ECM. Once being released from parent cells, (A) one of subpopulation of EVs are "bare EVs" within PS presenting on the inside membrane and directly taken up by cells. (B) another subset of EVs engage with the ECM through (i) hydrogen bonds between negatively charged PS on the outer membrane of the EVs and positively charged moieties within ECM proteins; or (ii) incorporating a molecular sequence, such as an RGD peptide that interacts with integrins, allows for the selective capture of specific subpopulations of EVs anchoring ECM. PS: Phosphatidylserine; RGD: amino acids arginine (R), glycine (G), and aspartic acid (D).

Surface biomolecules target EVs to ECM in bone metabolism

Integrins as one of most well-known adhesive transmembrane receptors expressed on the surface of EVs, contribute to EVs' selective targeting. Integrins consist of an alpha (18 types) and a beta (8 types) subunit that together provide selectivity of the integrin to binding specific ligands [37]. Collagen and laminin are examples of ECM components that contain motifs that are recognized by specific integrins. Typically, α3β1 are involved in binding to laminin, while α2β1 in collagen binding. For example, very recent study observed as MCF10 breast cancer EVs travel through the interstitium the EVs containing integrin α3β1 have the potential to bind to the laminin-rich ECM. This interaction influences the population of EVs entering blood and lymphatic capillaries and further determines the spatial distribution of bound and free MCF10 EVs within the interstitium [38]. In addition, α2β1 integrin mediated EVs derived from myofibroblasts to preferentially bind to type I collagen, promoting collagen crosslinking to regulate the activity of myofibroblasts in wound healing [39].

Other integrins subtype have been reported in bone metabolism. *Wellington et al.* reported that during the process of bone and tooth resorption more osteoclast EVs containing αVβ3 recognized to have affinity with hydrolyzed collagen [40], are detected in bone tissue, while more α4β1-positive osteoclast EVs are detected in dentine [41]. Based on this, they speculated it was the subtype of integrins that targeted EVs to specific ECM. Recently, one paper demonstrated that the proteomic analysis of the proteinaceous cargo of MSCs EVs revealed that identified proteins were predominantly associated with EVs. These MSCs EVs carry a variety of integrins and integrin ligands, such as collagen and laminin family molecules, implying the affinity of EVs to the corresponding ECM components in tissues [42].

Fibronectin 1 (FN1) is a glycoprotein that interacts with collagen, and proteoglycans made of heparan sulfate. The viscoelastic fibrils assembled by FN1 facilitate the maturation and tissue specificity of the ECM. Therefore, FN1 is often upregulated during embryonic development and wound healing [43]. For instance, the accumulation of the FN1 matrix in wound areas aids in the deposition of collagen and plays a role in the contraction of the wound, and α5β1 integrin as the main receptor on cells to bind FN matrix through Arg-Gly-Asp (RGD) peptide facilitate the attachment of nearby cells, enhancing the stability of the ECM [44]. *Greiling et al.* conducted a study showing that in vitro, the movement of fibroblasts from a collagen-rich matrix surrounding a wound to the wound bed relied on FN1. Their findings revealed that without FN1, the migration of fibroblasts into the fibrin clot was reduced by approximately 80%, indicating dependency on FN1 within the provisional matrix of the fibrin clot [45]. In fractures, FN1 functions as

an immediate three-dimensional framework post-injury, facilitating the formation of additional ECM components. During the inflammatory phase of healing, neutrophils secrete cellular FN1 as a provisional ECM, setting the stage for the healing process. The interaction of growth factors with FN's III 9-10/12-14 domains plays a role in attracting mesenchymal stem cells (MSCs), fibroblasts, and chondro/osteoprogenitor cells to the injury site [46].

It has been reported that FN1 on the EVs surface was involved in bone defect healing [47]. The researchers intravenously injected labeled injured neuron-derived EVs containing FN1 in rats with a tibial bone or calvarial defect. The EVs went into circulation and migrated to various organs. With optical imaging, they noted an exponential increase in the numbers of EVs in the bone tissues with defects. Moreover, the accumulation of EVs in the tissue of bone injury was reduced by coating FN1 inhibitory peptide, GRGDNP (Gly-Arg-Gly-Asp-Asn-Pro), suggesting FN1 directed EV targeting of bone.

Surface biomolecules target EVs to ECM in joint dysregulation

CD44, a member of the homing cell adhesion molecules (HCAMs), is involved in recruitment of immune cells and tumor cell metastasis [48, 49] and is regarded as the primary receptor of hyaluronan (HA) through an amino-terminal domain [50]. For instance, in bone metastases, HA retention on the surface of cancer cells is possibly mediated by CD44. *Hiraga et al.* reported that cell surface-associated HA decreased in CD44-knockdown cells and increased in CD44-overexpressing cells. Immunohistochemical examinations have shown that HA and CD44 frequently co-localize in bone metastases of certain cancer cells, suggesting that CD44-mediated capture may increase the local concentration of HA in bone metastases [51]. In addition, deposits of HA in the synovial compartment have been linked to RA. Research by *Hayes et al.* revealed that synovial tissue from RA patients exhibited a 3.5-fold increase in CD44 expression compared to that from osteoarthritis patients, and a 10.7-fold increase compared to patients with joint trauma but without chronic arthritis, suggesting a significant upregulation of CD44 in the synovial cells of RA patients, with the expression levels of CD44 in synovial tissue being associated with the intensity of inflammation [52]. Moreover, high molecular weight (HMW) HA polymers undergo depolymerization, resulting in the formation of HA fragments, which are hypothesized to activate inflammatory responses from inflammatory cells by signaling through CD44 [53].

Recently, a direct bond between EVs derived from adipose stem cells (ADSCs) and HA matrix has been reported in a model of human osteoarthritic synoviocytes.

In this study, ADSC-derived EVs were shown to have increased CD44 level when ADSCs were cultured on HA-coated surfaces and these EVs were preferably involved in the internalization process by fibroblast-like synoviocytes, meaning this interaction between the EVs and HA matrix was crucial for efficient recruitment. This interaction was supposed to be one of the mechanisms involved in superior cartilage regeneration upon intra-articular administration of stem cell EVs in combination with HA, compared to that of HA [54] or EVs alone. However, the increased CD44 level on EVs was limited and inconsistent in this study. To overexpress CD44 on EVs, stable cell lines CD44v6 (CD44 variant isoform 6) overexpression could be established using lentivirus transfection or gateway systems to produce more EVs CD44 [55].

FN1 plays a pivotal role in the development of synovial fibroblasts of RA [56]. This ECM protein, synthesized by synovial fibroblasts, contributes to the composition and structure of type III collagen along with laminin in joint, thereby influencing the architectural integrity of joints. In the context of RA, overexpression of FN1 is linked to synovial membrane thickening and pannus formation, a critical feature of rheumatoid arthritis characterized by immune cell invasion and subsequent cartilage and bone degradation [57].

Coherently, *Skriner et al.* reported that the presence of FN1 was distinctively observed in EVs derived from RA patients, in contrast to those from patients with reactive arthritis or osteoarthritis. This underscores that as one marker, FN1's specificity to RA pathophysiology, is particularly in relation to EVs [58]. *Foers et al.* reported that FN1 is detectable on human synovial fluid-derived EVs isolated and purified through ultracentrifugation in combination with size exclusion chromatography, as called “dense” or “corona” EVs [59]. Considering the documented pro-inflammatory properties of EV-fibronectin complexes, previous experimental findings might have been influenced by the potential co-isolation artifact of FN1 and EVs [39]. Moreover, in terms of EVs bioactivity and therapeutic roles, *Morteza et al.* summarized the interfering effects of protein corona on EVs [60], and FN1 in collaboration with albumin and prothrombin affected distribution capacity and targeted delivery of EVs after introduction in biofluids. They further demonstrated enzymatic treatments such as proteinase K and trypsin that target specific proteins in the corona on the surface of EVs could potentially lead to hydrolysis of those proteins, affecting the structure and function of the corona protein and the EVs themselves. Therefore, it is desirable to functionalize the EVs surface by these enzymes that hydrolyze attached soluble proteins upon EV administration.

Role of EV surface on ECM remodeling of bone and joint

ECM degradation in bone

Matrix metalloproteinases (MMPs) are well-known proteases including the metzincin superfamily [61]. They act on cholesterol, surface receptors on cell membranes, as well as nearly all kinds of ECM proteins [62]. It is known that osteoclasts activate proteinases such as MMPs and Cathepsin K, primarily associated with the breakdown of triple-helical type I collagen in bone [63]. Recently, *Lingxin et al.* observed that the double knockout of Mmp9/conditional Mmp14 mice exhibited decreased homeostatic bone turnover and were shielded from pathological bone loss [64].

According to *d'Angelo et al.,* latent transforming growth factor beta 2 (TGFb-2) was exposed and activated by matrix vesicles (MVs) containing MMP-13. They hypothesized that TGF-β activation further causes pre-osteoblastic cells to invade cartilage and differentiate into osteoblasts, accelerating the progress of OA [65]. Besides, *Tang et al.* knocked down the expression of MMP2 in mature osteoblasts-derived EVs and demonstrated its critical role in promoting endothelial cell migration, proliferation, and tube formation [66]. Interestingly, recent work reported on EVs containing tissue inhibitor of metalloproteinases 1 (TIMP1), derived from human urine-derived stem cells (USCs) and their impact on bone health among other aging-related characteristics. Specifically, the intravenous injection of USC-EVs in mouse models significantly enhanced bone quality, notably through delivering TIMP1 directly into the aging tissues to inhibit matrix MMPs, which are implicated in the aging process [67].

ECM degradation in joint

MMPs, such as MMP-1, MMP-2, and MMP-13, are commonly found in EVs derived from various cell types, including synovial cells, osteoclasts, and fibroblasts in OA and RA. These enzymes are involved in the breakdown of ECM components like collagen and proteoglycans, which are crucial for maintaining cartilage integrity. On the surface of EVs, MMPs actively contribute to ECM turnover by cleaving structural proteins, leading to degradation in joint tissues [68]. EVs expressing MMPs facilitate the modulation of inflammation and cellular invasion, both of which are essential for ECM remodeling in joint diseases. The presence of MMPs on the surface of EVs enables these vesicles to interact with recipient cells, triggering the production of additional matrix-degrading enzymes in these cells. For example, EVs from fibroblast-like synoviocytes (FLSs) in RA are involved in upregulating MMP-13 and ADAMTS-5 expression in chondrocytes, leading to further cartilage degradation and facilitating the pathological remodeling of ECM

in the joint [69]. These interactions promote tissue invasion and inflammation, accelerating joint destruction in conditions like RA. Thus, EV-associated MMPs not only contribute directly to ECM degradation but also play a pivotal role in the pathological processes that sustain inflammatory joint diseases. In addition, the formation of new blood vessels is driven by the inflammatory environment in the synovial tissue. As collagen and proteoglycans are degraded by MMPs present on EVs, the breakdown of the ECM leads to the release of pro-angiogenic factors like VEGF (vascular endothelial growth factor) and other cytokines [70]. These factors stimulate endothelial cells to proliferate and form new blood vessels, allowing for the increased delivery of inflammatory cells, nutrients, and immune mediators to the joint and exacerbating the inflammatory cycle and leading to further ECM degradation. Specifically, the presence of EVs carrying MMPs such as MMP-2, MMP-9, and MMP-13 can further enhance the degradation of ECM components and promote angiogenesis (formation of new blood vessels). This creates a vicious cycle of joint inflammation and tissue destruction MMP9 and MMP8 collaborate to activate MMP2 through the influence of reactive oxygen species, contributing to cartilage collagen breakdown and angiogenesis [71].

ECM mineralization in bone

Collagen type I in bone or collagen type X in endochondral ossification in articular cartilage become calcified due to a large amount of deposited hydroxyapatite crystals intertwined in the collagen triple helix structure [72, 73]. Matrix vesicles (MVs) secreted by osteoblasts, hypertrophic chondrocytes or macrophages are postulated to be the initial site of mineralization in the ECM [74]. Annexin calcium channeling proteins anchor MVs to collagen fibrils and subsequently facilitate an influx of calcium ions. The pre-apatitic mineral phase was then generated through the interaction of calcium with phospholipids (primarily phosphatidylserine) present in the inner membrane of the MVs. [75]. Specially, annexins (i.e. annexins II, IV, and V), alongside phosphatidylserine and tissue non-specific alkaline phosphate (TNAP), are concentrated on the MV surface, facilitating the sequestration of calcium ions necessary for the formation of hydroxyapatite crystals and shifting the ECM from a primarily organic structure to a composite of organic and inorganic materials in bone and endochondral mineralization processes [76, 77].

Furthermore, transforming growth factor beta receptor II interacting protein 1 (TRIP-1) is located in the ER and controls protein synthesis in conjunction with other initiation components [78]. It has been reported that TRIP-1 has an extracellular role as a modulator of matrix mineralization [79]. Recently, EVs derived from MC3T3-E1 cells showed to participate in transportation of TRIP-1 to the ECM, which takes up

calcium to precipitate calcium phosphate polymorphs [80], thereby facilitating matrix mineralization.

ECM synthesis in joint

HA is an anionic and non-sulfated glycosaminoglycan, involved in joint lubrication, cartilage maintenance and longitudinal bone growth [81, 82]. HA is a key element of the cartilage ECM, essential for preserving the health and function of joints. The size of HA molecules plays a significant role in how long they stay within bodily tissues. Specifically, HA with a higher molecular weight tends to stay in the joint or tissue longer before it is degraded and eliminated from the body, thereby extending its beneficial effects. Conversely, HA with a lower molecular weight can more readily move through ECM and interact with specific cells, which have a higher likelihood of inducing immune responses [83]. For example, an imbalance between the production and breakdown of HA in the synovial membrane leads to an accumulation of HA fragments, which intensifies inflammation by triggering immune cells and stimulating the release of inflammatory substances. These HA fragments, alongside CD44, play a role in sustaining ongoing inflammation and contribute to the continuous harm seen in the joints affected by RA [84].

EVs containing HA have shown to participate in ECM remodeling [85]. The amount of diffusive transfer of HA into matrix removed from the cell body may be low, but shedding EVs allow for horizontal transfer: the deposition of HA and other components, and the distribution of signaling molecules even at locations far from the cell of origin [85]. As such, the EVs surrounded by HA contribute to the creation of a regenerative microenvironment that supports stem cells and facilitates the replacement of damaged ECM through integration of other matrix elements [86]. For example, HA of synovial fluid influences the recruitment of stem cells to sites of injury and their differentiation into chondrocytes. It was reported that in OA and healthy synovial fluid, 66% of particles were identified as HA-coated EVs or HA particles, but lower proportion in RA [87]. Of note, recent work focused on the contamination of EV samples with HA and its implications for regenerative applications of corona EVs. *Goncalves et al.* demonstrated that low and medium molecular weight HA fragments, which might mimic or interfere with the immunomodulatory effects attributed to EVs, are retained in EV fractions isolated using size-exclusion chromatography and tangential flow filtration [88] **(Fig.2)**.

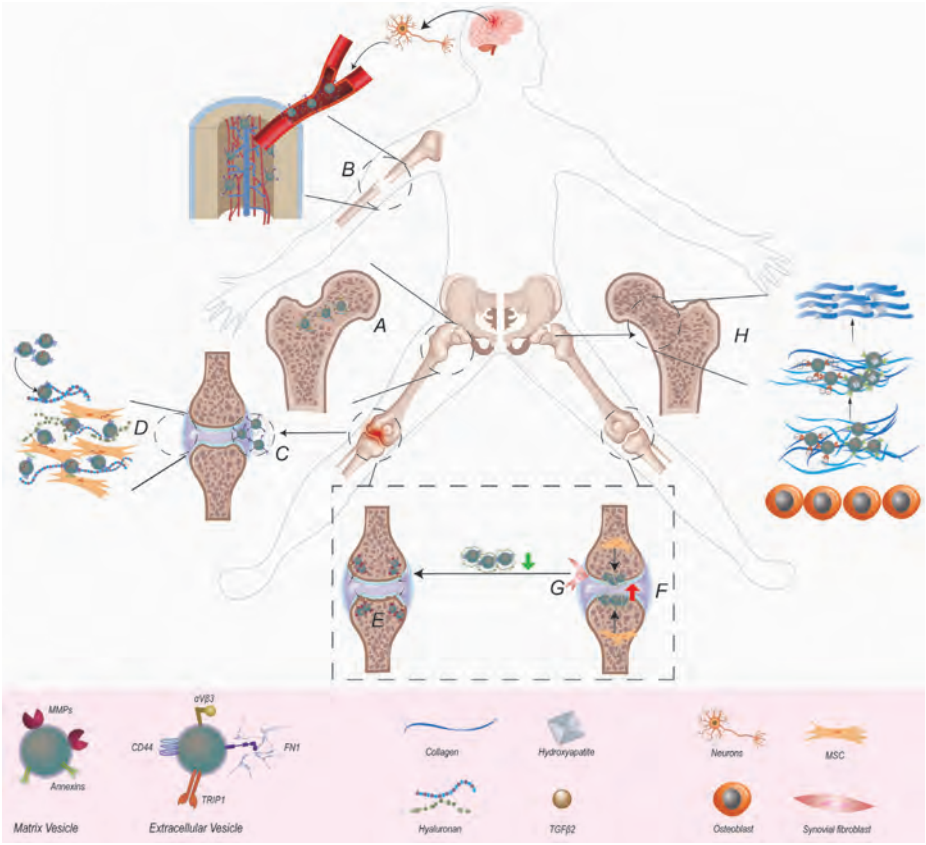

Fig. 2. EVs and ECM interaction as modulators in bone and joint homeostasis and dysregulation. (A) αVβ3 osteoclast EVs assemble in the sites of bone resorption. (B) The FN1 around the surface of EVs released by damaged neurons facilitated EV transportation to the site of bone injury via the circulatory system. (C) FN1 on EVs facilitates the attachment of EVs to cells and the internalization or better presentation of associated autoantigens to immune cells in RA. (D) Adipose MSC EVs interact with the HA of inflamed synovial membrane, promoting their accumulation and subsequent release of therapeutic cargos. (E) TGF-β activation by MMP13-MVs potentially induces the differentiation of pre-osteoblastic cells infiltrating the cartilage into osteoblasts, eventually causing the replacement of cartilage with bone tissue. (F) Hydroxyapatite crystals constituted by calcium and phosphate ions grow inside MVs containing annexins or around TRI1-MC3T3E1 derived EVs and align themselves with collagen fibers to mineralize ECM. (G) The HA-coated MSC-derived EVs are responsible for the reorganization and restoration of cartilage through integrating multiple ECM components such as FN1. (H) The decreased of HA-coated synovial fibroblast-derived EVs is implicated for the damage of synovial membrane and cartilage in RA. FN1: Fibronectin; RA: Rheumatoid Arthritis; MSC: Mesenchymal Stem Cell; TGF- β: Transforming Growth Factor Beta; MMP: Matrix metalloproteinases; HA: Hyaluronan; TRI1: Transforming Growth Factor Beta Receptor II Interacting Protein 1.

EV encapsuled in ECM-based biomaterials in bone and joint

Since MVs were first described as key players in endochondral ossification by Bonucci and Anderson in 1967, multiple reports have focused on the role of EVs derived from MSCs, macrophages, and fibroblasts regarding their contribution to bone and cartilage regeneration [89-91]. Furthermore, EVs have been applied as nanoparticles for systemic administration via intravenous or intraperitoneal injection and oral uptake, leading to systemic dispersion throughout the body. However, it seems straightforward to assume that the therapeutic efficacy of systemic administration is low for local lesions in skeletal tissues. Besides inevitably diluted due to EV clearance, the distant transportation likely makes most EVs fail to contact target tissues/organs and end up in others, such as lungs, liver, and brain [92]. Local injections have been used in preclinical research on therapeutic application in bone and joint disorders, using animal models such as antigen-induced synovitis in pigs and femoral fractures in mice [93, 94]. The results of these studies showed that EVs derived from MSCs have immunomodulatory properties and contribute to tissue regeneration. However, neither the biodistribution nor release kinetics of EVs alone are well regulated. Loaded EVs in or on biomaterials seems a feasible approach to achieve local availability and sustained release toward optimized therapeutic efficacy, especially for bone and cartilage defects, which often require relatively long healing times. Moreover, research on EVs encapsuled in ECM-based biomaterials (e.g. decellularized ECM, specific ECM components, or ECM-mimetic hydrogels) has consequently been investigated for tissue regeneration applications [95] **(Fig.3)**.

ECM-mimetic hydrogels

are particularly appealing to EVs due to their customizable mechanical characteristics and various surface modifications [96]. Typically, in a rat femoral fracture model, defect sites were treated with HA hydrogels with embedded EVs from human umbilical cord mesenchymal stem cells (hUMSCs) or human embryonic kidney 293 cells. The findings indicated that the hUMSC-derived EVs facilitated angiogenesis via the activation of HIF-1α-mediated pathways. More importantly, the animals experiment results implied these EVs loaded in HA hydrogel promoted bone regeneration. Since EV biodistribution or release kinetics were not reported, the function of the HA hydrogel as an EV carrier remains unknown [97]. Of note, other work demonstrated that in 14 days an injectable hydroxyapatite combined with HA-alginate hydrogel (i.e. a composite hydrogel) had a relatively slower EV release effect (~ 70%) than pure HA-alginate hydrogel (~ 85%) in vitro. However, it remains unclear which specific molecules contributed to the assembly of EVs on hydroxyapatite, which commonly acts as a ‘magnet’ for multiple biological

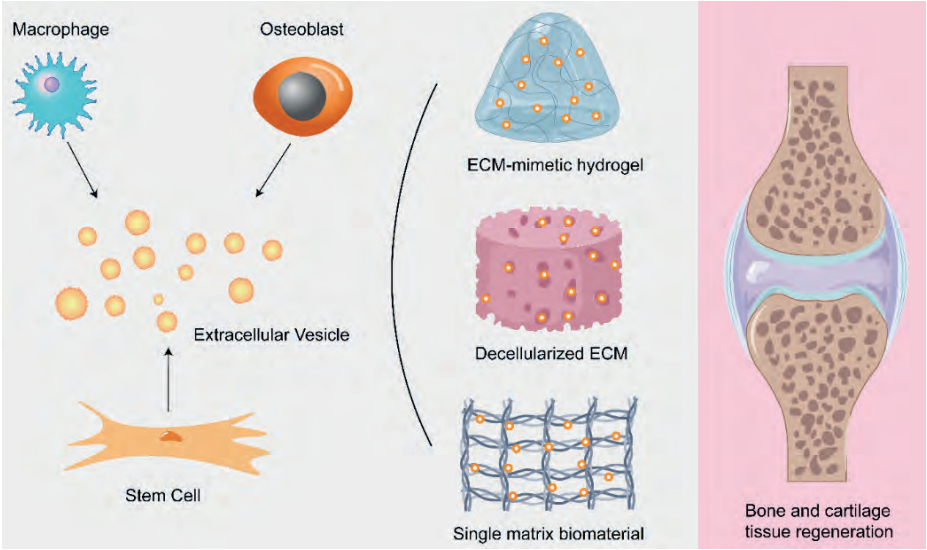

Fig. 3. The applications of EVs with ECM-based biomaterials in bone and cartilage regeneration. Once being released from stem cells or osteoblast or macrophages, EVs are loaded into different ECM-based biomaterials such as ECM-mimetic hydrogel, decellularized ECM as well as single matrix biomaterials to realize sustainable local EV delivery. The EV-functionalized ECM scaffolds have been implanted on the at sites of bone or cartilage tissue damage or degeneration to enhanced regeneration and repair.

molecules [98]. Furthermore, the effect of the different released amounts of EVs on bone regeneration is unknown in this study, as the experimental group utilizing pure HA-alginate hydrogel as a carrier of EVs was not included [99]. Recently, an ECM-mimetic hydrogel comprising chitosan-collagen was used to study delivery of murine osteoblast-derived EVs and promote hBMSCs osteogenic differentiation in vitro. This work showed the ratio of chitosan over collagen in hydrogels to play a positive role in immobilizing EVs and subsequent osteogenic effects on hBMSCs [100]. In the transwell system, compared with 8% EV release in 65%Chitosan-35%Collagen hydrogel and 2% in 0%Chitosan-100%Collagen hydrogel, 100% Chitosan-0%Collagen hydrogel had 20% EV release during 7-days observation, with optimal effects on osteogenesis. The researchers speculated that the difference in EV release may be due to the ECM types and EV affinity. Indeed, collagen type I connects with annexins or integrins present on the EV surface, while chitosan absorbs with EVs through electrostatic interactions [101]. Another study demonstrated that a hydrogel device, integrating MSC-EVs within an HA-based hydrogel matrix with specific formulation, has been designed for harnessing the osteogenic and angiogenic potential of the EVs in a controlled-release system, enhancing the regeneration of bone tissue. The study meticulously quantified the release of MSC-derived exosomes from the alginate-HA (ALG-HA) hydrogels. After

14 consecutive days of monitoring, a specific hydrogel ratio of ALG:HA (5%:2.5%) exhibited a slow but steady release of ~ 80% of encapsulated exosomes. In comparison, a different ratio of ALG:HA (5%:5%) showed a release of ~60%, and ALG: HA (2.5%:5%) showed the slowest release of ~40%. In the animal experiments, the ALG: HA (5%:5%) hydrogel was selected due to its favorable mechanical strength and moderate EVs release profile, and with 50% amount of EVs incorporation, this material had the most optimal effect on bone healing and regeneration [102].

Zhang et al. recently investigated a specially designed hydrogel combined with EVs as an innovative approach for cartilage repair [103]. Their work introduces the incorporation of EVs derived from BMSCs into a hydrogel composed of alginate-dopamine, chondroitin sulfate, and regenerated silk fibroin (AD/CS/RSF), which exhibits significant adhesive strength to wet cartilage surfaces. Moreover, the hydrogel sustainably released the encapsulated EVs for at least 14 days to ensure a continuous supply of EVs to the cartilage defect site. However, the detailed quantitative data for describing the percentage of EVs released at various time points within the 14-day period was not provided. A recent study reported a composition of EVs and hydrogel made of aldehyde-functionalized chondroitin sulfate and gelatin methacryloyl designed for enhancing ECM synthesis and chondrogenesis. A bicinchoninic acid assay was conducted to quantify the amount of EVs in hydrogel released into phosphate-buffered saline for two weeks, and it showed over 80% of the encapsulated EVs were released by day 14 [104].

Decellularized ECM

Xenogenic or allogenic bone tissue can be used to prepare decellularized bone ECM scaffolds. These fulfill the requirement for bioactive cellular support, resembling the natural extracellular environment more closely than artificial scaffolds [105]. For the decellularized ECM, bone-derived ECM, particularly decalcified bone matrix, is highly recommended due to its inherent osteoinductive properties that promote bone regeneration [106]. The species of origin should ideally be porcine or bovine ECM due to their biological similarity to humans, which enhances translational relevance [107]. Functionalizing dECM with EVs derived from MSCs is recommended, as EVs have been shown to promote angiogenesis and tissue regeneration. For example, *Xie et al.* reported on a bovine decalcified bone matrix coated with fibronectin that was investigated to carry MSC-derived EVs. After EV labeling by carboxyfluorescein succinimidylamino ester, scanning electron microscopy (SEM) images showed that EVs were dispersed evenly in the scaffolds (EV-modified scaffold). In this study, micro-computed tomography scanning and histological analysis showed that more bone formation was observed in EV-

modified dECM scaffolds. The Immunohistochemical staining for CD31 proved that vascularization happened in the EV-modified dECM scaffolds, implying enhanced bone regeneration. [108]. However, the EV release kinetics from the scaffolds remained unclear in this study. Moreover, one more control group (exogenous EV introduction after in vivo implantation of unmodified scaffold) for functional comparative analysis was lacking.

As for targeting cartilage tissues, cartilage ECM or adipose-derived ECM are desirable to support the differentiation of stem cells into chondrogenic or adipogenic lineages. One recent report demonstrated that the effects of acellular cartilage ECM scaffold (ACECMs) on osteochondral regeneration were enhanced by exogenous Wharton's jelly MSC-EVs injection. In a rabbit knee osteochondral defect model, an evident longitudinally aligned articular cartilage-like structure was formed at the implantation site. However, only the cytocompatibility of stained BMSCs on the ACECM was observed using scanning electron microscopy (SEM) and confocal laser scanning microscopy; no data on EV retention to the scaffold were described [109]. Similarly, a 3D printed ACECM construct consisting of gelatin methacrylate (GelMA) loaded with MSC-EVs was applied in a rabbit knee osteochondral defect model, potentiating cartilage repair [110]. It showed that this scaffold sustainably retained more EVs both in vitro (for 14 days; > 56%) and in vivo (> 7 days) through nanoparticle tracking analysis (NTA) and IVIS (in vivo imaging system) spectrum, compared to EVs in PBS. Another study observed the cumulative release efficiency of human ADSCs derived EVs from the printed decellularized extracellular matrix (dECM) scaffold was ~ 80% after 24 days, highlighting the hydrogel's capacity for prolonged EV delivery locally at the defect site [111]. In addition to EVs derived from stem cells as the main source of EVs, also other cell types have been used as a source for EVs. Typically, a combination of M2 macrophage-derived exosomes (M2D-Exo) and ACECM and decellularized Bone Matrix scaffolds is an innovative approach for osteochondral regeneration, in which M2D-Exo reduced the expression of pro-inflammatory factors and promote M2 polarization, beneficial for cartilage repair [112].

Single matrix biomaterial

Despite the use of decellularization techniques, isolating and obtaining sufficient tissues remains a time-consuming and costly process, and control over the exact composition of the ECM is limited due to donor variability. Consequently, research has focused on single components of ECM. *Huang & Narayanan* reported on CD63-labeled EVs from human dental pulp stem cells and hBMSCs that were quantified to assess their binding to fibronectin, which was blocked by RGD peptide. Moreover,

through determining the connection with collagen I membrane in vitro by ELISA assays, an increased amount of bound EV without saturation was observed. However, the role of collagen membrane on EVs delivery remained unclear after in vivo implantation [113, 114]. Interestingly, one study reported by the same research team demonstrated the prolonged delivery of functionally engineered EVs derived from BMP2 expressing human MSCs has been realized in 4% alginate hydrogels containing RGD peptide in vivo. Since alginate gels are known to exhibit nano-sized mesh networks (normally 10-100nm) that give alginate gels unique properties to entrap molecules, and the capacity to control the release of these molecules over time. Increasing the concentration of alginate will generally create smaller pores. It is not surprising that compared to 2% alginate, slower EVs release in higher concentration of alginate (4%) has been observed in this study. Furthermore, compared to nearly 50% EV release from 4% alginate hydrogels, similar hydrogels additionally containing RGD peptide showed much lower EV release (20%). Consistently, the use of these hydrogels in a rat calvarial defect model (with 4 and 8 weeks of implantation) showed improved bone regeneration for the 4% alginate hydrogels containing RGD peptide [115]. Similarly, confocal laser-scanning microscopy showed that human periodontal-ligament stem cell (hPDLSCs)-derived EVs, engineered by polyethyleneimine (PEI), had better capacity to adhere onto a commercially available collagen membrane (Evo; name of manufacturer) compared to the membrane without EVs, and promoted better bone regeneration in a calvarium defect animal model. However, the better effect of PEI-EVs on bone regeneration was ascribed to cellular internalization, which was due to the positive charge and proton-sponge property of PEI-EVs. The explanation for more PEI-EVs loaded onto the membrane compared with unmodified EVs was lacking [116] **(Table 1)**.

Table 1. Summary of EVs with ECM-based biomaterials in bone and cartilage regeneration.

Material	Specific Types & Source	Application	Results	Reference
ECM-mimetic hydrogel				
Hystem-HP hydrogel	Exosomes derived from hUCMSCs	Rat femoral osteotomy	Enhanced bone healing and angiogenesis for hUCMSCs derived exosomes than HEK293 cell derived exosome or empty control	(97)
HAP/HA-ALG	Exosomes derived from hUCMSCs	Rat cranial defect	1. In 14 days, nearly 70% exosomes release in HAP/ HA-ALG hydrogel, and 85% in HA-ALG hydrogel. 2. Increased bone healing for exosome +HAP/HA-ALG compared to HAP/HA-ALG or empty control.	(99)
Chitosan/Collagen I-b-glycerophosphate	EVs derived from murine osteoblast	Osteogenic differentiation of hBMSCs	1. In 7 days, 20% EV release in 100%Chitosan-Collagen hydrogel, and 8% in 65%Chitosan-35%Collagen hydrogel and 2% in 0%Chitosan-100%Collagen hydrogel 2. In transwell system, the best proliferation and osteogenesis of hBMSCs in 100%Chitosan-Collagen hydrogel + EVs.	(100)
Alginate/ HA	Exosomes derived from rat MSCs	Rat calvarial defect model	1. Hydrogel ratio of ALG:HA (5%:2.5%) exhibited a slow but steady release of ~ 80% of encapsulated exosomes. A different ratio of ALG:HA (5%:5%) showed a release of ~60%, and ALG: HA (2.5%:5%) had the slowest release rate at ~ 40%. 2. Best improvement in bone healing and regeneration in Alginate/ HA+ 50% EVs group	(102)
AD/CS/RSF	Exosomes derived from rat BMSCs	Rat osteochondral defect	1. Sustained release of encapsulated exosomes over at least 14 days from AD/CS/RSF hydrogel. 2. Improved outcomes in cartilage surface smoothness, continuity, and the generation of hyaline-like cartilage	(103)
Chondroitin sulfate/ gelatin methacryloyl	Exosomes derived from rat BMSCs	Rat distal femoral drill-hole growth plate injury model	1. Over 80% of the encapsulated exosomes were released by day 14. 2. Increased chondrocyte anabolism and enhanced growth plate injury repair through ECM remodeling.	(104)

Table 1. Continued

Material	Specific Types & Source	Application	Results	Reference
Decellularized ECM				
DBM	EVs derived from rat BMSCs	Nude mice subcutaneous	Increased bone induction and blood vessel formation for EVs+rBMSCs compared to other two components alone or scaffold only	(108)
ACECM	Exosomes derived from human umbilical cord Wharton's jelly MSC	Rat and Rabbit femoral trochlear osteochondral defect	Exosomes enhance M2 response compared to PBS. Exosomes +ACECM improves osteochondral regeneration compared to ACECM, Exosomes, PBS or sham only	(109)
2% cartilage ECM/GelMA	Exosomes derived from BMSCs	Rabbit patellar groove osteochondral defect	1. In 14 days, nearly 44% exosome release in ECM/GelMA scaffold in vitro. In 7 days, better EV retention in 3D printed ECM/ GelMA scaffold compared to control (Exosomes in PBS) in subcutaneous mouse model. 2. Enhanced M2 response, cartilage and subchondral bone regeneration by ECM/GelMA/Exosomes scaffold compared to no treatment group, GelMA scaffold group, and ECM/GelMA group	(110)
Hydrogel-dECM scaffold	Exosomes derived from hADSCs	Rat knee osteochondral defects	1. Over 80% of the encapsulated exosome were released by day 24. 2. The Exosomes-enriched groups showed superior outcomes in terms of the quality of regenerated tissue, including improved matrix deposition, enhanced cellular infiltration, and more robust integration with surrounding tissues.	(111)
ACECM ABECM	Exosomes derived from rat M2 macrophages	Osteochondral defect model of rats	The promotion of osteochondral regeneration and the regulation of the joint cavity's inflammatory microenvironment.	(112)

Table 1. Continued

Material	Specific Types & Source	Application	Results	Reference
Single matrix biomaterial				
Type I collagen	Exosomes derived from hDPSCs	Human root slice model in nude mice	Stimulated Exosomes+hDPSCs induced more dental pulp-like tissue regeneration than unstimulated Exosomes+hDPSCs and hDPSCs only	(113)
Type I collagen	Exosomes derived from hMSCs	Nice mice subcutaneous	Increased bone induction and vascularization for stimulated Exosomes +hMSCs than unstimulated Exosomes +hMSCs and hMSCsonly	(114)
Alginate hydrogels containing RGD peptide	EVs derived from BMP2 overexpressing hMSCs	Rat calvarial bone defect	In 7 days, 20% EV release in 4%-Alginate-RGD hydrogel, compared with 100% in 2% Alginate hydrogel and 50% in 4% Alginate hydrogel and 2%-Alginate-RGD hydrogel in vitro In 4 and 8 weeks, best bone repair in 4%-alginate-RGD hydrogel hydrogel + EVs, among 4%-alginate hydrogels + /- EVs, and alginate-RGD hydrogels only	(115)
Evolution collagen membrane	EVs derived from hPDLSCs (+/- PEI modification)	Rat calvarial bone injury	Improved bone healing observed for PEI-EVs+hPDLSCs than hPDLSCs or PEI-EVs only.	(116)

CONCLUSIONS

The small diameter of EVs leads to large surface-to-volume ratio of EVs [117], allowing for more surface interactions between EV surface structures and molecules within the ECM and on the cell surface. The molecular basis of the interaction between EVs and ECM is expected on the basis of their biochemical composition and chemical bonds. Specifically, hydrogen bonds have been mentioned before to bridge some subsets of EVs and fibronectin or collagen in heparin-binding domain. In addition, other subsets of EVs contain cysteines exposed to the extracellular space, forming covalent bonds with ECM proteins such as laminin [31]. The specificity of these interactions appears important for the regulation of the extracellular microenvironment of bone and joint tissue. In this view, considering the EV surface to interact with a biological environment is of utmost importance to fully exploit the potential of EVs for therapeutic applications. The interactions between EVs and the ECM have been studied for their role in altering the biodistribution of EVs, and considering EVs ability to penetrate tissue barriers, it highlights the growing importance of EV-based therapies.

The synergy between EVs and ECM-based scaffolds is central to the emerging therapeutic strategy. ECM-based biomaterials serve as biologically compatible delivery platforms that closely mimic the native tissue environment. The local delivery of EVs from ECM-based scaffolds is particularly advantageous for bone and joint regeneration. Bone tissue regeneration often requires prolonged therapeutic interventions due to the slow healing process and the need for precise spatiotemporal control over biomolecule delivery. ECM-based scaffolds address this challenge by providing sustained release mechanisms that ensure prolonged EV activity at the site of injury. In cartilage repair, where avascularity and limited cellular turnover present significant obstacles, ECM-based scaffolds embedded with EVs have been shown to enhance chondrocyte activity, protect against ECM degradation, and stimulate cartilage matrix synthesis. Therefore, it should be emphasized that the availability of EVs largely depends on control over EV release. In view of this, cells in the host tissues such as MSCs and endothelial cells are supposed to be recruited on or in the biomaterials [118]. In this review, we summarized that EVs are increasingly being utilized in conjunction with ECM-based biomaterials, such as ECM-mimetic hydrogels and decellularized ECM scaffolds. Moreover, some of these studies explicitly demonstrated the positive role of this hydrogen bond between EVs and ECM-based materials on tissue regeneration, and the essential biomolecules such as integrins and fibronectin have been applied.

Manufacturing challenges and Regulatory hurdles

While the therapeutic promise of EVs delivered via ECM-based scaffolds is clear, several challenges remain to be addressed. Achieving scalable production within low cost and consistent quality control as the regular manufacturing challenges on regenerative medicine. Moreover, the heterogeneity of EV populations poses significant barrier to clinical translation. EV heterogeneity implies that individual vesicles may not possess all the chemical or physical characteristics attributed to the bulk population, indicating that each vesicle might lack certain functional properties including ECM binding ability and related therapeutic functions that are associated with the bulk. For example, Y*ijun Zhou et al*. demonstrated that heparin-chromatography separated the two subpopulations of cancer cell-derived EVs. These two EVs had similar biophysical characteristics but non-heparin binding EVs did not induce ERK1/2 phosphorylation or Ki67 activation, while EVs with heparin binding property induced ERK1/2 phosphorylation and Ki67 activation [119]. Therefore, it is eminent to understand the detailed mechanisms underlying EV-ECM interactions, and optimizing scaffold formulations for specific applications is a critical topic for future research. In addition, the safety, ethical sourcing of both ECM materials and EVs, as well as demonstrating their long-term efficacy in human trials are current regulatory hurdles. By establishing standardized sourcing protocols for ECM materials and EVs, ethical practices, safety, and traceability can be ensured. More importantly, in addition to studying the functional properties of EV-ECM, monitoring for potential chronic toxicity and immune responses should be conducted.

Key findings and outlook

We summarized the EV surface molecules such as integrins, FN1 and CD44 that guide EVs to interact with ECM components in bone and joint tissues. In addition, MMPs, TRIP-1, and HA contribute to ECM remodeling by modulating key processes such as ECM degradation, mineralization, and synthesis. More importantly, ECM-based biomaterials including hydrogels and decellularized ECM scaffolds provide biologically compatible environments for localized and sustained release of EVs, contributing to bone and cartilage regeneration.

EV-based therapies have shown great promise in treating bone and joint diseases by leveraging combination with ECM-mimetic biomaterials. Future research should focus on optimizing EV-ECM interactions and improving the design of biomaterials to enhance targeted delivery, release control, and therapeutic efficacy. Despite the challenges, such as EV heterogeneity and the complexity of ECM compositions, combining EVs with advanced biomaterials offers a potential pathway for addressing bone and joint conditions like osteoarthritis and bone defects.

REFERENCES

1. Wang, X., et al., Matrix stiffness regulates osteoclast fate through integrin-dependent mechanotransduction. Bioact Mater, 2023. **27**: p. 138-153.
2. Komatsu, N. and H. Takayanagi, Mechanisms of joint destruction in rheumatoid arthritis - immune cell-fibroblast-bone interactions. Nat Rev Rheumatol, 2022. **18**(7): p. 415-429.
3. Reid, I.R., A broader strategy for osteoporosis interventions. Nat Rev Endocrinol, 2020. **16**(6): p. 333-339.
4. Price, A.J., et al., Knee replacement. Lancet, 2018. **392**(10158): p. 1672-1682.
5. Ferguson, R.J., et al., Hip replacement. Lancet, 2018. **392**(10158): p. 1662-1671.
6. Johnbosco, C., et al., Microencapsulated stem cells reduce cartilage damage in a material dependent manner following minimally invasive intra-articular injection in an OA rat model. Mater Today Bio, 2023. **22**: p. 100791.
7. Theocharis, A.D., et al., Extracellular matrix structure. Adv Drug Deliv Rev, 2016. **97**: p. 4-27.
8. Bailey, S., et al., Structural role of osteocalcin and its modification in bone fracture. Appl Phys Rev, 2023. **10**(1): p. 011410.
9. Qu, F., F. Guilak, and R.L. Mauck, Cell migration: implications for repair and regeneration in joint disease. Nat Rev Rheumatol, 2019. **15**(3): p. 167-179.
10. Buckley, C.D., et al., Location, location, location: how the tissue microenvironment affects inflammation in RA. Nat Rev Rheumatol, 2021. **17**(4): p. 195-212.
11. Liu, M., Y. Sun, and Q. Zhang, Emerging Role of Extracellular Vesicles in Bone Remodeling. J Dent Res, 2018. **97**(8): p. 859-868.
12. Malda, J., et al., Extracellular vesicles — new tool for joint repair and regeneration. Nat Rev Rheumatol, 2016. **12**(4): p. 243-9.
13. Zhang, Y., et al., Advanced extracellular vesicle bioinformatic nanomaterials: from enrichment, decoding to clinical diagnostics. J Nanobiotechnology, 2023. **21**(1): p. 366.
14. Ali, S.A., et al., The non-coding RNA interactome in joint health and disease. Nat Rev Rheumatol, 2021. **17**(11): p. 692-705.
15. Lei, F., et al., Treatment of inflammatory bone loss in periodontitis by stem cell-derived exosomes. Acta Biomater, 2022. **141**: p. 333-343.
16. Tian, J., et al., Small extracellular vesicles derived from hypoxic preconditioned dental pulp stem cells ameliorate inflammatory osteolysis by modulating macrophage polarization and osteoclastogenesis. Bioact Mater, 2023. **22**: p. 326-342.
17. Tan, S.H.S., et al., Mesenchymal stem cell exosomes in bone regenerative strategies-a systematic review of preclinical studies. Mater Today Bio, 2020. **7**: p. 100067.
18. Chen, C.Y., et al., Extracellular vesicles from human urine-derived stem cells prevent osteoporosis by transferring CTHRC1 and OPG. Bone Res, 2019. **7**: p. 18.
19. Raimondo, S., et al., Multiple myeloma-derived exosomes are enriched of amphiregulin (AREG) and activate the epidermal growth factor pathway in the bone microenvironment leading to osteoclastogenesis. J Hematol Oncol, 2019. **12**(1): p. 2.
20. Zhang, H.G., et al., A membrane form of TNF-alpha presented by exosomes delays T cell activation-induced cell death. J Immunol, 2006. **176**(12): p. 7385-93.

21. Zhang, L., et al., Nanoenzyme engineered neutrophil-derived exosomes attenuate joint injury in advanced rheumatoid arthritis via regulating inflammatory environment. Bioact Mater, 2022. **18**: p. 1-14.
22. Pieters, B.C.H., et al., Bovine Milk-Derived Extracellular Vesicles Inhibit Catabolic and Inflammatory Processes in Cartilage from Osteoarthritis Patients. Mol Nutr Food Res, 2022. **66**(6): p. e2100764.
23. Kim, H.I., et al., Recent advances in extracellular vesicles for therapeutic cargo delivery. Exp Mol Med, 2024. **56**(4): p. 836-849.
24. Lu, J., et al., Rejuvenation of tendon stem/progenitor cells for functional tendon regeneration through platelet-derived exosomes loaded with recombinant Yap1. Acta Biomater, 2023. **161**: p. 80-99.
25. Rong, Y., et al., Engineered extracellular vesicles for delivery of siRNA promoting targeted repair of traumatic spinal cord injury. Bioact Mater, 2023. **23**: p. 328-342.
26. Belov, L., et al., Extensive surface protein profiles of extracellular vesicles from cancer cells may provide diagnostic signatures from blood samples. J Extracell Vesicles, 2016. **5**: p. 25355.
27. Sung, B.H., et al., Directional cell movement through tissues is controlled by exosome secretion. Nat Commun, 2015. **6**: p. 7164.
28. Buzas, E.I., The roles of extracellular vesicles in the immune system. Nat Rev Immunol, 2023. **23**(4): p. 236-250.
29. Arntz, O.J., et al., Rheumatoid Arthritis Patients With Circulating Extracellular Vesicles Positive for IgM Rheumatoid Factor Have Higher Disease Activity. Front Immunol, 2018. **9**: p. 2388.
30. Wong, S.W., et al., Matrix biophysical cues direct mesenchymal stromal cell functions in immunity. Acta Biomater, 2021. **133**: p. 126-138.
31. Debnath, K., et al., Extracellular vesicle-matrix interactions. Nat Rev Mater, 2023. **8**(6): p. 390-402.
32. Al Halawani, A., et al., Extracellular Vesicles: Interplay with the Extracellular Matrix and Modulated Cell Responses. Int J Mol Sci, 2022. **23**(6).
33. Bailey, S., et al., The role of extracellular matrix phosphorylation on energy dissipation in bone. Elife, 2020. **9**.
34. Tang, T.T., et al., Employing Macrophage-Derived Microvesicle for Kidney-Targeted Delivery of Dexamethasone: An Efficient Therapeutic Strategy against Renal Inflammation and Fibrosis. Theranostics, 2019. **9**(16): p. 4740-4755.
35. Zhou, L., et al., Role of CD44 in increasing the potency of mesenchymal stem cell extracellular vesicles by hyaluronic acid in severe pneumonia. Stem Cell Res Ther, 2021. **12**(1): p. 293.
36. Debnath, K., et al., Extracellular vesicle–matrix interactions. Nature Reviews Materials, 2023. **8**(6): p. 390-402.
37. Kechagia, J.Z., J. Ivaska, and P. Roca-Cusachs, Integrins as biomechanical sensors of the microenvironment. Nat Rev Mol Cell Biol, 2019. **20**(8): p. 457-473.
38. Sariano, P.A., et al., Convection and extracellular matrix binding control interstitial transport of extracellular vesicles. J Extracell Vesicles, 2023. **12**(4): p. e12323.
39. Arif, S., et al., The diffusion of normal skin wound myofibroblast-derived microvesicles differs according to matrix composition. J Extracell Biol, 2024. **3**(1): p. e131.
40. McHugh, K.P., et al., Role of cell-matrix interactions in osteoclast differentiation. Adv Exp Med Biol, 2007. **602**: p. 107-11.

41. Holliday, L.S., L.P. Faria, and W.J. Rody, Jr., Actin and Actin-Associated Proteins in Extracellular Vesicles Shed by Osteoclasts. Int J Mol Sci, 2019. **21**(1).
42. Wang, X., et al., Exosomes influence the behavior of human mesenchymal stem cells on titanium surfaces. Biomaterials, 2020. **230**: p. 119571.
43. Dalton, C.J. and C.A. Lemmon, Fibronectin: Molecular Structure, Fibrillar Structure and Mechanochemical Signaling. Cells, 2021. **10**(9).
44. Singh, P., C. Carraher, and J.E. Schwarzbauer, Assembly of fibronectin extracellular matrix. Annu Rev Cell Dev Biol, 2010. **26**: p. 397-419.
45. Greiling, D. and R.A. Clark, Fibronectin provides a conduit for fibroblast transmigration from collagenous stroma into fibrin clot provisional matrix. J Cell Sci, 1997. **110 (Pt 7)**: p. 861-70.
46. Martino, M.M., et al., Engineering the growth factor microenvironment with fibronectin domains to promote wound and bone tissue healing. Sci Transl Med, 2011. **3**(100): p. 100ra89.
47. Xia, W., et al., Damaged brain accelerates bone healing by releasing small extracellular vesicles that target osteoprogenitors. Nat Commun, 2021. **12**(1): p. 6043.
48. Lesley, J. and R. Hyman, CD44 structure and function. Front Biosci, 1998. **3**: p. d616-30.
49. Alaniz, L., et al., Interaction of CD44 with different forms of hyaluronic acid. Its role in adhesion and migration of tumor cells. Cell Commun Adhes, 2002. **9**(3): p. 117-30.
50. Suzuki, A., et al., Localization of CD44 and hyaluronan in the synovial membrane of the rat temporomandibular joint. Anat Rec A Discov Mol Cell Evol Biol, 2006. **288**(6): p. 646-52.
51. Hiraga, T., S. Ito, and H. Nakamura, Cancer stem-like cell marker CD44 promotes bone metastases by enhancing tumorigenicity, cell motility, and hyaluronan production. Cancer Res, 2013. **73**(13): p. 4112-22.
52. Haynes, B.F., et al., Measurement of an adhesion molecule as an indicator of inflammatory disease activity. Up-regulation of the receptor for hyaluronate (CD44) in rheumatoid arthritis. Arthritis Rheum, 1991. **34**(11): p. 1434-43.
53. Jiang, D., J. Liang, and P.W. Noble, Hyaluronan as an immune regulator in human diseases. Physiol Rev, 2011. **91**(1): p. 221-64.
54. Ragni, E., et al., Interaction with hyaluronan matrix and miRNA cargo as contributors for in vitro potential of mesenchymal stem cell-derived extracellular vesicles in a model of human osteoarthritic synoviocytes. Stem Cell Res Ther, 2019. **10**(1): p. 109.
55. Xie, Z., et al., Exosome-delivered CD44v6/C1QBP complex drives pancreatic cancer liver metastasis by promoting fibrotic liver microenvironment. Gut, 2022. **71**(3): p. 568-579.
56. Xu, J., et al., Identification of Candidate Genes Related to Synovial Macrophages in Rheumatoid Arthritis by Bioinformatics Analysis. Int J Gen Med, 2021. **14**: p. 7687-7697.
57. Yang, J., et al., Fibronectin-1 is a dominant mechanism for rheumatoid arthritis via the mediation of synovial fibroblasts activity. Front Cell Dev Biol, 2022. **10**: p. 1010114.
58. Skriner, K., et al., Association of citrullinated proteins with synovial exosomes. Arthritis Rheum, 2006. **54**(12): p. 3809-14.
59. Foers, A.D., et al., Enrichment of extracellular vesicles from human synovial fluid using size exclusion chromatography. J Extracell Vesicles, 2018. **7**(1): p. 1490145.
60. Heidarzadeh, M., et al., Protein corona and exosomes: new challenges and prospects. Cell Commun Signal, 2023. **21**(1): p. 64.
61. Kumar, L., et al., Role of Matrix Metalloproteinases in Musculoskeletal Diseases. Biomedicines, 2022. **10**(10).

62. Grillet, B., et al., Matrix metalloproteinases in arthritis: towards precision medicine. Nat Rev Rheumatol, 2023. **19**(6): p. 363-377.
63. Zaidi, M., Skeletal remodeling in health and disease. Nat Med, 2007. **13**(7): p. 791-801.
64. Zhu, L., et al., Osteoclast-mediated bone resorption is controlled by a compensatory network of secreted and membrane-tethered metalloproteinases. Sci Transl Med, 2020. **12**(529).
65. D'Angelo, M., et al., Authentic matrix vesicles contain active metalloproteases (MMP). a role for matrix vesicle-associated MMP-13 in activation of transforming growth factor-beta. J Biol Chem, 2001. **276**(14): p. 11347-53.
66. Tang, H., et al., Exosomal MMP2 derived from mature osteoblasts promotes angiogenesis of endothelial cells via VEGF/Erk1/2 signaling pathway. Exp Cell Res, 2019. **383**(2): p. 111541.
67. Rao, S., et al., Extracellular vesicles from human urine-derived stem cells delay aging through the transfer of PLAU and TIMP1. Acta Pharm Sin B, 2024. **14**(3): p. 1166-1186.
68. Thuault, S., et al., A Journey on Extracellular Vesicles for Matrix Metalloproteinases: A Mechanistic Perspective. Front Cell Dev Biol, 2022. **10**: p. 886381.
69. Nawaz, M., et al., Extracellular Vesicles and Matrix Remodeling Enzymes: The Emerging Roles in Extracellular Matrix Remodeling, Progression of Diseases and Tissue Repair. Cells, 2018. **7**(10).
70. Turpin, D., et al., Role of extracellular vesicles in autoimmune diseases. Autoimmun Rev, 2016. **15**(2): p. 174-83.
71. Bian, Y., et al., Immunomodulatory roles of metalloproteinases in rheumatoid arthritis. Front Pharmacol, 2023. **14**: p. 1285455.
72. Buckwalter, J.A. and R.R. Cooper, Bone structure and function. Instr Course Lect, 1987. **36**: p. 27-48.
73. Shen, G., The role of type X collagen in facilitating and regulating endochondral ossification of articular cartilage. Orthod Craniofac Res, 2005. **8**(1): p. 11-7.
74. New, S.E. and E. Aikawa, Role of extracellular vesicles in de novo mineralization: an additional novel mechanism of cardiovascular calcification. Arterioscler Thromb Vasc Biol, 2013. **33**(8): p. 1753-8.
75. Davies, O.G., et al., Annexin-enriched osteoblast-derived vesicles act as an extracellular site of mineral nucleation within developing stem cell cultures. Sci Rep, 2017. **7**(1): p. 12639.
76. Rogers, M.A., et al., Annexin A1-dependent tethering promotes extracellular vesicle aggregation revealed with single-extracellular vesicle analysis. Sci Adv, 2020. **6**(38).
77. Boyan, B.D., et al., The Role of Matrix-Bound Extracellular Vesicles in the Regulation of Endochondral Bone Formation. Cells, 2022. **11**(10).
78. Herrmannová, A., et al., Structural analysis of an eIF3 subcomplex reveals conserved interactions required for a stable and proper translation pre-initiation complex assembly. Nucleic Acids Res, 2012. **40**(5): p. 2294-311.
79. Ramachandran, A., et al., TGF beta receptor II interacting protein-1, an intracellular protein has an extracellular role as a modulator of matrix mineralization. Sci Rep, 2016. **6**: p. 37885.
80. Chen, Y. and A. George, TRIP-1 Promotes the Assembly of an ECM That Contains Extracellular Vesicles and Factors That Modulate Angiogenesis. Front Physiol, 2018. **9**: p. 1092.
81. Sprott, H. and C. Fleck, Hyaluronic Acid in Rheumatology. Pharmaceutics, 2023. **15**(9).
82. Bastow, E.R., et al., Hyaluronan synthesis and degradation in cartilage and bone. Cell Mol Life Sci, 2008. **65**(3): p. 395-413.
83. Chistyakov, D.V., et al., High and Low Molecular Weight Hyaluronic Acid Differentially Influences Oxylipins Synthesis in Course of Neuroinflammation. Int J Mol Sci, 2019. **20**(16).

84. Olsson, M., et al., Fragmented hyaluronan has no alarmin function assessed in arthritis synovial fibroblast and chondrocyte cultures. Innate Immun, 2018. **24**(2): p. 131-141.
85. Arasu, U.T., et al., Human mesenchymal stem cells secrete hyaluronan-coated extracellular vesicles. Matrix Biol, 2017. **64**: p. 54-68.
86. Phinney, D.G. and M.F. Pittenger, Concise Review: MSC-Derived Exosomes for Cell-Free Therapy. Stem Cells, 2017. **35**(4): p. 851-858.
87. Mustonen, A.M., et al., Characterization of hyaluronan-coated extracellular vesicles in synovial fluid of patients with osteoarthritis and rheumatoid arthritis. BMC Musculoskelet Disord, 2021. **22**(1): p. 247.
88. Goncalves, J.P., et al., Hyaluronic acid: An overlooked extracellular vesicle contaminant. J Extracell Vesicles, 2023. **12**(9): p. e12362.
89. Lu, X., et al., Exosomes loaded a smart bilayer-hydrogel scaffold with ROS-scavenging and macrophage-reprogramming properties for repairing cartilage defect. Bioact Mater, 2024. **38**: p. 137-153.
90. Jin, S., et al., M2 macrophage-derived exosome-functionalized topological scaffolds regulate the foreign body response and the coupling of angio/osteoclasto/osteogenesis. Acta Biomater, 2024. **177**: p. 91-106.
91. Cao, H., et al., Bio-nanoparticles loaded with synovial-derived exosomes ameliorate osteoarthritis progression by modifying the oxidative microenvironment. J Nanobiotechnology, 2024. **22**(1): p. 271.
92. Aqil, F., et al., Exosomes for the Enhanced Tissue Bioavailability and Efficacy of Curcumin. Aaps j, 2017. **19**(6): p. 1691-1702.
93. Casado, J.G., et al., Mesenchymal Stem Cell-Derived Exosomes: Immunomodulatory Evaluation in an Antigen-Induced Synovitis Porcine Model. Front Vet Sci, 2017. **4**: p. 39.
94. Furuta, T., et al., Mesenchymal Stem Cell-Derived Exosomes Promote Fracture Healing in a Mouse Model. Stem Cells Transl Med, 2016. **5**(12): p. 1620-1630.
95. De Jong, O.G., et al., Extracellular vesicles: potential roles in regenerative medicine. Front Immunol, 2014. **5**: p. 608.
96. Zhang, K., et al., Nanocomposite hydrogels stabilized by self-assembled multivalent bisphosphonate-magnesium nanoparticles mediate sustained release of magnesium ion and promote in-situ bone regeneration. Acta Biomater, 2017. **64**: p. 389-400.
97. Zhang, Y., et al., Exosomes from human umbilical cord mesenchymal stem cells enhance fracture healing through HIF-1α-mediated promotion of angiogenesis in a rat model of stabilized fracture. Cell Prolif, 2019. **52**(2): p. e12570.
98. Kadu, K., et al., Role of surface charges on interaction of rod-shaped magnetic hydroxyapatite nanoparticles with protein. Colloids Surf B Biointerfaces, 2019. **177**: p. 362-369.
99. Yang, S., et al., Integration of Human Umbilical Cord Mesenchymal Stem Cells-Derived Exosomes with Hydroxyapatite-Embedded Hyaluronic Acid-Alginate Hydrogel for Bone Regeneration. ACS Biomater Sci Eng, 2020. **6**(3): p. 1590-1602.
100. Man, K., et al., An ECM-Mimetic Hydrogel to Promote the Therapeutic Efficacy of Osteoblast-Derived Extracellular Vesicles for Bone Regeneration. Front Bioeng Biotechnol, 2022. **10**: p. 829969.
101. Ju, Y., et al., Extracellular vesicle-loaded hydrogels for tissue repair and regeneration. Mater Today Bio, 2023. **18**: p. 100522.

102. Wan, L., et al., Development of an integrated device utilizing exosome-hyaluronic acid-based hydrogel and investigation of its osteogenic and angiogenic characteristics. Materials & Design, 2024. **237**: p. 112565.
103. Zhang, F.X., et al., Injectable Mussel-Inspired highly adhesive hydrogel with exosomes for endogenous cell recruitment and cartilage defect regeneration. Biomaterials, 2021. **278**: p. 121169.
104. Guan, P., et al., Exosome-loaded extracellular matrix-mimic hydrogel with anti-inflammatory property Facilitates/promotes growth plate injury repair. Bioact Mater, 2022. **10**: p. 145-158.
105. Bryksin, A.V., et al., Learning from nature - novel synthetic biology approaches for biomaterial design. Acta Biomater, 2014. **10**(4): p. 1761-9.
106. Yu, M., et al., Regeneration of Mechanically Enhanced Tissue-Engineered Cartilage Based on the Decalcified Bone Matrix Framework. ACS Biomater Sci Eng, 2023. **9**(8): p. 4994-5005.
107. Capella-Monsonís, H. and D.I. Zeugolis, Decellularized xenografts in regenerative medicine: From processing to clinical application. Xenotransplantation, 2021. **28**(4): p. e12683.
108. Xie, H., et al., Extracellular Vesicle-functionalized Decalcified Bone Matrix Scaffolds with Enhanced Pro-angiogenic and Pro-bone Regeneration Activities. Sci Rep, 2017. **7**: p. 45622.
109. Jiang, S., et al., Enhancement of acellular cartilage matrix scaffold by Wharton's jelly mesenchymal stem cell-derived exosomes to promote osteochondral regeneration. Bioact Mater, 2021. **6**(9): p. 2711-2728.
110. Chen, P., et al., Desktop-stereolithography 3D printing of a radially oriented extracellular matrix/mesenchymal stem cell exosome bioink for osteochondral defect regeneration. Theranostics, 2019. **9**(9): p. 2439-2459.
111. Li, Q., et al., 3D Printing of Microenvironment-Specific Bioinspired and Exosome-Reinforced Hydrogel Scaffolds for Efficient Cartilage and Subchondral Bone Regeneration. Adv Sci (Weinh), 2023. **10**(26): p. e2303650.
112. Yin, H., et al., M2 macrophages-derived exosomes combined with acellular cartilage matrix scaffolds promote osteochondral regeneration via modulatory microenvironment. Materials & Design, 2023. **226**: p. 111672.
113. Huang, C.C., et al., Exosomes as biomimetic tools for stem cell differentiation: Applications in dental pulp tissue regeneration. Biomaterials, 2016. **111**: p. 103-115.
114. Narayanan, R., C.C. Huang, and S. Ravindran, Hijacking the Cellular Mail: Exosome Mediated Differentiation of Mesenchymal Stem Cells. Stem Cells Int, 2016. **2016**: p. 3808674.
115. Huang, C.C., et al., 3D Encapsulation and tethering of functionally engineered extracellular vesicles to hydrogels. Acta Biomater, 2021. **126**: p. 199-210.
116. Diomede, F., et al., A novel role in skeletal segment regeneration of extracellular vesicles released from periodontal-ligament stem cells. Int J Nanomedicine, 2018. **13**: p. 3805-3825.
117. Zendrini, A., et al., On the surface-to-bulk partition of proteins in extracellular vesicles. Colloids Surf B Biointerfaces, 2022. **218**: p. 112728.
118. Li, W., et al., Tissue-Engineered Bone Immobilized with Human Adipose Stem Cells-Derived Exosomes Promotes Bone Regeneration. ACS Appl Mater Interfaces, 2018. **10**(6): p. 5240-5254.
119. Zhou, Y., et al., Large-scale heparin-based bind-and-elute chromatography identifies two biologically distinct populations of extracellular vesicles. J Extracell Vesicles, 2023. **12**(6): p. e12327.

Chapter 5

Collagen Binding Properties Separate Two Functionally Distinct Subpopulations of Milk Extracellular Vesicles Regarding Bone Regenerative Capacity

Peng Wang, Yang Zhang, Onno J. Arntz, Marina C. Oliveira, Taozhao Yu, Zhihua Yang, Peter M. van der Kraan, Jeroen J.J.P. van den Beucken, Fons A.J. van de Loo

Materials Today Bio. 2025 Jul 18:33:102115.

ABSTRACT

Extracellular vesicles (EVs) are heterogeneous in their composition. The proteins on their surface determine their binding properties to the meshwork of extracellular matrix (ECM). Here, we report that type I collagen-binding property separates two subpopulations of EVs from cow milk (mEVs): collagen-binding mEVs ($^{cb+}$mEVs) and non-collagen binding mEVs ($^{cb-}$mEVs). $^{cb+}$mEVs showed noticeable uptake by human bone marrow mesenchymal stromal cells (hBMSCs) and osteogenic functionality *in vitro* (1.2-fold increase in mineralization). By proteomics profiling we identified Annexin V (AnxV) and confirmed its enrichment on CD9 positive $^{cb+}$mEVs using immunomagnetic separation. By implanting a hydrogel construct enriched with $^{cb+}$mEVs into a femoral condyle defect in osteoporotic rats, we demonstrated their superior bone regenerative capacity *in vivo* (2.4-fold increase in bone formation). Our study suggests that EV binding to the ECM protein type I collagen can be used to isolate a functional mEV subpopulation for bone tissue regeneration. This approach represents an important step forward in relating EV properties to their functionality, which will promote clinical translation.

Keywords: extracellular vesicles, interactome, extracellular matrix, bone defects

Graphical abstract

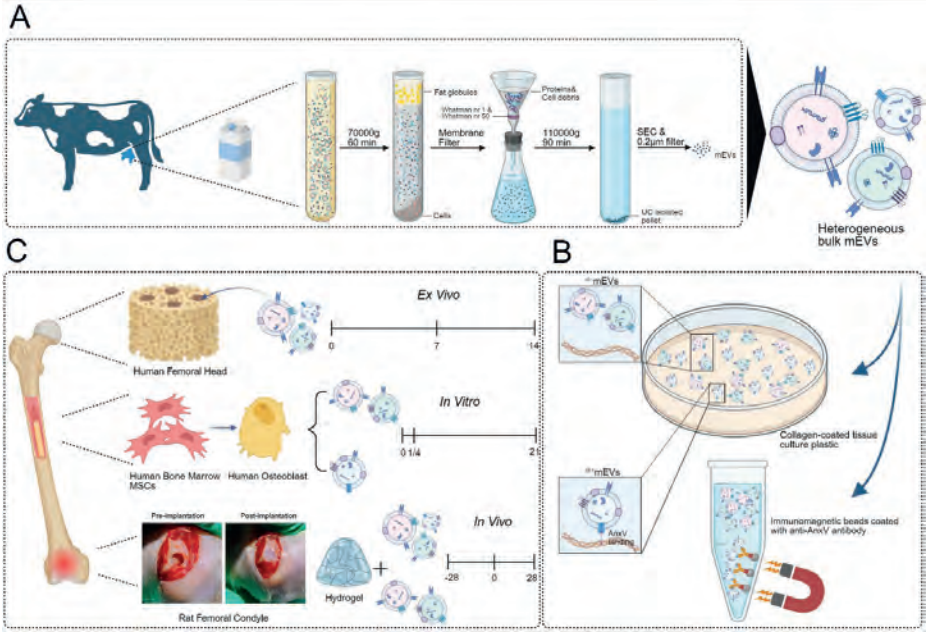

INTRODUCTION

Osteoporotic fractures are often accompanied by bone defects due to changes in bone microarchitecture, decreasing deposits of bone mineral and bone matrix components, sparseness of bone trabeculae, decreased bone strength, and increased bone fragility [1]. A bone defect is defined as a significant disruption in the integrity of bone tissue [2, 3]. Globally, fracture-related bone defects such as non-unions and segmental bone defects are significant public health issues. There are approximately 178 million new bone fractures worldwide every year, with a substantial increase in prevalence since 1990 [4]. Bone defects and related conditions can lead to long-term disability, affecting a patient's ability to work and participate in daily activities and reducing the quality of life [5]. Moreover, the treatment of bone defects in the United States incurs an annual cost of approximately $5 billion, with significant expenses related to bone grafts and surgical interventions for non-unions and other complications [6]. The current standard for treating osteoporotic bone defects primarily involves surgical interventions that use autologous bone grafts to fill the defects [7], which are considered the gold standard due to their osteoinductive and osteogenic properties. However, this method is not without limitations, including donor site morbidity, limited supply, and variable clinical outcomes [8]. As for allografts and xenografts, they offer key advantages such as wide availability, ease of use, and avoidance of donor-site morbidity [9]. While they lack osteogenic potential, they provide an effective osteoconductive scaffold and, in some cases (e.g., Demineralized Bone Matrix), limited osteoinductive capacity. Their ready-to-use nature makes them valuable alternatives when autografts are not feasible [10].

Emerging cutting-edge therapies in bone tissue engineering and regenerative medicine such as using cells predominantly mesenchymal stromal cells (MSCs), growth factors and extracellular vesicles (EVs) in scaffolds are being developed to address these limitations and improve patient outcomes [11, 12]. EVs are cell-secreted lipid bilayer vesicles that consist of sterols, membrane proteins and encloses an aqueous solution containing proteins, nucleic acids, and metabolites capable of influencing biological functions [13]. EVs are non-tumorigenic, biocompatible, and can be stored and transported more easily, reducing risks associated with cell-based therapies such as immune rejection and tumor formation. Additionally, compared to growth factor-based therapies that are often limited to specific signaling pathways and may require repeated administration due to their short half-lives, the versatility and stability of EVs makes EVs suitable for a wide range of therapeutic applications, including drug delivery and tissue repair [14, 15].

EVs play a crucial role in cellular communication during bone remodeling [16]. Furuta *et al.* demonstrated that CD9-knockout mice showed impaired femur fracture healing due to reduced exosome secretion, emphasizing the significance of EVs in bone regeneration [17]. For therapeutic purposes, EVs can be isolated from cell cultures or body fluids [18]. Specifically, EVs derived from MSCs act as key posttranscriptional regulators of osteoblasts. In return, osteoblasts communicate with MSCs via EVs, creating a positive feedback loop to stimulate osteogenesis [19]. However, the main concern of enrichment of MSC-EVs from cell culture media is the contamination with exogenous EVs present in fetal bovine serum (FBS). The presence of FBS-EVs may confound the therapeutic or diagnostic analyses of EVs derived from cultured cells [20].

Recent work reported that the BMP2 and MAPK signaling pathways are crucial for the osteogenic effects of human milk derived EVs. These pathways facilitate the differentiation and mineralization of osteoblasts, thereby promoting bone regeneration [21]. While the use of human milk derived EVs faces limitations due to ethical problems, limited resources, individual heterogeneity that limit scalability and standardization of the EV product which complicates their widespread therapeutic use [22, 23]. Cow milk EVs (mEVs) are known for their species cross-reactivity [24], and robust stability as they can survive the gastrointestinal tract's harsh conditions, making them effective carriers for bioactive molecules and potential drug delivery systems [25]. The scalable isolation of high-quality purified mEVs has been achieved through novel purification methods, which ensure minimal contamination from milk proteins, thus paving the way for their industrial-scale application [26]. Our previous work demonstrated that mEVs regulate bone homeostasis through influencing the activity of osteoblasts and osteoclasts [27, 28]. Moreover, mEVs showed systemic osteoprotective properties in an ovariectomized (OVX) bone loss mouse model and a high-refined carbohydrate diet-induced obesity mouse model via RANKL/OPG regulation [29, 30]. Recent work demonstrated that the local delivery of mEVs promoted bone repair using a mice skull defect model [31]. *Dong et. al* revealed the mechanism behind the osteogenic functionality of bulk mEVs involves the upregulation of the osteogenic gene GJA1 through the transcription factor AP3B1, providing valuable insights into how mEVs could be utilized in bone regeneration therapies.

Despite the involvement of EVs in regulating bone metabolism, functional differences among EV subpopulations, based on their inherent features such as physical characteristics and molecular cargos, present challenges for clinical translation [32]. EV heterogeneity implies that individual vesicles lack few or all of

the chemical or physical characteristics of the entire population, meaning that they lack the functional properties attributed to the bulk [33, 34]. This acts as a double-edged sword: it provides functional versatility, enabling EVs to perform diverse therapeutic roles and target multiple tissues, which enhances their potential in personalized medicine. Additionally, this variability complicates standardization, reproducibility, and regulatory approval, as only a subset of EVs may be bioactive while others remain inert or even counterproductive. Therefore, to validate the quality of EV preparations for therapeutic applications, the EV-inherent features could be harnessed to qualify them as suitable for subsequent clinical functional testing applications [35]. The common EV categorization is by size range, which classifies EVs as exosomes (~30-150 nm) or microvesicles (~100-1000 nm) [36]. Some functional aspects of EVs are known to vary with size [37, 38]. For instance, recent work demonstrated that by size exclusion chromatography (SEC) three cardiac progenitor cell-EVs subpopulations with different sizes were isolated and that these showed distinct differential effects on angiogenesis [39]. In this study, we investigated small mEVs (<200 nm), separated from the larger particles by using a standard 0.2 µm filter after SEC purification [40]. Additionally, the variation in the composition of proteins on EV surface has attracted attention, as it may play a key role in determining the functional subpopulations of EVs [41]. As the size decreases, the dynamic changes in the surface-to-volume ratio make small EVs more surface-active than luminal-active [42]. Therefore, tackling EV heterogeneity and isolating the optimal EV subpopulation are supposed to be realized through utilizing surface biomolecules present on EVs [43, 44]. Typically, matrix vesicles (MVs) represent one subset of small EVs released by osteoblasts, chondrocytes, or odontoblasts onto which phosphatidylserine (PS) is highly abundant on the outside the membrane. It has been reported that via the high affinity of PS for calcium ions, MVs can adhere to the extracellular matrix (ECM) by allowing calcium ions to form a bridge between the PS on the MV surface and negatively charged ECM [45].

Emerging data demonstrated that EVs actively interact with ECM components, including collagen, laminin, and fibronectin through adhesion molecules expressed on their surface [46]. The molecular foundation of the interactions between EVs and ECM components is anticipated to depend on their biochemical composition and chemical bonds. Specifically, hydrogen bonds have been identified as linking certain subsets of EVs with fibronectin or collagen in the heparin-binding domain, while other subsets of EVs possess exposed cysteines that form covalent bonds with ECM proteins like laminin [47]. Understanding the interaction of the EV surface with the biological environment is essential to fully harness the potential of EVs for applications [48]. For example, recent work observed that the migration of

EVs derived from tumors cells through the interstitium depends on the presence of integrin α3β1 and α6β1 on their surface, which contribute to their binding potential to laminin-rich ECM [49]. This integrin-mediated ECM binding influences the population of EVs entering blood and lymphatic capillaries and further determines the spatial distribution of bound and free EVs within the interstitium. In bone ECM, the predominant protein is type I collagen, which plays an important role in bone regeneration [50]. During the process of new bone formation, type I collagen secreted by osteoblasts serves as a template to initiate and propagate mineralization [51]. Previous work showed that identifying an active collagen-binding domain from bioactive proteins can offer a novel approach for targeted osteogenic differentiation [52]. Specifically, *Choi et. al* investigated the interaction between binding peptide and collagen matrix activates the ERK1/2 and Akt signaling pathways and increases osteoblastic differentiation in human osteosarcoma cells. *In vivo*, a hydroxyapatite scaffold modified with the peptide significantly improved bone formation in a rabbit calvarial defect model, highlighting its potential as a bioactive agent for bone tissue engineering [53]. It has been demonstrated that the binding sites of collagen for artificial peptide present on the surface of MSC-EVs enhance EVs retention and further accelerate tissue regeneration [54]. Considering EV heterogeneity hence we regard collagen-binding capacity as an eminent "EV-inherent feature" regarding the osteogenic functionality of an EV subpopulation.

We herein demonstrate the osteogenic functionality of bulk mEVs using *in vitro* MSC-osteogenic differentiation and *ex vivo* human bone organ culture models. Through harnessing collagen binding properties, we next separate two subpopulations of mEVs: collagen-binding mEVs ($^{cb+}$mEVs) and non-collagen binding mEVs ($^{cb-}$mEVs) and demonstrate their distinct functional properties regarding osteogenic functionality *in vitro*. By proteomic profiling, we identify Annexin V (AnxV) and show its role in $^{cb+}$mEV subpopulation-induced osteogenesis. Most importantly, we reveal that $^{cb+}$mEVs enriched for AnxV represent the functional mEV subpopulation that promotes bone defect repair under osteoporotic conditions *in vivo*.

MATERIALS AND METHODS

Cow milk extracellular vesicles isolation

mEVs were isolated from commercial semi-skimmed milk derived from Holstein-Friesian cows (breed of large dairy cattle originating in northern Holland) as previously described [55]. Briefly, the milk was centrifuged for 60 min at 70.000 g at 4 °C in a SW60 rotor (Beckman Coulter). Afterwards, the fat layer and cells were

removed, and supernatant was collected and filtered with Whatman nr 1 and Whatman nr 50. Thereafter the samples were centrifuged again for 90 min 110,000 g at 4°C. After discarding the supernatant, PBS was added to dissolve the pellets, which were then filtered using a 0.22 µm filter and stored at 4°C for future use. Thereafter, the subsequent SEC was utilized to remove the co-isolated protein contamination. In short, sepharose CL-2b (Cytiva; GE17-0140-01) was stacked in a 10 ml syringe (56 mm). mEVs (500 mL) were loaded on top of the column and eluted with PBS, and fractions 4 and 5 were collected. After SEC, the samples were filtered in 0.22 µm filter and were stored at 4°C until further use.

Cow milk extracellular vesicles characterization

The concentration and size distribution of mEVs were determined using the NanoSight Tracking Analysis (NTA) NS300 system (Malvern, UK). Cryo-electron microscopy (Cryo-EM) was used for visualization of mEVs. In short, Cryo-EM samples were prepared by applying 3 µL mEV solution on glow discharged 200 mesh gold Quantifoil (2/2) grids (Electron Microscopy Sciences, USA). The grids were vitrified in liquid ethane using a Vitrobot Mark IV (Thermo Fisher, NL). Images were acquired using a TALOS F200C-G2 (Thermo Fisher, NL) operated in low dose mode at 200 kV and equipped with a Falcon 4i detector (Thermo Fisher, NL).

The expressions of EVs common markers were detected by western blotting (WB). In brief, mEVs were washed with PBS and RIPA lysis buffer (Millipore) with a proteinase inhibitor cocktail (Roche diagnostics, cOmplete™) was added. Proteins were separated by electrophoresis on 10% bisacrylamide gels in 1x electrophoresis buffer. Afterwards the proteins were transferred to a 0.45 µm nitrocellulose (NC) blotting membrane (GE Healthcare) using wet transfer. The blots were blocked with 1x animal-free blocking buffer (Cell Signaling Technologies, 15019) overnight at 4°C. Thereafter, the blots were washed three times with TBS-Tween® (TBST) for 10 minutes and then incubated overnight with corresponding antibody: CD81 (Santa Cruz Biotech, sc-166029), Alix (Santa Cruz Biotech, sc-53540), HSP-70 (Santa Cruz Biotech, sc-32239), CD9 (Thermo Fischer, MA1-80307), AnxV (Santa Cruz Biotech, sc-74438) in 2% bovine serum albumin (BSA) (Sigma Aldrich) dissolved in TBS-T. The blots were treated with enhanced chemiluminescence (ECL) using ECL Prime Western Blotting Detection Reagent Kit (GE Healthcare) to visualize the protein bands with ChemiDoc™MP Imaging System (Bio-Rad) machine and Imagelab 6. software.

To identify EVs surface markers, the EV analyses were performed with Cytek® Amnis® CellStream® Flow Cytometer: To 3µl mEVs, 3µl CD81-Alexa488 (1:100, R&D

Systems, Inc., Minneapolis, MN, USA), or 3µl CD9-Alexa647 (1:100, R&D Systems, Inc., Minneapolis, MN, USA) antibodies were added. Thereafter 10 µl PBS was added and samples were incubated overnight at 4°C. The next day PBS was added to a volume of 150 µL. Small particle setting was used and detection was set up for 60 seconds with the following settings FSC=5 and SSC=5. As negative controls, only antibodies were measured with the same settings. The gating strategy was based on fluorescence channel 488 and 647, and positive events per ml were determined.

Cell culture

Human bone marrow MSCs (hBMSCs, passage 2-5) were maintained in a log phase in a humidified atmosphere with 5% CO_2 at 37°C with cell culture media composed of α-MEM (A14090, Gibco) supplemented with 10% fetal bovine serum (Gibco) and 1% penicillin–streptomycin (Gibco). hBMSCs were isolated from bone fragments obtained as surgical excess material following total hip arthroplasty at the Department of Orthopedics (Radboudumc, Nijmegen, the Netherlands) from anonymized patients. In line with the criteria as set by the International Society for Cellular Therapy (ISCT), hBMSCs were immunophenotypically characterized to express MSC markers (>95% immunopositive for CD90 and CD105, and >85% immunonegative for CD45).

Osteogenic differentiation in vitro

To initial osteogenic differentiation of hBMSC basic osteogenic induction media (OM) that are α-MEM containing 10% v/v EV-depleted FBS prepared by 18 hours UC [56] and 1% penicillin-streptomycin, as well as 10 mM β-glycerophosphate disodium salt hydrate, 10^{-8} M dexamethasone and 50 µg/ml ascorbic acid were utilized for cell culture. On day 7 of osteogenic differentiation the expression of type I collagen by cells was tested through western blotting. Cells were washed with PBS and RIPA lysis buffer (Millipore) with a proteinase inhibitor cocktail (Roche diagnostics, cOmplete™) was added. Equal proteins were loaded onto 10% SDS-PAGE and subsequently transferred onto 0.45 µm NC membrane for 120 min at 275mA. The membrane was blocked with 5% skim milk overnight at 4°C. After that the blots were incubated overnight with anti-col1a1 (1:1000, Merck ABT257).

The alkaline phosphatase enzymatic activity (ALP) and the calcium content were tested as previously described [57]. Briefly, 0.5 M alkaline buffer solution (Sigma) and samples (1:5) were incubated with substrate solution (5mM pNPP disodium salt hexahydrate) (Sigma) for 1 hour at 37°C. The conversion in this assay results in 4-Nitrophenol, and the absorbance was read at 405 nm with Clariostar spectrometer (BMG Labtech). To measure calcium content the cell culture wells were incubated

overnight in 0.5 M acetic acid at room temperature. The working solution consisted of 5% 14.8 M ethanolamine (Merck)/boric acid buffer (BOOM) [pH 11], 5% Ortho-Cresolphthalein Complexone (Merck), and 2% hydroxyquinoline (Sigma). Samples mixed with working solution and incubated at RT for 10 minutes. The absorbance of the plates was measured with Clariostar spectrometer (BMG Labtech) at 570 nm.

To visualize mineralization, histochemical staining of hBMSCs was performed. hBMSCs were washed with PBS and then fixed in 200 µl 70% ethanol for 10 minutes. Then the wells were washed one time with demi water. Afterwards the wells were stained with 200 µl 2% alizarin red s for 10 minutes. Then the cells were washed with demi water twice and photographed with Nikon D7500.

Human bone organ preparation and culture

Human femoral heads were freshly obtained from the Department of Orthopedics (Radboudumc, Nijmegen, the Netherlands) as surgical excess material following total hip arthroplasty from anonymized patients. Procedures were performed in accordance with the Dutch code of conduct for responsible use of human tissue in medical research. To create standard-sized bone discs, trabecular osteochondral cores were inserted into a custom-made mold with a diameter of 8 mm and a height of 4 mm. The bone discs were secured into a custom-made holder, after which four defects (Ø1.1 mm x 3 mm) were drilled into the bone discs using a drill press (8450468, Bosch PBD40, Germany). mEVs were injected into all defects four times in two weeks. Bone discs were cultured in a 24-well plate within OM and stored in an incubator at 37°C with 5% CO_2.

Fluorochrome labeling

Two fluorochrome labels (Calcein (CO3050, Sigma-Aldrich); Alizarin Red (Alizarin-3-methyliminodiacetic acid, A3882, Sigma-Aldrich) were administered on the 7th and 14th day respectively through OM at a concentration of 25 µg/ml for 24 hours [58]. After 24 hours of incubation, bone discs were transferred to a clean 24-well plate and washed one time with PBS for 5 minutes before fresh OM was added. Post-incubation, bone discs were imaged using widefield microscopy (Zeiss Axio Imager 2). To quantify fluorescence intensity along the walls of defects, the donuts labeling centered on the hole have been designed and areas within inner circles have been excluded. Two corresponding and separate channels for Calcein Green and Alizarin Red were utilized in Fiji/ImageJ (National Institutes of Health (NIH), United States).

Binding of mEVs to Type I collagen

mEVs were fluorescently labeled using the PKH67 Green Fluorescent Cell Linker Kit kit (Merck). The quantitative binding experiment was performed in 100 µg/ml collagen-coated tissue culture plastic (Advanced Biomatrix® Collagen I, bovine, Cat# 5005). Fluorescently labeled mEVs were added in increasing doses to the wells and incubated for 24 hours at 4°C. The receiving media (unbound part of mEVs) were collected and regarded as $^{cb-}$mEVs. The wells were washed 3× with PBS and the fluorescence from $^{cb+}$mEVs was quantitatively measured using a fluorescent plate reader (BioTek), and observed using IVIS (Xenogen VivoVision IVIS Lumina II, PerkinElmer, Waltham, MA, USA).

mEVs labeling and cellular uptake

mEVs were labeled with DiD stain (Invitrogen) according to the manufacturer's instructions. Briefly, EVs were mixed with DiD stain (10 µM) and incubated at room temperature for 15 min in the dark. The labeled EVs were then washed two times with PBS at 100,000 g for 90min at 4°C. The final EV pellet was suspended in PBS. For uptake assay, 3×10^4 hBMSCs were seeded in each well of collagen-coated tissue culture plastic and incubated with DiD-labeled EVs at 37°C. After 6 h, cells were washed with PBS and fixed with 4 % paraformaldehyde. The cell nucleuses were stained with DAPI. The imaging was performed using a confocal laser-scanning microscopy (Nikon, Japan).

Proteomic analysis of mEVs and $^{cb-}$mEVs

Proteins associated with or incorporated in mEVs and $^{cb-}$mEVs were identified through mass spectrometry by the Radboud Technology Center. Briefly, mEVs (2e+09 particles/each well) were added to collagen-coated tissue culture plastics and incubated for 24 hours at 4 °C to collect $^{cb-}$mEVs. mEVs and $^{cb-}$mEVs (10 µg in PBS) were precipitated by adding 3 ml ice cold ethanol to 1 ml of sample followed by overnight precipitation at -80°C and subsequent 15min centrifugation at 14.000 g. Protein pellets were dissolved in 30 µl 8M urea 10 mM Tris-HCl (pH 8) prior to subsequent reduction and alkylation of cysteine residues by addition of 1 µl 50 mM dithiothreitol and 1 µl 50 mM chloroacetamide and subsequent incubation at room temperature for 30 minutes in the dark, respectively. Next, 120 µl 50 mM ammoniumbicarbonate (pH 8) and 0.5 µl Trypsin (0.2 µg/µl) were added and samples were incubated overnight at 37 °C. Tryptic digests were analyzed by nanoflow liquid chromatography (Evosep One, Evosep Biosystems) coupled online to a trapped ion mobility spectrometry – quadrupole time-of-flight mass spectrometer (timsTOF Pro2, Bruker Daltonics) via a nanoflow electrospray ionization source (CaptiveSprayer, Bruker Daltonics). Tryptic peptides were separated by C18 reversed phase liquid

chromatography (Evosep EV1137 30SPD performance column; 150 mm length x 0.150 mm internal diameter, 1.5 µm C18AQ particles) using the pre-programmed 30 samples per day (30SPD) Evosep One method. The mass spectrometer was operated in positive ionization mode using the default data independent acquisition – Parallel Accumulation SErial Fragmentation (dia-PASEF) [59] instrument method: 0.6 – 1.6 1/K0 mobility range, 100 - 1700 *m/z* mass range, 100ms accumulation time, 100ms ramp time, 26 Da mass width, 1 Da mass overlap, 32 mass steps per cycle, 0 mobility overlap, 1 mobility window. Acquired spectra were streamed directly to ProteoScape (v2025b, Bruker Daltonics) for protein identification and label-free quantitation against the Uniprot Bovine protein sequence database (downloaded Jan 2024) using the following settings: Spectronaut v19 directDIA+ (Fast) workflow, 0.2 precursor PEP cutoff, 0.01 precursor Q-value cutoff, 0.01 protein Q-value cutoff global, 0.01 protein Q-value cutoff, 0.75 protein PEP cutoff, full tryptic specificity, allowed up to 2 missed cleavages, carbamidomethyl (C) as fixed modification and Oxidation (M) as variable modifications, protein group specific peptides were used for quantitation.

To determine enrichment of protein in $^{cb+}$mEVs, the following formula on EV-protein intensity of single protein in $^{cb+}$mEVs was utilized:

$$\text{EV-protein intensity} = \frac{1 - \text{PI}_{\text{cb-mEVs}} / \text{PI}_{\text{mEVs}}}{2 \times (\text{PN}_{\text{cb+mEVs}} / \text{PN}_{\text{mEVs}})}$$

Where PI refers to protein intensity and PN refers to particle number. Protein with an EV-protein intensity more than 1 was considered enriched in $^{cb+}$mEVs.

Immunomagnetic separation of mEVs

EVs expressing specific surface markers could be isolated through immunomagnetic separation [60]. Likewise, we incubated mEVs (4e+10 particles) with protein A/G immunomagnetic beads (~500 µg, MCE) pre-coated 20 µg/ml AnxV antibody (Santa Cruz Biotech, sc-32321) in a roller bench for 1 h at room temperature. According to the manufacturer protocol the beads-unbound mEV were isolated using a DynaMag magnet (Thermo Fisher, USA), washed with 0.2-µm-filtered 0.5% Tween-20-supplemented PBS four times. We collected the supernatant from the first wash as AnxV depleted mEVs ($^{AnxV-}$mEVs). In addition, the beads-bound AnxV positive mEVs were eluted and collected for NTA measurements and flow cytometry analyses.

Preparation of mEVs-laden hydrogel construct

To prepare EVs-laden hydrogel constructs, acidulated collagen solution was mixed with 10 × PBS, neutralized with 0.023 µL of 1 N sodium hydroxide per µL of

collagen to achieve the final concentration of 3 mg/mL using 1× PBS. Then 30 µL of neutralized collagen was added per well of 96-well plates and allowed to polymerize at 37°C for 60 min. For EVs encapsulation, DiD-labeled mEVs were incorporated into the collagen solution before polymerization. The distribution of mEVs in hydrogel construct was observed using confocal laser-scanning microscopy. Moreover, the *in-vitro* release kinetic of mEVs was assessed by NTA. Briefly, mEVs-laden hydrogel construct was incubated in sterile PBS at 37 °C. On day 1, 3, 6, and 10, the receiving media was collected and replaced by an equal volume of fresh PBS. On day 14, 200 U/ml collagenase D (Roche) was added for digestion of hydrogel after incubation at 37°C incubator for 1h. The percentage of mEVs released was calculated from the initial quantity of EVs added prior to gelation. For hBMSCs mineralization in 3D collagen-based hydrogel, 2×10^4 hBMSCs were mixed either hydrogel only (Ctrl-col) or containing mEVs (mEVs-col), $^{cb-}$mEVs ($^{cb-}$mEVs-col) and $^{AnxV-}$mEVs ($^{AnxV-}$mEVs-col) and cultured within OM medium for 14 days.

Evaluation of bone repair within mEVs, cb-mEVs or AnxV-mEVs-laden hydrogel construct *in vivo*

All animal care and related experimental procedures were carried out according to the guidelines of Chinese Research Council's and all procedures were approved by the ethical committee for animal care and use of Shenzhen University (SYXK 2022-0302). To evaluate the bone repair effect of three types of mEVs-laden constructs *in vivo*, we created the femoral condyle defect model in OVX-induced osteoporotic SD rats (females; 320-380g, 16 weeks old) according to the previously described method [61, 62].

Surgical procedure Firstly, bilateral ovariectomies were performed to induce osteoporosis under general anesthesia in SD rats (females; 200-250g, 12 weeks old). After four weeks the bilateral femoral condyle defects operation was conducted in all rats. Each animal was anesthetized and immobilized in a supine position. A longitudinal incision was made along the direction of the sartorius muscle, and the distal femur was exposed after opening the skin and separating the muscle. After exposure of distal femur, the knee was flexed, and the soft tissues including muscle and ligament were moved aside to let the femoral condyles completely expose. A defect (2.4 mm in diameter, 3 mm in depth) was created between two femoral condyles. After the creation of the femoral condyle defect, the defected holes were covered by implanting either ctrl-col or containing 9e+07 particles of mEVs-col, $^{cb-}$mEVs-col and $^{AnxV-}$mEVs-col. All rats were housed and maintained in Specific Pathogen Free facility.

Micro-CT scanning Four weeks post operation, all rats were euthanized to excise the femur for fixation in neutral buffered formalin for 36 h. To assess the bone repair at defect sites, the collected samples were scanned by high-resolution micro-computed tomography (μCT) system (Quantum FX, Perkin-Elmer); The scanning parameters were as follows: 70 kV, 100 μA, 144μm. The μCT analyser software (Analyze 14.0, Mayo, USA) was used to define a region of interest (ROI) based on the two-dimensional (2D) images which representing the defects surrounding newly formed bone tissue to obtain a volume of interest (VOI) dataset. Once the views around the ROI were reconstructed, bone volume/total volume (BV/TV) was measured.

Histological analysis Formalin-fixed femoral condyles were decalcified in 10% ethylenediaminetetraacetic acid (EDTA) solution followed by embedding in paraffin for 4 weeks. The tissues were then sectioned into 7 μm thick slices. The sectioned tissues were placed on slides and dried overnight for subsequent histological analysis, including hematoxylin-eosin (HE) and Verhoeff's Van Gieson (EVG) staining as previous study [61]. Sections were further scanned with a NanoZoomer Digital Pathology System (Hamamatsu, Bridgewater, USA).

Statistical analysis

Results were analyzed in GraphPad Prism 9 using unpaired two-tailed Student's t tests with two groups and one-way ANOVA with a Dunnett post hoc test with more than two groups as per specific *ex vivo* experiment. Data for animal experiments were evaluated using paired two-tailed Student's t tests within each group (Ctrl-col & mEVs-col; Ctrl-col & $^{cb-}$mEVs-col; Ctrl-col & $^{AnxV-}$mEVs-col). A p-value below 0.05 ($p<0.05$) was considered to be statistically significant.

RESULTS

Isolation and characterization of mEVs

Cryo-EM showed that mEVs were relatively regular in morphology with a circular shape, surrounded by a well-defined lipid bilayer membrane with diameters < 200 nm (Fig. **1A**), having a yield of 5e+10 particles/ml and a median particle size of 118 nm as determined by NTA (Fig. **1B**). The EV protein content used as an indication of EV purity [63] was 0.5±0.05 fg/particle (Fig. **1C**). WB results further confirmed that mEVs expressed the common EV markers HSP-70, Alix, and CD81 (Fig. **1D**). Of note, CD81 or CD9 positive mEVs were also identified with flow

cytometry (Fig. **1E**). Taken together, these results proved the successful extraction of mEVs from cow milk.

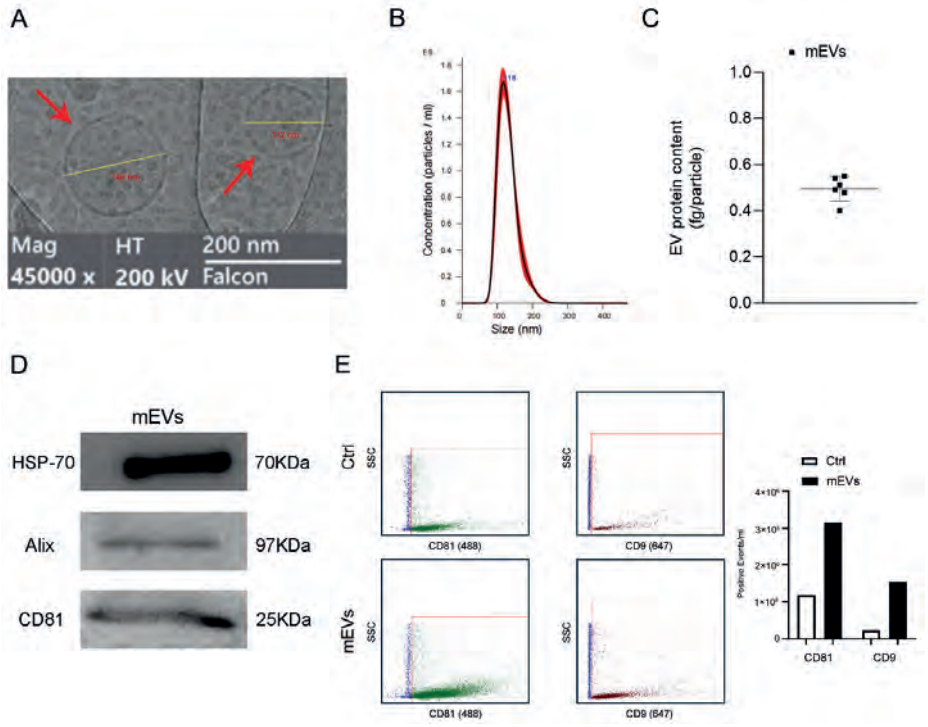

Fig. 1. Isolation and characterization of mEVs. A. Morphological appearance of mEVs upon electron microscopy (Cryo-EM). B. Size distribution of mEVs (n=3). C. Determination of mEV protein content (n=6). D. Western blotting analysis of protein levels of HSP-70, Alix, and CD81 in mEV lysates. E. Flowcytometry measurement of mEVs expressing CD81 (fluorescence channel 488 nm) or CD9 (fluorescence channel 647 nm). Ctrl: corresponding antibody in pbs. SSC: side scatter. Data were expressed as means ± standard deviation (SD).

mEVs stimulate osteogenesis in cell and organ cultures

To clearly assess whether bulk SEC-purified mEVs have a pro-osteogenic effect on MSCs, we exposed hBMSCs to basic OM with or without supplementation with mEVs (5e+06 particles/ml). EV supplementation resulted in an enhanced expression of type I collagen at day 7 (Fig. **2A**) as determined by WB, increased activity of ALP at day 14 (Fig. **2B**), and a higher calcium deposition at day 21 (Fig. **2C**). Furthermore, a human bone *ex vivo* organ culture model was established, in which hBMSCs and osteoblasts are preserved in their native three-dimensional environment [64]. After 14 days of culture in OM, methylene blue/basic fuchsine staining showed preservation of trabecular bone structures with viable osteocytes. To test the effect of local mEV delivery on repair of a bone defect, 4 holes were drilled into the bone

explant directly after preparation (Fig. **2D**). mEV injection into these holes of the bone explants showed to increase fluorochrome uptake along the walls of these holes after day 14 of culture (Fig. **2E-F**). Collectively, these results imply that mEVs stimulate osteogenic differentiation of hBMSCs *in vitro* and bone formation *ex vivo.*

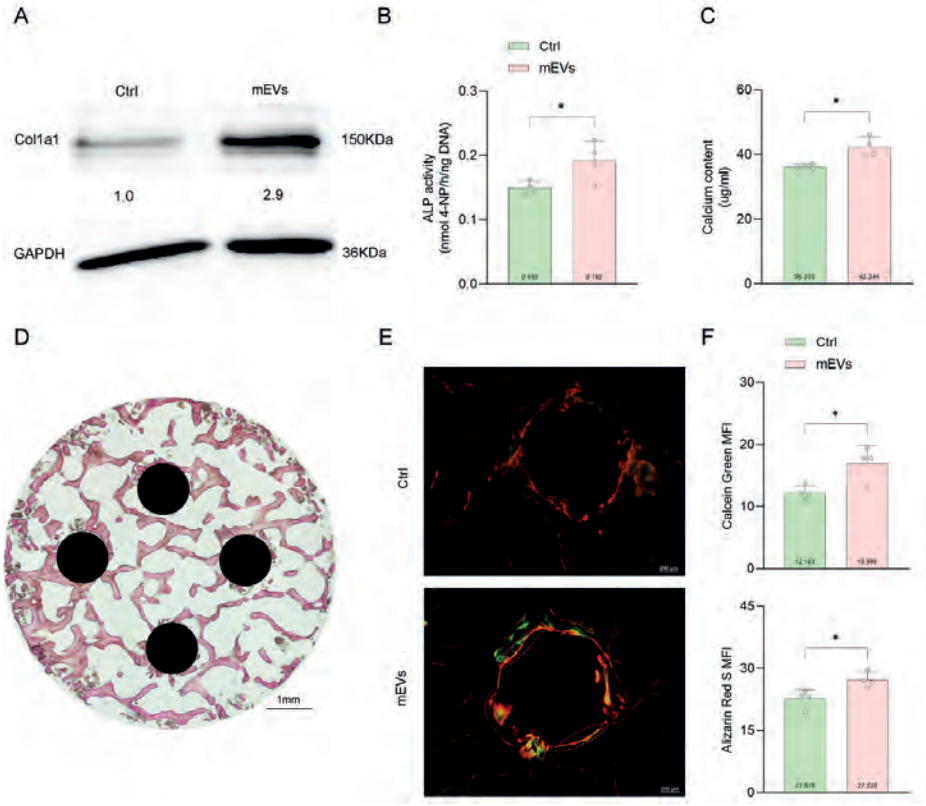

Fig. 2. mEVs stimulate osteogenesis in cell and organ cultures. A. Western blotting for Col1a1 protein expression at day 7. B. Quantification of ALP activity at day 14 and C) Calcium content of hBMSCs cultured in OM (Ctrl) or OM within mEVs at day 21 (n=4). D. Methylene blue/basic fuchsine staining of the bone disc within four drilled holes (indicated by black circles). E. Representative images of the drilled holes stained with calcein green on the 7th day and alizarin red s on the 14th day for ctrl (pbs) and mEVs injection. F. Mean fluorescence intensity (MFI) of calcein green and alizarin red s on inner edges of defects (dots represent holes of each sample). Scale bars correspond to 1mm in 2D and 200 µm in 2E. Data were expressed as means ± standard deviation (SD). *$p < 0.05$.

Binding to collagen separates mEVs with osteogenic functionality in cell cultures

Using a collagen-binding experiment for mEVs with collagen-coated tissue culture plastic, the binding curve revealed that 4% of the input particles were able to bind to collagen, and saturation occurred from mEVs numbers of 3e+09

particles (Fig **3A**). Moreover, fluorescently labeled $^{cb+}$mEVs were observed and the signal intensities were calculated using IVIS optical imaging (Fig **3B**-**C**). To evaluate the effect of $^{cb+}$mEVs on osteogenic differentiation of hBMSCs, cells were seeded on the collagen-coated plate with or without $^{cb+}$mEVs (Fig **3D**). Within 6h (from cell seeding to fixation), we observed that more than 60% of hBMSCs specifically took up $^{cb+}$mEVs (Fig S1: Fluorescence image of negative control). Both mEVs and $^{cb-}$mEVs were internalized by adherent cells within 6 hours. However, noticeably fewer labeled $^{cb-}$mEVs were observed in the perinuclear region compared to mEVs (Fig **3E**). By Cryo-EM and NTA analysis we confirmed that $^{cb-}$mEVs are true EVs of similar size and purity as bulk mEVs (Fig S2). More importantly, alizarin red s staining showed significantly more mineralization after 21 days of OM culture by hBMSCs cultured on collagen-coated plates with $^{cb+}$mEVs and mEVs, and less mineralization was observed with $^{cb-}$mEVs stimulation (Fig **3F**). Consistently, the calcium content of hBMSCs under control (PBS) conditions was 91.4 ± 5.5 μg/ml while $^{cb+}$mEVs presence resulted in 106.9 ± 4.4 μg/ml and 99.9 ± 4.8 μg/ml with mEVs stimulation but 90.8 ± 4.6 μg/ml upon $^{cb-}$mEVs stimulation, respectively (Fig **3G**). Taken together, these data show that $^{cb+}$mEVs are the functional subpopulation of mEVs that drives osteogenic differentiation of hBMSCs.

AnxV mediates the osteogenic effect of $^{cb+}$mEVs

As we cannot isolate sufficient quantity of the $^{cb+}$mEV subpopulation for proteomic analysis, we performed proteomic profiling of (bulk) mEVs and $^{cb-}$mEVs to investigate proteins enriched in $^{cb+}$mEVs that facilitate collagen binding. The comprehensive mass spectrometric analysis revealed that mEVs possess over 260 quantifiable proteins. Given that $^{cb+}$mEVs account for 4% of the bulk mEVs, the EV-protein intensity of 73 proteins is greater than 1, which were selected for further analysis (Table S1). The GO term "cellular components" showed that all 73 selected proteins were main EV-associated proteins (Fig **4A**), indicating the specific binding between type I collagen and EVs. Next, proteins located in the extracellular region and their interactions were mapped (Fig **4B**). One single interaction chain was identified, comprising CD9, CD81 and AnxV that was digitally stained as heparin-binding protein. Three casein-related proteins have been labelled as milk protein. The EV-protein intensity of the extracellular proteins exceeded 1.90 (Fig **4C**). Since CD9 has been reported as one specific marker among tetraspanins present on some EV subpopulations [65, 66], we speculated AnxV was enriched in CD9 positive $^{cb+}$mEVs. WB results showed that compared to (bulk) mEVs the protein levels for CD9 and AnxV decreased 40% and 30% in $^{cb-}$mEVs (Fig **4D**).

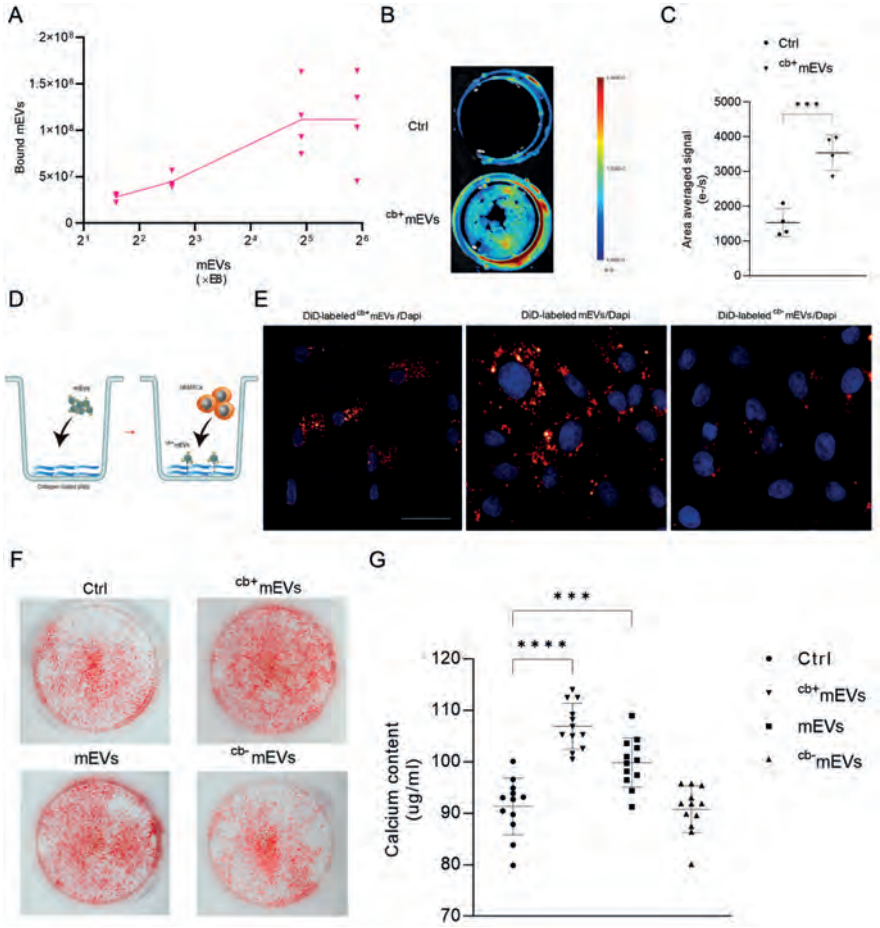

Fig. 3. Binding to collagen separates mEVs with osteogenic functionality in cell cultures. A. Quantification of mEV with collagen binding properties (n=4). B. Representative IVIS image showing fluorescently labeled cb+mEVs bound to collagen-coated tissue culture plastic (Ctrl: label agent in pbs). (C) Quantitative area averaged signal in from fluorescently labeled cb+mEVs bound to collagen-coated tissue culture plastic (Ctrl: label agent in pbs) (n=4). (D) Schematic representation showing sequential mEVs loading and hBMSCs seeding on collagen-coated tissue culture plastic. (E) Uptake of cb+mEVs, mEVs, cb-mEVs by hBMSCs within 6h. (F) Representative alizarin red staining of hBMSCs cultured on collagen-coated tissue culture plastic (PBS control, cb+mEVs, mEVs or cb-mEVs) at day 21. (G) Calcium content of hBMSCs cultured on collagen-coated tissue culture plastic (PBS control, cb+mEVs, mEVs or cb-mEVs) at day 21 (n=12). Data were expressed as means ± standard deviation (SD). ***$p < 0.001$; ****$p < 0.0001$. Scale bars correspond to 100 µm in 3E.

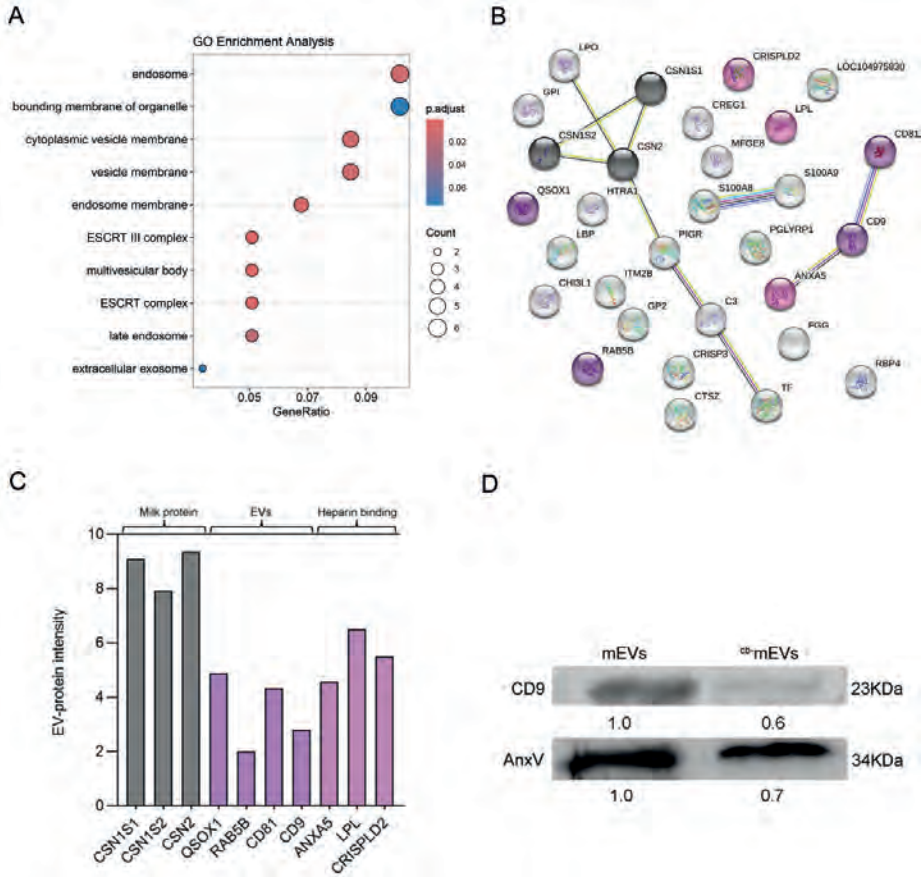

Fig. 4. AnxV was enriched in CD9 positive $^{cb+}$mEVs. A. The classification of proteins enriched in $^{cb+}$mEVs according to the cellular components. B. The STRING analysis of the proteins in extracellular region for protein-protein interactions. C. The EV-protein intensity of proteins (extracellular components) in $^{cb+}$mEVs. D. Western blotting analysis of protein levels of CD9, AnxV in mEVs and $^{cb-}$mEVs lysates.

Thereafter, to assess the role of AnxV on mEVs-induced osteogenesis, immunomagnetic beads separation was conducted to collect $^{AnxV+}$mEVs and $^{AnxV-}$mEVs. The particle amount of $^{AnxV+}$mEVs was 1.9e+08 particles per 10 μg beads (Fig **5A**). Flow cytometry analysis confirmed the presence of CD9 on $^{AnxV+}$mEVs (Fig **5B**). In addition, NTA analysis showed the shifted size distribution of mEVs due to the removal of the fraction captured by anti-coated AnxV beads (Fig **5C**). WB revealed that the protein levels for CD9 decreased 40% in $^{AnxV-}$mEVs compared to mEVs (Fig **5D**). More importantly, we observed that hBMSCs took up much fewer $^{AnxV-}$mEVs (Fig **5E**). Calcium deposition in hBMSCs was significantly reduced after

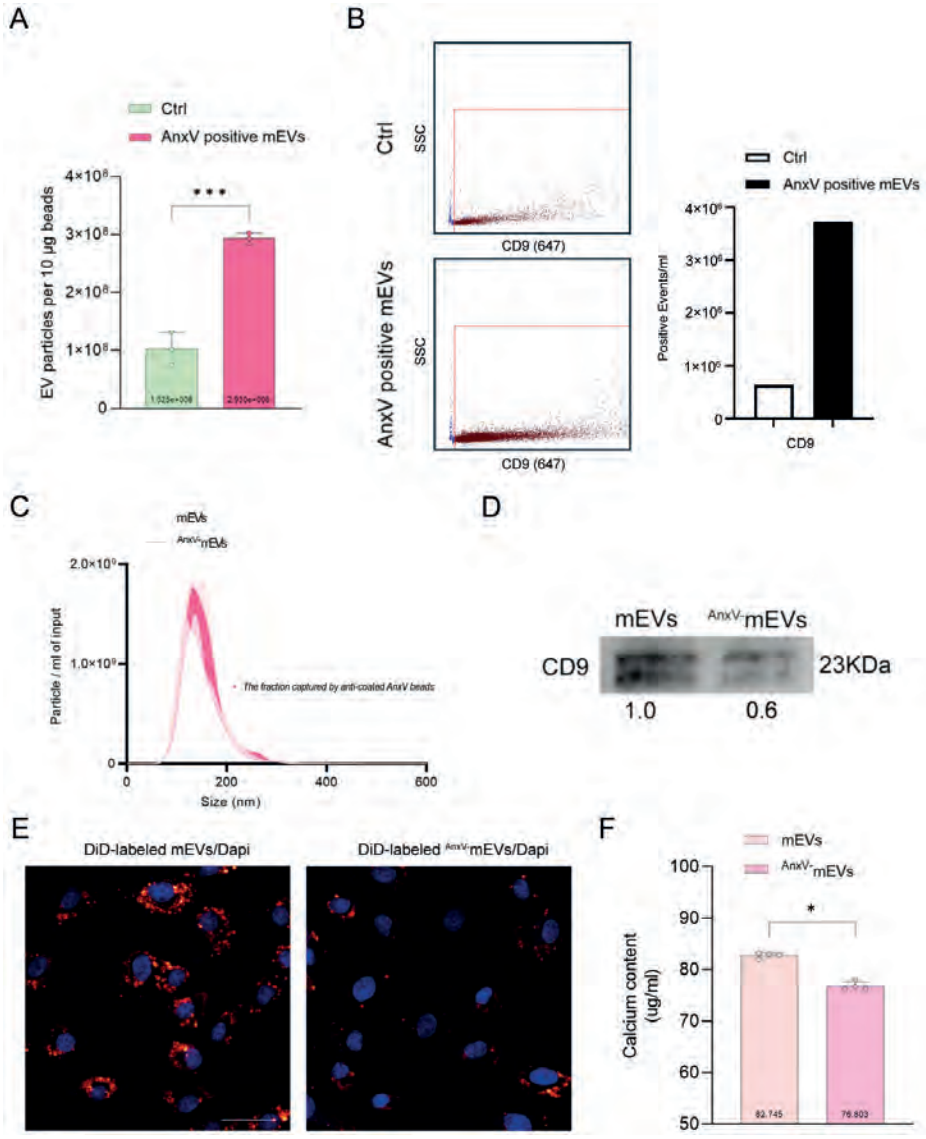

Fig. 5. Depleting AnxV diminished mEV-induced hBMSCs osteogenesis. A. Number of AnxV positive mEVs (n=3). Ctrl: beads-AnxV antibody-pbs complex. B. Flowcytometry measurement of AnxV positive mEVs expressing CD9. Ctrl: corresponding antibody in pbs. C. NTA of mEVs before and after incubation (inc.) with magnetic beads coated with anti-AnxV antibody (n=2). D. Western blotting analysis of protein levels of CD9 in mEVs and $^{AnxV-}$mEVs lysates. E. The uptake of mEVs or $^{AnxV-}$mEVs by adherent hBMSCs within 6h. F. Calcium content of hBMSCs cultured in OM within mEVs or $^{Anxv-}$mEVs (n=4). Data were expressed as means ± standard deviation (SD). *$p < 0.05$, ***$p < 0.001$. Scale bars correspond to 100 µm in 5E.

21 days of OM culture with $^{AnxV-}$mEVs stimulation compared to mEVs (Fig **5F**). In addition, to investigate the role of AnxV on mEVs binding to collagen, we checked the binding capacity of $^{AnxV-}$mEVs in collagen-coated plates. IVIS imaging showed less signal of labeled collagen-binding $^{AnxV-}$mEVs ($^{cb+\ AnxV-}$mEVs) compared to that of $^{cb+}$mEVs. Decreased calcium deposition by hBMSCs was determined in coated collagen plate within $^{cb+\ AnxV-}$mEVs (Fig S3). Collectively, these data strongly suggest that AnxV is enriched on $^{cb+}$mEVs and contributes to mEV-induced osteogenesis.

$^{cb+}$mEVs in 3D hydrogel constructs enhance hBMSCs mineralization

Next, we strived to apply mEV subpopulations therapeutically to heal bone defects. For this, we engineered hydrogel constructs with encapsulated mEVs and determined the EV release kinetics for 14 days in PBS at 37°C. Fluorescently labeled mEVs were observed in 3D hydrogel constructs at day 0 using laser confocal microscopy (Fig. **6A**). Robust release of mEVs was observed from day 1 to day 6, during which 68.1 $\pm$8.7% mEVs was released from the hydrogel construct. However, thereafter the release plateaued and between day 6 up to day 10 only 7.8%$\pm$1.2 mEVs was released. Because the particle amount of mEVs in receiving PBS on day 14 was undetectable with NTA, we degraded the hydrogel to measure the particle amount of still encapsulated mEVs and found 15.6%$\pm$2.5 mEVs to be still entrapped in the hydrogel (Fig. **6B**). Next, we mixed hBMSCs into the EVs containing hydrogel constructs and after 14 days of culture in OM medium more calcium staining was apparent from Alizarin red S staining for mEVs-col compared to $^{cb-}$mEVs-col and $^{AnxV-}$mEVs-col (Fig. **6C**). The highest calcium content by hBMSCs was found for mEVs-col (Fig. **6D**). Consequently, these data demonstrate that mEVs were successfully encapsulated in 3D hydrogel constructs and we deduced from these data that in particular the $^{cb+}$mEVs population is responsible for the enhanced hBMSCs mineralization *ex vivo*.

Removal of $^{cb+}$mEVs eliminates the effect of mEVs-mediate acceleration of osteoporotic bone regeneration

To further evaluate mEV and $^{cb+}$mEVs efficacies toward bone regeneration, we implanted the mEVs, $^{cb-}$mEVs and $^{AnxV-}$mEVs laden-hydrogel constructs into femoral condyle defects of OVX-induced osteoporotic rats. 2D micro-CT X-ray images revealed massive bone loss in the distal femoral diaphysis from longitudinal view, confirming OVX-induced osteoporotic bone conditions following ovariectomy. New bone formation occurred in all experimental groups but was the most pronounced for bone defects filled with mEVs-laden hydrogels (Fig. **7A**). Bone morphometry analysis showed that only the mEVs-col group exhibited a 2.4-fold

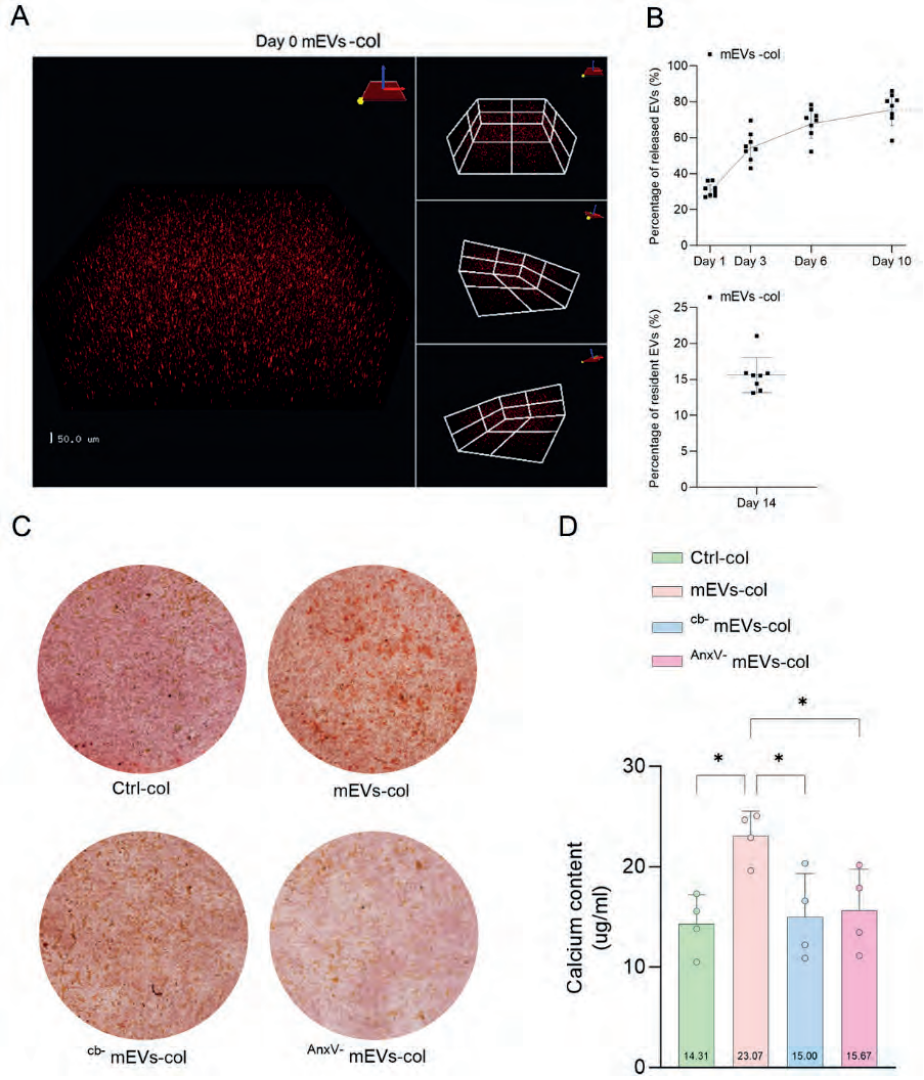

Fig. 6. $^{cb+}$mEVs in 3D hydrogel constructs enhance hBMSCs mineralization. A. Laser scanning-confocal microscope showing fluorescently labeled mEVs in 3D collagen hydrogel at day 0. B. Graphical representation of 3D encapsulated fluorescently labeled mEVs release from collagen-based hydrogels over time (n=8). C. Representative alizarin red staining of hBMSCs and D) Calcium content of hBMSCs encapsulated in 3D collagen-based hydrogel containing PBS (Ctrl) or mEVs or $^{cb-}$EVs or $^{AnxV-}$mEVs for 21day OM culture (n=4). Data were expressed as means ± standard deviation (SD). *$p < 0.05$. Scale bars correspond to 50 µm in 6A.

increase in bone tissue volume/total tissue volume (BV/TV%) compared to collagen controls, while groups lacking $^{cb+}$mEVs showed no improvement for this parameter (Fig. **7B**). Thereafter, we performed a histological analysis to investigate the ossification within the ROI. The images within closed defects surrounded by mature bone are the eligible ones for ROI determination. The inclusion of samples was based on careful selection of properly created bone defects (Table S2). H&E staining showed that new blood vessels identified by yellow cell nuclei in luminal structures around the newly formed bone were present in the ROI of all included samples slides (Fig. **7C**). To distinguish between connective tissue (yellow), newly formed bone (pink) and host bone tissue (bright red), we carried out EVG staining (Fig. **7D**). Moreover, we quantified the amount of newly formed bone within the ROI using consecutive sections. The area fractions of newly formed bone in the defects implanted with mEVs-col exhibited a 1.4-fold increase compared to collagen controls (Fig. **7E**), while removal of $^{cb+}$mEVs abolished the effect of mEVs on bone formation. Collectively, these data support the contribution of the $^{cb+}$mEVs subpopulation to mEV-mediated acceleration of orthotopic osteoporotic bone defect regeneration.

DISCUSSION

Most research on EVs focuses on their use in drug delivery, regenerative medicine, and the identification of EV-based biomarkers [68, 69], where EVs have been regarded as a single, homogeneous population. However, emerging evidence has emphasized the presence of distinct EV subpopulations [70, 71]. This study builds on these findings by highlighting the functional heterogeneity of mEVs, which can be explored after separating mEV subpopulations based on their collagen-binding property. This supports our hypothesis that ECM-binding capacity is an "EV-inherent feature" associated with functionality toward bone regeneration.

Emerging evidence shows that non-EV particles and proteins independent of EVs are susceptible to being co-isolated during ultracentrifugation (UC), leading to sample contamination [72]. Introducing SEC purification following ultracentrifugation, we obtained mEVs with higher purity expressing CD9 and CD81. These UC/SEC isolated mEVs were shown to stimulate mineral apposition of *ex vivo* bone and kept the positive effect on BMSC commitment toward an osteogenic phenotype without supplementing additional factors such as Ca^{2+} or bone morphogenetic protein 2 (BMP2) [73-75]. Attributing functional performance to a specific EV size fraction in downstream assessments is challenging [71]. It has been demonstrated that CD9

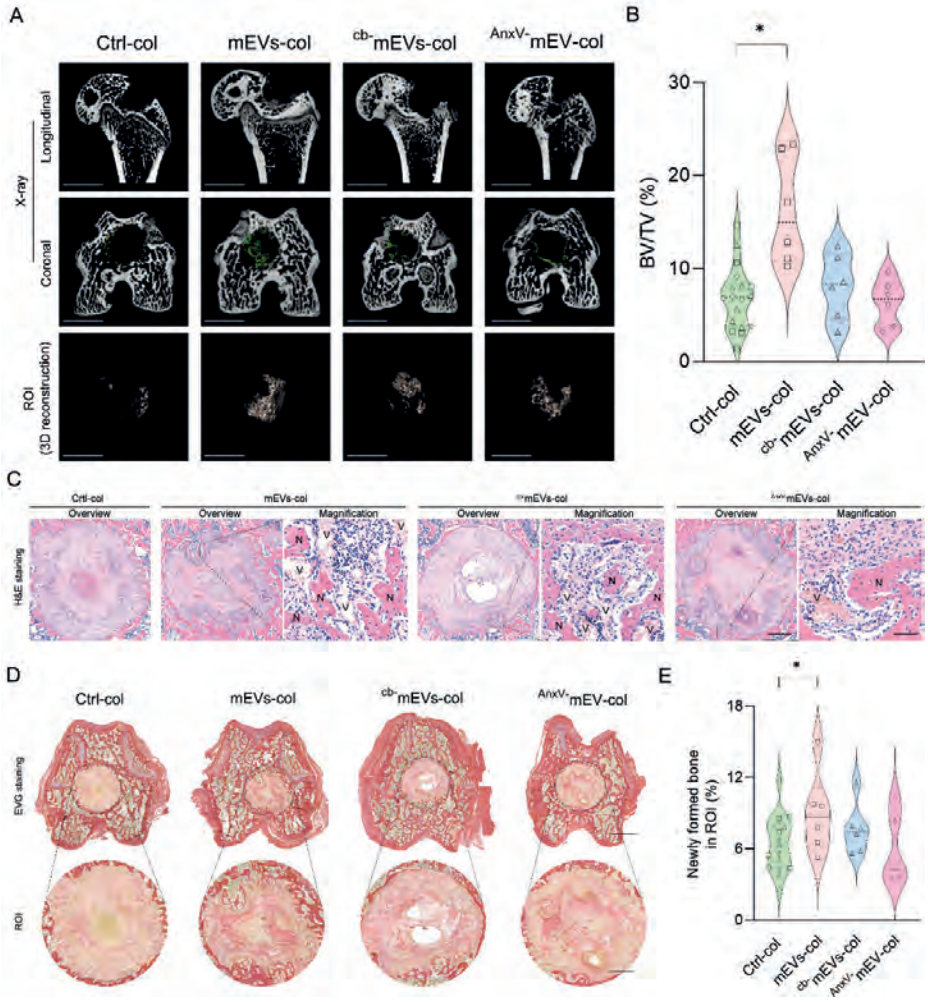

Fig. 7. Removal of $^{cb+}$mEVs eliminates the effect of mEVs-mediated acceleration of osteoporotic bone regeneration. A. Representative 2D micro-CT X-ray images from longitudinal and coronal view (The newly formed bone tissues within the defects were highlighted by green) and 3D reconstructions of ROI in femoral condyle defects. B. Bone morphometry analysis at 4 weeks of bone defects treated with ctrl-col, mEVs-col, cb-mEVs-col, or AnxV-mEVs-col (n=6 for each comparison). C. Representative images of H&E staining of the femoral condyle defects with mEVs-col, $^{cb-}$mEVs and $^{AnxV-}$mEVs in collagen, or collagen only (ctrl). N: newly formed bone, V: micro-vessels. D. Representative images of EVG staining of the femoral condyle defects mEVs-col, $^{cb-}$mEVs and $^{AnxV-}$mEVs in collagen hydrogel, or collagen hydrogel only (ctrl). Semi-quantitative analysis of (E) the area fractions of newly formed bone by staining intensity in separate channels through ImageJ software (n=6 for mEVs-col and cb-mEVs-col groups comparison and n=5 for AnxV-mEVs-col group). "☐" refers to the rats received mEVs-col and Ctrl-col treatment; "△" refers to the rats received cb-mEVs -col and Ctrl-col treatment; "◇" refers to the rats received AnxV-mEVs-col and Ctrl-col treatment. *$p < 0.05$. Scale bars correspond to 2.5 mm in 7A. In histology analysis, scale bar = 500 μm for overviewed image and 50 μm for magnified image in 7C; scale bar = 1 mm for overviewed EVG staining image and 500 μm for ROI image in 7D.

positive EVs mainly are present in the size range 50-100 nm and CD81 in 50-200 nm [71], meaning during SEC isolation the 70 nm resin pore size inevitably resulted in a large loss of CD9 and CD81 positive mEVs smaller than 70 nm. In the present study, the vast majority of mEVs are within the range of 100-200 nm according to cryo-EM imaging and NTA analysis. Therefore, to determine functional subpopulations within bulk mEVs, we turned to their surface moieties [49, 76].

Specific molecules present on the surface of EVs are considered to facilitate the EV-ECM interactions through covalent or hydrogen bonding [47]. Typically, to increase EVs retention within hydrogels for eliciting specific biological response, selective molecular interactions are desirable. A very recent paper demonstrated that EVs' immobilization in the type I collagen hydrogel was mediated by surface proteins RGD-binding integrins in a composition-dependent manner [77]. Furthermore, this specificity on surface biomolecules shapes EVs heterogeneity. For instance, *Lai et al.* leveraged specific lipid-binding ligands such as cholera toxin B and shiga toxin B to selectively isolate different MSC-EV subtypes with different protein and RNA contents. Notably, only shiga toxin B-binding EVs were found to express fibronectin with extra domain that are associated with promoting recruitment and adhesion of reparative cells [78]. In our study, we made use of the binding between mEVs and type I collagen to separate subpopulations, and a constant proportion of input mEVs binding to the collagen was calculated. The complete loss of osteogenic functionality in mEVs after the removal of $^{cb+}$mEVs implied that $^{cb+}$mEVs have been efficiently separated from the bulk mEVs. In addition, it has been reported that EVs still can be taken up by surrounding cells such as human endothelial colony-forming cells in the collagen-bound condition [54]. Herein, labeled $^{cb+}$mEVs accumulated massively around the nuclei of hBMSCs during culture on collagen plates and influenced the osteogenic differentiation of hBMSCs. This suggests that $^{cb+}$mEVs dynamically detached from collagen and entered into the cells.

Through bioinformatics analysis, we deduced that AnxV is associated with CD9 and CD81 in the $^{cb+}$mEV subpopulation. This is interesting as one recent paper reported that AnxV derived from MVs plays a central role in mediating MV adhesion to collagen and bone mineralization [79]. Specifically, MVs have been isolated from osteoblasts of mice in normal or osteoporotic conditions. In their cases, the inter-subpopulation heterogeneity (compositional and functional differences amongst EVs from various sources) contributed to distinguishing two types of EVs with massive difference in amount of AnxV. Herein the subsets of mEVs stemmed from the same bulk, as called intra-subpopulation heterogeneity (differences in EVs within subpopulations derived from the same source), have been identified

and isolated through immunomagnetic separation. However, the cellular uptake experimental data from the two studies indicated that the reduction of AnxV affects the receptor cells' uptake of EVs. AnxV, widely recognized as an EV marker [80], has been reported to be present in cow milk and capable of binding to collagen [81]. Calcium binding AnxV proteins are essential in mediating proteoliposome attachment to collagen fibrils [82]. The 2D coated type I collagen has negatively charged regions, including specific sites that resemble heparin structures. Therefore, the heparin-binding domain of AnxV could interact with these negatively charged regions on collagen. Moreover, the binding specificity was further enhanced with stabilization by calcium ions [83]. During OM culture, BMSCs can expose PS on their cell membrane facilitating interaction with annexin proteins and calcium-binding proteins like S100A9. These interactions enhance MV uptake by BMSCs and promote mineralization [84]. In our study, the inefficient cellular uptake observed in $^{AnxV-}$mEVs suggests that PS on BMSCs plays a role. Impaired uptake leads to a reduction in calcium mineralization for hBMSCs, indicating that the binding and potential uptake of mEVs are essential for functionality, and this process depends on AnxV on mEVs.

It is well established that integrin-mediated adhesion to collagen promotes stromal cell osteogenic differentiation [85]. This interaction has been utilized to immobilize EVs within collagen hydrogels for various clinical applications [86]. *Hao et al.* showed that functionalizing a material surface with the integrin α4β1 ligand, LLP2A, improved the binding of MSC-derived EVs and enhanced vascularization [87]. However, the proteomic analysis in the present study did not detect any integrin protein. We speculated that most of the mEVs are small EVs (exosomes), and integrin markers such as integrin β1, are not present on the surface of exosomes [88, 89]. Additionally, recent work reported that milk fat globule-EGF factor 8 (MFGE8) was identified as a principal protein in the corona around EVs released by human pluripotent stromal cells (hPSCs) that helps facilitate the uptake of EVs by recipient cells, a process that is crucial for maintaining the self-renewal and pluripotency of hPSCs [90]. In our study, MFGE8 as a protein found in milk, has been deduced as one of extracellular proteins enriched in $^{cb+}$mEVs. Previous paper reported that MFGE8 bound to type I collagen, resulting in promotion of collagen uptake by macrophages and decrease in severity of tissue fibrosis [91]. Therefore, we speculated this contributes to the mEVs binding to the collagen but might alleviate mEVs-induced osteogenesis of hBMSCs.

Collagen hydrogel is a highly biocompatible material, providing a suitable environment for cell adhesion and proliferation. Previously, we demonstrated that

osteoclasts and osteoclast-derived EVs encapsulated in collagen hydrogel promote bone regeneration using a mouse tibial bone defect model [92]. Considering the large fraction of mEVs released from collagen hydrogel over 14 days *in vitro*, we here collected the rat femoral condyles in the early phase of bone healing (4 weeks). Osteoporotic bone conditions serve as a challenging scenario for bone healing because it is characterized by decreased bone density, disrupted microarchitecture, and imbalance of bone turnover. These factors collectively weaken the regenerative capacity of bone and delay effective repair [93]. In these conditions, EVs could bring about a more obvious effect on bone regeneration [94]. Therefore, we tested the effect of mEV-laden collagen hydrogels on bone defect repair in an OVX-induced osteoporotic rat bone defect model. To minimize OVX-related variability, each animal received both an experimental and a control treatment. Of note, we observed the presence of microvascular networks in all the samples, which provide essential nutrients, and growth factors to the regenerating bone tissue. EVG staining was conducted to quantify the area fractions of newly formed bone [63]. It showed the collagen deposition appeared from various positions of the defect edges and had the tendency to spread outward. We observed the $^{cb-}$mEV or $^{AnxV-}$mEVs groups showed comparable amount of pink, randomly oriented collagen fiber compared to the control group. However, a noticeable increase in fiber density was found in defects filled with hydrogel constructs containing mEVs, suggesting that it is $^{cb+}$mEV subpopulation stimulates mEV-mediated bone formation *in vivo* at 4 weeks after implantation.

A notable innovation of this study is utilizing the specific biomolecular interaction between mEVs and type I collagen for EV subpopulation selection. The foundation for utilizing this inherent property is the high purity of mEVs. EVs isolated from body liquids comprise more lipoprotein and protein contaminants compared to EVs isolated from cell culture, typically MSCs [95]. Therefore, SEC isolation is an essential procedure for purifying mEVs in the present study. While for MSCs-EVs, EVs come from FBS are the main contamination problem. To obtain homogenous functional MSCs-EVs using PEG EVdepleted FBS [96], in combination of further collagen-binding selection could be a desirable method. It has been reported that MSCs-EVs contain the collagen-binding property. In consistent with the binding experiment results of our study, *Huang et al.* demonstrated a constant proportion of bulk MSCs-EVs bound to type I collagen [97]. However, their further research direction turned to control EVs release through introducing mimetic peptides within hydrogel construct. Controlling EVs release by functionalizing the biomaterials has been the focus of investigation, especially in bone regeneration. *Sophie Cox et al.* reported that pre-osteoblast derived-EVs had various release kinetics in different ratio of

chitosan-collagen, and 65%/35% chitosan-collagen has been utilized as the optimal construct for EVs delivery [81]. However, the released data on EVs in 100% collagen in their study showed CD63 positive EVs were barely detected in the receiving media, implying CD63 positive EVs have the optimal collagen binding property. Moreover, in the contactless transwell system, the most calcium depositions were observed the 100% chitosan containing EVs group, suggesting the CD63 positive EVs had the best osteogenic functionality. Recently, enhancing the collagen-binding property by conjugating some artificial peptides has been explored, which contributes to the retention of EVs at target sites [54, 98]. However, it seems that these studies overlook the heterogeneity of EVs. Although this approach aids in the retention of EVs, it might not be the bulk effect of EVs that alleviates the inflammatory response, promotes angiogenesis and osteogenesis, but rather the binding peptide that contributes to these effects. In the current study, we focused on native EVs and did not introduce external factors to explore a subset of EVs with collagen-binding properties that can promote osteogenesis.

It is a challenge that EV enrichment technologies have not kept pace with characterization tools in addressing the heterogeneity of EVs [71]. EVs could be characterized at the single-vesicle level but could not be easily enriched. This makes EV subpopulation recovery more difficult in the context of therapeutic applications, where large numbers of EVs are often required [39]. This limited our study to isolate $^{cb+}$mEVs and forced us to indirectly investigate the protein composition in $^{cb+}$mEVs by comparing mEVs and $^{cb-}$mEVs and use only the bulk and negative functional mEVs parts *in vivo*. However, the images of $^{cb-}$mEVs uptake by cells implied the presence of $^{cb-}$mEVs in mEVs may not compete with $^{cb+}$mEVs to enter the recipient cells and negatively influence the effect of mEVs in driving osteogenesis. Therefore, it is imperative to evaluate whether $^{cb+}$mEVs could truly perform better compared to the bulk mEVs in boosting bone regeneration. Future research should explore ways to enrich collagen-binding mEVs. For example, 3D collagen-coated microspheres can be used to increase the binding area for $^{cb+}$mEVs. However, it is not recommended to load mEVs into the microspheres, as the physical properties of EVs and ECM might affect their binding. Furthermore, by exploring the biomolecular interactions between EVs and ECM, we can establish a standard procedure, such as collagen binding (domain) chromatography, to isolate collagen-binding mEVs. Nevertheless, column EV desorption using high salt or acid may harm the integrity of EVs. Knowing which binding protein mediates the collagen attachment or using a unique marker of this EV subpopulation remains essential for further high yield immunoaffinity purification.

The clinical translational potential of $^{cb+}$mEVs is significantly enhanced by overcoming the challenge of heterogeneity common in broader EV populations. Unlike bulk mEVs, which vary in cargo and function, $^{cb+}$mEVs represent a standardized subset, ensuring consistent and predictable therapeutic outcomes. This consistency allows for more reliable clinical applications, particularly in bone repair, compared to EV-functionalized biomaterials, where variability in EV quality compromises results. Compared to traditional materials like autografts and allografts, $^{cb+}$mEVs offer a non-invasive, cell-free alternative, eliminating risks of immune rejection and donor site morbidity, while also providing better integration into the bone matrix due to their collagen-binding properties. Additionally, $^{cb+}$mEVs are more effective than synthetic bone substitutes or growth factor therapies, as they deliver regenerative factors more precisely, promoting localized bone regeneration with fewer side effects. Thus, with their resolved heterogeneity, $^{cb+}$mEVs offer a safe, scalable, and cost-effective solution for bone repair, positioning them as a promising alternative to both traditional and emerging bone repair materials.

CONCLUSION

We demonstrate the osteogenic functionality of UC/SEC bulk mEVs. More importantly, focusing on mEV heterogeneity, we harnessed collagen binding to separate $^{cb+}$mEVs and $^{cb-}$mEVs. Using *in vitro* osteogenic differentiation, *ex vivo* osteogenesis, and *in vivo* osteoporotic bone defect regeneration, we show that the $^{cb+}$mEV subpopulation is responsible for the osteogenic functionality of mEVs but $^{cb-}$mEVs, that represent the largest proportion of bulk mEVs, have no bone-promoting capacity. AnxV was found to be enriched in the $^{cb+}$mEV subpopulation and essential for mEVs collagen binding and mEVs-mediated bone regeneration.

REFERENCES

1. von Rüden, C. and P. Augat, Failure of fracture fixation in osteoporotic bone. Injury, 2016. **47 Suppl 2**: p. S3-s10.
2. Li, Y., et al., Bone defect animal models for testing efficacy of bone substitute biomaterials. J Orthop Translat, 2015. **3**(3): p. 95-104.
3. Hadji, P., et al., The epidemiology of osteoporosis--Bone Evaluation Study (BEST): an analysis of routine health insurance data. Dtsch Arztebl Int, 2013. **110**(4): p. 52-7.
4. Global, regional, and national burden of bone fractures in 204 countries and territories, 1990-2019: a systematic analysis from the Global Burden of Disease Study 2019. Lancet Healthy Longev, 2021. **2**(9): p. e580-e592.
5. Mora, R., et al., Economic Burden and Practical Considerations, in Hexapod External Fixator Systems: Principles and Current Practice in Orthopaedic Surgery, M. Massobrio and R. Mora, Editors. 2021, Springer International Publishing: Cham. p. 285-289.
6. Perez, J.R., et al., Tissue Engineering and Cell-Based Therapies for Fractures and Bone Defects. Front Bioeng Biotechnol, 2018. **6**: p. 105.
7. Zhang, H., et al., Expert consensus on the bone repair strategy for osteoporotic fractures in China. Front Endocrinol (Lausanne), 2022. **13**: p. 989648.
8. Jimi, E., et al., The current and future therapies of bone regeneration to repair bone defects. Int J Dent, 2012. **2012**: p. 148261.
9. Ferraz, M.P., Bone Grafts in Dental Medicine: An Overview of Autografts, Allografts and Synthetic Materials. Materials (Basel), 2023. **16**(11).
10. Amini, Z. and R. Lari, A systematic review of decellularized allograft and xenograft-derived scaffolds in bone tissue regeneration. Tissue Cell, 2021. **69**: p. 101494.
11. Vo, T.N., F.K. Kasper, and A.G. Mikos, Strategies for controlled delivery of growth factors and cells for bone regeneration. Adv Drug Deliv Rev, 2012. **64**(12): p. 1292-309.
12. Davies, O.G., Extracellular vesicles: From bone development to regenerative orthopedics. Mol Ther, 2023. **31**(5): p. 1251-1274.
13. Yáñez-Mó, M., et al., Biological properties of extracellular vesicles and their physiological functions. J Extracell Vesicles, 2015. **4**: p. 27066.
14. Kalluri, R. and V.S. LeBleu, The biology, function, and biomedical applications of exosomes. Science, 2020. **367**(6478).
15. S, E.L.A., et al., Extracellular vesicles: biology and emerging therapeutic opportunities. Nat Rev Drug Discov, 2013. **12**(5): p. 347-57.
16. Yu, T., et al., Extracellular vesicle-functionalized bioactive scaffolds for bone regeneration. Asian J Pharm Sci, 2024. **19**(5): p. 100945.
17. Furuta, T., et al., Mesenchymal Stem Cell-Derived Exosomes Promote Fracture Healing in a Mouse Model. Stem Cells Transl Med, 2016. **5**(12): p. 1620-1630.
18. Sanz-Ros, J., et al., Extracellular Vesicles as Therapeutic Resources in the Clinical Environment. Int J Mol Sci, 2023. **24**(3).
19. Liu, M., Y. Sun, and Q. Zhang, Emerging Role of Extracellular Vesicles in Bone Remodeling. J Dent Res, 2018. **97**(8): p. 859-868.
20. Eitan, E., et al., Extracellular vesicle-depleted fetal bovine and human sera have reduced capacity to support cell growth. J Extracell Vesicles, 2015. **4**: p. 26373.

21. Jiao, Y., et al., Advances in the Study of Extracellular Vesicles for Bone Regeneration. Int J Mol Sci, 2024. **25**(6).
22. Miracle, D.J., et al., Contemporary ethical issues in human milk-banking in the United States. Pediatrics, 2011. **128**(6): p. 1186-91.
23. Chutipongtanate, S., A.L. Morrow, and D.S. Newburg, Human Milk Extracellular Vesicles: A Biological System with Clinical Implications. Cells, 2022. **11**(15).
24. Sanwlani, R., et al., Milk-Derived Extracellular Vesicles in Inter-Organism, Cross-Species Communication and Drug Delivery. Proteomes, 2020. **8**(2).
25. Barathan, M., et al., Milk-Derived Extracellular Vesicles: A Novel Perspective on Comparative Therapeutics and Targeted Nanocarrier Application. Vaccines (Basel), 2024. **12**(11).
26. Marsh, S.R., et al., Novel Protocols for Scalable Production of High Quality Purified Small Extracellular Vesicles from Bovine Milk. Nanotheranostics, 2021. **5**(4): p. 488-498.
27. Oliveira, M.C., et al., Milk extracellular vesicles accelerate osteoblastogenesis but impair bone matrix formation. J Nutr Biochem, 2016. **30**: p. 74-84.
28. Oliveira, M.C., et al., Milk-Derived Nanoparticle Fraction Promotes the Formation of Small Osteoclasts But Reduces Bone Resorption. J Cell Physiol, 2017. **232**(1): p. 225-33.
29. Oliveira, M.C., et al., Bovine Milk Extracellular Vesicles Are Osteoprotective by Increasing Osteocyte Numbers and Targeting RANKL/OPG System in Experimental Models of Bone Loss. Front Bioeng Biotechnol, 2020. **8**: p. 891.
30. Silva, F.R.F., et al., Bovine Milk Extracellular Vesicles as a Preventive Treatment for Bone Dysfunction and Metabolic Alterations in Obese Mice Fed a High-Refined Carbohydrate Diet. Mol Nutr Food Res, 2025: p. e70139.
31. Dong, M., et al., Milk-derived small extracellular vesicles: nanomaterials to promote bone formation. J Nanobiotechnology, 2022. **20**(1): p. 370.
32. Nguyen, V.V.T., et al., Functional assays to assess the therapeutic potential of extracellular vesicles. J Extracell Vesicles, 2020. **10**(1): p. e12033.
33. Sharma, S., et al., Impact of isolation methods on the biophysical heterogeneity of single extracellular vesicles. Sci Rep, 2020. **10**(1): p. 13327.
34. Xiang, B., et al., Microenvironmental Modulation for Therapeutic Efficacy of Extracellular Vesicles. Adv Sci (Weinh), 2025. **12**(18): p. e2503027.
35. Adamo, G., et al., DetectEV: A functional enzymatic assay to assess integrity and bioactivity of extracellular vesicles. J Extracell Vesicles, 2025. **14**(1): p. e70030.
36. Davidson, S.M., et al., Methods for the identification and characterization of extracellular vesicles in cardiovascular studies: from exosomes to microvesicles. Cardiovasc Res, 2023. **119**(1): p. 45-63.
37. Caponnetto, F., et al., Size-dependent cellular uptake of exosomes. Nanomedicine, 2017. **13**(3): p. 1011-1020.
38. Shami-Shah, A., B.G. Travis, and D.R. Walt, Advances in extracellular vesicle isolation methods: a path towards cell-type specific EV isolation. Extracell Vesicles Circ Nucl Acids, 2023. **4**(3): p. 447-460.
39. van de Wakker, S.I., et al., Size matters: Functional differences of small extracellular vesicle subpopulations in cardiac repair responses. J Extracell Vesicles, 2024. **13**(1): p. e12396.
40. Arntz, O.J., et al., Profiling of plasma extracellular vesicles identifies proteins that strongly associate with patient's global assessment of disease activity in rheumatoid arthritis. Front Med (Lausanne), 2023. **10**: p. 1247778.

41. Nikoloff, J.M., et al., Identifying extracellular vesicle populations from single cells. Proc Natl Acad Sci U S A, 2021. **118**(38).
42. Zendrini, A., et al., On the surface-to-bulk partition of proteins in extracellular vesicles. Colloids Surf B Biointerfaces, 2022. **218**: p. 112728.
43. Mitchell, M.I., et al., Extracellular Vesicle Capture by AnTibody of CHoice and Enzymatic Release (EV-CATCHER): A customizable purification assay designed for small-RNA biomarker identification and evaluation of circulating small-EVs. J Extracell Vesicles, 2021. **10**(8): p. e12110.
44. Kang, Y.T., et al., Isolation and Profiling of Circulating Tumor-Associated Exosomes Using Extracellular Vesicular Lipid-Protein Binding Affinity Based Microfluidic Device. Small, 2019. **15**(47): p. e1903600.
45. Iwayama, T., et al., Matrix Vesicle-Mediated Mineralization and Potential Applications. J Dent Res, 2022. **101**(13): p. 1554-1562.
46. Genschmer, K.R., et al., Activated PMN Exosomes: Pathogenic Entities Causing Matrix Destruction and Disease in the Lung. Cell, 2019. **176**(1-2): p. 113-126.e15.
47. Debnath, K., et al., Extracellular vesicle-matrix interactions. Nat Rev Mater, 2023. **8**(6): p. 390-402.
48. Wang, P., et al., ECM-binding properties of extracellular vesicles: advanced delivery strategies for therapeutic applications in bone and joint diseases. Cell Commun Signal, 2025. **23**(1): p. 161.
49. Sariano, P.A., et al., Convection and extracellular matrix binding control interstitial transport of extracellular vesicles. J Extracell Vesicles, 2023. **12**(4): p. e12323.
50. Fan, L., et al., The Use of Collagen-Based Materials in Bone Tissue Engineering. Int J Mol Sci, 2023. **24**(4).
51. Ferreira, A.M., et al., Collagen for bone tissue regeneration. Acta Biomater, 2012. **8**(9): p. 3191-200.
52. Shin, M.K., et al., A novel collagen-binding peptide promotes osteogenic differentiation via Ca2+/calmodulin-dependent protein kinase II/ERK/AP-1 signaling pathway in human bone marrow-derived mesenchymal stem cells. Cell Signal, 2008. **20**(4): p. 613-24.
53. Choi, Y.J., et al., Enhanced osteogenesis by collagen-binding peptide from bone sialoprotein in vitro and in vivo. J Biomed Mater Res A, 2013. **101**(2): p. 547-54.
54. Hao, D., et al., Engineered extracellular vesicles with high collagen-binding affinity present superior in situ retention and therapeutic efficacy in tissue repair. Theranostics, 2022. **12**(13): p. 6021-6037.
55. Silva, F.R.F., et al., Protective Effect of Bovine Milk Extracellular Vesicles on Alveolar Bone Loss. Mol Nutr Food Res, 2024. **68**(3): p. e2300445.
56. Shelke, G.V., et al., Importance of exosome depletion protocols to eliminate functional and RNA-containing extracellular vesicles from fetal bovine serum. J Extracell Vesicles, 2014. **3**.
57. Husch, J.F.A., et al., Comparison of Osteogenic Capacity and Osteoinduction of Adipose Tissue-Derived Cell Populations. Tissue Eng Part C Methods, 2023. **29**(5): p. 216-227.
58. Hall, T.A.G., et al., Active osseointegration in an ex vivo porcine bone model. Front Bioeng Biotechnol, 2024. **12**: p. 1360669.
59. Meier, F., et al., diaPASEF: parallel accumulation-serial fragmentation combined with data-independent acquisition. Nat Methods, 2020. **17**(12): p. 1229-1236.
60. Zhang, D.X., et al., αvβ1 integrin is enriched in extracellular vesicles of metastatic breast cancer cells: A mechanism mediated by galectin-3. J Extracell Vesicles, 2022. **11**(8): p. e12234.
61. Wang, Z., et al., Cisplatin-functionalized dual-functional bone substitute granules for bone defect treatment after bone tumor resection. Acta Biomater, 2025. **191**: p. 158-176.

62. Wang, P., et al., Hydroxysafflor yellow A promotes osteogenesis and bone development via epigenetically regulating β-catenin and prevents ovariectomy-induced bone loss. Int J Biochem Cell Biol, 2021. **137**: p. 106033.
63. Webber, J. and A. Clayton, How pure are your vesicles? J Extracell Vesicles, 2013. **2**.
64. Cramer, E.E.A., et al., Culture system for longitudinal monitoring of bone dynamics ex vivo. Biotechnol Bioeng, 2025. **122**(1): p. 53-68.
65. Karimi, N., et al., Tetraspanins distinguish separate extracellular vesicle subpopulations in human serum and plasma - Contributions of platelet extracellular vesicles in plasma samples. J Extracell Vesicles, 2022. **11**(5): p. e12213.
66. Saftics, A., et al., Single Extracellular VEsicle Nanoscopy. J Extracell Vesicles, 2023. **12**(7): p. e12346.
67 Roefs, M.T., J.P.G. Sluijter, and P. Vader, Extracellular Vesicle-Associated Proteins in Tissue Repair. Trends Cell Biol, 2020. **30**(12): p. 990-1013.
68 Sluijter, J.P.G., et al., Extracellular vesicles in diagnostics and therapy of the ischaemic heart: Position Paper from the Working Group on Cellular Biology of the Heart of the European Society of Cardiology. Cardiovasc Res, 2018. **114**(1): p. 19-34.
69. Zhang, H., et al., Identification of distinct nanoparticles and subsets of extracellular vesicles by asymmetric flow field-flow fractionation. Nat Cell Biol, 2018. **20**(3): p. 332-343.
70. Carney, R.P., et al., Harnessing extracellular vesicle heterogeneity for diagnostic and therapeutic applications. Nat Nanotechnol, 2024.
71. Visan, K.S., et al., Comparative analysis of tangential flow filtration and ultracentrifugation, both combined with subsequent size exclusion chromatography, for the isolation of small extracellular vesicles. J Extracell Vesicles, 2022. **11**(9): p. e12266.
72. Carluccio, M., et al., Adult mesenchymal stem cells: is there a role for purine receptors in their osteogenic differentiation? Purinergic Signal, 2020. **16**(3): p. 263-287.
73. Vermeulen, S., et al., An in vitro model system based on calcium- and phosphate ion-induced hMSC spheroid mineralization. Mater Today Bio, 2023. **23**: p. 100844.
74. Martin-Iglesias, S., et al., BMP-2 Enhances Osteogenic Differentiation of Human Adipose-Derived and Dental Pulp Stem Cells in 2D and 3D In Vitro Models. Stem Cells Int, 2022. **2022**: p. 4910399.
75. Kamerkar, S., et al., Exosomes facilitate therapeutic targeting of oncogenic KRAS in pancreatic cancer. Nature, 2017. **546**(7659): p. 498-503.
76. Tam, N.W., et al., Extracellular Vesicle Mobility in Collagen I Hydrogels Is Influenced by Matrix-Binding Integrins. ACS Nano, 2024. **18**(43): p. 29585-29601.
77. Lai, R.C., et al., MSC secretes at least 3 EV types each with a unique permutation of membrane lipid, protein and RNA. J Extracell Vesicles, 2016. **5**: p. 29828.
78. Su, G., et al., Annexin A5 derived from matrix vesicles protects against osteoporotic bone loss via mineralization. Bone Res, 2023. **11**(1): p. 60.
79. Dietz, L., et al., Uptake of extracellular vesicles into immune cells is enhanced by the protein corona. J Extracell Vesicles, 2023. **12**(12): p. e12399.
80. Man, K., et al., An ECM-Mimetic Hydrogel to Promote the Therapeutic Efficacy of Osteoblast-Derived Extracellular Vesicles for Bone Regeneration. Front Bioeng Biotechnol, 2022. **10**: p. 829969.
81. Davies, O.G., et al., Annexin-enriched osteoblast-derived vesicles act as an extracellular site of mineral nucleation within developing stem cell cultures. Sci Rep, 2017. **7**(1): p. 12639.
82. Capila, I., et al., Interaction of heparin with annexin V. FEBS Lett, 1999. **446**(2-3): p. 327-30.

83. Zhang, C., et al., Coupling of Integrin α5 to Annexin A2 by Flow Drives Endothelial Activation. Circ Res, 2020. **127**(8): p. 1074-1090.
84. Kundu, A.K. and A.J. Putnam, Vitronectin and collagen I differentially regulate osteogenesis in mesenchymal stem cells. Biochem Biophys Res Commun, 2006. **347**(1): p. 347-57.
85. Ramírez, O.J., et al., Type I collagen hydrogels as a delivery matrix for royal jelly derived extracellular vesicles. Drug Deliv, 2020. **27**(1): p. 1308-1318.
86. Hao, D., et al., Extracellular Matrix Mimicking Nanofibrous Scaffolds Modified With Mesenchymal Stem Cell-Derived Extracellular Vesicles for Improved Vascularization. Front Bioeng Biotechnol, 2020. **8**: p. 633.
87. Baietti, M.F., et al., Syndecan-syntenin-ALIX regulates the biogenesis of exosomes. Nat Cell Biol, 2012. **14**(7): p. 677-85.
88. Babaker, M.A., et al., The Therapeutic Potential of Milk Extracellular Vesicles on Colorectal Cancer. Int J Mol Sci, 2022. **23**(12).
89. Lee, Y., et al., MFGE-8, a Corona Protein on Extracellular Vesicles, Mediates Self-Renewal and Survival of Human Pluripotent Stem Cells. J Extracell Vesicles, 2025. **14**(4): p. e70056.
90. Wang, M., et al., MFG-E8 activates proliferation of vascular smooth muscle cells via integrin signaling. Aging Cell, 2012. **11**(3): p. 500-8.
91. Faqeer, A., et al., Cleaved SPP1-rich extracellular vesicles from osteoclasts promote bone regeneration via TGFβ1/SMAD3 signaling. Biomaterials, 2023. **303**: p. 122367.
92. Cheung, W.H., et al., Fracture healing in osteoporotic bone. Injury, 2016. **47 Suppl 2**: p. S21-6.
93. Shaheen, M.Y., et al., Impact of Single or Combined Drug Therapy on Bone Regeneration in Healthy and Osteoporotic Rats. Tissue Eng Part A, 2021. **27**(9-10): p. 572-581.
94. Brennan, K., et al., A comparison of methods for the isolation and separation of extracellular vesicles from protein and lipid particles in human serum. Sci Rep, 2020. **10**(1): p. 1039.
95. Wang, P., et al., Polyethylene glycol precipitation is an efficient method to obtain extracellular vesicle-depleted fetal bovine serum. PLoS One, 2023. **18**(12): p. e0295076.
96. Huang, C.C., et al., 3D Encapsulation and tethering of functionally engineered extracellular vesicles to hydrogels. Acta Biomater, 2021. **126**: p. 199-210.
97. Jeon, S., et al., Controlled delivery of HIF-1α via extracellular vesicles with collagen-binding activity for enhanced wound healing. J Control Release, 2025. **380**: p. 330-347.

SUPPLEMENTAL INFORMATION

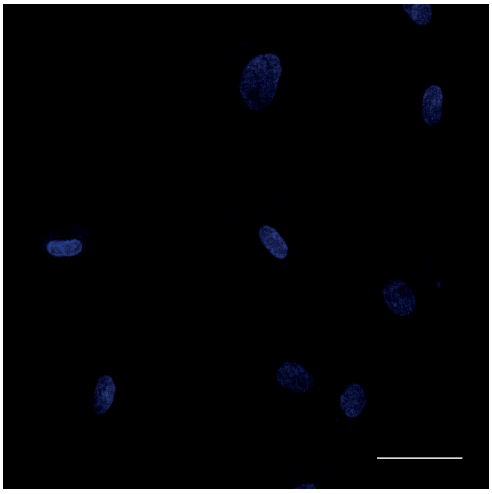

Fig. S1. Fluorescence image of dapi-stained hBMSCs cultured on collagen-coated tissue plastic without $^{cb+}$mEVs in 6h (Ctrl). Scale bars correspond to 100 µm.

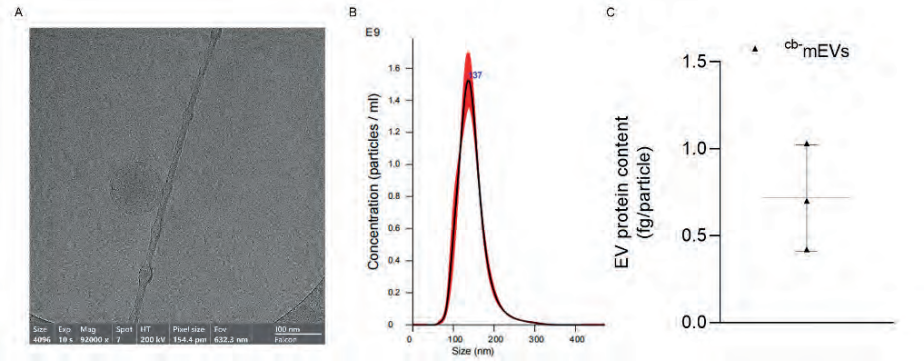

Fig. S2. $^{cb-}$mEVs characterization. A. Observation of the morphology of $^{cb-}$mEVs under Cryo-EM (92000x). B. NTA detection of the median particle size of $^{cb-}$mEVs (n=3). C. Determination of particle/protein ratio as $^{cb-}$mEVs protein content (n=3). Data were expressed as means ± standard deviation (SD).

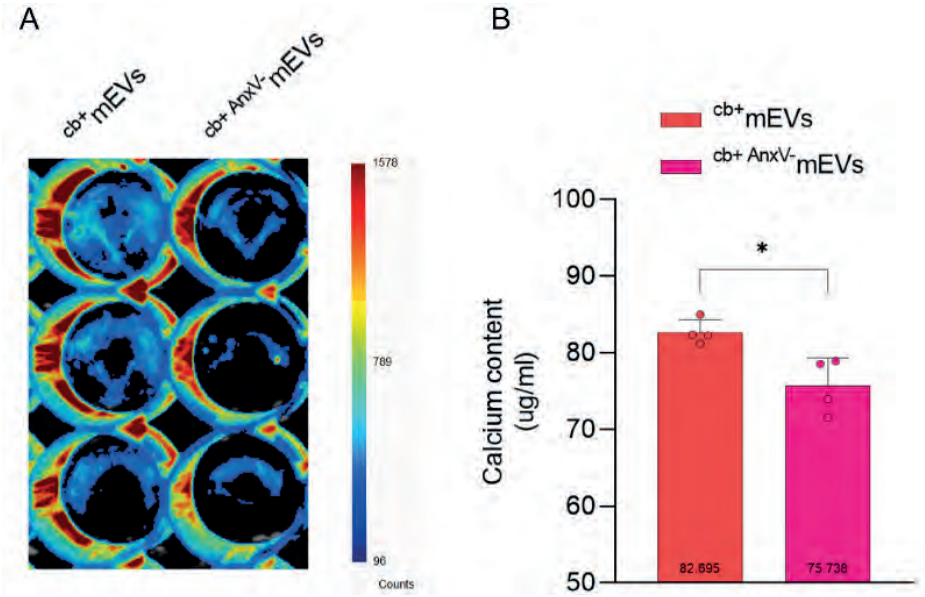

Fig. S3. Depleting AnxV diminished mEVs-collagen binding. A. IVIS image showing a representative image of the binding of fluorescently labeled $^{cb+}$mEVs and $^{cb+\ AnxV-}$mEVs. B. Calcium content of hBMSCs cultured in OM in collagen-coated tissue culture plastic within $^{cb+}$mEVs or $^{cb+\ AnxV-}$mEVs for 21 days (n=4). Data were expressed as means ± standard deviation (SD). *$p < 0.05$.

Table S1. List of proteins enriched in $^{cb+}$mEVs.

S.No	Protein accession	Gene symbol	Intensity mEVs-1	Intensity mEVs-2	Intensity $^{cb-}$mEVs-1	Intensity $^{cb-}$mEVs -2
1	Q5E946	PARK7	21.0	50.4	7.3	
2	P28783	S100A9	36.0	24.7	7.6	
3	A0AAA9T9Y7	CSN2	306.1	1479.5	167.4	283.6
4	D3TJT8	CSN1S1	233.9	17.8	34.4	
5	A5D7Q6	PCDHGA2	98.3	166.5	47.4	46.3
6	P02663	CSN1S2	5850.5	441.7	2177.3	131.8
7	Q28049	LALBA	91.4	91.7	28.2	43.8
8	Q2UVX4	C3	197.8	31.7	64.5	27.0
9	F1N1Z8	LOC104975830	255.1	105.2	118.9	37.3
10	Q3SYR8	JCHAIN	2012.8	1329.6	1095.6	424.6
11	Q8SPP7	PGLYRP1	28.0	62.1	17.5	25.0
12	F1N026	ITM2B	19.3	11.0	7.1	
13	P81265	PIGR	725.7	780.5	511.3	208.5
14	P11151	LPL	728.7	624.3	361.2	288.3
15	A4FV54	RAB8A	66.7	52.7	45.5	15.2
16	Q862Q3	B2M	129.1	282.8	129.2	83.5
17	Q0VBY4	TPD52L1	8.0	17.0	6.7	
18	P30922	CHI3L1	42.8	24.6	18.5	
19	D1Z306	CRISPLD2	42.8	26.9	19.5	
20	E1BGX8	HHIPL2	113.4	60.6	49.3	
21	Q95M40	TXNDC17	29.6	18.9	20.8	6.9
22	G3X6N3	TF	152.6	125.8	49.7	110.2
23	Q0IIA4	GP2	1092.1	244.4	726.2	80.7
24	Q3ZCL0	CRISP3	105.9	875.0	71.8	523.6
25	F1MM32	QSOX1	158.1	67.5	106.9	30.8
26	F1N152	HTRA1	15.7	11.3	8.4	
27	P05689	CTSZ	62.5	40.7	32.4	
28	P80195	GLYCAM1	4661.2	1796.5	2441.8	1638.6
29	P81287	ANXA5	97.7	147.7	69.0	87.1
30	Q2TBI0	LBP	51.7	15.4	21.6	
31	Q95JH2	AGPAT1	65.5	50.5	37.4	
32	Q3ZCD0	CD81	34.9	114.1	32.4	64.9
33	Q148D9	CREG1	37.8	15.5	17.5	
34	Q3T0D7	SAR1A	88.3	41.9	85.7	
35	P20072	ANXA7	35.9	58.8	32.7	

Table S1. Continued

S.No	Protein accession	Gene symbol	Intensity mEVs-1	Intensity mEVs-2	Intensity ^{cb}mEVs-1	Intensity ^{cb}mEVs -2
36	Q32L41	GCHFR	69.3	10.0	41.2	14.2
37	P80025	LPO	264.7	87.8	151.2	99.5
38	A0A3Q1LGW7	KRT76	5873.0	13577.5	4573.2	9889.2
39	Q95114	MFGE8	7021.0	1880.1	5397.8	1249.3
40	F1N6Y1	GANAB	41.3	27.1	26.1	
41	G3N2D8	GGT1	2843.6	3402.9	2601.1	2240.7
42	P30932	CD9	1446.3	198.6	1178.1	99.1
43	Q5EA79	GALM	602.4	69.5	489.1	32.9
44	Q3SZZ9	FGG	71.1	44.2	45.4	
45	Q5E994	CHMP1B	405.9	49.1	307.8	50.7
46	Q8SPJ1	JUP	55.7	320.8	94.4	202.8
47	Q0VCK0	ATIC	43.4	3.0	18.4	
48	A0AAA9T9N7	PANK1	567.6	339.0	280.9	437.9
49	Q2KJ22	MINDY1	104.9	11.0	80.1	12.3
50	F1MXH7	CSF2RB	46.7	23.0	28.1	
51	Q17QE5	CIB1	325.3	144.2	275.0	104.2
52	P00727	LAP3	198.9	36.3	178.0	13.6
53	E1BKT9	DSP	12.7	53.0	32.4	21.2
54	Q32KV6	SIL1	17.5	30.2	4.4	34.9
55	Q8MJ50	OSTF1	81.2	20.1	42.1	
56	Q3ZBD7	GPI	194.6	97.2	191.8	50.7
57	A0AAA9TDJ4	SDCBP	101.0	19.5	57.8	43.2
58	F1MNI4	RAB5B	72.0	29.6	78.7	6.7
59	P50448	SERPING1	134.8	82.0	81.1	101.8
60	E1BP42	CSAD	36.1	17.3	22.6	
61	P50227	SULT1A1	56.4	14.4	54.0	6.5
62	Q4GZT4	ABCG2	2891.3	1587.0	2175.1	1672.3
63	Q3T000	YKT6	202.1	55.9	192.3	32.0
64	Q3T0U5	CHMP2A	435.1	51.4	352.1	77.4
65	Q28161	PKP1	31.3	47.0	34.6	
66	F1MYJ3	GGT5	32.4	4.7	16.4	
67	A6QR35	SCAMP2	74.5	20.7	80.9	3.7
68	Q32KR9	CHMP1A	193.1	14.7	185.3	
69	Q27960	SLC34A2	3688.2	758.6	3443.0	539.8
70	Q3SZU5	SPCS3	281.1	72.0	160.7	

Table S1. Continued

S.No	Protein accession	Gene symbol	Intensity mEVs-1	Intensity mEVs-2	Intensity $^{cb-}$mEVs-1	Intensity $^{cb-}$mEVs -2
71	A1L5C6	HPN	42.7	136.9	56.3	108.7
72	P28782	S100A8	224.0	9.0		
73	Q32L14	RBP4	20.9	8.7		

Intensity: Mass spectrometric signal intensity for a peptide is an indicator for its respective amount in the sample.

Tables S2. Defects for Histological Analysis in ROI.

Groups	Defects Created	Defects Included in Analysis
Ctrl-col	18	17
mEVs-col	6	6
$^{cb-}$mEVs-col	6	6
$^{AnxV-}$mEVs-col	6	5

Chapter 6

Ex vivo human femoral head bone discs: a model for studying bone regeneration

Peng Wang, Gerry Koons, Zhule Wang, Jetze Visser, Fons van de Loo,
Jeroen JJP van den Beucken

In preparation

ABSTRACT

Preclinical assessment of regenerative capacity on the treatment of bone defects is underpinned by a large burden for laboratory animals. We here evaluated the feasibility of an *ex vivo* human bone defect model to assess effects on bone regeneration from extracellular vesicle (EVs). This approach potentially offers a humanized alternative to animal testing for the evaluation of bone regeneration. A standardized protocol was developed to create human bone discs of uniform size and maintain sterility throughout the procedure. AlamarBlue™ assays revealed sustained viability of healthy cells originating from the bone discs over a 14-day culture period. Histological images confirmed the presence of CD14 positive monocyte-lineage cells and microvessels in bone marrow of bone discs next to abundant adipocytes. Levels of pro-inflammatory cytokines (i.e. IL6, IL1b, TNFa) and TRAP activity in supernatant of human bone discs confirmed that bone discs retain the inherent immune response and marginal resorption activity for bone remodeling. Flow cytometry and gene expression data further demonstrated that bone marrow mesenchymal stromal cells (hBMSCs) resided in the human bone discs during ex vivo culture and kept their osteogenic differentiation capacity. Most importantly, fluorochrome uptake proved increased bone formation evoked by cow milk EVs during ex vivo culture of human bone discs. These findings underscore that this ex vivo bone model provides a 3D bone microenvironment comprising vital trabecular bone and bone marrow, which resembles important features of physiological bone tissue. Overall, this ex vivo human bone model holds promise as an appealing platform for investigating bone biology and evaluating novel regenerative therapeutic strategies.

INTRODUCTION

Bone defects, frequently resulting from trauma, tumor removal, or age-related conditions like osteoporosis, severely affect patients' mobility, independence, and overall quality of life [1]. An estimated 10 million people worldwide suffer from bone defects each year, leading to global healthcare costs for bone healing that exceed $50 billion [2]. The natural healing process is initiated by an inflammatory response, which is crucial for recruiting immune cells such as neutrophils and macrophages that secrete cytokines and growth factors [3]. Thereafter, mesenchymal stromal cells (MSCs) differentiate into osteoblasts, playing pivotal roles in bone formation [4], and multinucleated osteoclasts gradually form and become active during the remodeling phase to resorb excess or disorganized bone [5]. Besides, angiogenesis is crucial for supplying the necessary oxygen and nutrients to healing tissue and for removing metabolic waste [6]. For the treatment of large bone defects requiring surgical intervention, autologous and allogeneic bone grafts are commonly employed. Allogeneic grafts are often combined with biomaterials and biological agents—such as cells, growth factors, or extracellular vesicles (EVs)—to enhance bone repair [7].

EVs comprise a diverse type of membrane-bound structure secreted by various cell types. They are key mediators of intercellular communication, delivering bioactive cargo—such as microRNAs (miRNAs), proteins, and lipids—to target cells, where they activate specific signaling pathways [8]. EVs has been implicated in playing a vital role in mediating cellular communication throughout the bone remodeling process [9]. It has been reported that CD9-knockout mice exhibited impaired femoral fracture healing due to diminished exosome secretion, underscoring the importance of EVs in bone regeneration [10]. Our previous studies showed that EVs isolated from cow milk (mEVs) contribute to bone homeostasis by modulating the activity of osteoblasts and osteoclasts [11, 12]. Recent work demonstrated that the local delivery of mEVs promoted bone repair using a mice skull defect model [13]. The local injections of EVs with biomaterials, such as hydrogel constructs, have been commonly used in preclinical research on therapeutic application in bone regeneration, using animal models such as calvarial defects, femoral fractures, and tibia defects in mice, rats and rabbits [14, 15]. Nonetheless, it should be noted that the bone structure, remodeling processes, and anatomy of these animal models differ significantly from the human bone. In addition, the ethical debate on the utilization of animals in research has strongly intensified over the last years [16]. Therefore, *ex vivo* tissue culture models utilizing discarded vital bone could provide a valuable alternative to animal models, bridging the gap between well-established *in vitro* and *in vivo* investigation platforms [17, 18].

Ex vivo bone models are increasingly recognized as valuable tools in bone research, offering a more physiologically relevant alternative to traditional *in vitro* and animal models [19]. For instance, the *ex vivo* human bone organ model developed by *Zankovic et al.* allows for the evaluation of osseointegration of implant materials, demonstrating that the geometry of test substrates influences cell growth and survival over a 28-day period [20]. Similarly, *Choudhary et al.* have utilized an *ex vivo* 3D bone model to study osteocyte responses to metastatic prostate cancer, revealing significant and clinically relevant changes in the expression of key factors like fibroblast growth factor 23 and alkaline phosphatase (ALP), which were not mirrored in 2D cultures [21]. Furthermore, *ex vivo* models are used to test the biocompatibility of biomaterials, as demonstrated by *Schnieders et al.*, who evaluated calcium phosphate composites in a human trabecular bone bioreactor, maintaining bone metabolism in a physiological environment [22]. *Ex vivo* cultures of intact human bone fragments contain essential cell-cell and cell-matrix interactions, enabling the study of bone cells within their natural 3D environment. Additionally, using human bones in organ cultures more closely replicates human conditions and provides an appealing tool for testing patient-specific responses.

Toward a reliable model for bone biology with optimal resemblance to human tissue physiology, we here developed an *ex vivo* human bone model comprising viable human trabecular bone discs. To investigate the intact bone system for regeneration in this model, we identified various cell types within the bone discs. The viability of bone discs was confirmed for up to 14 days. In addition, the presence of microvessels and multinucleated cells in bone marrow of bone discs were histologically assessed and immunohistochemistry was used to identify monocytes in the bone marrow of bone discs. Moreover, we comparatively evaluated the expression levels of typical pro-inflammatory cytokines in supernatant after lipopolysaccharide (LPS) stimulation to controls. We further identified human bone marrow MSCs (hBMSCs) growing out from bone discs by flow cytometry and determined the expressions levels of osteogenic genes of whole bone tissues upon *ex vivo* culture in osteogenic media (OM). Finally, we assessed the effect of mEV injection into defects created in the bone discs for stimulating osteogenic responses.

MATERIALS AND METHODS

Preparation of standard-sized human bone discs

Human femoral heads were obtained from the Department of Orthopedics (Radboudumc and Canisius-Wilhelmina Hospital; Nijmegen, the Netherlands)

from patients undergoing total hip replacement. After surgery, femoral heads were transported in a sterile container and stored at 4°C for no longer than 48 hours until bone disc preparation. Before preparation, the workplace and all materials used were soaked in 70% ethanol for sterilization. Afterwards, all the following steps for obtaining the *ex vivo* bone discs were performed under aseptic conditions. A vice (Fig. **1A**) was secured to the table and wrapped in a surgical drape. The human femoral head was fixed into the vice (Fig. **1B**) and drilled by using an Ø 8 mm hollow trephine drill (MF Dental, Weiherhammer, Germany) (Fig. **1C-D**). The drilling process was performed under constant cooling with sterile DPBS (14190-094, GibcoTM, Thermo Fisher Scientific) to minimize the damage caused by heat generated during drilling.

To obtain approximately 14 mm long cylindrical osteochondral cores, a custom-made hollow metal tube, serving as a breaking tool, was used. The osteochondral cores were then secured into a custom-made mold (Ø8mm×4mm) (Fig. **1E**) and cut perpendicular to the longitudinal axis using a minitom diamond saw (4431361, Struers, Rodovre, Denmark), again under constant cooling with sterile DPBS. First, the articular cartilage of the bone was removed and then proximal end of the bone, resulting in *ex vivo* bone discs (Ø8mm x 4mm). The bone discs were then secured into a custom-made holder, after which four defects (Ø1.1mm x 3mm) were drilled into the bone discs using a drill press (8450468, Bosch PBD40, Germany) (Fig. **1F**). Between steps, bone discs were stored in sterile medium consisting of α-MEM (A10490-01, GibcoTM, Thermo Fisher Scientific), 10 % v/v FBS (BCBV7611, Sigma-Aldrich) and 2% Pen/Strep (15140-122, GibcoTM, Thermo Fisher Scientific). Afterwards, bone discs were transferred to 24-well plates and cultured for mentioned time periods (Fig. **1G**).

One bone disc was devitalized by undergoing two freeze-thaw cycles: frozen at -80°C for 24 hours and then thawed at room temperature in 70% ethanol. The devitalized bone disc served as negative control.

Ex vivo bone disc culture

All bone discs were initially cultured in 24-well plates in proliferation media (PM) composed of α-MEM supplemented with 10% fetal bovine serum and 1% penicillin–streptomycin for three days. Thereafter, bone discs were cultured in PM supplemented with (0 or 10 ng/ml) LPS for 3 days and transferred to the new well plates at day 3. For osteogenic differentiation, bone discs were cultured in basic OM (α-MEM containing 10% v/v EV-depleted FBS prepared by 18 hours ultracentrifugation [23] and 1% penicillin-streptomycin, 10mM β-glycerophosphate disodium salt hydrate, 10^{-8} M dexamethasone and 50 µg/ml ascorbic acid) and

stored in an incubator at 37°C with 5% CO_2. For local mEVs delivery, each defect of bone discs was injected with mEVs (2.5E+08 particles in 2.5 µl) two times per week for a culture period of two weeks.

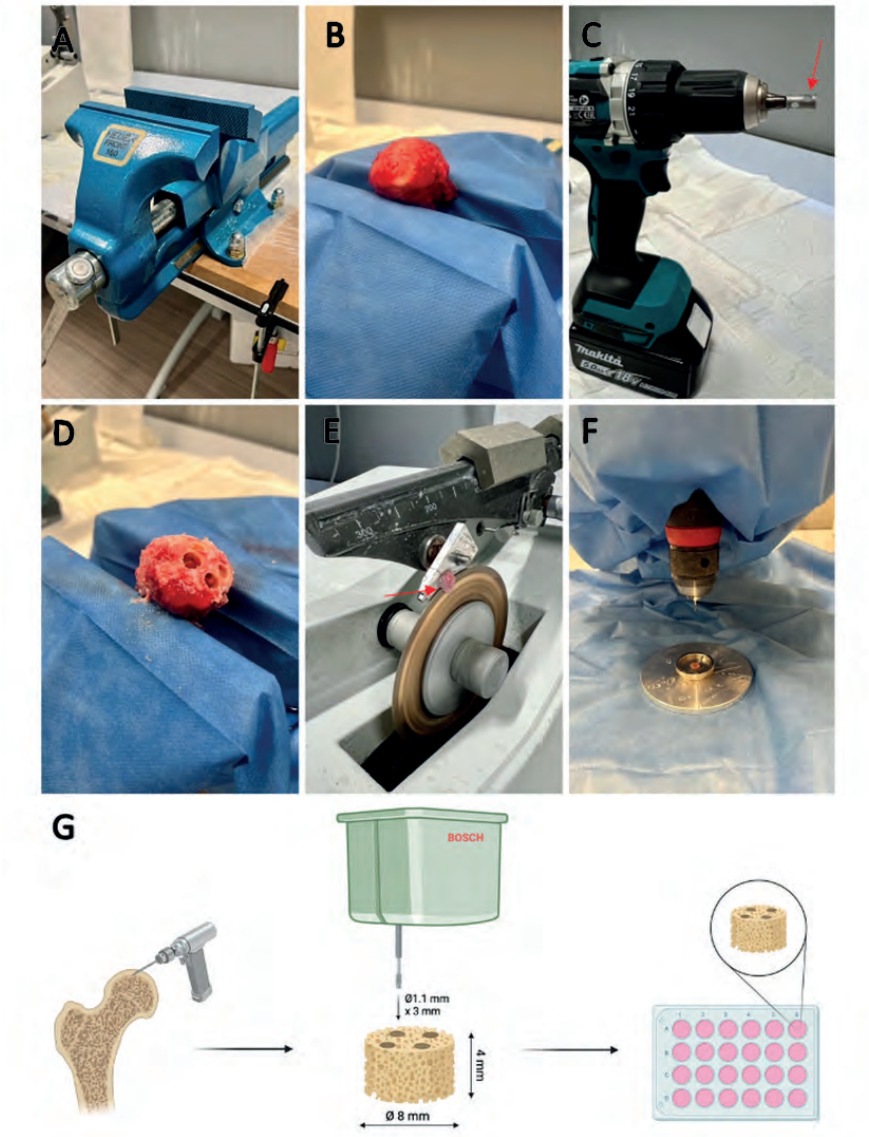

Fig.1. Tools used for ex vivo bone disc isolation. A. Vice to hold femoral head B. Femoral head positioned in vice C. Drill with Ø8 mm hollow trephine drill D. Femoral head after drilling E. Custom-made mold to make bone discs (Ø8mm×4mm) F. Drill-press used to make four standardized circular defects (Ø1.1mm×3mm). G. Schematic overview of ex vivo bone disc isolation (partly created in BioRender.com).

Assessment of cell viability of ex vivo bone discs

AlamarBlue™ (BUF012B, Bio-Rad Laboratories, USA) assays were performed non-destructively to determine cell viability of the bone discs during ex vivo culture following recommendations of the manufacturer. Cell viability was measured at days 1,3,6,10 and 14. Working solutions were made by adding AlamarBlue™ to the desired culture medium at a concentration of 10% (v/v). Bone discs were then transferred to a fresh 24-well plate and 1 ml of working solution was added. After 4 hours incubation at 37°C and 5% CO_2, 100 µl of the medium was added to a black 96-wells plate. Fluorescence intensity was then measured using a plate reader (70908, Synergy HTX Multimode Reader, BioTek, USA) at excitation 560/40 nm and emission 620/40 nm. Measured fluorescence values were adjusted by subtracting the fluorescence values of medium samples from controls (medium without bone discs). Thereafter, samples were washed two times for 5 minutes using sterile DPBS (14190-094, GibcoTM, Thermo Fisher Scientific). After washing, samples were transferred to a clean 24-well plastic plate and fresh medium was added.

Histological analysis

Bone discs were transferred to tissue cassettes and fixed for 24 hours in 10% formalin. Decalcification of bone discs was performed prior to embedding using a Sakura TDETM30 Electrolysis Decalcifier System (1460, Sakura Finetek, CA, USA) and Sakura TDETM30 Decalcifier Solution (Sakura Finetek, CA, USA). After decalcification, samples were washed with tap water and placed in the tissue processor (TP1020, Leica, Wetzlar, Germany) for dehydration through a graded series of ascending alcohol solutions and embedded in paraffin wax. Sections perpendicular to the defects in the bone discs were cut using a rotary microtome to a thickness of 5 µm and mounted on microscope slides. Slides were then deparaffinized, rehydrated, and stained with Hematoxylin and Eosin (H&E) and CD14 immunohistochemistry.

For H&E staining, sections were stained with Delafield Hematoxylin for 8 minutes, followed by rinsing in running tap water for 10 minutes. The sections were then dehydrated through a graded ethanol series (50%, 70%, 80%, and 96%), moving them up and down ten times in each solution. After dehydration, the sections were stained with eosin for 2 minutes, followed by two short immersions in 96% ethanol and four short immersions in 100% ethanol. The sections were then treated with a mixture of xylene and ethanol (100%) (1:1) for 4 minutes, followed by two 5-minute immersions in xylene. Finally, the sections were mounted in DPX and left in a fume hood to dry overnight.

To perform CD14 immunohistochemistry (IHC) on decalcified bone discs, deparaffinize the tissue sections with xylene and ethanol. Antigen retrieval is performed using a Tris-EDTA buffer at pH 9 (prepared with 1.21 g Tris and 0.37 g EDTA in 1 L water), followed by microwave heating at half power for 2 minutes and a 10-minute cool-down at room temperature. Quench endogenous peroxidase activity using 3% hydrogen peroxide (H_2O_2) in PBS for 15 minutes. Next, block non-specific binding with a buffer containing 10% normal goat serum (NGS), 1–2% bovine serum albumin (BSA), and TBS-Tween (0.05%) for 30 minutes. Incubate the sections with rabbit anti-human CD14 (Merck Clone EPR3653)—diluted 1:150 in the blocking buffer, for 60 minutes at 4°C. After thorough washing with TBS-Tween, apply the biotinylated goat anti-rabbit secondary antibody (Vector PK-6101) at 1:400 for 30 minutes. This is followed by incubation with the ABC-HRP complex (Avidin-Biotin Complex, 1:200) for another 30 minutes. For visualization, use DAB (3,3'-diaminobenzidine) as the chromogen to produce a brown stain at the site of CD14 expression. The sections were counterstained with hematoxylin, dehydrated through a graded series of ethanol and xylene, and then mounted using Permount.

Measurement of pro-inflammatory cytokines levels in culture supernatants

Culture supernatant was collected at days 1 and 3 to analyze pro-inflammatory cytokines levels. The release of IL6, IL1b and TNFa were measured using Luminex multianalyte technology, using the Bio-Rad Bio-Plex™ 200 System with specific magnetic beads according to the manufacturer's guidelines.

TRAP activity

To assess differentiation towards osteoclast, tartrate-resistant acid phosphatase (TRAP) activity was quantified in culture medium collected at day 1,3,6,10 and 14. On these days, 0.6 ml medium was collected in an Eppendorf tube and stored at -80°C until further assessment. To measure TRAP activity, a p-nitrophenyl phosphate TRAP assay buffer (pNPP TRAP) was prepared by mixing 15 ml Stock assay buffer (200 ml PBS, 8.3 ml 3 M NaAc [0.1M] and 2.5 ml 10% Triton X-100 [0.1%], adjusted to pH 5.5), one tablet pNPP and 450 µl tartrate solution. 10 µl 1 mM p-nitrophenol standards were added two times in concentrations of 0, 0.5, 2, 6 and 9 to the 96 wells plate for creating a standard curve. For the assay, 10 µl of medium supernatant was added to 90 µL of the buffer and incubated for 1.5 hours at 37°C, 5% CO_2. The reaction was stopped with 100 µL of 0.3 M NaOH stop solution. Absorbance was measured at 405 nm using a plate reader. The standards with known p-nitrophenol concentrations (0-0.9 µmol/mL) were used to calculate TRAP activity per explant.

Bright-field imaging

Bright-field images were taken from bone disc repetitively during ex vivo culture to monitor the morphology and migration of cells out of the bone discs. Bright-field images were taken at day 7 and day 14. All images were taken before AlamarBlue™ assays using a Leica DM IL LED Inverted Laboratory Microscope.

Flow cytometry analysis

Cells migrated away from bone discs were collected and used for flow cytometric staining. The viability dye, eFluor 780 (eBioscience™) was 1:1000 diluted in PBS and added to the cell vials. The vials were covered in aluminum foil and incubated for 30 minutes at 4°C. Fluorescence-activated cell sorting (FACS) staining solution containing 1:20 PE anti-human CD90 (Thy1) antibody (Biolegend), 1:20 FITC anti-human CD105 (Biolegend) and 1:100 Brilliant violet 510 anti-human CD45 antibody (Biolegend) and was made in FACS buffer on ice. 100 µL pbs was added and the samples were centrifuged 3 minutes at 300g at 4°C. Afterwards the supernatant was removed and FACS staining solution was added to pellets. The samples were resuspended and incubated for 20 minutes at room temperature with aluminum foil around the vials. Afterwards 100 µL FACS buffer was added, and the samples were centrifuged for 3 minutes at 300g at 4°C. The supernatant was removed and 100 µL FACS buffer was added. The samples were analyzed in Beckman Coulter Cytoflex flow cytometer and analyzed with Kaluza analysis (version 2.1).

Real-time qPCR

The osteogenic differentiation-related gene expressions, including ALPL, Runx2, and collagen type 1 (COL1a1) were determined through real-time qPCR (qRT-PCR). In brief, bone discs were deposited in 3 ml of TRIzolTM Reagent (15596018, Thermo Fisher Scientific) to isolate total RNA. By using a TissueRuptor (QIAGEN, Hilden, Germany), bone discs were fractioned until a pellet of bone tissue was clearly visible at the bottom of the 15 ml tubes. The concentration and quality of the total RNA samples were assessed using a Nanodrop spectrophotometer (Thermo Fisher Scientific Inc.). After DNA contamination was removed, complementary DNA (cDNA) was diluted 20x in dH_2O. RT-qPCR was performed in 10 µl reaction mixture containing 5 µl Power Sybr Green Master Mix (4309155, Thermo Fisher Scientific Inc.), 1 µl (2 µM) of each forward (FW) and reverse (RV) primer for each gene of interest and 3 µl of diluted cDNA. Glyceraldehyde-3-phosphate-dehydro-genase (GAPDH), a reference gene, was used as a control. The reaction was carried out using an QuantStudio™ 1 Real-time PCR System (Thermo Fisher Scientific Inc.). Relative expression levels for each target gene were normalized to the Ct value of GAPDH and calculated using the delta-delta Ct method. All experimental groups were determined in triplicate.

Then the fold change from the control group was used to analyze the change in gene expression. The forward and reverse primer sequences are listed below in Table 1.

Table 1. List of forward and reverse primer sequences for genes measured in qRT-PCR.

Gene	Forward primer	Reverse primer
GAPDH	ATCTTCTTTTGCGTCGCCAG	TTCCCCATGGTGTCTGAGC
COL1A1	AGATCGAGAACATCCGGAG	AGTACTCTCCACTCTTCCAG
RUNX2	GCAAGGTTCAACGATCTGAGA	TTCCCGAGGTCCATCTACTG
ALP	TGGGAGATGGGATGGGTGTCT	CTGGGCATTGGTGTTGTACGT

Fluorochrome labeling

Two fluorochrome labels (Calcein (CO3050, Sigma-Aldrich); Alizarin Red (Alizarin-3-methyliminodiacetic acid, A3882, Sigma-Aldrich) were administered on the 7th and 14th day respectively through OM at a concentration of 25 µg/ml for 24 hours [24]. After 24 hours of incubation, bone discs were transferred to a clean 24-well plate and washed one time with PBS for 5 minutes before fresh OM was added. Post-incubation, bone discs were imaged using widefield microscopy (Zeiss Axio Imager 2).

Statistical analysis

Statistical analyses were performed, and graphs were prepared, using Prism version 10.2 (GraphPad, San Diego, USA). Data were checked for normal distribution using the Kolmogorov–Smirnov test. Unpaired Student's t-tests were used for comparisons between two groups (0 & 10 LPS ng/ml; PM & OM; PBS control & mEVs). Data are represented as mean ± standard deviation. A p-value of <0.05 was considered statistically significant.

RESULTS

Bone discs remained vital during *ex vivo* culture

To establish the *ex vivo* culture condition, each bone disc was placed in the center of a well in a 24-well plastic plate, with 1 ml of culture medium added to fully cover the bone disc. The defect opening was oriented upward to allow for mEVs injection (Fig. **2A**). Further, AlamarBlue™ data showed a significant increase in fluorescence intensity over time in the vital bone discs while no noticeable change was observed in the devitalized bone disc, indicating that the cells in the bone discs remained vital and continued to proliferate during *ex vivo* bone disc culture (Fig. **2B**).

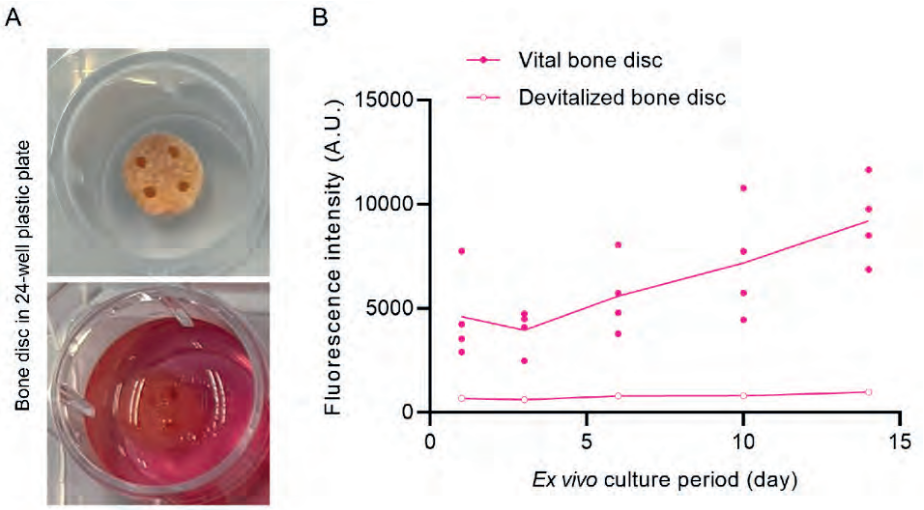

Fig. 2. Bone discs remained vital during ex vivo culture. A. Bone discs (Ø8mm x 4mm) cultured in 24-well plastic plates. B. AlamarBlue™ assay results for vital bone disc and devitalized bone disc *ex vivo* culture within PM.

Inflammatory cells within the bone discs respond to LPS-stimulation

To investigate overall histological appearance of the vital bone disc, H&E staining was conducted to visualize the typical trabecular structure with intertrabecular spaces filled with bone marrow (Fig. **3A**). The bone trabeculae showed to comprise nucleated osteocytes and were surrounded by adipose bone marrow tissue. Moreover, we carried out CD14 IHC staining to verify the presence of monocytes/macrophages in the bone marrow compartment of the bone discs. These images showed that massive cell numbers within the bone marrow stained positively for CD14, indicating that indeed the bone marrow compartment comprised abundant cells of the monocyte-lineage (including monocytes and macrophages) (Fig. **3B-C**). Given that CD14 plays a role in recognizing bacterial LPS as part of the innate immune response [25], bone discs were stimulated with LPS for three days to investigate their responsiveness to an immunogenic stimulus (Fig. **3D**). AlamarBlue™ data showed that LPS stimulation significantly decreased the viablility activity from day 6 to day 14 compared to control bone discs (0 ng/ml LPS) (Fig. **3E**). More importantly, the concentrations of pro-inflammatory cytokines in supernatant showed a robust and significant increase upon LPS stimulation. More specifically, 10 ng/ml LPS induced a 64-fold increase in expression levels of human IL6 and IL1b, and a 1024-fold increase of human TNFa compared to control bone discs (0 ng/ml LPS) within 1 day. LPS-stimulation remained to evoke high expression levels of these cytokines by day 3 (Fig. **3F**). Collectively, these data clearly

demonstrate that the bone marrow compartment in human bone discs contained monocytes/macrophages that retained highly responsive to LPS stimulation.

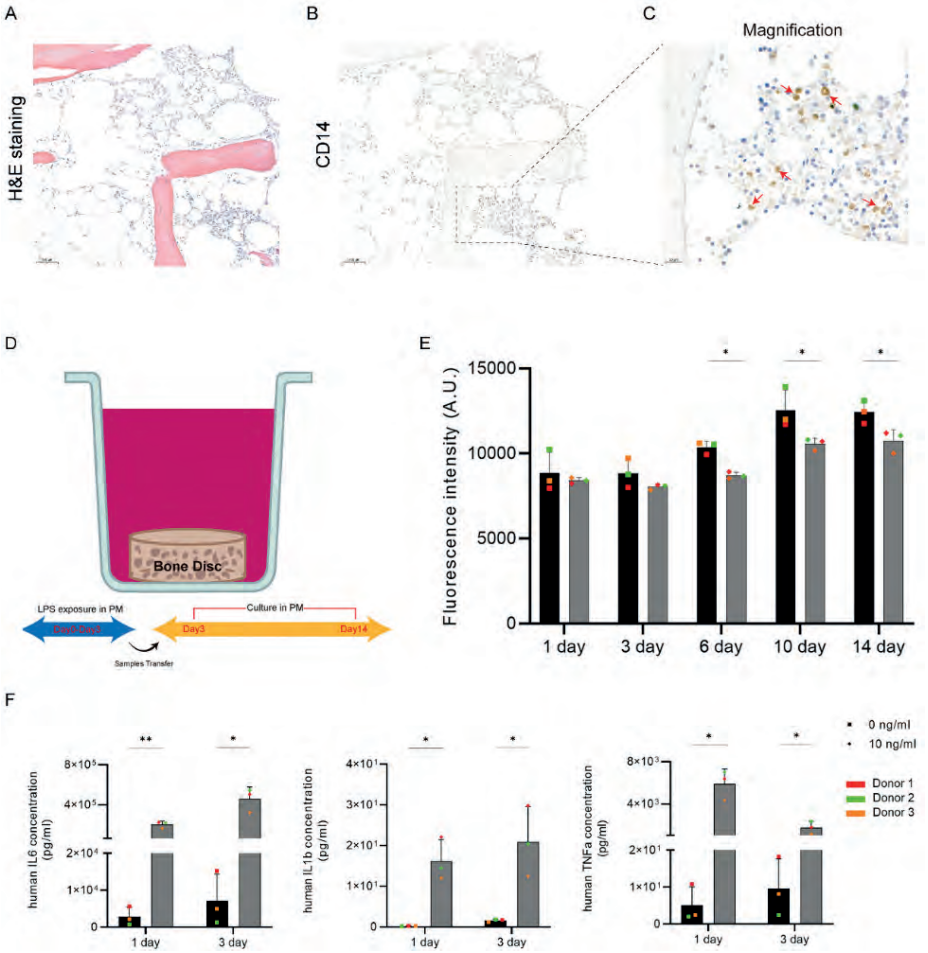

Fig. 3. LPS induced immune responses of bone disc. A. Representative image of H&E staining of bone discs at day 3 showing trabeculae containing nucleated osteocytes and abundant adipose bone marrow. B. Representative image of CD14 IHC of bone discs at day 3 showing adipose bone marrow with regions of high cellularity. C. Magnification showing CD14-positive immune cells (brown) indicated by red arrows in bone marrow regions of high cellularity. Scale bars correspond to 100 µm in 3A and 20 µm in 3C. D. Schematic representation showing the process of bone discs cultured in PM supplemented with LPS. E. AlamarBlue™ assay results for bone discs within PM containing LPS (0, 10 ng/ml) at day 1, 3, 6, 10, 14 (n=3). F. The expression levels of pro-inflammatory cytokines (IL6, IL1b, TNFa) measured in supernatant within LPS (0, 10 ng/ml) exposure used for culturing bone discs at days 1 and 3 (n=3). Data were expressed as means ± standard deviation (SD). *$p < 0.05$, **$p < 0.01$.

Vessel-like structures and multinucleated cells remain present in bone discs during *ex vivo* culture

Since the presence of viable osteocytes, adipose bone marrow, and responsive monocytes/macrophages therein was confirmed, we further investigated the presence of micro-vessels and multinucleated cells in the bone discs. H&E staining of bone discs after two weeks of *ex vivo* culture revealed the presence of vessel-like structures containing erythroid precursors in their lumen, located near the trabecular bone tissue (Table 2). In addition, cells exhibiting osteoclast characteristics, including multinucleation and location on the surface of bone trabeculae were observed (Fig. **4A**). Moreover, measurements of TRAP activity confirmed the presence of active osteoclasts, as TRAP levels slightly increased during *ex vivo* culture (Fig. **4B**). Taken together, these data imply that bone discs retain micro-vessels and multinucleated osteoclastic-like cells on the surface of bone trabeculae during ex vivo culture.

Viable BMSCs persist in bone discs during prolonged *ex vivo* culture

After 7 days of *ex vivo* culture, we observed that cells with a fibroblast-like morphology were growing on the tissue culture plastic around the bone discs (Fig. **5A**). Flow cytometry was performed to assess the identity of these cells. Expecting BMSCs, we included routinely used positive and negative stem cell markers for this assessment. We observed that these cells were CD45-negative, confirming they are not of hematopoietic origin. Conversely, a high proportion (95.02%) of the CD45-negative population expressed CD90 and CD105. Consequently, this immunophenotyping indicates that outgrowing cells from the bone discs are hBMSCs (Fig. **5B**). Further, to investigate the osteogenic differentiation capacity of these hBMSCs in the bone discs, bone discs were subjected to PM and OM culture conditions for 7 and 14 days. qRT-PCR data showed that culture in OM significantly increased ALPL expression (~2-fold) compared to culture in PM at day 7. Moreover, by day 14, the expression levels of ALPL and Col1a1 mRNA were still significantly increased in OM compared to PM cultures. These data indicate that viable hBMSCs persist in the bone discs and suggest that these cells could undergo osteogenic differentiation in the bone discs during *ex vivo* culture in OM medium.

Table 1. Summary of blood and multinucleated cells in H&E staining from 4 donors.

	Age/Gender	Vascular cavities	Multinucleated cells
Donor 1	61, Male	✔	✔
Donor 2	78, Female	✔	✖
Donor 3	66, Female	✔	✔
Donor 4	56, Male	✔	✖

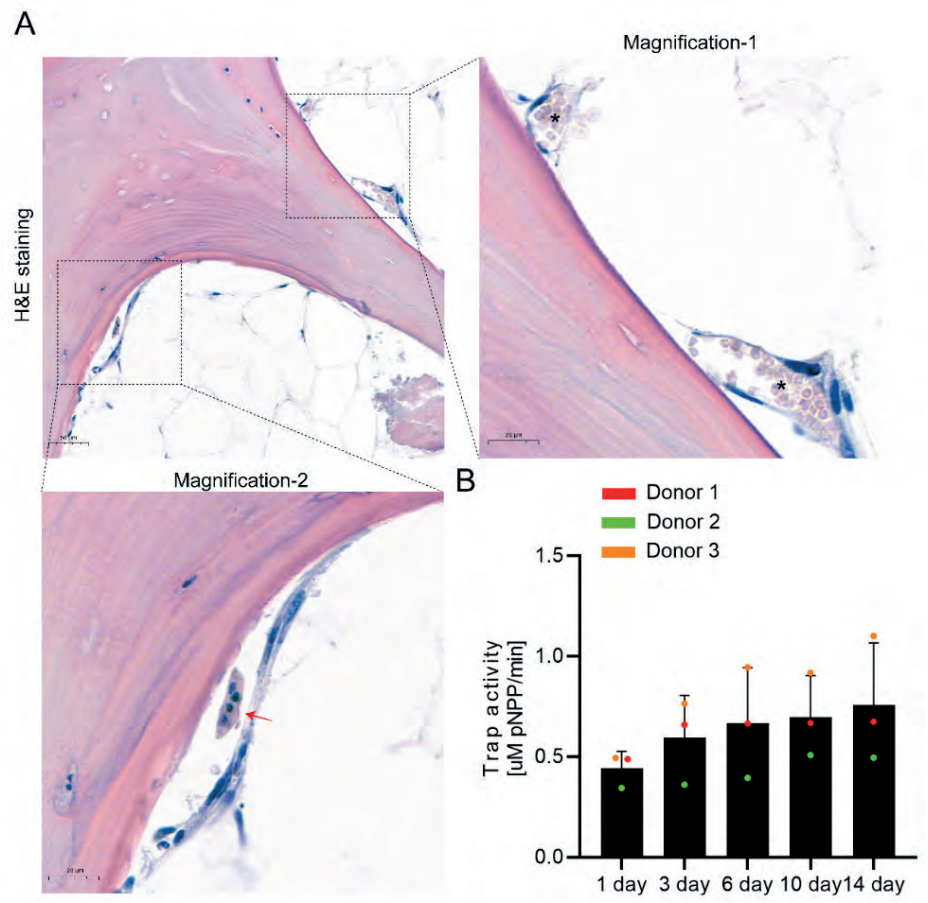

Fig. 4. Blood vessels and multinucleated cells are present in bone discs during *ex vivo* culture. A. Representative image of H&E staining of bone discs at day 14. Vessel-like structuresweremarked with asterisks and show luminal presence of erythrocytes; multinucleated cells are indicated with red arrow. B. Trap activity in supernatant collected during culture at day 1, 3, 6, 10, 14 (n=3).

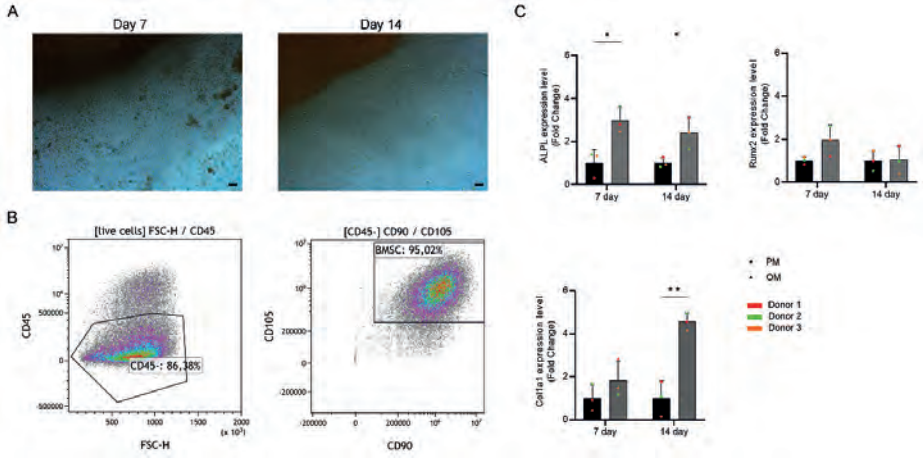

Fig. 5. BMSCs persist in ex vivo cultured bone discs. A. General observations of cell migration away from bone discs cultured in 24-well plastic plates from 7 and 14 days. Scale bars correspond to 100 µm in 5A. B. CD45, CD90, and CD105 flow cytometry staining of fibroblast-like cells grown away from bone discs after 14 days of bone disc culture. C. qRT-PCR analysis of osteogenic differentiation-related mRNA expressions of whole bone discs tissues under PM or basic OM culture conditions at day 7 and day 14 (n=3). Data were expressed as means ± standard deviation (SD). *$p < 0.05$, **$p < 0.01$.

mEVs stimulate bone formation in bone discs

We hypothesized that the viable cells of mesenchymal and hematopoietic origin in the *ex vivo* cultured bone discs might resemble the process of bone repair. Consequently, we next investigated the effects of mEVs on bone regeneration using this *ex vivo* human bone culture model. For this, we created defects in the bone discs and injected mEVs into these defects. We first tested the ALPL, Runx2 and Col1a1 mRNA expression levels of whole bone discs tissues within mEVs injection. The data demonstrated a significant increase in Runx2 expression by 104% under OM culture conditions at day 7 (Fig. **6A**), In addition, mEV injection into these defects in the bone discs showed to increase fluorochrome uptake along the defect walls during ex vivo culture (Fig. **6B-C**). Collectively, these results suggest that mEVs stimulated bone formation in bone discs.

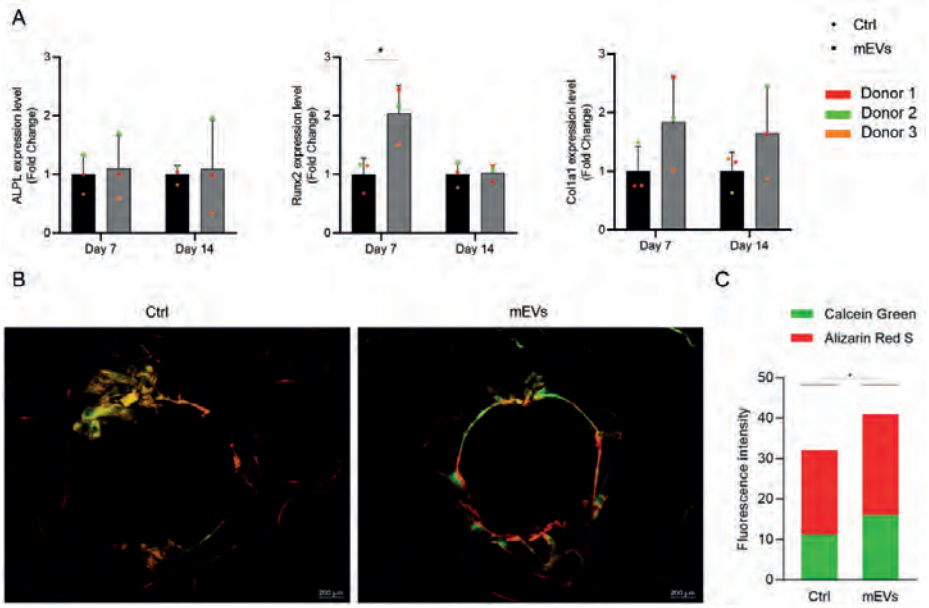

Fig. 6. mEVs stimulated bone formation in bone discs. A. qRT-PCR analysis of osteogenic differentiation-related mRNA expressions of whole bone discs tissues with or without mEVs injection at day 7 and day 14 (n=3). B. Representative images of the drilled holes stained with calcein green on the 7th day and alizarin red s on the 14th day for ctrl (pbs) and mEVs injection. C. Mean fluorescence intensity (MFI) of calcein green and alizarin red s on inner edges of defects (dots represent holes of each sample). Scale bars correspond to 200 μm in 6B. Data were expressed as means ± standard deviation (SD). *$p < 0.05$.

DISCUSSION

A human *ex vivo* bone model previously showed to be a valuable tool for assessing bone repair processes upon treatment with bone substitute materials [26]. In the process of *in vivo* bone healing, circulating monocytes are recruited to the injury site, where they differentiate into macrophages and pre-osteoclasts within the blood clot. Concurrently, MSCs mainly BMSCs are attracted to the area and differentiate into osteoblasts, which drive the synthesis, deposition, and mineralization of the bone matrix [27]. Therefore, once the bone tissue is separated from the human body, the limited number of immune cells and MSCs should be evaluated for their viability and activity. Compared to complicated conditions *in vivo*, *ex vivo* models are more convenient to control. Researchers could investigate and adjust experimental parameters, as *ex vivo* models are instrumental in the preclinical testing of medical devices and therapies [28]. Previous studies using EVs as therapeutic agents for bone fractures or defects still face a challenge due to the inability to monitor bone

tissue in real time through non-invasive methods—unlike soft tissues, such as the gastrointestinal tract, which can be observed using doppler color ultrasound [29]. It is still uncertain whether locally administered free EVs can truly reach the target sites from outside the body, such as through the skin. Furthermore, the controlled release behavior of EVs within certain biomaterial delivery systems remains insufficiently characterized. Given that bone healing is a prolonged and multi-phase process, it is challenging to achieve precise temporal regulation of EV dosage at specific stages of tissue regeneration in animal models. This limitation hinders the ability to align EV availability with the dynamic biological demands of each healing phase [30]. In this work, we characterized an *ex vivo* human bone model and employed it to assess the effects of mEVs on bone formation.

To verify viable cells in the human bone discs during ex vivo culture, we non-destructively assessed metabolic activity at multiple moments. The AlamarBlue™ assay results demonstrated that cells within bone discs remain vital during the culture. More importantly, there was no viability detected in the devitalized bone disc, which indicates the complete absence of viable cells, thereby confirming the successful devitalization process. The devitalized bone serves as critical comparison for assessment of viability of cells within bone dics, but this sample is not suitable for other experiments as it could influence the results interpretation. For example, devitalized bones have lost their cell membranes and the active transport regulation of calcium, which can result in a higher concentration of calcium ions in the extracellular matrix. This increased calcium availability makes fluorochrome dyes in vivo more likely to bind [31] potentially leading to a misinterpretation of the results [32]. In addition, 3-day LPS exposure impacted the viability of bone discs significantly meanwhile triggered the strong immune responses of bone discs. The contradictory results indicated a diverse cellular three-dimensional environment in bone discs, in which hBMSCs, osteoblasts, osteocytes and immune cells are preserved. It has been well-known that LPS induces apoptosis in osteoblasts by activating the c-Jun N-terminal kinase (JNK) pathway, which leads to increased expression of pro-apoptotic markers such as Bax and caspase-3 [33]. Moreover, by triggering DNA damage and activating stress-related pathways, including $p16^{Ink4a}$, p21, and p53, LPS could cause massive osteocyte senescence [34]. We selected three classical pro-inflammatory cytokines to assess the immune responses of bone discs under the LPS conditions. Of note, the sequence and timing of peak levels for TNFa, IL1b, and IL6 vary *in vitro* and *in vivo* studies. In brief, TNFa is often the first to peak—usually within 1–2 hours; IL1b and IL6 tend to peak somewhat later (around 4–6 hours) [35, 36]. In this study, following 3 days of LPS exposure, TNFa expression declined marginally, while IL1b and IL6 continued to show a slight upward trend.

This suggests that the three-dimensional tissue structure and resident bone cell populations in the *ex vivo* model may have played a role in mediating a delayed yet sustained cytokine response, closely resembling the inflammatory kinetics observed *in vivo*.

It has not been investigated whether specific resident cell populations are lost during bone explant isolation or persist in a viable state [37]. In relation to bone cells, osteoclasts and osteoblast-like cells, MSC-like cells, and morphologically intact osteocytes located within their lacunae are supposed to be evaluated. Osteoclasts form from hematopoietic precursors, specifically from the monocyte/macrophage lineage. Under the influence of M-CSF and RANKL, mononuclear monocytes fuse to form multinucleated osteoclasts [38]. Herein multinucleated cells have been found in H&E staining from 2 out 4 donors (50%). In all cases, these multinucleated cells were located close to the surface of trabeculae. Moreover, TRAP activity as a marker of osteoclast activity slightly increased during *ex vivo* culture, indicating the presence of viable osteoclasts. Recent work on *ex vivo* human bone discs reported a rapid reduction in TRAP activity, with osteoclast viability significantly compromised by day 4, and an absence of bone resorption under static culture condition [39]. However, their investigation focused on osteochondral explants containing both cartilage and subchondral components, rather than pure trabecular bone tissue used in this work. In their work, both tissue types were maintained viable throughout the culture period. Given that their donor samples were obtained from osteoarthritis patients, it is plausible that the inflamed cartilage created a locally anti-resorptive microenvironment by releasing factors such as osteoprotegerin (OPG) and anti-inflammatory cytokines (e.g., IL-10, TGF-β), which may inhibit osteoclast activity, and hence downregulate TRAP expression [40]. Under OM culture conditions, gene expression of ALPL and Col1a1 increased significantly, indicating BMSCs within bone discs retained their osteogenic capacity during *ex vivo* culture. Recent work compared ALP activity of *ex vivo* bone under low (10nM dexamethasone) and high osteogenic stimulation (100nM dexamethasone). Through increasing the concentration of dexamethasone and adding β-glycerophosphate in the culture media, higher ALP activity was observed but with lower procollagen 1 c-terminal propeptide as an indicator for collagen formation [41]. They speculated that resorption-formation coupling was disturbed by high stimulation with osteogenic factors, suggesting mineralization occurred independently of proper organic matrix production. In our study, the basic OM was used, taking into account the co-culture system in the *ex vivo* bone. Compared to PM (no dexamethasone and β-glycerophosphate) culture conditions,

both gene expression of ALPL and Col1a1 were increased in OM culture conditions, suggesting BMSCs undergo regular osteogenic differentiation.

Several main limitations can be stated regarding this study on bone regeneration within *ex-vivo* human bone discs. Donor variability is a significant limitation. Human bone samples can vary widely in terms of age, health status, genetic background and previous medical history. Even in the sample donors, it should be highlighted that bone discs from distinct anatomical regions exhibit variability in cellular composition, including differences in the density of cells such as osteocytes and immune cells due to variations in mechanical loading and vascular supply [42, 43]. In this case, we do not recommend collecting as many bone discs as possible from one donor. Instead, the bone discs for comparison in the experiments should be in a similar position. Additionally, bone samples were collected from elderly patients undergoing total hip arthroplasty, who are more prone to comorbidities (such as osteoporosis and diabetes) that can impact cellular composition and activity. In addition, this study did not incorporate mechanical loading, which is a significant factor in bone regeneration. Specifically, osteocytes, embedded within the bone matrix, play a crucial role in sensing mechanical stimuli and regulating bone formation and degradation. They respond to mechanical loading by producing signaling molecules that influence osteoblast and osteoclast activity, thereby modulating bone remodeling [44]. The absence of mechanical loading in an *ex-vivo* setup means that the bone regeneration observed may not be fully replicated *in vivo* conditions.

CONCLUSION

We here developed, characterized, and analyzed a novel human *ex vivo* bone model, offering insights into the dynamic behavior of various cells involved in bone regeneration in an *ex vivo* environment. We demonstrated that bone discs remained viable over extended *ex vivo* culture periods of 14 days. Histology confirmed trabecular bone tissue with viable osteocytes and adipose bone marrow comprising monocytes/macrophages. Further, vessel-like structures and multinucleated cells were during prolonged ex vivo culture. The data on pro-inflammatory cytokines responses and osteoclastic activity reflected that bone discs retain inherent immune response and resorption activity. More importantly, MSCs can proliferate and undergo osteogenic differentiation in the bone discs. Using this human ex vivo bone model, loading of mEVs into bone defects showed to stimulate bone formation.

REFERENCES

1. Duda, G.N., et al., The decisive early phase of bone regeneration. Nat Rev Rheumatol, 2023. **19**(2): p. 78-95.
2. Global, regional, and national burden of bone fractures in 204 countries and territories, 1990-2019: a systematic analysis from the Global Burden of Disease Study 2019. Lancet Healthy Longev, 2021. **2**(9): p. e580-e592.
3. Suh, D.H., B.M. Koo, and J.W. Kang, Current Concepts of Bone Healing. J Musculoskelet Trauma, 2020. **33**(3): p. 171-177.
4. Saul, D., et al., Bone Healing Gone Wrong: Pathological Fracture Healing and Non-Unions-Overview of Basic and Clinical Aspects and Systematic Review of Risk Factors. Bioengineering (Basel), 2023. **10**(1).
5. Xiang, Q., et al., Beyond resorption: osteoclasts as drivers of bone formation. Cell Regen, 2024. **13**(1): p. 22.
6. Bahney, C.S., et al., The multifaceted role of the vasculature in endochondral fracture repair. Front Endocrinol (Lausanne), 2015. **6**: p. 4.
7. Han, J., A.N. Rindone, and J.H. Elisseeff, Immunoengineering Biomaterials for Musculoskeletal Tissue Repair across Lifespan. Adv Mater, 2024. **36**(28): p. e2311646.
8. Welsh, J.A., et al., Minimal information for studies of extracellular vesicles (MISEV2023): From basic to advanced approaches. J Extracell Vesicles, 2024. **13**(2): p. e12404.
9. Yu, T., et al., Extracellular vesicle-functionalized bioactive scaffolds for bone regeneration. Asian J Pharm Sci, 2024. **19**(5): p. 100945.
10. Furuta, T., et al., Mesenchymal Stem Cell-Derived Exosomes Promote Fracture Healing in a Mouse Model. Stem Cells Transl Med, 2016. **5**(12): p. 1620-1630.
11. Oliveira, M.C., et al., Milk extracellular vesicles accelerate osteoblastogenesis but impair bone matrix formation. J Nutr Biochem, 2016. **30**: p. 74-84.
12. Oliveira, M.C., et al., Milk-Derived Nanoparticle Fraction Promotes the Formation of Small Osteoclasts But Reduces Bone Resorption. J Cell Physiol, 2017. **232**(1): p. 225-33.
13. Dong, M., et al., Milk-derived small extracellular vesicles: nanomaterials to promote bone formation. J Nanobiotechnology, 2022. **20**(1): p. 370.
14. Hwang, H.S. and C.S. Lee, Exosome-Integrated Hydrogels for Bone Tissue Engineering. Gels, 2024. **10**(12).
15. Tan, S.H.S., et al., Mesenchymal stem cell exosomes in bone regenerative strategies-a systematic review of preclinical studies. Mater Today Bio, 2020. **7**: p. 100067.
16. Schilling, A.F., et al., Transgenic and knock out mice in skeletal research. Towards a molecular understanding of the mammalian skeleton. J Musculoskelet Neuronal Interact, 2001. **1**(3): p. 275-89.
17. Stein, M., et al., Why Animal Experiments Are Still Indispensable in Bone Research: A Statement by the European Calcified Tissue Society. J Bone Miner Res, 2023. **38**(8): p. 1045-1061.
18. Schafrum Macedo, A., et al., Animal modeling in bone research-Should we follow the White Rabbit? Animal Model Exp Med, 2019. **2**(3): p. 162-168.
19. Cramer, E.E.A., K. Ito, and S. Hofmann, Ex vivo Bone Models and Their Potential in Preclinical Evaluation. Curr Osteoporos Rep, 2021. **19**(1): p. 75-87.
20. Zankovic, S., et al., A Method for the Evaluation of Early Osseointegration of Implant Materials Ex Vivo: Human Bone Organ Model. Materials (Basel), 2021. **14**(11).

21. Choudhary, S., et al., Human ex vivo 3D bone model recapitulates osteocyte response to metastatic prostate cancer. Sci Rep, 2018. **8**(1): p. 17975.
22. Schnieders, J., et al., Ex vivo human trabecular bone model for biocompatibility evaluation of calcium phosphate composites modified with spray dried biodegradable microspheres. Adv Healthc Mater, 2013. **2**(10): p. 1361-9.
23. Shelke, G.V., et al., Importance of exosome depletion protocols to eliminate functional and RNA-containing extracellular vesicles from fetal bovine serum. J Extracell Vesicles, 2014. **3**.
24. Hall, T.A.G., et al., Active osseointegration in an ex vivo porcine bone model. Front Bioeng Biotechnol, 2024. **12**: p. 1360669.
25. Liu, J., R. Kang, and D. Tang, Lipopolysaccharide delivery systems in innate immunity. Trends Immunol, 2024. **45**(4): p. 274-287.
26. Klüter, T., et al., An Ex Vivo Bone Defect Model to Evaluate Bone Substitutes and Associated Bone Regeneration Processes. Tissue Eng Part C Methods, 2020. **26**(1): p. 56-65.
27. Mandracchia, V.J., S.C. Nelson, and E.A. Barp, Current concepts of bone healing. Clin Podiatr Med Surg, 2001. **18**(1): p. 55-77.
28. Malfertheiner, M.V., et al., Ex vivo models for research in extracorporeal membrane oxygenation: a systematic review of the literature. Perfusion, 2020. **35**(1_suppl): p. 38-49.
29. Dolinger, M.T. and M. Kayal, Intestinal ultrasound as a non-invasive tool to monitor inflammatory bowel disease activity and guide clinical decision making. World J Gastroenterol, 2023. **29**(15): p. 2272-2282.
30. Pinheiro, A., et al., Extracellular vesicles: intelligent delivery strategies for therapeutic applications. J Control Release, 2018. **289**: p. 56-69.
31. van Gaalen, S.M., et al., Use of fluorochrome labels in in vivo bone tissue engineering research. Tissue Eng Part B Rev, 2010. **16**(2): p. 209-17.
32. Miroshnichenko, L.A., et al., Review of Local Cellular and Molecular Processes of Bone Tissue Regeneration Induced by Calcium Phosphate Materials. Cell and Tissue Biology, 2024. **18**(2): p. 148-162.
33. Guo, C., et al., Lipopolysaccharide (LPS) induces the apoptosis and inhibits osteoblast differentiation through JNK pathway in MC3T3-E1 cells. Inflammation, 2014. **37**(2): p. 621-31.
34. Aquino-Martinez, R., et al., LPS-induced premature osteocyte senescence: Implications in inflammatory alveolar bone loss and periodontal disease pathogenesis. Bone, 2020. **132**: p. 115220.
35. Amiot, F., et al., Lipopolysaccharide-induced cytokine cascade and lethality in LT alpha/TNF alpha-deficient mice. Mol Med, 1997. **3**(12): p. 864-75.
36. Lotter, K., et al., In vivo efficacy of telithromycin on cytokine and nitric oxide formation in lipopolysaccharide-induced acute systemic inflammation in mice. J Antimicrob Chemother, 2006. **58**(3): p. 615-21.
37. Cramer, E.E.A., et al., Culture system for longitudinal monitoring of bone dynamics ex vivo. Biotechnol Bioeng, 2025. **122**(1): p. 53-68.
38. Sun, Y., et al., Macrophage-Osteoclast Associations: Origin, Polarization, and Subgroups. Front Immunol, 2021. **12**: p. 778078.
39. Cramer, E.E.A., et al., Integration of osteoclastogenesis through addition of PBMCs in human osteochondral explants cultured ex vivo. Bone, 2024. **178**: p. 116935.

40. Wang, B., et al., Chondrocytes-Specific Expression of Osteoprotegerin Modulates Osteoclast Formation in Metaphyseal Bone. Sci Rep, 2015. **5**: p. 13667.
41. de Wildt, B.W.M., et al., The Impact of Culture Variables on a 3D Human In Vitro Bone Remodeling Model: A Design of Experiments Approach. Adv Healthc Mater, 2023. **12**(27): p. e2301205.
42. Chiba, K., et al., Heterogeneity of bone microstructure in the femoral head in patients with osteoporosis: an ex vivo HR-pQCT study. Bone, 2013. **56**(1): p. 139-46.
43. He, Y., et al., Increased vascularization of the subchondral region in human osteoarthritic femoral head in the elderly. Histochem Cell Biol, 2025. **163**(1): p. 39.
44. Klein-Nulend, J., R.G. Bacabac, and A.D. Bakker, Mechanical loading and how it affects bone cells: the role of the osteocyte cytoskeleton in maintaining our skeleton. Eur Cell Mater, 2012. **24**: p. 278-91.

Chapter 7

General discussion

The primary aim of this thesis was to explore the precise utilization of EVs, encompassing their characterization, isolation, and therapeutic applications: Developing strategies to eliminate FBS contamination for isolating EVs from *in vitro* cultures of human ADSCs, and exploring the osteogenic potential of specific EV subpopulations isolated from body fluids (cow milk). Several conclusions can be drawn from our results:

1) PEG precipitation is the efficient method to obtain EV depleted FBS for MSC EVs enrichment with minimal FBS EV contamination.
2) mEVs facilitate osteogenic differentiation of hBMSCs in an inverse dose-dependent manner, during which mitochondrial aerobic metabolism is enhanced with a fused and functionally active state of mitochondria.
3) ECM-binding property is an "EV-inherent feature" and involved in EV-regulated bone tissue homeostasis and pathological conditions.
4) The property of binding to type I collagen separates two subpopulations of mEVs, and those mEVs that bind to type I collagen are key for the osteogenic functionality of mEVs.
5) An *ex vivo* bone defect model can be developed by using viable human trabecular bone, and this model provides a 3D bone microenvironment for investigating bone regeneration and evaluating EV-based therapeutic strategies.

Still, multiple limitations and challenges remain to be addressed in future research.

First, we optimized the PEG precipitation method for depleting FBS-derived EVs from MSCs-EVs. Compared to the other two commonly used approaches, this method achieves maximal removal of EVs from FBS while retaining essential proteins necessary for *in vitro* cell culture in **Chapter 2**. However, our analysis did not encompass the RNA constituents of the FBS milieu. The presence of residual RNA complexes in FBS may introduce variables that complicate the interpretation of experiments, notably those focused on EV-associated RNA species [1]. Moreover, in human application of MSC-EVs the alternative is to use artificial serum replacement media or autologous human serum. We did not test the efficiency of PEG method on human serum in the present study. In addition, our study included insufficient representation of cell types. Besides MSCs from bone marrow or adipose tissue, MSC-like populations have been isolated from various sources such as skin, foreskin [2], synovial fluid [3], and Wharton's jelly [4]. Further, EVs derived from other cultured cells, including macrophages and endothelial cells, have been shown to promote angiogenesis and regulate inflammatory responses in the context of targeted tissue regeneration [5]. To make the conclusion more convincing and enrich the

applicable field of PEG precipitation FBS EV depletion protocol, it is of significant research importance to evaluate the presence and abundance of RNAs in PEG EVdFBS or PEG EV depleted human serum in various cells-derived EVs through high-throughput RNA sequencing in further research.

Second, the bioenergetic metabolism during mEVs-induced osteogenic differentiation of MSCs should be further evaluated in detail. In **Chapter 3,** glucose is the main energy source for fueling OXPHOS during osteogenic differentiation with mEVs stimulation, while the investigation on utilization of fatty acids derived from FBS *in vitro* culture conditions remains unclear. As one of the specific transmembrane proteins in milk and milk derived EVs [6], cluster of differentiation 36 (CD36) has been widely reported to facilitate the uptake and transport of long-chain fatty acids across cell membranes [7, 8]. Therefore, it is meaningful to determine whether fatty acid consumption is involved in mEVs-induced osteogenesis and explore the role of CD36 therein. Moreover, data showed the main effect of mEVs is probably the stimulation of collagen type I synthesis and not perse the stimulation of calcium deposition. It has been reported that collagen synthesis is related to the effect on mitochondria [9]. Is the protein synthesis in cells and mitochondria enhanced by mEVs, leading to increased ATP/OXPHOS and subsequently more collagen production? Could there potentially be a causal relationship between the two? Additionally, further research should be conducted to explain the optimal osteogenic functionality in the lowest dosage of mEVs. One explanation might be the abnormally high ROS level. A recent paper reported that high doses of EVs may overwhelm cells, leading to stress responses and nonspecific uptake [10]. Herein we demonstrated the inverse-dose related effect of mEVs on driving osteogenic differentiation. The data demonstrated an increase in superoxide production, along with elevated SOD2 gene expression, at the lowest dose of mEVs. This indicated enhanced ROS level was moderate and had no impact on further osteogenic differentiation. But the data on mitochondrial activity and ROS level upon stimulation of higher dosage of mEVs are missing. Moreover, it has been demonstrated that a low dose EVs more closely mimics physiological interactions, suggesting surface-mediated signaling is more prominent at low doses [10]. As the size of EVs decreases, the dynamic changes in the surface-to-volume ratio make small EVs more surface-active than luminal-active [11], reminding us to investigate the role of surface biomolecules of mEVs.

Third, in **Chapter 5**, the presence of distinct mEV subpopulations has been emphasized. We investigated the osteogenic functionality of mEVs through *in vitro, ex vivo* and *in vivo* experiments. Moreover, the surface biomolecules of mEVs are

dedicated to the separation of functional mEVs subsets regarding bone-promoting properties. Future research should explore possibilities toward the enrichment of the collagen-binding mEVs to evaluate their sole effects on bone regeneration. By exploring the interactions method between EVs and ECM, we could establish one standard procedure such as heparin-binding chromatography to isolate ECM-binding EVs [12]. It is important to note that the EV corona is absent in the present study [13]. The presumed EV corona is a layer of biomolecules that spontaneously forms on the outside of the EV membrane. The EV corona may contain proteins, nucleic acids, and lipids that are loosely associated with an EV. It has not been investigated whether EV corona retained specific heterogeneity and influenced EVs subsets identification. More research is needed to investigate this concept, but heparin-chromatography followed by SEC may have utility in enriching or depleting EVs with an extensive corona. Additionally, the images of mEVs and $^{cb-}$mEVs uptake by cells showed that the negative functional subset of mEVs barely entered into the recipient cell. This indicated a very specific uptake under low dose mEVs stimulation through surface molecules AnxV-mediated membrane docking and subsequent internalization [14]. We speculated that high dose mEVs can lead to bypassing of normal recognition mechanisms and $^{cb-}$mEVs uptake through less selective or passive pathways, such as macropinocytosis or non-specific endocytosis. Therefore, it can be predicted that mEVs and $^{cb+}$mEVs have similar osteogenic functionality at low doses; however, further research is needed to collect $^{cb+}$mEVs and use them at higher doses, which may better promote bone regeneration.

Finally, to explore the feasibility of a model verifying therapeutic application of EVs on bone regeneration by local delivery, we developed a standardized protocol to establish an *ex vivo* bone defect model using discarded human bone tissue from total hip arthroplasty patients for the generation of viable bone discs with mEVs injection in **Chapter 6**. Our data indicated that healthy cells in the *ex vivo* bone discs remained viable over 14-day culture period. But the donor variability limited the determination of more parameters on osteogenesis. To avoid variability in cellular composition of bone discs [15, 16], future work should focus on comparing the paired bone discs isolated from the similar positions in the sample donor and collecting as many donors as possible for the quantification analysis. Moreover, using this source of human material is that it is often from pathological conditions such as osteoarthritis, osteoporotic or diabetic patients. This is suitable when studying bone repair in these diseases but might not be the correct bone source when studying other diseases such as bone cancer. In addition, osteoclasts are crucial for bone regeneration and remodeling. Herein we revealed the activity of multinucleated osteoclasts but the images of trap staining in histological analysis

are missing to quantify the positive number of osteoclasts. In addition, future experiments also can focus on adding cellular components such as RANKL and M-CSF [17], which may boost osteoclasts differentiation in the presence of immune cells within the bone discs. Furthermore, measures such as applying exogenous mechanical stimuli or establishing a blood supply by establishing some culture chamber system [18] should be used to further refine or advance the model to explore the therapeutic application of EVs or EVs-based materials on human bone and other tissue regeneration.

In addition to the refinements discussed earlier, several issues require attention. Firstly, understanding the scalable production of pure and homogenous EVs is important for EV therapeutic applications in bone tissue regeneration in clinical settings. Regarding current technology on obtaining cell-EVs *in vitro*, any alteration is likely to impact on the properties of cell-EVs such as production and cargos. In practical work, the inevitable contamination arising from FBS or human serum causes improper assessment on the true effect of cell-EVs, lowering the standardization for scalable production. Additionally, the starving strategy (during cell culture with medium NOT supplemented with the nutritional element FBS) requires deeper consideration, which may contribute to the massive loss in inherent cargos of cell-EVs and inefficient EVs enrichment. Secondly, it is imperative to establish one more standardization procedure for isolating EVs from body liquids due to their high heterogeneity. Instead of focusing on the advanced technologies on identifying single EVs from individual cells, the awareness of subsets of bulk EVs should be cultivated, and more isolation tools should be developed for EV subpopulations enrichment commonly based on the surface biomolecules. Thirdly, the comprehensive assessment of effects of EVs in treating bone defects using suitable models should be highlighted. Developing suitable animal models that more closely mimic human bone fractures/defects caused by conditions such as osteoporosis, infection, and diabetes are essential to clarify the factors of a bone regenerative microenvironment. In this case, instead of investigating multiple functionalities of native EVs or engineered EVs in bone remodeling such as anti-inflammatory, anti-resorptive, or angiogenesis, the schedule of applicating homogenous EVs with one main property is more essential to be accurately regulated.

These chapters collectively represented a significant advancement in precision utilization of EVs from isolation to application for bone regeneration, as current research often ignores EVs heterogeneity, heavily compromising clinical translation [19]. By developing methods of identifying/separating/isolation pure and homogenous EVs,

the EV-based therapy on bone and other tissue regeneration could simplify treatment protocol and enhance patient outcomes and reduce dependency on advanced biomaterials for delivery. This has profound implications for tissue regeneration and may require and establish new standards of care for bone fracture/defects patients.

Due to EV heterogeneity as a critical hurdle upstream of barriers to clinical application, the approaches to effectively use EVs have not yet been materialized -there currently is no EV formulation approved by the US Food and Drug Administration (FDA) [20]. From a regulatory perspective, our work may influence the approval and regulation of EVs for specific therapeutic applications. This hastens the translation of research from the laboratory to clinical practice, benefiting patients requiring improved bone fracture/defect treatment. On a clinical level, precise utilization of EVs could offer more personalized and effective supporting treatment options for patients with bone fractures/defects. By customizing the route of administration of EVs (such as pills for system administration; liquid agent or lyophilized EVs implanted in bone grafts for local injections) to suit individual patients' needs, clinicians could devise tailored therapeutic strategies to optimize treatment outcomes.

REFERENCES

1. Shelke, G.V., et al., Importance of exosome depletion protocols to eliminate functional and RNA-containing extracellular vesicles from fetal bovine serum. J Extracell Vesicles, 2014. **3**.
2. Riekstina, U., et al., Characterization of human skin-derived mesenchymal stem cell proliferation rate in different growth conditions. Cytotechnology, 2008. **58**(3): p. 153-62.
3. Morito, T., et al., Synovial fluid-derived mesenchymal stem cells increase after intra-articular ligament injury in humans. Rheumatology (Oxford), 2008. **47**(8): p. 1137-43.
4. Hou, T., et al., Umbilical cord Wharton's Jelly: a new potential cell source of mesenchymal stromal cells for bone tissue engineering. Tissue Eng Part A, 2009. **15**(9): p. 2325-34.
5. Cheng, P., et al., Hypoxia endothelial cells-derived exosomes facilitate diabetic wound healing through improving endothelial cell function and promoting M2 macrophages polarization. Bioact Mater, 2024. **33**: p. 157-173.
6. Xia, M., et al., Milk-derived small extracellular vesicles inhibit the MAPK signaling pathway through CD36 in chronic apical periodontitis. Int J Biol Macromol, 2024. **274**(Pt 2): p. 133422.
7. Chen, Y., et al., CD36, a signaling receptor and fatty acid transporter that regulates immune cell metabolism and fate. J Exp Med, 2022. **219**(6).
8. Glatz, J.F.C. and J. Luiken, Dynamic role of the transmembrane glycoprotein CD36 (SR-B2) in cellular fatty acid uptake and utilization. J Lipid Res, 2018. **59**(7): p. 1084-1093.
9. Guillard, J. and S. Schwörer, Metabolic control of collagen synthesis. Matrix Biol, 2024. **133**: p. 43-56.
10. Hagey, D.W., et al., The cellular response to extracellular vesicles is dependent on their cell source and dose. Sci Adv, 2023. **9**(35): p. eadh1168.
11. Zendrini, A., et al., On the surface-to-bulk partition of proteins in extracellular vesicles. Colloids Surf B Biointerfaces, 2022. **218**: p. 112728.
12. Zhou, Y., et al., Large-scale heparin-based bind-and-elute chromatography identifies two biologically distinct populations of extracellular vesicles. J Extracell Vesicles, 2023. **12**(6): p. e12327.
13. Buzas, E.I., Opportunities and challenges in studying the extracellular vesicle corona. Nat Cell Biol, 2022. **24**(9): p. 1322-1325.
14. Su, G., et al., Annexin A5 derived from matrix vesicles protects against osteoporotic bone loss via mineralization. Bone Res, 2023. **11**(1): p. 60.
15. Chiba, K., et al., Heterogeneity of bone microstructure in the femoral head in patients with osteoporosis: an ex vivo HR-pQCT study. Bone, 2013. **56**(1): p. 139-46.
16. He, Y., et al., Increased vascularization of the subchondral region in human osteoarthritic femoral head in the elderly. Histochem Cell Biol, 2025. **163**(1): p. 39.
17. Cramer, E.E.A., et al., Integration of osteoclastogenesis through addition of PBMCs in human osteochondral explants cultured ex vivo. Bone, 2024. **178**: p. 116935.
18. Cramer, E.E.A., et al., Culture system for longitudinal monitoring of bone dynamics ex vivo. Biotechnol Bioeng, 2025. **122**(1): p. 53-68.
19. Carney, R.P., et al., Harnessing extracellular vesicle heterogeneity for diagnostic and therapeutic applications. Nat Nanotechnol, 2025. **20**(1): p. 14-25.
20. Lener, T., et al., Applying extracellular vesicles based therapeutics in clinical trials - an ISEV position paper. J Extracell Vesicles, 2015. **4**: p. 30087.

Chapter 8

Summary

Bone defects and fractures, particularly non-unions and segmental defects that result in long-term disability, represent a major public health concern [1]. The treatment of bone defects and fractures in the United States costs approximately $5 billion annually [2], largely due to surgical interventions and grafting procedures—such as autologous bone grafts, allografts, and xenografts—used to address non-unions and other complications [3, 4]. However, these methods/materials come with inherent drawbacks, including donor site morbidity and limited osteoinductive capacity [5]. In response to these challenges and in pursuit of satisfactory clinical outcomes, there is a growing need for advanced (nano) technology in bone tissue engineering, such as EVs-based therapy as a promising cell-free therapeutic strategy to promote bone regeneration. In view of this, this PhD thesis aimed to explore various aspects of EVs from isolation to application for precision utilization in treating bone defects. Specifically, this thesis focused on identification and utilization of pure and homogenous EVs by developing methods of depleting native EVs from FBS for *in vitro* cell culture and exploring the osteogenic potential of specific subpopulations of EVs. To this end, **Chapter 1** provided a broad introduction on bone defects and fractures, their current standard-of-care treatments and cutting-edge therapies including EVs isolated from *in vitro* cell culture and body liquids. A brief description of the objectives of this thesis is provided based on addressed research questions.

Which EV-depletion method of FBS is the best to use in MSC cultures to obtain pure MSC-EVs with minimal FBS EV contamination whilst not impairing cell growth and differentiation?

The majority of EVs used for tissue regeneration are obtained from *in vitro* cultures of MSCs. However, the main concern of enrichment of MSC-EVs is the contamination with exogenous EVs present in FBS needed as nutritional supplement of cell culture medium for optimal growth of cells. The presence of FBS-EVs confounds the therapeutic efficacy of MSC-EVs [6]. During the standard FBS-EVs depletion process via ultracentrifugation, serum components such as proteins, lipids, and lipoproteins often aggregate and are eliminated from the FBS, resulting in a less effective and incomplete supplement for MSC culture. Therefore, studying optimization methods for highly selective FBS-EVs depletion is necessary. In **Chapter 2**, we tested the three approaches ultracentrifugation (UC), ultrafiltration (UF), and polyethylene glycol (PEG) precipitation to evaluate efficient methods for EV depletion from FBS. Our results demonstrated that the EV depletion efficiency was similar for PEG (95.6%) and UF (96.6%), but less with UC (82%) relative to standard FBS. However, protein loss varied significantly across methods: PEG (47%), UF (87%), and UC (51%), resulting in EV depletion-to-protein loss ratios of 2.03 (PEG), 1.11 (UF), and 1.61 (UC). Notably,

UF treatment led to a marked reduction in TGFβ/Smad signaling in MSCs, a pathway critical for MSC growth and function. After 96 hours of culture in media containing 5% FBS or 5% EVdFBS, hADSC osteogenic potential remained intact. Consistent with the low confluency observed using light microscopy, hADSC proliferation was significantly reduced in media supplemented with 5% UF EVdFBS. Importantly, hADSCs cultured in 5% PEG EVdFBS media yielded a higher quantity and purity of EVs, which remained biologically active, as evidenced by their ability to upregulate Col1a1 and TIMP1 expression in human knee synovial fibroblasts. These findings indicate that PEG precipitation is the most effective method for preparing EV-depleted FBS, offering high EV depletion with acceptable protein loss and enabling efficient enrichment of MSC-derived EVs with minimal contamination from FBS-derived EVs.

What is the effect of mEVs on energy metabolism during EV stimulated osteogenic differentiation of hBMSCs?

During osteogenic differentiation, MSCs undergo a transition from glycolysis to aerobic mitochondrial OXPHOS, marked by mitochondrial biogenesis, and increased membrane potential, as well as higher intracellular ATP levels [7]. This metabolic shift is crucial as it supports the energy-intensive process of osteogenic differentiation. In **Chapter 3**, we aimed to investigate the role of cow milk-derived (m)EVs stimulation in energy metabolism during the early phase of osteogenic differentiation of hBMSCs. Supplementation with mEVs (5E+06 particles/ml) showed an optimal effect on driving osteogenic differentiation with a 120% increase in type I collagen expression at day 7, 40% increase in ALP activity at day 14, and 20% increase in mineralization at day 21. Consistently, mEV stimulation at 5E+06 particles/ml resulted in 30% increase in cellular ATP levels compared to controls at day 2 and day 6 of osteogenic differentiation of hBMSCs through strengthening aerobic energy metabolism within glucose as main source of energy production. By measuring mitochondrial membrane potential and superoxide production, our data showed that mEV stimulation enhanced mitochondrial activity in hBMSCs during their differentiation into osteoprogenitor cells, while maintaining ROS levels at a moderate level by improving SOD2 expression. Additionally, the expressions of mitochondrial regulatory genes were determined by RT-qPCR. Compared to controls, mEV stimulation resulted in a 40% increase in mRNA expression of the mitochondrial fusion gene MFN2 and a 27% decrease in the fission gene DRP1. Additionally, the mitochondrial transcription genes TEFM and TFB2M showed expression increases of 140% and 30%, respectively—altogether indicating a fused, functionally active mitochondrial state. These data demonstrated that mEVs facilitate osteogenic differentiation of hBMSCs through activating classical mitochondrial aerobic metabolism.

What is the significance of ECM-binding properties of EVs in the therapeutic treatment of skeletal diseases?

To obtain an overview of available knowledge on the interaction of EV-ECM in bone and joint, **Chapter 4** presented a comprehensive review on this specific topic based on clear inclusion and exclusion criteria for related literature [8]. PubMed and Web of Science were searched to identify relevant literature and study selection was limited to research articles that: i) included both *in vivo* and *in vitro* bone or joint studies, and ii) reported on *in vitro* and *in vivo* ECM and EVs. Studies that only investigated ECM or EVs were excluded. After the introduction of EV and ECM in bone and joint tissues, this review summarized i) the surface biomolecules of EVs and their interactions with ECM components that are crucial for regulating bone remodeling, cartilage maintenance, and immune responses, and ii) the effect of ECM-based biomaterials encapsulating EVs for efficient EV delivery in regenerative and immunomodulatory therapies in bone and joint diseases. The small diameter of EVs leads to large surface-to-volume ratio of EVs [9], causing the contribution of surface molecules to become relatively more significant compared to the interior of the EVs. The molecular basis for the interaction between EVs and ECM is expected on the basis of their biochemical composition and chemical bonds. The specificity of these interactions appears important for the regulation of the extracellular microenvironment of bone and joint tissue. Moreover, this synergy between EVs and ECM-based scaffolds is central to the emerging therapeutic strategy. ECM-based biomaterials serve as biologically compatible delivery platforms that closely mimic the native tissue environment. The local delivery of EVs from ECM-based scaffolds is particularly advantageous for bone and joint regeneration. While the therapeutic promise of EVs delivered via ECM-based scaffolds is clear, several challenges remain to be addressed. First, achieving scalable production at low cost and with consistent quality as the regular manufacturing challenges on regenerative medicine. More importantly, the heterogeneity of EV populations poses a significant barrier to clinical translation. EV heterogeneity implies that individual vesicles may not possess all the chemical or physical characteristics attributed to the bulk population, indicating that each vesicle might lack certain functional properties including ECM binding ability and related therapeutic functions that are associated with the bulk. Therefore, it is eminent to understand the detailed mechanisms underlying EV-ECM interactions, and optimizing scaffold formulations for specific applications is a critical topic for future research.

What is the role of the mEV subpopulation with the capacity to bind collagen in preclinical bone regeneration?

EV heterogeneity impacts on functional performance in therapeutics [10]. The proteins on the EV surface determine their binding properties to the meshwork of ECM. To

explore the correlation between ECM-binding properties of EV subpopulations and their functionality, we investigated the role of the mEV subpopulation with the capacity to bind to type I collagen in treating bone defects in **Chapter 5**. By injecting mEVs into the defects of bone explants, accumulation of fluorochromes in the newly formed bone revealed that bulk mEVs stimulate bone formation *ex vivo*. Using a collagen-binding experiment for bulk mEVs with collagen-coated tissue culture plastic, the binding curve revealed that approximately 4% of the input particles (bulk mEVs) were able to bind to collagen, and their presence resulted in 106.9 ± 4.4 μg/ml of calcium content of hBMSCs while 91.4 ± 5.5 μg/ml in control conditions. In addition, confocal microscopy showed noticeably fewer labeled $^{cb-}$mEVs were observed in the perinuclear region compared to bulk mEVs, and the calcium content of hBMSCs with mEVs stimulation was 99.9 ± 4.8 μg/ml and 90.8 ± 4.6 μg/ml for $^{cb-}$mEVs stimulation, respectively, suggesting $^{cb+}$mEVs are the functional subpopulation of mEVs that enhances osteogenic differentiation of hBMSCs. Further, proteomic profiling of (bulk) mEVs and $^{cb-}$mEVs and western blotting results demonstrated that the binding between type I collagen and mEVs is specific and that AnxV was enriched (more than 400%) in CD9 positive $^{cb+}$mEVs. Consistently, compared to mEVs, calcium deposition in hBMSCs was significantly reduced after 21 days of OM culture with $^{AnxV-}$mEVs isolated by utilizing immunomagnetic separation. NTA analysis showed release kinetics of mEV encapsulated in 3D hydrogel constructs during 14 days in PBS at 37°C. Specially, robust release of mEVs was observed from day 1 to day 6, during which 68.1 ± 8.7% mEVs were released from the hydrogel construct. 7.8% ± 1.2 mEVs were released between day 6 up to day 10 and 15.6% ± 2.5 mEVs remained entrapped in the hydrogel. The data on alizarin red S staining and calcium content of hBMSCs with mEVs-col, $^{cb-}$mEVs-col and $^{AnxV-}$mEVs-col demonstrated that mEVs were successfully encapsulated in 3D hydrogel constructs and that in particular the $^{cb+}$mEVs population is responsible for the enhanced hBMSCs mineralization *ex vivo*. *In vivo* assessment of regenerative capacity in a rat femoral condyle defect model, employing high-resolution micro-computed tomography scanning and various histology staining methods, demonstrated that the contribution of the $^{cb+}$mEVs subpopulation to mEV-mediated acceleration of orthotopic osteoporotic bone defect regeneration. These findings underscored that EV binding to the ECM protein type I collagen can be used to isolate a functional mEV subpopulation for bone tissue regeneration. This approach represents an important step forward in relating EV properties to their functionality, which will promote clinical translation.

Can we develop an *ex vivo* vital human bone model to study bone regeneration?

Preclinical assessment of regenerative therapy on treating bone defects is underpinned by a tremendous animal experimentation burden. The ethical

debate on the utilization of animals in research has strongly intensified over the last years [11]. Moreover, it should be noted that the bone structure, physiological remodeling processes, and anatomy of these animal models differ significantly from the human bone. In **Chapter 6**, we established an *ex vivo* human bone model and loaded EVs into defects, thereby offering a promising approach that assesses bone regeneration in a 3D setting. A standardized protocol was developed to create bone discs of uniform size and maintain sterility throughout the procedure. AlamarBlue™ assays revealed sustained viability of healthy cells originating from the bone discs over a 14-day culture period. Histological images confirmed that bone discs contained CD14 positive monocyte-lineage cells and the presence of microvessels in bone marrow compartments. By testing pro-inflammatory cytokines (IL6, IL1b, TNFa) and TRAP activity in supernatant of bone discs, we demonstrated that bone discs respond to an immunological stimulus and retain marginal osteoclastic activity for bone remodeling. Flow cytometry and RT-qPCR data demonstrated the presence of hBMSCs that kept their osteogenic differentiation property in the bone discs. More importantly, fluorescent imaging showed more bone formation-related fluorochrome (calcein green, alizarin red s) uptake upon injection of mEVs into defects in viable human bone discs. These findings underscore that our ex vivo bone model provides a 3D bone microenvironment resembling important aspects of the regenerative processes observed in physiological bone defects/fractures. Future research may explore modifications such as mechanical stimuli or blood supply (perfusion system) to create a more comprehensive bone regenerative micro-environment. Overall, our *ex vivo* human bone model appears to be a valuable platform for investigating bone biology and evaluating novel regenerative therapeutic strategies such as the effect of EVs either from *in vitro* cell cultures or body liquids.

REFERENCES

1. Mora, R., et al., Economic Burden and Practical Considerations, in Hexapod External Fixator Systems: Principles and Current Practice in Orthopaedic Surgery, M. Massobrio and R. Mora, Editors. 2021, Springer International Publishing: Cham. p. 285-289.
2. Perez, J.R., et al., Tissue Engineering and Cell-Based Therapies for Fractures and Bone Defects. Front Bioeng Biotechnol, 2018. **6**: p. 105.
3. Zhang, H., et al., Expert consensus on the bone repair strategy for osteoporotic fractures in China. Front Endocrinol (Lausanne), 2022. **13**: p. 989648.
4. Ferraz, M.P., Bone Grafts in Dental Medicine: An Overview of Autografts, Allografts and Synthetic Materials. Materials (Basel), 2023. **16**(11).
5. Jimi, E., et al., The current and future therapies of bone regeneration to repair bone defects. Int J Dent, 2012. **2012**: p. 148261.
6. Eitan, E., et al., Extracellular vesicle-depleted fetal bovine and human sera have reduced capacity to support cell growth. J Extracell Vesicles, 2015. **4**: p. 26373.
7. Li, Q., et al., The role of mitochondria in osteogenic, adipogenic and chondrogenic differentiation of mesenchymal stem cells. Protein Cell, 2017. **8**(6): p. 439-445.
8. Wang, P., et al., ECM-binding properties of extracellular vesicles: advanced delivery strategies for therapeutic applications in bone and joint diseases. Cell Commun Signal, 2025. **23**(1): p. 161.
9. Zendrini, A., et al., On the surface-to-bulk partition of proteins in extracellular vesicles. Colloids Surf B Biointerfaces, 2022. **218**: p. 112728.
10. Carney, R.P., et al., Harnessing extracellular vesicle heterogeneity for diagnostic and therapeutic applications. Nat Nanotechnol, 2025. **20**(1): p. 14-25.
11. Schilling, A.F., et al., Transgenic and knock out mice in skeletal research. Towards a molecular understanding of the mammalian skeleton. J Musculoskelet Neuronal Interact, 2001. **1**(3): p. 275-89.

Chapter 9

Samenvatting

Botdefecten en fracturen, in het bijzonder niet-verbonden botbreuken en segmentale botdefecten die leiden tot langdurige invaliditeit, vormen een groot probleem voor de volksgezondheid [1]. De behandeling van botdefecten en fracturen in de Verenigde Staten kost jaarlijks ongeveer 5 miljard dollar [2], voornamelijk door chirurgische ingrepen en transplantaties zoals autologe-, allogene- en xenogene bottransplantaties, die worden gebruikt om niet-verbonden botbreuken en botdefecten te behandelen [3, 4]. Deze aanpak kent echter inherente nadelen, waaronder het risico op afsterven van donorweefsel en geringe osteoinductieve eigenschappen van het gebruikte donorweefsel [5]. In het streven naar betere klinische uitkomsten spelen geavanceerde (nano)technologieën een steeds grotere rol bij het ontwikkelen van botvervangers, al dan niet in combinatie met transplantatie van bot- of stamcellen en het bijvoegen van botgroei bevorderende middelen. Recentelijk is er veel aandacht voor het toepassen van extracellulaire vesicles (EVs); dit zijn uitgescheiden celblaasjes, die veelal gebruikt worden ter vervanging van cellen en groeifactoren om botregeneratie te bevorderen. In dit proefschrift werd onderzocht of uit koemelk verkregen EVs voor dit doel gebruikt kunnen worden.

In cel- en weefselkweken wordt meestal foetaal runderserum (FBS) gebruikt als toevoeging om de groei en levensvatbaarheid van cellen te ondersteunen. Om de effecten van koemelk-EVs hierop te testen, is het van belang dat FBS zelf geen runder-EVs bevat. Dit geldt ook bij therapeutisch gebruik van stamcel-EVs, die meestal uit celkweken verkregen worden. Het is namelijk bewezen, dat de aanwezigheid van FBS-EVs de therapeutische effectiviteit van MSC-EVs verstoort [6]. In Hoofdstuk 2 vergeleken we drie gangbare methoden om EVs te verwijderen uit serum: ultracentrifugatie (UC), ultrafiltratie (UF) en polyethyleenglycol (PEG) precipitatie. Naast het meten van de EV-verwijderingsefficiëntie hebben we ook gekeken of deze behandelingen consequenties hadden op het gebruik van FBS als toevoeging aan de celkweek. Twee van de drie gebruikte methoden resulteerden in vergelijkbare verwijdering van EVs (PEG 95,6% en UF 96,6%), maar UC was duidelijk minder efficient (82%). Echter, het eiwitverlies varieerde aanzienlijk tussen de gebruikte methoden: PEG (47%), UF (87%) en UC (51%). Na 96 uur kweken van MSCs in media met 5% FBS of 5% EV-vrij FBS was er geen verschil in de botdifferentiatie van MSCs, maar was de celgroei lager bij 5% UF EV-vrij FBS en leverde de kweek met 5% PEG EV-vrij FBS een hogere opbrengst op van biologisch actieve MSC-EVs, bepaald naar hun vermogen om de genexpressie van collageen en TIMP1 in humane fibroblasten (uit knie synovium) te induceren. Deze bevindingen geven aan dat PEG behandeling de meest effectieve methode is voor het bereiden van EV-vrij FBS en het verkrijgen van zuivere MSC-EVs uit kweek.

In een voorgaande studie hadden we reeds aangetoond dat het toevoegen van koemelk-EVs aan kweken van stamcellen uit beenmerg (BMSCs) de differentiatie tot osteoblasten, de cellen die verantwoordelijk zijn voor de aanmaak van nieuw botweefsel, bevordert. Het is algemeen bekend dat tijdens deze osteogene differentiatie de stamcellen overschakelen van glycolyse naar aerobe mitochondriale energieproductie (OXPHOS), gekarakteriseerd door mitochondriale biogenese, verhoogd membraanpotentieel en hogere intracellulaire ATP-niveaus [7]. Mitochondriën zijn de 'energiecentrales' van cellen. Deze metabole verschuiving is cruciaal omdat dit het energie-intensieve proces van botdifferentiatie ondersteunt. In Hoofdstuk 3 onderzochten we het effect van koemelk-EVs op het energiemetabolisme tijdens de botdifferentiatie van humane BMSCs. We vonden dat een concentratie van 5E+06 koemelk-EVs/ml optimaal was om de botdifferentiatie te bevorderen met 120% toename van type I collageen-expressie op dag 7, een 40% toename in ALP-activiteit op dag 14 en een 20% toename in mineralisatie op dag 21. Bij dezelfde dosering zagen we dat koemelk-EVs leidden tot 30% toename in cellulaire ATP-niveaus op dag 2 en dag 6 van de botdifferentiatie. Door het meten van de mitochondriale membraanpotentiaal en de productie van superoxide, toonden onze gegevens aan dat koemelk-EVs de mitochondriële activiteit in humane BMSCs versterken tijdens hun differentiatie naar botvormende cellen. Bovendien verhoogde koemelk-EVs de expressie van mitochondriale, regulerende genen in deze cellen met een 40% toename van de mRNA-expressie van MFN2 (een eiwit betrokken bij het fuseren van mitochondriën wat leidt tot hogere energieproductie), en een 27% afname van DRP1 (een eiwit betrokken bij deling van mitochondriën wat leidt tot minder energieproductie). Bovendien verhoogde koemelk-EVs de expressie van TEFM (140%) en TFB2M (30%), twee eiwitten die betrokken zijn bij de genregulatie in mitochondriën. Dit alles toonde aan dat toevoeging van koemelk-EVs aan humance BMSC kweken niet alleen de energieproductie van mitochondriën verhoogt, maar ook zorgt voor efficiënte en gezonde mitochondriën tijdens de transitie van stamcellen naar botvormende cellen.

Het is bekend dat EVs in lichaamsvloeistoffen een heterogene groep vormen en dat geldt ook voor de koemelk-EVs. We speculeerden dat in analogie met EVs afkomstig van kraakbeencellen (matrix-vesicles genoemd), de binding van koemelk-EVs aan de extracellulaire matrix (ECM) van belang kan zijn met betrekking tot hun botstimulerende eigenschappen. In hoofdstuk 4 beschrijven we de huidige kennis omtrent de ECM bindingseigenschappen van EVs die gebruikt zijn in bot- of gewrichtsstudies en rapporteerden over ECM binding. Dat resulteerde in een overzicht van de oppervlaktemoleculen van EVs, die betrokken zijn bij binding aan ECM en ook cruciaal zijn bij het remodelleren van bot- en kraakbeenweefsel. Tevens gaf het ons het inzicht dat EVs in combinatie met ECM-gebaseerde biomaterialen

kunnen leiden tot efficiëntere regeneratieve en immuun-modulerende therapieën bij bot- en gewrichtsziekten.

Hoewel de therapeutische belofte van EVs die via ECM-gebaseerde biomaterialen beschikbaar komen duidelijk is, blijven er verschillende uitdagingen om aan te pakken. Ten eerste, het bereiken van opschaalbare productie tegen lage kosten en met consistente kwaliteit van EVs. Echter, de heterogeniteit van EV-populaties vormt een aanzienlijke barrière voor de klinische toepassing. Want EV-heterogeniteit betekent dat subpopulaties verschillende en mogelijk tegenovergestelde eigenschappen hebben, waardoor de therapeutische effecten kleiner zijn en neveneffecten groter kunnen zijn. Op basis van dit literatuuronderzoek is de vraag: bevatten koemelk EVs ook een ECM bindende subpopulatie en zijn deze dan ook beter in het ondersteunen van nieuwe botvorming?

In hoofdstuk 5 geven we op deze vraag een antwoord. Een hechtingstest van EVs aan collageen gecoate microtiterplaten toonde aan dat ongeveer 4% van koemelk-EVs ($^{cb+}$mEVs genoemd) deze bindingseigenschap heeft. Kweken we vervolgens humane BMCs op deze collageen microtiterplaten en meten we na verloop van tijd de calcium afzetting van deze cellen, dan was die 106,9 ± 4,4 µg/ml in aanwezigheid van deze subpopulatie koemelk-EVs, terwijl dit 91,4 ± 5,5 µg/ml was in controles zonder toevoeging van koemelk-EVs. Ter vergelijking, de calciumafzetting van humane BMSCs met de bulk mEV-stimulatie was 99,9 ± 4,8 µg/ml en 90,8 ± 4,6 µg/ml voor $^{cb-}$mEVs (beiden niet collageen-bindende koemelk-EVs). Dit suggereert dat $^{cb+}$mEVs de functionele subpopulatie van koemelk-mEVs is, die de botdifferentiatie van humane BMSCs kan bevorderen. Met proteomics (het in kaart brengen van de eiwitten in/op EVs) en verificatie met Westernblotting bevestigden we dat de $^{cd+}$mEVs inderdaad verschillen van de overige koemelk-EVs en dat ze positief zijn voor de markers annexine-V (AnxV) en CD9. Van AnxV is bekend dat het collageen kan binden en nieuwe botvorming kan stimuleren, terwijl CD9 een bekende EV marker is. Consistent hiermee was onze bevinding dat de calciumafzetting door humane BMSCs significant lager was na 21 dagen botdifferentiatie met AnxV-negatieve koemelk-EVs ($^{AnxV-}$mEVs), geïsoleerd door immunomagnetische scheiding, vergeleken met de totale koemelk EV populatie.

Van de collageen-bindende eigenschappen wilden we gebruik maken door koemelk-EVs op te nemen in collageen-hydrogels, een veelgebruikt biomateriaal voor het bevorderen van botregeneratie. Onder fysiologische omstandigheden komen deze koemelk-EVs vanuit de collageen-hydrogels langzaam vrij. Zoals verwacht kwam de eerste 6 dagen 68,1% van de koemelk-EVs vrij en tussen dag 6 en

10 slechts 7,8%, waarmee nog 15,6% achterbleef in de hydrogel op dag 10, hetgeen met grote waarschijnlijkheid de $^{cb+}$mEVs zullen zijn. In opvolgende kweken van humane BMSCs in hydrogels die mEVs, cb-mEVs-col of AnxV-mEVs bevatten, zagen we een verschil in calcium-specifieke alizarine rood kleuring en calciumgehaltes, waaruit we concludeerden dat met name de $^{cb+}$mEVs-populatie in koemelk-EVs verantwoordelijk is voor de versterkte calcium afzetting van humane BMSCs. Vervolgens hebben we de collageen-hydrogels getest in een kniedefect-model in ratten met osteoporotisch bot. Micro-computed tomography scanning van hoge resolutie en verschillende histologische kleuringstechnieken toonden aan dat de bijdrage van de cb+mEVs subpopulatie significant was in de mEV-gemedieerde regeneratie van osteoporotische botdefecten. Deze bevindingen benadrukten dat de binding van EVs aan het ECM-eiwit type I collageen kan worden gebruikt om een functionele koemelk-EV-subpopulatie te verkrijgen voor botregeneratieve toepassingen. Deze benadering vertegenwoordigt een belangrijke stap vooruit in de klinische toepassing van EVs in de behandeling van botfracturen en -defecten.

Hoofdstuk 6 beschrijft het vitaal menselijk botmodel dat we ontwikkeld hebben om botregeneratie te bestuderen met als doel de effecten van EVs te kunnen bepalen. Daarnaast zijn momenteel voor de preklinische beoordeling van regeneratieve therapieën voor de behandeling van botdefecten (veel) dierexperimenten nodig. Het ethische debat over het gebruik van proefdieren in onderzoek is de afgelopen jaren sterk toegenomen [8]. Bovendien moet worden opgemerkt dat de botstructuur, fysiologische remodelleringsprocessen en anatomie van deze diermodellen aanzienlijk verschillen van die in menselijke bot. Een ex vivo vitaal menselijk botmodel zou een aanzienlijke vermindering in het gebruik van proefdieren kunnen opleveren en relevante gegevens opleveren.

In hoofdstuk 6 hebben we het ex vivo menselijk botmodel gebruikt en de koemelk-EVs in de aangebrachte botdefecten geladen, wat een veelbelovende benadering biedt om botregeneratie in een 3D-omgeving te beoordelen. Een gestandaardiseerd protocol werd ontwikkeld om botschijfjes van uniforme grootte te maken en de steriliteit gedurende de procedure te behouden. AlamarBlue™-testen toonden aan dat gezonde cellen afkomstig van de botschijfjes gedurende een kweekperiode van 14 dagen hun vitale capaciteit behielden. Histologische analyses bevestigden dat de botschijfjes CD14-positieve monocyten bevatten alsook de aanwezigheid van kleine bloedvaten in de beenmergcompartimenten. Door pro-inflammatoire cytokines (IL6, IL1b, TNFa) en TRAP-activiteit in het medium van de botschijfjes te testen, toonden we aan dat de botschijfjes reageren op een immunologische stimulus en marginale osteoclastische activiteit behouden voor botremodellering.

Flowcytometrie- en gen-expressie data toonden de aanwezigheid van humane BMSCs aan, die hun botdifferentiatiecapaciteit in de behielden. Belangrijker nog, fluorescente beeldvorming toonde een verhoogde opname van botvormings-gerelateerde fluorochromen (calceïne groen, alizarinrood S) aan na injectie van koemelk-EVs in de defecten in de vitale menselijke botschijfjes. Deze bevindingen benadrukken dat dit ex vivo humane botmodel een 3D-bot(micro)omgeving biedt, die belangrijke aspecten nabootst van de regeneratieve processen die worden waargenomen bij fysiologische botdefecten/-fracturen. Toekomstig onderzoek kan modificaties aan dit model verkennen, zoals mechanische belasting of bloedtoevoer (perfusiesysteem), om een meer uitgebreide botregeneratieve (micro-)omgeving te creëren. Al met al lijkt dit ex vivo menselijke botmodel een waardevol platform voor het onderzoeken van botbiologie en het evalueren van nieuwe regeneratieve therapeutische strategieën, zoals het effect van EVs, zowel uit in vitro celkweken als lichaamsvloeistoffen.

REFERENCES

1. Mora, R., et al., Economic Burden and Practical Considerations, in Hexapod External Fixator Systems: Principles and Current Practice in Orthopaedic Surgery, M. Massobrio and R. Mora, Editors. 2021, Springer International Publishing: Cham. p. 285-289.
2. Perez, J.R., et al., Tissue Engineering and Cell-Based Therapies for Fractures and Bone Defects. Front Bioeng Biotechnol, 2018. **6**: p. 105.
3. Zhang, H., et al., Expert consensus on the bone repair strategy for osteoporotic fractures in China. Front Endocrinol (Lausanne), 2022. **13**: p. 989648.
4. Ferraz, M.P., Bone Grafts in Dental Medicine: An Overview of Autografts, Allografts and Synthetic Materials. Materials (Basel), 2023. **16**(11).
5. Jimi, E., et al., The current and future therapies of bone regeneration to repair bone defects. Int J Dent, 2012. **2012**: p. 148261.
6. Eitan, E., et al., Extracellular vesicle-depleted fetal bovine and human sera have reduced capacity to support cell growth. J Extracell Vesicles, 2015. **4**: p. 26373.
7. Li, Q., et al., The role of mitochondria in osteogenic, adipogenic and chondrogenic differentiation of mesenchymal stem cells. Protein Cell, 2017. **8**(6): p. 439-445.
8. Schilling, A.F., et al., Transgenic and knock out mice in skeletal research. Towards a molecular understanding of the mammalian skeleton. J Musculoskelet Neuronal Interact, 2001. **1**(3): p. 275-89.

Chapter 10

Acknowledgements

I have never forgotten the first time I met with Dr. Fons van de Loo in person. The sky was clear, and weather was not as cold as I imagined. He was friendly and just showed me around in the lab, introducing me to all the colleagues in the lab. My working unit had been cleaned with a comfortable chair. That position was very convenient for me to turn to my co-supervisor for help in time. Everything was new but positive to me. As time goes by, I am now typing these words and memorizing the past PhD time. I know it is time to say goodbye to this small place I have grown to love deeply. It was an incredible journey which made me become a qualifiable researcher that I could not imagine before. With so many people's helps, I learnt a lot in my research field and finished my PhD thesis. Without you, I would not have made it this far. I would like to express my deep acknowledgement in this chapter.

First, I would like to express my sincere gratitude to my supervisor, Dr. Fons van de Loo, Dr. Jeroen van den Beucken, and Dr. Artz Onno. Dear Fons, thank you for showing me what it truly means to be a researcher. Your lifelong passion for EV research has been a constant source of inspiration to me. Whenever I ran into questions or setbacks and turned to you for help, you responded with patience and clarity, offering key solutions grounded in your own experience and the latest literature. You rarely issued directives. Instead, you trusted me to explore ideas and encouraged me to run the experiments I felt compelled to try. In the early months of my PhD, when I felt discouraged about my direction and even considered moving to another department, you did not blame or pressure me. You spoke with me openly and kindly, and you proposed a joint-supervision arrangement that helped me regain confidence and momentum. When an unexpected family emergency forced me to pause my studies and return home for a time, you gave me your full support. You assured me that I could take the time I needed and come back to continue our work once things are settled. That promise sustained me through a difficult period. Although I am your last PhD student, you have remained exceptionally responsible and responsive—your prompt emails and your willingness to welcome me into your office without an appointment made me feel seen and supported. Through your example, I learned not only methods and rigor, but also generosity, integrity, and curiosity. Thank you for every piece of advice, every careful edit, and every quiet vote of confidence. I will carry your mentorship with me throughout my career and hope to pay it forward to my own students one day. I wish you a joyful, healthy, and fulfilling retirement—you have more than earned it. Dear Jeroen, I want to express my heartfelt gratitude for giving me the opportunity to work in the Dentistry Department. It has been an immense honor to be your student, and I am truly proud to have had the chance to learn under your guidance. I vividly recall our first conversation, during which I spoke somewhat hesitantly in English. I was

filled with worries—what if I couldn't express myself or my research plan clearly? What if you didn't think my ideas were worth pursuing, and you wouldn't allow me to work with you in the Dentistry Department? These concerns weighed heavily on my mind, but as the conversation progressed, I was relieved to find it relaxed and enjoyable. Your openness, directness, and the simplicity with which you explained your thoughts made a significant impact on me. You always made everything clear using accessible and familiar language, which immediately made me feel more at ease. Your suggestions were incredibly helpful, and they gave me the confidence I needed to pursue my research in the Dentistry Department as a guest PhD student. I also deeply appreciate your constant encouragement: "Don't be shy, we are open here, and if you face any technical challenges, feel free to contact me or our technicians—we're all happy to help you." Given your extremely busy schedule, I have always been impressed by how promptly you respond to my emails, even in the early mornings. Your willingness to engage with me and offer your time has truly made a difference in my academic journey. Whenever we discussed my recent data, you patiently provided valuable suggestions that helped me refine our story, making it both more logical and compelling. This made me feel that the work I was doing was worthwhile and valued, which, as you know, was a great source of motivation. Moreover, during the final stages of my PhD, your support in enabling me to conduct animal experiments was invaluable. You facilitated my connection with Dr. Yang Zhang at Shenzhen University, which allowed me to quickly gather the necessary in vivo data for my final paper. Thanks to your help, I was able to complete my work and publish the paper on time, which was a significant achievement for me. The collaboration with you was truly pleasant, and I will forever cherish that experience. I am deeply grateful for the opportunity to work with you, and I am determined to follow in your footsteps, continuously striving to improve in my academic career. Your guidance and support have been instrumental in shaping my growth, and I hope to carry the lessons you've taught me as I move forward in my work. Dear Onno, thank you for the countless times you offered immediate support and practical help. Even when I didn't have an appointment, I could come to you with puzzles and misunderstandings, and you always made space for me. From setting up the NTA instrument to tracking down small but critical reagents and supplies, you helped me arrange everything—especially coordinating with colleagues in other departments so we could access specialized equipment for our experiments. Although you are my co-supervisor and senior in experience, you have always felt like an older brother to me. Every conversation with you was open and relaxed; I never felt shy or uncomfortable sharing my ideas, doubts, or half-formed results. As a department manager with a heavy workload, you still found time whenever I knocked on your door, and your quick replies were

both impressive and reassuring. As EV researchers in our department, we became especially close collaborators. You generously shared everything you knew about EVs, and your passion continually inspired me. Whenever I walked past your unit, I would ask myself, "Can I carry this same energy and dedication when I reach Onno's age?" English is the language I used most often with you. At first, I struggled to fully understand your meaning and to clearly express my own. But as time went by, we came to understand each other completely—about research and about daily life. I vividly remember our trip to Vienna for the Annual EV meeting. It was a wonderful journey: we presented our work to colleagues from around the world, learned a great deal in the sessions, and enjoyed the city. On the first evening, we went to a Chinese restaurant. Before we left, you worried the food might be too spicy—but in the end you ordered the special spicy dish. After finishing, you told me it was your first time trying Chinese food abroad, and that it was excellent. I will always smile when I think of that moment. Thank you again for your instant support, your patience, and your example. I will do my best to learn from your passion and to keep a positive, forward-looking attitude in my work and life. I am truly grateful to have had the chance to work with you. Dear Peter, thank you for welcoming me into your lab; it has been a privilege to work under your supervision. Although EVs and bone biology are not your primary focus, you consistently gave my project your full attention—especially during the annual checkpoint meetings—and offered thoughtful, actionable advice. Your presentations exemplify rigorous thinking and a compelling research vision; I have learnt a great deal from them, including how to shape ideas into persuasive funding proposals. I wish you a vibrant and fulfilling retirement.

I am also grateful to my Master supervisor, Prof. Haibin Wang and Prof. Liangliang Xu who played vital roles in starting my academic career. Dear Haibin, you set the highest standard of what it means to be an exceptional orthopedic doctor, and your dedication is truly inspiring. To me, you are someone who not only excels in your field but also continually strives to improve and push the boundaries of your own capabilities. Your energy and passion for bettering yourself are unmatched, and they motivate those around you, myself included, to keep striving for excellence. You are a true researcher—someone who never stops learning, even after achieving so much. Despite having already reached such an impressive level in your career, you told us that you still spend time in your office studying during workweeks, rather than seeking entertainment or relaxation like most people would. You once shared with me, "You should never stop chasing the best. Learn as much as you can while you are young." When others say things like this, I often think it's just empty rhetoric, but with you, I've seen your actions align perfectly with your words.

Thank you for providing me with such a valuable platform to explore the world of academic research in bone and joint diseases. It was through your guidance that I was able to receive the CSC scholarship, which opened doors for me and allowed me to see a much broader world than I could have imagined. I'll always be grateful for your mentorship and the opportunities you've helped me unlock. Now, after hearing the difficult news, I sincerely hope that you will recover swiftly. Please know that my thoughts are with you, and I wish for your health and well-being every day. With deepest gratitude and warmest wishes for your recovery. Dear Liangliang, I consider myself incredibly lucky to have had the opportunity to work with you and to be one of your students in the field of stem cell research. Looking back, especially at the beginning of my master's period, I realize just how much I benefited from your guidance. At that time, you were also new to the university, and we navigated this journey together. We not only worked side by side but also shared meals and conversations, and through it all, you taught me the hands-on techniques I needed to carry out experiments. This personal involvement in my learning process sparked my passion for science and helped me grow tremendously. Without your mentorship, I would not have been able to achieve such significant milestones, such as publishing my first paper and getting the National Undergraduate Scholarship. These accomplishments were incredibly meaningful to me, and they would not have been possible without your unwavering support and guidance. You have always been incredibly friendly, approachable, and open. Whenever I faced difficulties or felt lost in my experiments, I knew I could count on you to provide thoughtful and patient advice. Your willingness to help me, no matter the situation, made a huge difference in my academic journey. Thank you so much for your selfless dedication to my academic growth, and for the generosity you showed in supporting me throughout this journey. I will always be grateful for everything you have done. I sincerely wish that your research life continues to flourish, and that you achieve even greater success in the years ahead. With sincere gratitude and best wishes for your future endeavors.

Then, I would like to thank other supervisors and senior colleagues from the Experimental Rheumatology Department, including Dr. Marije Koenders, Dr. Martijn van den Bosch, Dr. Arjan van Caam, Dr. Esmeralda Blaney Davidson, Dr. Arjen Blom, Dr. Daphne Dorst, Dr. Henk van Beuningen. Dear Marije, I will always cherish the warmth of your smile every time we met, as well as the genuine interest you showed in both my research and daily life. Even though you were not my supervisor, your kind and thoughtful greetings always lifted my spirits and motivated me to work with greater enthusiasm for the rest of the day. Thank you so much for your constant encouragement and kindness! Dear Martijn, I have always been impressed

by the depth of your insights during our discussions. You strike me as a dedicated and meticulous researcher, and your relentless commitment to your work is clearly reflected in the impressive funding you've secured. You set a strong example for all of us, and I aspire to learn from your exemplary scientific rigor and attitude. I wish you continued success and a brighter future in your research endeavors! Dear Arjan, Your patience in answering my questions has been invaluable. Your vast knowledge and logical approach to research have often inspired me, helping me generate meaningful and reliable data. I am truly grateful for your guidance, and I hope you continue to have a brilliant research career ahead! Dear Esmeralda, Although I understand that your focus on education has limited our time for discussions in the lab, I always enjoyed our conversations. I particularly remember how considerate you were during Peter's 40th work anniversary celebration, when you suggested others speak in English to facilitate my communication with you. That thoughtful gesture meant a lot to me. I appreciate your kindness and hope you continue to shine as an outstanding educator! Dear Arjen, even though we were not in the same research group, I truly appreciated the personal messages and emails you sent to congratulate me whenever I made progress in my PhD. Your encouragement greatly boosted my confidence and motivated me to keep moving forward. You are also such a kind and approachable person, always ready to lend a helping hand. It's been a pleasure to have you in the department—thank you! Dear Daphne, as an international PhD student, I always enjoyed listening to your presentations and discussions. Your ability to convey complex ideas in a clear and accessible manner never failed to impress me. Beyond your research expertise, I admire how effortlessly you balance work and family life. You are a true role model, and I look forward to learning even more from you! Dear Henk, I often see you working diligently in the lab, even after hours and on weekends. Your passion for research is infectious and has been a source of great motivation for me. Additionally, I've thoroughly enjoyed the moments we've shared as teammates during the lab outings, playing games together. You're not only an inspiring researcher but also a fun and friendly colleague. Thank you for being such a positive influence! Subsequently, I would like to express my sincere gratitude to the technical staff of our department. Dear Birgitte, thank you for your expert support with histology; you are invariably the first person I turn to when a lab question arises. Dear Elly, I am grateful for your assistance with the cell experiments, particularly the work on mitochondria—your persistence and steady professionalism have inspired me throughout. Dear Monique and Annet, thank you for performing the Luminex and qPCR assays; without your expertise and timely help, this PhD thesis would not have been possible. I would like to thank the technicians in the Dentistry Department. Dear Dr. Vincent, thank you for generously sharing your imaging expertise and for

proposing practical solutions to my research challenges. I remain impressed by the breadth of your knowledge and the truly comprehensive way you view scientific problems. Dear Natasja, thank you for your support with histology. Although I am only a visiting PhD researcher, you always made time to guide me and assist with the staining protocols. Your help was indispensable to my most recent publication. Dear Ingrid, thank you for all your assistance with cell culture and fluorochrome-based histology. I have learnt a great deal from your rigorous standards and strict adherence to good laboratory practice.

I would like to extend my acknowledgements to my outstanding colleagues in the Experiments Rheumatology department. Dear Xinlai (Chen), it felt natural that we spoke so often during the workday; your energy and steady support kept me going at the bench. You have been unfailingly kind—a true big sister in the lab. Without you, this PhD would not feel complete. I wish you every success with your own PhD and a smooth, on-time thesis submission. I am also looking forward to showing you around my hometown. Dear Wessel, thank you for agreeing to be one of my paranymphs—your support means a great deal. Although we haven't talked extensively, I always remember how clearly you explained things whenever I asked for help. You also looked out for me during the lab day out. You are impressively fit and energetic, and you model a healthy balance between work and life; I hope to learn from your example. Wishing you a bright future in research. Dear Nienke, thank you for providing the bone tissues from CWZ and for your kind, enthusiastic help. You have always been patient with my questions, and I truly appreciate it. I wish you a happy and fulfilling life after your PhD. Dear Theo, you are a standout among us. I am consistently impressed by your excellent research skills—your ability to marshal resources, communicate across groups, and build strong collaborations is exemplary. Most of all, your work ethic inspires me; I will not forget the late nights you spent at the computer refining your manuscript. Wishing you a happy and brilliant next chapter at Leiden University. Dear Angela, I only wish we had met sooner—thank you for inviting me to the animation screening; it was fascinating. It's a pity your PhD began in my final year, but I hope you have a wonderful PhD journey ahead. I would also like to thank Joyce Aarts, Natalia Valdrighi, Ritchie Timmermans, Yvonne Bartels, Margot Neefjes, Nathalie Thielen, Donna Vegt, and Anne Essen. I feel very lucky to have been your colleague; your presence truly enriched my time in the lab.

Then I would like to thank some colleagues in the Dentistry Department. Dear xiaosong (Xiang), it is a pity that we met only in the later phase of my PhD, but I am truly glad to have had you as a neighbor. I miss your delicious cooking, and

I deeply appreciate all the support you have provided in my daily life. Thank you for being one of my paranymphs. I admire your hard work and enthusiasm. I hope you continue to pursue your research with the same passion and that your PhD journey becomes even brighter and more fruitful! Dear Zhule (Wang), thank you for all your guidance in the Dentistry lab. I feel incredibly fortunate to have been part of Jeroen's group, especially during your final year. Your logical thinking has constantly inspired and enlightened me. You are a true researcher, and I wish you all the best in achieving an outstanding academic career! Dear Johanna, I cannot thank you enough for all the help you provided during my first year of PhD. You guided me through the lab and taught me how to conduct experiments. Whenever I had questions, you were always there with patience and clarity. Without your support, I would not have adapted so quickly to the work in the Dentistry Department. I wish you nothing but success in your postdoc journey in Twente. Dear Gerry, I feel lucky to have met you in the later phase of my PhD. My interest in deep machine learning has grown, and you have been incredibly supportive in guiding me through this field. I truly appreciate your attention to the bone discs research; although it is now complete, I've gained so much from our discussions. Your logical thinking and words of encouragement have had a lasting impact. I wish you all the best in your future academic career! Dear Lei (Li), working with you to observe cells and label EVs using the NanoLive machine has been an amazing research experience. I've always enjoyed our conversations, which have been both insightful and enlightening. Beyond the research, I also miss the food we shared and the computer games we played together. I hope your career in this field continues to shine brightly. Dear Qianfeng (Xiang), as one of the PhD candidates in Jeroen's group, even though we didn't have many research interactions, it's always been a pleasure discussing our future careers as physicians. I also miss the basketball games we played together, and the great food and drinks, especially in Shenzhen with Dr. Yang Zhang. I hope you have a rewarding year as you approach the final phase of your PhD. Dear Zhihao (Wang), we arrived in the Netherlands at the same time, and now, we're about to graduate around the same time. Although we didn't have much contact, I still vividly remember the first time we played "Wolf Killer" together at my place. Time has flown by so quickly! I wish you all the best in the future and hope you have a wonderful life ahead. Dear Chong (Huang), keyi (Wu), Lingyun (Cao), I wish you all the best for your PhD study and life in the Netherlands.

Subsequently, I would like to thank several friends. Dear Xianzong Meng, I feel incredibly fortunate to have met you in Nijmegen. Basketball brought us together, and from there, we discovered so much more to talk about. You have been like a brother to me—helping me find a place to live, guiding me through the process

of moving, and sharing invaluable tips for life in the Netherlands. I miss the meals we shared in your room and the long conversations we had every night. You've always been a reliable friend, ready to join me for a game of basketball, and our conversations seem to have no end. You are kind, friendly, and enthusiastic, and I've truly enjoyed spending time with you. My PhD experience would not have been the same without you. I wish you all the best as you begin your postdoc journey with your previous team. I know this is the perfect next step for you, and I hope your future is full of success! Dear Zhiming (Wu) and Delong (Chen), my fellow master's colleagues, it feels like fate brought us together to pursue our PhDs in the Netherlands. I fondly remember our trip to Paris and the meals we shared together. Visiting Rotterdam or Utrecht to meet you both added so much to my weekends. I wish both of you vibrant and fulfilling PhD journeys. I look forward to meeting you again in Guangzhou in the future! Dear Junjie (Cao), Shenghang (Wang), Zhikang (Cheng), Yubo (Zhang), I felt so lucky to meet you in the Netherlands. Your presence has enriched my life. Hope to see you in the future!

最后，我想感谢我的父母和我的妻子。感谢爸妈三十多年的照顾和关心。每当遇到困难的时候，第一个想要求助的人总是我的父亲母亲。希望两位在未来的日子里可以好好享受生活，希望您们健健康康，事事顺心，长命百岁。 还要感谢我的妻子，谢谢你的支持，谢谢你能在我不在的时候照顾好自己和我们的孩子。如今我已毕业回到了家乡，希望我们的日子会越来越好。也感谢我自己，感谢自己的坚持和努力。未来要继续加油!

Peng Wang

王鹏

30/9/2025

Chapter 11

Research data management
PhD Portfolio
List of publications
Curriculum Vitae

RESEARCH DATA MANAGEMENT

Medical and ethical approval

Human studies being part of this thesis were conducted in accordance with the principle of the Declaration of Helsinki and were approved by the medical ethics committee (Commissie Mensgebonden Onderzoek Arnhem-Nijmegen). Procedures were performed in accordance with the Dutch code of conduct for responsible use of human tissue in medical research as set by the International Society for Cellular Therapy (ISCT).

For chapter 2 data, human subcutaneous adipose tissue from two healthy male donors, with an age range of 33–47 years, was obtained from the Department of Plastic Surgery (Radboudumc) after ethical approval (Commissie Mensgebonden Onderzoek; dossier number #3252) and informed consent. The privacy of the participants in study was warranted by the use of fully anonymous data.

For chapter 3, 5, 6 data, human femoral heads and were freshly obtained from the Department of Orthopedics (Radboudumc, Nijmegen, the Netherlands) as surgical excess material following total hip arthroplasty from anonymized patients and human bone marrow MSCs were isolated from bone fragment of corresponding human femoral heads.

All animal care and related experimental procedures were carried out according to the guidelines of Chinese Research Council's and all procedures were approved by the ethical committee for animal care and use of Shenzhen University (SYXK 2022-0302).

Data collection and storage

Data for chapters 2, 3 and 6 was obtained through laboratory experiments involving anonymous or non-human materials and data for chapter 5 was obtained from experiments involving animals. Data for chapters 2, 3, 5 and 6 from NTA analysis, qPCR, Western blot, IVIS imaging, flow cytometry, microBCA test, proteomics sequencing analysis, micro-CT scanning, bone tissue staining are stored and analyzed on the private network server of Experimental Rheumatology Department and Department of Dentistry – Regenerative Biomaterials and are only accessible by project members working at the Radboudumc. These secure storage options safeguard the availability, integrity and confidentiality of the data.

Data sharing according to the FAIR principles

Chapters 2, 4 and 5 are published open access. DOI (s): Chapter 2: http://doi.org/10.1371/journal.pone.0295076.Chapter 4: http://doi.org/10.1186/s12964-025-02156-5. Chapter 5: http://doi.org/10.1016/j.mtbio.2025.102115. Chapter 3 and 6 are not published currently. Chapter 4 is based on existing data which was obtained from published literature. The data underlying the chapters 2, 3, 5, and 6 in this thesis comprise laboratory data that are generated specifically for the purpose of this thesis and are unlikely to be suitable for reuse. The data referenced in chapters 2 and 5 are stored in a DAC titled 'Utilization of Extracellular Vesicles for Bone Repair' within the Radboud Data Repository, with restricted access for 10 years (DOI: https://doi.org/10.34973/as1p-2e38). The data used in the unpublished chapters 3 and 6 are archived at the Experimental Rheumatology Department and Department of Dentistry – Regenerative Biomaterials. Upon publication of these chapters, the data will also be archived for 10 years in a DAC of the Radboud Data Repository with closed access (DOI: https://doi.org/10.34973/as1p-2e38).

PHD PORTFOLIO

Name PhD candidate: P. Wang Department: Experimental Rheumatology
PhD period: 01/03/2021-01/03/2025
PhD promotor(s): Prof. dr. Peter M. van der Kraan, Dr. Jeroen J.J.P. van den Beucken
PhD Co- promotor(s): Dr. Fons A.J. van de Loo, Dr. Onno J. Arntz.

TRAINING ACTIVITIES	Hours
Courses	
Radboudumc – Introduction Day (2021)	6.00
RIMLS – Introduction courses "In the lead of my PhD" (2021)	15.00
RU- Scientific Writing for PhD candidates (2022)	84.00
Radboudumc – Scientific integrity (2024)	20.00
RU - Academic English Conversation and Pronunciation (2021)	42.00
Seminars	
Science Meeting and Working Discussion in Experimental Rheumatology (2021-2025)	192.00
Mini-symposium on EVs at Radboudumc (**) (2024, 2025)	6.00
Radboudumc Research Round (X10) (2021-2025)	10.00
Conferences	
PhD retreat (*) (2024)	21.00
ISEV Annual Meeting (##) (2022, 2025)	48.00
APSEV 2024 Asia Pacific Spotlight on EV (2024)	48.00
NLSEV 2024	48.00
Teaching activities	
Supervision of one master student (2023)	100.00
Supervision of one master student (2023)	56.00
Total	**696.00**

Oral and poster presentations are indicated with a * and # after the name of activity, respectively.

LIST OF PUBLICATIONS

First author publications related to this thesis

1. **Peng Wang**, Yang Zhang, Onno J. Arntz, Marina C. Oliveira, Taozhao Yu, Zhihua Yang, Peter M. van der Kraan, Jeroen J.J.P. van den Beucken, Fons A.J. van de Loo. Collagen Binding Properties Separate Two Functionally Distinct Subpopulations of Milk Extracellular Vesicles Regarding Bone Regenerative Capacity. Materials Today Bio. 2025 Jul 18:33:102115.
2. **Peng Wang**, Johanna F.A. Husch, Onno J. Arntz, Peter M. van der Kraan, Fons A.J. van de Loo, Jeroen J.J.P. van den Beucken. ECM-Binding Properties of Extracellular Vesicles: Advanced Delivery Strategies for Therapeutic Applications in Bone and Joint Diseases. Cell Commun Signal. 2025 Apr 2;23(1):161.
3. **Peng Wang**, Onno J. Arntz, Johanna F.A. Husch, Van der Kraan PM, Jeroen J.J.P. van den Beucken, Fons A.J. van de Loo. Polyethylene Glycol Precipitation is an Efficient Method to Obtain Extracellular Vesicle-Depleted Fetal Bovine Serum. PLoS One. 2023 Dec 5;18(12):e0295076.
4. **Peng Wang**, Onno J. Arntz, Xinlai Chen, Theodoros Ioannis Papadimitriou, Peter M. van der Kraan, Jeroen J.J.P. van den Beucken, Arjan van Caam, Fons A.J. van de Loo. Milk Extracellular Vesicles Promote the Osteogenesis of Bone Marrow Stromal Cell Through Mitochondrial Oxidative Phosphorylation. In preparation.
5. **Peng Wang**, Gerry Koons, Zhule Wang, Jetze Visser, Fons van de Loo, Jeroen JJP van den Beucken. Ex vivo human femoral head bone discs: a model for studying bone regeneration. In preparation.

Other first author publications

6. **Peng Wang**, Min Wang, Tingling Zhuo, Ying Li, Weiping Lin, Lingli Ding, Meng Zhang, Chi Zhou, Jinfang Zhang, Gang Li, Haibin Wang, Liangliang Xu. Hydroxysafflor yellow A promotes osteogenesis and bone development via epigenetically regulating β-catenin and prevents ovariectomy-induced bone loss. Int J Biochem Cell Biol. 2021 Aug: 137: 106033.
7. **Wang P**, Cao Y, Zhan D, Wang D, Wang B, Liu Y, Li G, He W, Wang H, Xu L. Influence of DNA methylation on the expression of OPG/RANKL in primary osteoporosis. 2018 Oct 3;15(13):1480-1485.

CURRICULUM VITAE

Peng Wang was born on 23 June, 1994 and grew up in Nanchang, China. In 2012, he was enrolled in School of Medicine, Guangzhou University of Chinese Medicine (Guangzhou, China), majoring Chinese Clinical Medicine. He obtained his bachelor's degree with honors in June 2017. After this, he continued with a 3-year master's medical education in the Chinese Orthopedic Department under the supervision of Prof. dr. Haibin Wang at Traditional Chinese Medicine University of Guangzhou No.1 Affiliated Hospital (Guangzhou, China). In 2020, he received his master's degree with honors from Guangzhou University of Chinese Medicine. From March 2021 onward, he worked as a Ph.D. candidate in the department of Experimental Rheumatology and Density-Regenerative Biomaterials, Radboud University Medical Center under the supervision of Dr. Fons van de Loo, Dr. Jeroen J.J.P. van den Beucken, Prof. dr. Peter M. van der Kraan and Dr. Onno J. Arntz. His project focused on the precision utilization of EVs in treating bone defects. The results of his PhD projects are described in this thesis and have been published or will be published as separate research articles in scientific journals. During the doctor study, he actively participated in several (inter)national scientific conferences by presenting (parts of) his research via poster presentations (e.g. meetings of the International Society for Extracellular Vesicles, ISEV; Lyon, France 2022 & Vienna, Austria 2025). Additionally, he strengthened collaborative research via a research visit at Dr. Yang Zhang's laboratory at Shenzhen University (Shenzhen, China). After completing his PhD, he aims to pursue a clinical and academic career devoted to orthopedics and regenerative medicine.

9 789465 151915 >

Radboudumc university medical center

IN DEI NOMINE FELICITER

Radboud University